Model-Independent Approaches to QCD and B Decays

by

Christian Arnesen

Submitted to the Department of Physics
in partial fulfillment of the requirements for the degree of

Doctorate of Philosophy

at the

MASSACHUSETTS INSTITUTE OF TECHNOLOGY

May 2007

Author .....
Department of Physics
May 30, 2007

Certified by .....
Iain W. Stewart
Assistant Professor
Thesis Supervisor

Accepted by .....
Thomas J. Greytak
Associate Department Head for Education

Model-Independent Approaches to QCD and B Decays

by

Christian Arnesen

Submitted to the Department of Physics
on May 30, 2007, in partial fulfillment of the
requirements for the degree of
Doctorate of Philosophy

Abstract

We investigate theoretical expectations for B-meson decay rates in the Standard Model. Strong-interaction effects described by quantum chromodynamics (QCD) make this a challenging endeavor. Exact solutions to QCD are not known, but an arsenal of approximation techniques have been developed. We apply effective field theory methods, in particular the sophisticated machinery of the soft-collinear effective theory (SCET), to B decays with energetic hadrons in the final state. SCET separates perturbative interactions at the scales m_b and $\sqrt{m_b \Lambda_{\rm QCD}}$ from hadronic physics at $\Lambda_{\rm QCD}$ by expanding in ratios of these scales.

After a review of SCET, we construct a complete reparametrization-invariant basis for heavy-to-light currents in SCET at next-to-next-to-leading order in the power-counting expansion. Next we classify $\Lambda_{\rm QCD}/m_b$ corrections to non-leptonic $B \to M_1 M_2$ decays, where $M_{1,2}$ are charmless mesons (flavor singlets excluded). The leading contributions to annihilation amplitudes as well as the leading "chirally enhanced" contributions are calculated and depend on twist-2 two-parton and twist-3 three-parton distributions. We demonstrate that non-perturbative strong phases in annihilation are suppressed. Using simple models, we find that the three-parton and two-parton terms have comparable magnitude, both consistent with the expected size of power corrections. Finally, we present a method for determining $|V_{ub}|$ from $B \to \pi \ell \nu$ data that is competitive with inclusive methods. At large q^2, the form factor is taken from unquenched lattice QCD. At $q^2 = 0$, we impose a model-independent constraint obtained from $B \to \pi\pi$ using SCET, and the form factor shape is constrained using QCD dispersion relations. Theory error is dominated by the input points, with negligible uncertainty from the dispersion relations.

Thesis Supervisor: Iain W. Stewart
Title: Assistant Professor

Biographical Sketch

The author was born Mark Christian Arnesen on August 9, 1979, to Mark Allen Arnesen and Patricia Marie Arnesen (née Ahrens). He attended primary school at Wooddale Montessori Academy in Edina, Minnesota, followed by middle and high school at the International School of Minnesota, in Eden Prairie, where he graduated as valedictorian in 1997. He continued his education at the California Institute of Technology, in Pasadena, majoring in physics. Notable honors from that time include a Carnation Merit Scholarship for academic achievement (1/3rd tuition for his junior year), and a letter in varsity basketball in each of his four years. He received his Bachelor of Science degree with honors from Caltech in 2001. His graduate studies took place from 2002-2007 at the Massachusetts Institute of Technology in Cambridge, the first two years of which he was supported by the Karl Taylor Compton fellowship. This thesis is the culmination of those studies.

Acknowledgments

I would like to thank my collaborators in the research described in this thesis: Ben Grinstein, Joydip Kundu, Zoltan Ligeti, Ira Rothstein, and in particular, Iain Stewart for collaboration and supervision. In the course of my graduate studies, I have benefitted from discussions with numerous physicists including: Mauro Brigante, Qudsia Ejaz, Casey Huang, Ambar Jain, Alejandro Jenkins, Bjorn Lange, Keith Lee, Hong Liu, Sonny Mantry, Claudio Marcantonini, Vivek Mohta, Dan Pirjol, Krishna Rajagopal, Sean Robinson, Rishi Sharma, and Jessie Shelton. I deeply appreciate the support and encouragement that all my family and friends have given, none more than my parents, Mark and Pat, and the kind people I have lived with, Jessica Halverson, Sophie Hood, and Francis MacDonald. Finally, I acknowledge funding from the Karl Taylor Compton fellowship, the MIT physics department, and the Department of Energy under cooperative research agreement DOE-FC02-94ER40818.

Contents

Chapter 1

Introduction

1.1 The Standard Model

In the 20th century, it became clear that the sub-atomic world required a radical departure from the classical physics of daily life. Special relativity, important for large velocities, redefined the relationship between space and time. Quantum mechanics, important for short distances, had particles acting like waves and energy coming only in discrete nuggets, or quanta. Quantum field theory (QFT) incorporated both of these advances into a single mathematical framework. In such a theory, fields replace particles as the basic building block, and particles emerge as quantized excitations of those fields. This representation formalizes in a natural way the wave-particle duality and indisinguishability of elementary particles that had puzzled physicists for decades.

By the end of the 1970s, a coherent theoretical picture had emerged. The Standard Model (SM) of particle physics, a QFT, built all matter from a relatively small number of elementary particles: six "flavors" of quark (up, down, charm, strange, top, bottom) which can interact via the strong force, and six leptons (e, μ, τ, ν_e, ν_μ, ν_τ) which feel only electromagnetic and weak forces. Interactions[1] derive from a symmetry principle, local gauge invariance, a simple mathematical statement with far-reaching consequences. By the 1990s, predictions of the Standard Model had been verified by a

[1] Gravity, negligible for the processes described in this thesis, is not included in the SM.

multitude of experiments probing energies over many orders of magnitude. The sector of the theory governing quark flavor transitions through weak interactions, however, was still poorly constrained, and theoretical tools for understanding the influence of strong interactions were still being developed.

1.2 B physics

Quark flavor transitions can be studied by observing weak decays of hadrons. Since the late 1980's, the CLEO collaboration at the Cornell Electron Storage Ring has been measuring decay rates of D mesons, $c\bar{q}$ bound states, and B mesons, $b\bar{q}$ bound states, where q is a light quark. As the lightest charmed and bottomed hadrons, respectively, these mesons can only decay through weak interactions.[2] For the last decade, the B factories, Belle at the KEK facility in Japan and BaBar at the Stanford Linear Accelerator Center in California, have produced B mesons in abundance. All three of these experiments exploit an efficient and effective B-production mechanism. Accelerated electrons and positrons annihilate creating a new fermion anti-fermion pair. The center-of-mass energy is tuned to the rest mass of the $\Upsilon(4s)$ $b\bar{b}$ bound state such that when a b and a $\bar{b}$ are created, they hadronize into this bound state. The $\Upsilon(4s)$ decays almost exclusively (>96%) via strong interactions to a B meson and its anti-matter counterpart. Half the B pairs are charged, B^+B^-, and half are neutral, $B^0\bar{B}^0$. The B factories have created a billion $B\bar{B}$ pairs from more than an inverse attobarn of total integrated luminosity between them.

The stated primary goal of the B factories and the inspiration behind their innovative design is the investigation of CP violation. Until 1964 it was widely assumed that the combined operation of charge conjugation C, (exchanging particles and anti-particles), and parity P (spatial inversion) was an exact symmetry of nature. Then Cronin, Fitch and collaborators observed that CP is only an approximate symmetry of the neutral kaon Hamiltonian [65]. CP violation can be even more dramatic B decays, and can manifest in several ways. The easiest type of CP asymmetry

[2]The top quark, with a width $\Gamma_t \approx 1.5$GeV, decays too quickly to hadronize.

to understand conceptually is *direct* CP violation when the rate for a certain decay differs from the rate for the CP-conjugate version of that decay. For example, $\mathcal{A}_{K\pi} = -0.113 \pm 0.020$ (world average by the Heavy Flavor Averaging Group [91]) tells us that the rate for $B^0 \to K^+\pi^-$ is larger than the rate for $\bar{B}^0 \to K^-\pi^+$ with a statistical significance of more than 5.5 standard deviations. The rates would be equal in a CP-symmetric world. Many such direct CP asymmetries have been measured independently by CLEO, BaBar, and Belle in both charged and neutral B decays.

The B factories have a compelling design advantage over CLEO for measuring CP-violating observables. Asymmetric energies for the electron and positron beams mean that the $\Upsilon(4s)$ rest frame is boosted and time-dilated relative to the lab frame. B's are naturally long-lived because they require a flavor-changing weak interaction in order to decay. With the boost inherited from the parent $\Upsilon(4s)$, the B's travel measurable distances, several hundred micrometers, before decaying. The decay products can be traced back to the point in space and time where the decay occurred. This additional piece of information allows the B factories to measure so-called time-dependent CP asymmetries.

CP-violating observables only constitute a fraction of the measurements made by CLEO and the asymmetric B factories. The large b-quark mass opens a plethora of decay modes. The relatively clean environment of a lepton collider, together with high luminosities and an efficient production mechanism, has allowed a truly amazing variety of CP-averaged B-decay rates to be measured or bounded (23 pages worth, more than 500 modes, in the most recent Partcle Physics Booklet extracted from the Review of Particle Physics by the Particle Data Group [140]). Rare decays such as $B \to K^*\gamma$, $B \to X_s\gamma$, and $B \to X_s\ell^+\ell^-$, do not occur at tree level in the Standard Model. They proceed through an electroweak loop and could receive significant contributions from "new physics," *i.e.* particles and interactions *not* included in the Standard Model.

Semi-leptonic decays with $b \to c\ell\bar{\nu}$ or $b \to u\ell\bar{\nu}$ at the quark level are an unlikely place to see CP violation or evidence for new physics, since in the SM they are dominated by a single tree-level weak transition. This simplicity of semi-leptonic

decays benefits a major goal of the B factories: measurement of entries in the unitary Cabbibo-Kobayashi-Maskawa (CKM) matrix that parametrizes the strength of interactions of quark currents with the charged weak bosons [105]. Exclusive $B \to D^{(*)}\ell\bar{\nu}$ and inclusive $B \to X_c\ell\bar{\nu}$, where we sum over hadronic final states with net charm 1 (*e.g.* D, D^*, $D\pi\ldots$), both provide an accurate determination of $|V_{cb}|$. Similarly $B \to X_u\ell\bar{\nu}$ gives our best direct measurement of $|V_{ub}|$, which is one of least-constrained CKM parameters. A model-independent method for determining $|V_{ub}|$ using $B \to \pi\ell\bar{\nu}$ constitutes part of the original work presented in this thesis.

The question for theorists is whether the Standard Model, with a single value of its input parameters, is consistent with the observed pattern of CP violation and CP-averaged decay rates.

1.3 Quantum chromodynamics

The goals of the B-physics program emphasized in the previous section, measurement of CP violation and weak mixing parameters, with a chance of new physics, are often cited as the reasons why one should be interested in (and fund production of) B's. Far less often are B decays recognized as an exceptional laboratory for strong interactions. For, within just a few years of the first proofs of asymptotic freedom in quantum chromodynamics (QCD) in 1973 [131, 89], it was widely accepted as the correct QFT for describing the strong force. There is now overwhelming evidence that this is the case, and as the saying goes, "Yesterday's sensation is today's calibration and tomorrow's background."[3] For many, QCD's tomorrow is today. Certainly a quantitative understanding of strong-interaction effects is required to extract short-distance physics from collider data. Understanding QCD, however, is a worthwhile and interesting endeavor in its own right, and the decays mentioned in the last section can be reinterpreted in this context.

CP violation results, in the Standard Model, from a single complex phase in the

[3]This quote is most often attributed to Richard Feynman (see [116] for example), but Ikaros Bigi credits Valentine Telegdi [41].

CKM matrix. A physical observable, however, depends only on the *magnitude* of its quantum mechanical amplitude. Direct CP violation, for example, requires not only that the decay proceeds through two or more paths with differing weak phases, but also that those paths have differing strong phases. (See the BaBar Physics Book [93] for a review). We need a detailed understanding of strong-interaction effects in CP violating processes in order to make quantitative statements about their consistency within the Standard Model. This is particularly challenging since with rare exception (*e.g.* $B^0 \to K^*(892)^0\gamma$), CP violation has only been observed in channels with both a hadronic initial state, *i.e.* B, and a final state composed of hadrons. The resounding success of the Standard Model encourages us to reverse this line of reasoning: assume that the CKM phase is in fact the sole source of CP non-conservation and then these observables test our understanding of the strong force. This is the philosophy with which B decays to two light mesons are approached in Chapter 4.

Any claim of new physics in rare decays requires an accurate SM prediction, in particular, of QCD effects. $B \to X_s\gamma$ has not shown signs of new physics, but it does provide information about the B-meson shape function, which describes the probability distribution of b-quark momenta inside the meson. Using effective field theory, knowledge of this shape function can in turn be used to extract $|V_{ub}|$ from $B \to X_u\ell\bar{\nu}$ data (see Lange et al. [109] for a recent analysis). This value of $|V_{ub}|$ can be compared to the value extracted from $B \to \pi\ell\bar{\nu}$ with the $B \to \pi$ form factor normalization taken from lattice monte carlo simulations of QCD [127, 73]. The weak physics of these decays is well-understood, and we view the consistency of these determinations as a validation of the theoretical techniques used to calculate the strong interactions. Similarly, $|V_{cb}|$ from $B \to D\ell\bar{\nu}$ and from $B \to X_c\ell\bar{\nu}$ can be compared as a check on the QCD tools used in those extractions (at leading order, heavy-quark symmetry and quark-hadron duality plus an operator product expansion, respectively [125]). The primary theoretical technique applied in this thesis, effective field theory, is outlined in the next section.

1.4 Effective field theory

It is not known how to find exact solutions to the Standard Model. Instead, each prediction is expressed as a power series in a number of small expansion parameters: gauge coupling constants and ratios of energy scales defined by both dynamics and kinematics. Generally, each term in the series requires a more complicated calculation than the previous term and the series must be truncated. The predictive accuracy of the truncated series is limited by the magnitude of the terms left out, which can be estimated by parameter counting. Such approximate solutions do not have the same aesthetic appeal as exact ones. Physics, however, is an experimental science and the accuracy of a theoretical prediction need only be comparable to the accuracy of the data. One powerful mathematical formalism used to derive such series expansions is effective field theory (EFT). (See Georgi [83] or Manohar [121] for a review.)

The idea behind EFT is a familiar one in physics: low-energy models should not require a detailed knowledge of what happens at higher energies. Any physical model consists of a mathematical framework and a set of rules and input parameters, and gives a theoretical expectation for a variety of processes. Comparing expectation and observation for a fraction of the processes fixes the value of the input parameters. The expectations for the remainder then become predictions. For example, non-relativistic quantum mechanics is the appropriate framework for calculating atomic energy levels. The mass, charge, and magnetic moment of the electron and nuclei can all be thought of as low-energy input parameters. The high-energy theory, once known, provides deeper insight. In this case, quantum field theory justifies the fermionic indistinguishability of electrons, which is simply adopted as a rule in QM. It also reveals that the electron's magnetic moment can be calculated in terms of its charge and mass. The goal of particle physics then is not only a unified theory of everything, but also the theories that provide a detailed understanding of low-energy processes.

The Standard Model itself is an effective field theory valid up to some scale where "new physics" becomes important. Its parameters have to be fit from experimental data since that new physics is presently unknown. Within the Standard Model, EFTs

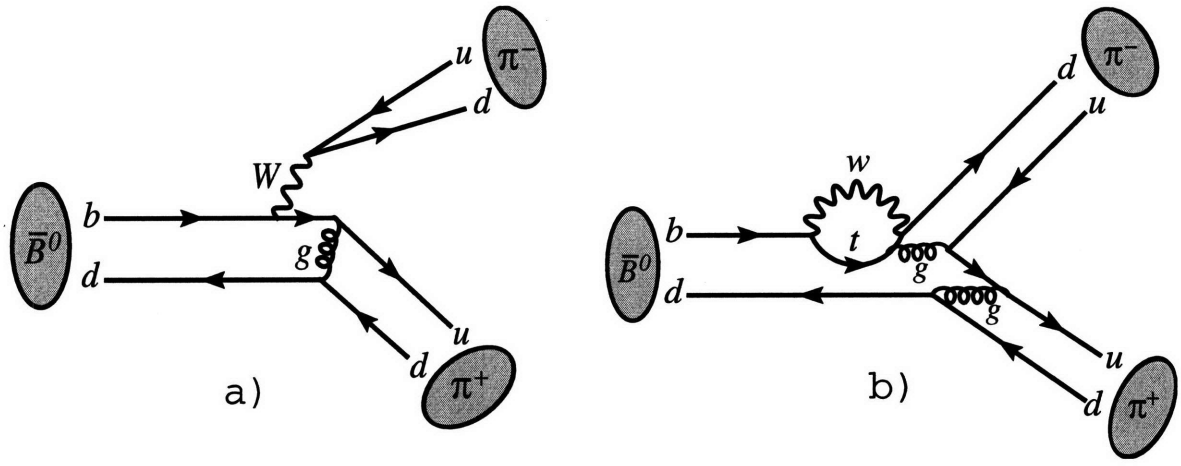

Figure 1-1: Two diagrams that contribute to $\bar{B}^0 \to \pi^+\pi^-$: a) "tree" topology b) "penguin" topology

are used to disentangle strong interaction effects at disparate energy scales. As an example, consider the decay $\bar{B}^0 \to \pi^+\pi^-$. Two SM diagrams that contribute to this process are shown in Figure 1-1. The lowest scale in the problem is not determined by kinematics; curiously, $\Lambda_{\rm QCD} \approx 300$MeV is generated dynamically in QCD. It can be thought of as the scale at which the theory becomes strongly coupled. At one-loop order (in dimensional regularization with $\overline{\rm MS}$ renormalization), the strong coupling has

$$\alpha_s(\mu) = \frac{12\pi}{(33 - 2N_q)\log(\mu^2/\Lambda^2_{\rm QCD})} \tag{1.1}$$

where N_q is the number of light quark flavors. Strong-interaction effects below, at, or near $\Lambda_{\rm QCD}$ cannot be treated perturbatively as a series in α_s. Equation (1.1) is no longer even valid near these scales. The transition to the strongly-coupled region is intimately associated with confinement: quarks and gluons have never been observed as isolated free particles, only as constituents of composite color-neutral bound states.

These non-perturbative QCD effects pose a significant challenge for theorists. In some cases, such as the B to π semi-leptonic form factor with $E_\pi \lesssim 1$GeV in the B rest frame, the hadronic physics can be estimated numerically using lattice monte carlo techniques [127, 73]. Current technology, however, does not support lattices of sufficient volume to simulate the nearly light-like pions in $B \to \pi\pi$, which have $E_\pi = 2.6\text{GeV} \approx 20 m_\pi$. EFTs allow us to reduce and quantify these pervasive hadronic

uncertainties by relating non-perturbative effects from distinct processes. In the case at hand, EFT methods reveal a relationship between $B \to \pi\pi$ and the $B \to \pi$ form factor at large momentum transfer using perturbation theory at the scale m_b [19]. In fact, if perturbation theory is valid at the "intermediate" scale $\sqrt{\Lambda_{\rm QCD} m_b}$, then all non-perturbative effects in $B \to \pi\pi$ enter as moments of distribution functions of the individual mesons [124]. These moments are universal in the sense that they are process-independent properties of the mesons themselves. EFTs help us understand the relevant scales in a problem, and how such relationships emerge.

There are several important scales in $B \to \pi\pi$ for which α_s *is* small. The top quark appears as an off-mass-shell intermediate state in penguin loop diagrams such as Figure 1-1(b). Its mass, $m_t = (170.9 \pm 1.8)$GeV in the most recent update from the Tevatron Electroweak Working Group [80], is the largest scale in the problem. The charged weak bosons W are responsible for quark flavor change. They also have a large mass $m_W = 80.403 \pm 0.029$GeV [140]. Far below the weak scale is the b-quark mass $m_b \approx 4.7$GeV which makes up the majority of the mass of the B meson and of the energy of the pions $E_\pi = m_B/2$. Between m_b and the non-perturbative region is the intermediate scale $\sqrt{\Lambda_{\rm QCD} m_b}$, the lowest scale in this problem that we treat perturbatively. $\Lambda_{\rm QCD} m_b$ is the virtuality of a propagator that carries the typical momentum of both an initial state parton and a final state parton, such as the gluon in Figure 1-1(a).

Effective field theories clarify and facilitate the calculation of QCD effects at these perturbative scales. In the full-theory SM diagrams in Figure 1-1, it is not clear what should be chosen for the renormalization parameter μ, since each diagram contains several disparate scales. The situation is even worse for radiative corrections; one finds large logarithms, $\log(m_W^2/\mu^2)$, $\log(m_b^2/\mu^2)\ldots$, multiplying α_s at every order in the "naive" perturbative expansion. The EFT approach leads to a decay amplitude of the schematic form

$$A(B \to \pi\pi) = C \times H \otimes J \otimes S\,. \tag{1.2}$$

The functions C, H, J, and S contain strong interactions of the scales m_W, m_b,

$\sqrt{m_b\Lambda_{\rm QCD}}$, and $\Lambda_{\rm QCD}$, respectively, and $\otimes$ refers to possible convolutions among the functions. C is calculated as an expansion in $\alpha_s(m_W)$ by *matching* the Standard Model onto a QFT that is otherwise identical, but without the top quark and weak bosons. In reference to Feynman's path integral formulation of quantum mechanics, we say that those massive degrees of freedom have been *integrated out.* The electroweak physics, expanded in $1/m_W^2$, is reproduced by a set of local operators called the weak effective Hamiltonian, whose coupling constants, C, are called *Wilson coefficients.* The matching procedure isolates perturbative strong interaction effects at m_W, encoding them in the Wilson coefficients. We solve a renormalization group equation (RGE) to lower the renormalization parameter μ to a scale $\sim m_b$ appropriate for b-quark decay, effectively resumming the large logs mentioned above.[4]

The focus of this thesis is strong-interaction effects at and below m_b. The soft-collinear effective theory (SCET) [13, 15, 27, 22] separates m_b, $\sqrt{m_b\Lambda_{\rm QCD}}$, and $\Lambda_{\rm QCD}$ in B decays to energetic hadrons or hadronic jets. At the "hard" scale m_b, QCD and the weak effective Hamiltonian are matched onto operators in a theory $\mathrm{SCET_I}$. The matching integrates out fluctuations with virtualities $\sim m_b^2$. The resulting Wilson coefficients, H, of the $\mathrm{SCET_I}$ operators are calculated as an expansion in $\alpha_s(m_b)$. At the intermediate scale, we match $\mathrm{SCET_I}$ onto a theory containing only non-perturbative degrees of freedom, fields that interpolate for partonic constituents of individual hadrons. For inclusive decays that theory is the heavy-quark effective theory [125], while for exclusive B decays to light energetic hadrons, the appropriate infrared effective theory is $\mathrm{SCET_{II}}$. The Wilson coefficients, J, that result from this matching step encode strong interactions at the intermediate scale, and are calculated as an expansion in $\alpha_s(\sqrt{m_b\Lambda_{\rm QCD}})$. These effective theories are discussed in some detail in the next chapter.

[4]Matching and running is sometimes referred to as renormalization-group-improved perturbation theory.

1.5 Plan of the Thesis

Chapter 2 gives an overview of the effective theories used in calculations in the subsequent chapters. These are the weak effective Hamiltonian, the heavy-quark effective theory, and the soft-collinear effective theories I and II. Chapters 3, 4, and 5 describe original research published in [2], [3, 4], and [5], respectively.

In Chapter 3, we construct a complete basis for heavy-to-light currents to second order in the SCET power counting. These operators, of the form $\bar{q}\Gamma b$, where q is a light collinear quark and Γ is a Dirac structure, enter many SCET calculations, including $B \to X_s\gamma$ and $B \to X_u\ell\bar{\nu}$ in the endpoint region of large energy but moderate invariant mass. We derive relations between the currents' Wilson coefficients by enforcing reparametrization invariance (RPI), which effects Lorentz invariance in the effective theory. Our RPI relations determine subleading Wilson coefficients in terms of the leading ones to all orders in α_s without the need for additional matching calculations.

In Chapter 4, we classify, according to their perturbative order and strong phases, all the $\Lambda_{\rm QCD}/m_b$–suppressed decay amplitudes for B decays to two light mesons (flavor singlets excluded). Among these, we calculate the leading "annihilation" contributions, where the spectator quark is Wick-contracted with a field in the weak effective Hamiltonian. Some have speculated that such annihilation contributions are responsible for the large relative phase between the "penguin" and "tree" amplitudes extracted from non-leptonic data. We show, using recent results on mode factorization in quantum field theory [124], that the leading annihilation amplitude is real with a magnitude of $\sim 15\%$ of the observed penguin amplitude. The origin of the large phase has yet to be determined, but our results eliminate one of the suggested SM explanations.

In Chapter 5, the theoretical tools of complex analysis and QCD dispersion are the basis for a model-independent method for determining $|V_{ub}|$ based on the exclusive mode $B \to \pi\ell\bar{\nu}$. The current best estimate of $|V_{ub}|$ (with 5% uncertainty) assumes CKM unitarity and infers the SM flavor parameters from a global fit to unitarity tri-

angle measurements [55]. The best direct measurement (quoted with 7% uncertainty in a world average by the Heavy Flavor Averaging Group [91]) uses the inclusive rate $B \to X_u \ell \nu$. These two estimates differ from each other, however, by more than a combined 2σ, and our method provides an important complementary determination. Previous estimates of $|V_{ub}|$ from $B \to \pi \ell \bar{\nu}$ used experimental data from only the largest q^2 bin (leptonic invariant mass squared $\geq 16\text{GeV}^2$), where lattice QCD gives information on the relevant $B \to \pi$ form factor f_+. Alternatively they relied on light-cone sum rules or models to extrapolate to low q^2. Our analysis expands f_+ as a power series in a kinematic variable whose magnitude is small ($< .35$) in the physical region, and uses a dispersion relation to put a QCD-derived bound on the size of the coefficients (see Boyd and Savage [51], for example). $|V_{ub}|$ and the series coefficients enter as the free parameters in a χ^2 minimization. The fit contains information about the form factor from unquenched lattice QCD and heavy-hadron chiral perturbation theory, experimental data on the decay rate (total and binned), and the product of $|V_{ub}|$ and f_+ at $q^2 = 0$ derived from SCET and $B \to \pi\pi$ data. The dispersive bound limits the shape of the form factor between input points and allows us to calculate the error associated with our choice of functional form (model-dependence), which we find to be negligible. The dominant part of our 13% uncertainty comes from lattice inputs, and the method will compete with the current best estimates as the lattice data improves.

Concluding remarks are given in Chapter 6.

Chapter 2

Theory

This chapter reviews the quantum field theories used to calculate B-meson decay rates in this thesis.

2.1 The Standard Model

We calculate theoretical expectations for physical processes using the Standard Model of particle physics, a local quantum field theory containing all known fundamental particles and their strong, weak, and electromagnetic interactions.[1] The matter field content is a scalar Higgs doublet and three families of spin-1/2 fermion fields. Interactions by vector boson exchange follow from imposing a local non-abelian gauge invariance on the matter field Lagrangian. The gauge group of the Standard Model is $SU(3)_{\text{Color}}$ for the strong interactions times $SU(2)_{\text{Left}} \times U(1)_{\text{Hypercharge}}$ for the unified electroweak interactions. Electroweak gauge symmetry is spontaneously broken to U(1)-electromagnetic by the vacuum expectation value (VEV) of the Higgs doublet. Expanding the Higgs field about its VEV gives mass terms to the weak gauge bosons and charged fermions. The photon, gluon, and neutrinos remain massless.

We work in a basis of flavor eigenstate fields where the fermion mass matrices are diagonal. In this basis, the massive weak bosons, W and Z, couple to fermions

[1] The Standard Model is, by now, standard material, and as such we will generally omit citations. See Peskin and Schroeder [128] for a more thorough introduction and additional references.

through a term in the Lagrangian density

$$\Delta\mathcal{L} = g_2(W^+_\mu J^{\mu+}_W + W^-_\mu J^{\mu-}_W + Z_\mu J^\mu_Z) \tag{2.1}$$

where g_2 is the $\mathrm{SU(2)_L}$ gauge coupling, and the fermion currents are described below. The charged current is

$$J^{\mu+}_W = \frac{1}{\sqrt{2}}(\bar{\nu}^\ell_L \gamma^\mu \ell_L + \bar{q}^f_L \gamma^\mu V_{ff'} q^{f'}_L) \tag{2.2}$$

where the lepton flavor index takes on values $\ell \in \{e, \mu, \tau\}$, and the quark current turns a down-type quark $f' \in \{d(\text{own}), s(\text{trange}), b(\text{ottom})\}$ into an up-type quark $f \in \{u(\text{p}), c(\text{harm}), t(\text{op})\}$. Only left-handed fermion fields $\psi_L = P_L\psi$ where $P_{R,L} = (1 \pm \gamma^5)/2$ participate in the weak interactions. The unitary Cabibbo-Kobayashi-Maskawa (CKM) matrix [105]

$$V = \begin{pmatrix} V_{ud} & V_{us} & V_{ub} \\ V_{cd} & V_{cs} & V_{cb} \\ V_{td} & V_{ts} & V_{tb} \end{pmatrix} \tag{2.3}$$

relates the quark mass eigenstates to the quark weak interaction eigenstates. The unitarity condition

$$V^*_{uf} V_{ub} + V^*_{cf} V_{cb} + V^*_{tf} V_{tb} = 0 \qquad f \in \{d, s\} \tag{2.4}$$

is often expressed geometrically for b to d transitions as the unitarity triangle (Figure 2-1). Alternatively, V can be parametrized explicitly as a unitary matrix. Quark field phase redefinitions reduce to four the number of independent real numbers necessary for such a parametrization. One convention [56] has angles $\theta_{12}, \theta_{13}, \theta_{23}$, and δ with

$$V = \begin{pmatrix} c_{12}c_{13} & s_{12}c_{13} & s_{13}e^{-i\delta} \\ -s_{12}c_{23} - c_{12}s_{23}s_{13}e^{i\delta} & c_{12}c_{23} - s_{12}s_{23}s_{13}e^{i\delta} & s_{23}c_{13} \\ s_{12}s_{23} - c_{12}c_{23}s_{13}e^{i\delta} & -c_{12}s_{23} - s_{12}c_{23}s_{13}e^{i\delta} & c_{23}c_{13} \end{pmatrix} \tag{2.5}$$

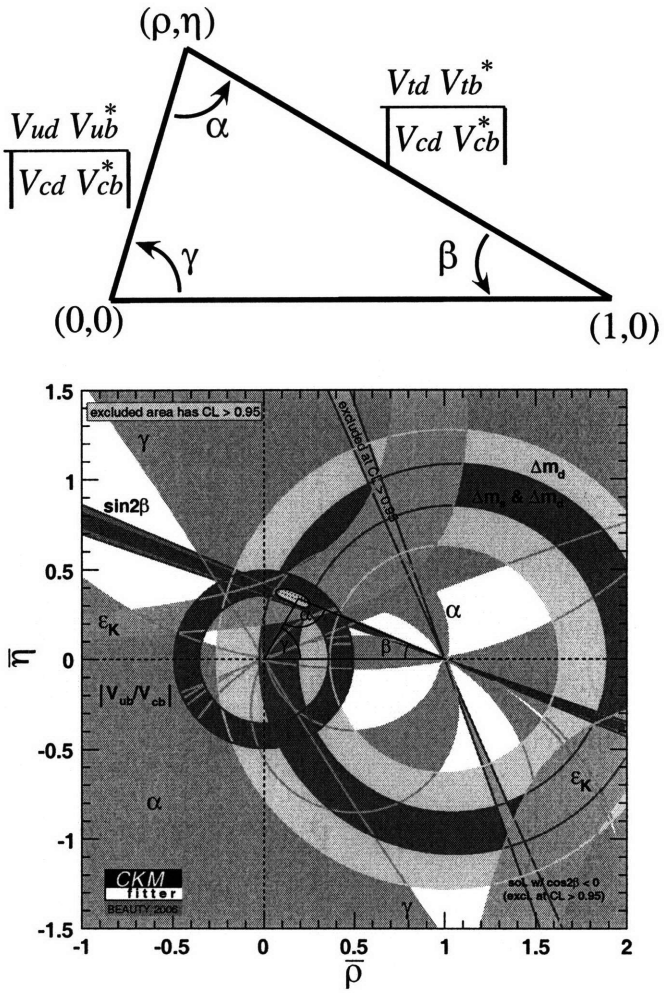

Figure 2-1: The unitarity triangle is obtained by dividing both sides of Eq. (2.4) with $f = d$ by the absolute value of $V_{cd}V_{cb}^*$, which is chosen to be real by phase convention. The colored regions are experimental constraints from a variety of sources. Plot by CKMfitter group [55].

where $c_{ij} = \cos\theta_{ij}$ and $s_{ij} = \sin\theta_{ij}$. The complex phase δ is the sole source of CP-violation in the Standard Model.[2]

The entries of the CKM matrix are free parameters in the Standard Model whose values must be determined through observation of flavor-changing processes. Chapter 5 of this thesis presents a method for determining $|V_{ub}|$ based on $B \to \pi\ell\bar{\nu}$. Experiment has revealed a hierarchy in the components of V that is conveniently illustrated by using Wolfenstein parameters (λ, A, ρ, η) [138]. In terms of the parametrization Eq. (2.5), define $s_{12} = \lambda$, $s_{23} = A\lambda^2$, and $s_{13}e^{-i\delta} = A\lambda^3(\rho - i\eta)$, then

$$V = \begin{pmatrix} 1 - \lambda^2/2 & \lambda & A\lambda^3(\rho - i\eta) \\ -\lambda & 1 - \lambda^2/2 & A\lambda^2 \\ A\lambda^3(1 - \rho - i\eta) & -A\lambda^2 & 1 \end{pmatrix} + \mathcal{O}(\lambda^4) \tag{2.6}$$

where $\lambda \approx |V_{us}| \approx 0.22$.

The hierarchy is important to keep in mind in our Standard Model calculations. For example, in Chapter 4 we consider B decays to two light mesons, M_1, M_2. We use the unitarity condition Eq. (2.4) to write the decay amplitude as a sum of two terms, each with a different product of CKM factors,

$$A(\bar{B} \to M_1 M_2) = V_{ub}V_{uf}^* T + V_{cb}V_{cf}^* P\,, \tag{2.7}$$

where $f \in \{d, s\}$, T is called the "tree" amplitude for the decay, and P is the "penguin" amplitude, (not to be confused with tree and penguin *diagrams* as described in Figure 2-3). $f = d$ for $\Delta S = 0$ and the weak prefactors are comparable in size. For $\Delta S = 1$ decays with $f = s$, the tree prefactor is λ^2-"Cabbibo suppressed" relative to the penguin weak coupling prefactor. The two terms in Eq. (2.7) could be comparable, giving large interference effects or the penguin could even dominate. Classification of B decays based on the weak structure is discussed at length in the BaBar Physics Handbook [93].

[2]Another possible source of CP-violation, the "θ" term $\mathcal{L}_\theta \propto \epsilon^{\mu\nu\rho\sigma} G^a_{\mu\nu} G^a_{\rho\sigma}$ where G is a gluon field strength tensor, has been shown to be negligible by the absence of a neutron electric dipole moment.

In the basis of flavor eigenstates, the neutral current in Eq.(2.1) has a somewhat lengthy expression. The most important feature of interactions between the Z boson and fermions is that they are flavor diagonal. In other words, the Standard Model has no flavor-changing neutral currents at tree level. For illustration, we give the expression for J_Z for first-family fermions, e, ν_e, u, d,

$$\begin{aligned} J_Z^\mu = \frac{1}{\cos\theta_W}\Big[&\bar{\nu}_L^e\gamma^\mu\big(\tfrac{1}{2}\big)\nu_L^e + \bar{e}_L\gamma^\mu\big(-\tfrac{1}{2}+\sin^2\theta_W\big)e_L + \bar{e}_R\gamma^\mu\big(\sin^2\theta_W\big)e_R + \\ &\bar{u}_L\gamma^\mu\big(\tfrac{1}{2}-\tfrac{2}{3}\sin^2\theta_W\big)u_L + \bar{u}_R\gamma^\mu\big(-\tfrac{2}{3}\sin^2\theta_W\big)u_R + \\ &\bar{d}_L\gamma^\mu\big(-\tfrac{1}{2}+\tfrac{1}{3}\sin^2\theta_W\big)d_L + \bar{d}_R\gamma^\mu\big(\tfrac{1}{3}\sin^2\theta_W\big)d_R\Big], \end{aligned} \tag{2.8}$$

where the weak mixing angle θ_W relates the two neutral $SU(2) \times U(1)$ weak boson fields to the Z and photon fields. Z exchange and photon exchange contribute to B decays in electroweak penguin operators as described below and as shown in Figure 2-3.

Strong interaction effects described by quantum chromodynamics (QCD) pose the most significant challenge to making quantitative predictions with the Standard Model. The QCD Lagrangian is

$$\mathcal{L}_{\rm QCD} = \sum_{f=u,d,s,c,b,t} \bar{q}^f(i\not{D} - m_f)q^f - \frac{1}{4}G^2, \tag{2.9}$$

with covariant derivative $iD^\mu = i\partial^\mu + g_sA^\mu$ and field strength tensor $[D^\mu, D^\nu] = ig_sG^{\mu\nu}$ where g_s is the $\mathrm{SU(3)_{Color}}$ gauge coupling. Spinor and color indices have been suppressed in Eq. (2.9). For example, the gauge field is a 3×3 matrix in color space, $A_\mu = A_\mu^a T^a$ where $\{T^a\}$ are eight 3×3 generators of $\mathrm{SU(3)_{Color}}$ normalized $\mathrm{Tr}\,[T^aT^b] = \delta^{ab}/2$. Similarly $G_{\mu\nu} = G_{\mu\nu}^a T^a$.

In addition to the Lagrangian, physical predictions require a regularization and renormalization scheme, which invariably introduces a dimensionful scale parameter μ. The renormalized couplings and mass parameters depend on μ, which can be thought of as the energy at which the theory is defined. QCD is "asymptotically free": $g_s(\mu)$ tends asymptotically to 0 as μ goes to infinity. Conversely, as μ is low-

ered to a scale $\mu \sim \Lambda_{\rm QCD} \approx 300$MeV, QCD becomes strongly coupled $g_s(\Lambda_{\rm QCD}) \sim 1$, and a perturbative expansion in $\alpha_s = g_s^2/(4\pi)$ is no longer justified. Typically, the most convenient scheme is dimensional regularization with modified minimal subtraction $\overline{\rm MS}$. It is gauge invariant and it simplifies calculations. Because $\overline{\rm MS}$ is a mass-independent scheme, heavy particles do not automatically decouple from low-energy processes such as B decays. Instead they are removed by hand by a matching procedure described in the next section. It is useful to think about μ in this context as the *resolution* of the theory. The W-boson in b-quark decay has typical virtuality m_W^2, and only propagates over a short distance $\sim m_W^{-1}$. Our theory at a scale $\mu \sim m_b$ appropriate for b-quark decays cannot resolve this propagation; the effects of W exchange are reproduced by local operators in an effective theory in which particles with mass greater than m_b have been integrated out.

2.2 Weak effective Hamiltonian

To calculate B decays with the Standard Model, the full theory is *matched* at the electroweak scale $\mu \sim m_W$ onto a quantum field theory without the W, Z, and t. The infrared (in this case low-mass) degrees of freedom and regulators must be the same in both theories. The effects of the heavy particles are reproduced by a set of local operators called the weak effective Hamiltonian and denoted H_W. The coupling constants of the operators, called Wilson coefficients, are chosen such that transition matrix elements give the same result in both theories when expanded in the strong coupling and the ratio of low-energy kinematic invariants to the heavy particle mass. For applications in B decays considered in this thesis, only the leading $\Delta B = 1$ flavor-changing operators in the $1/m_W^2$ expansion are needed. For these, H_W is of the form

$$H_W = \frac{G_F}{\sqrt{2}} \sum_i V_i^{\rm CKM} C_i(\mu) O_i(\mu) \tag{2.10}$$

where $G_F = g_2^2/(4\sqrt{2}m_W^2)$, $V_i^{\rm CKM}$ contains CKM matrix factors, $\{O_i\}$ are a complete set of mass-dimension-6 operators and C_i are their Wilson coefficients, which depend

on the dimensional regularization scale parameter μ.

The matching procedure defines the C_i's at $\mu \sim m_W$ as a expansion in $\alpha_s(m_W)$. Since the infrared structure is the same in both theories by construction, the renormalized Wilson coefficients encode strong interactions at the electroweak scale. Physics below m_W is still described by propagating fields and their interactions. To lower μ to a scale appropriate for b decay, we use renormalization group equations derived as follows. The renormalized operators $O(\mu)$ are related to bare operators $O^{(0)}$ constructed from bare fields by a renormalization matrix Z

$$O_i^{(0)} = Z_{ij} O_j \,. \tag{2.11}$$

Z is chosen to remove UV poles at $d = 4$ in Green's functions with an insertion of O. (Operator renormalization is conventional for H_W, but alternatively we could introduce bare and renormalized couplings, $C^{(0)} = Z_C C$, as is conventional for Lagrangian terms). Neither the bare operators nor H_W depend on the renormalization scale. From this it is straightforward to derive a renormalization group equation governing the μ dependence of the Wilson coefficients,

$$\mu \frac{\mathrm{d}}{\mathrm{d}\mu} C_i = \gamma_{ji} C_j \,, \tag{2.12}$$

where

$$\gamma_{ji} = Z^{-1}_{jk} \Big(\mu \frac{\mathrm{d}}{\mathrm{d}\mu} Z_{ki} \Big) \tag{2.13}$$

is called the anomalous dimension matrix. The RGE is used to evolve from $\mu \sim m_W$ to $\mu \sim m_b$, effectively resumming the large logs that appear in "naive" perturbation theory. After matching and running, the Wilson coefficients C_i encapsulate QCD effects above m_b, while the remaining long-distance physics is described by EFT dynamics, *i.e.* propagating fields and their Lagrangian and Hamiltonian interactions.

For the semi-leptonic decay $\bar{B}^0 \to \pi^+ \ell \bar{\nu}$ considered in Chapter 5, just one operator

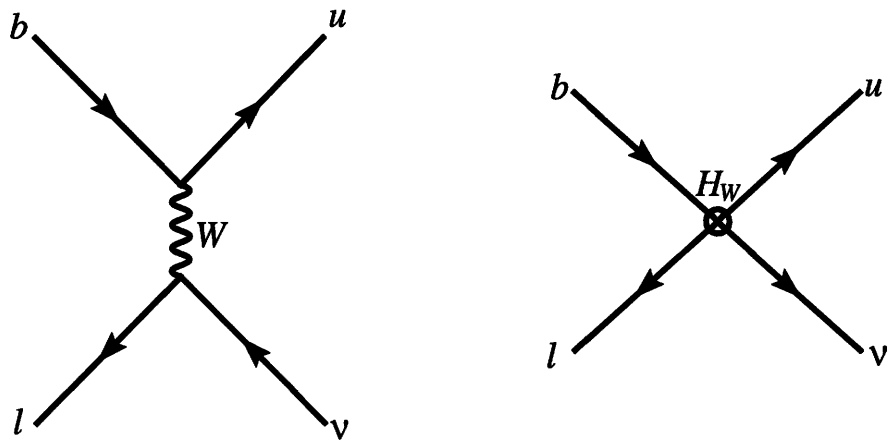

Figure 2-2: Tree-level matching diagrams for H_W for $b \to u\ell\bar{\nu}$. Left: full-theory. Right: weak effective Hamiltonian insertion.

is relevant in the Standard Model calculation,

$$H_W = \frac{4G_F}{\sqrt{2}} V_{ub} (\bar{u}_L \gamma_\mu b_L)(\bar{\ell}_L \gamma^\mu \nu_L) \,. \tag{2.14}$$

This operator also mediates the *inclusive* semi-leptonic decay $B \to X_u \ell\bar{\nu}$. The quark-field bilinear $\bar{u}\gamma_\mu b$ is an example of a heavy-to-light current whose soft-collinear effective theory representatives are discussed at length in Chapter 3. The tree-level diagrams for the perturbative matching onto Eq. (2.14) are shown in Figure 2-2. With the prefactors as in Eq. (2.14), the Wilson coefficient is unity at tree level. In massless QCD, $\bar{u}\gamma^\mu P_L b$ is a conserved current of a quark flavor symmetry. This means that with our mass-independent renormalization scheme, this operator is not renormalized by radiative corrections. The Wilson coefficient is scale independent, unity to all orders in perturbation theory.

For other processes, the weak effective Hamiltonian is more complicated. For uncharmed non-leptonic B decays considered in Chapter 4, there are $\Delta S = 0$ terms for $b \to d q_1 \bar{q}_2$ transitions and $\Delta S = 1$ terms for $b \to s q_1 \bar{q}_2$. For $\Delta S = 0$ it reads

$$H_W = \frac{G_F}{\sqrt{2}} \sum_{p=u,c} V_{pb} V_{pd}^* \Big(C_1 O_1^p + C_2 O_2^p + \sum_{i=3}^{10,7\gamma,8g} C_i O_i \Big), \tag{2.15}$$

where the operators we will need are

$$
\begin{aligned}
O_1^u &= (\bar{u}b)_{V-A}\,(\bar{d}u)_{V-A}, & O_2^u &= (\bar{u}_\beta b_\alpha)_{V-A}\,(\bar{d}_\alpha u_\beta)_{V-A}\,,\\
O_1^c &= (\bar{c}b)_{V-A}\,(\bar{d}c)_{V-A}, & O_2^c &= (\bar{c}_\beta b_\alpha)_{V-A}\,(\bar{d}_\alpha c_\beta)_{V-A}\,,\\
O_3 &= \textstyle\sum_{q'}(\bar{d}b)_{V-A}\,(\bar{q}'q')_{V-A}\,, & O_4 &= \textstyle\sum_{q'}(\bar{d}_\beta b_\alpha)_{V-A}\,(\bar{q}'_\alpha q'_\beta)_{V-A}\,,\\
O_5 &= \textstyle\sum_{q'}(\bar{d}b)_{V-A}\,(\bar{q}'q')_{V+A}\,, & O_6 &= \textstyle\sum_{q'}(\bar{d}_\beta b_\alpha)_{V-A}\,(\bar{q}'_\alpha q'_\beta)_{V+A}\,,\\
O_7 &= \textstyle\sum_{q'}\frac{3e_{q'}}{2}\,(\bar{d}b)_{V-A}\,(\bar{q}'q')_{V+A}\,, & O_8 &= \textstyle\sum_{q'}\frac{3e_{q'}}{2}\,(\bar{d}_\beta b_\alpha)_{V-A}\,(\bar{q}'_\alpha q'_\beta)_{V+A}\,,\\
O_9 &= \textstyle\sum_{q'}\frac{3e_{q'}}{2}\,(\bar{d}b)_{V-A}\,(\bar{q}'q')_{V-A}\,, & O_{10} &= \textstyle\sum_{q'}\frac{3e_{q'}}{2}\,(\bar{d}_\beta b_\alpha)_{V-A}\,(\bar{q}'_\alpha q'_\beta)_{V-A}\,,\\
O_{7\gamma} &= -\frac{e}{8\pi^2}\,m_b\,\bar{d}\,\sigma^{\mu\nu}F_{\mu\nu}(1+\gamma_5)b\,, & O_{8g} &= -\frac{g}{8\pi^2}\,m_b\,\bar{d}\,\sigma^{\mu\nu}G^a_{\mu\nu}T^a(1+\gamma_5)b\,.
\end{aligned}
\tag{2.16}
$$

The subscripts $V \pm A$ indicate the Dirac structure $\gamma^\mu(1 \pm \gamma^5) = 2\gamma^\mu P_{R,L}$. α and β are color indices. The quark bilinear $\bar{d}\sigma^{\mu\nu}b$ in $O_{7\gamma,8g}$ is another example of a heavy-to-light current considered in Chapter 3. Standard Model diagrams that match onto operators in Eq. (2.16) are shown in Figure 2-3. Here $O^u_{1,2}$ and $O^c_{1,2}$ are current-current operators, O_{3-6} are strong penguin operators and O_{7-10} are electroweak penguin operators, with a sum over flavors $q' = u, d, s, c, b$, and electric charges $e_{q'}$. Results for $\Delta S = 1$ transitions are obtained by replacing $d \to s$ in Eqs. (2.15) and (2.16). The coefficients in Eq. (2.15) are known at next-to-leading-log order [53] (we have $O_1^p \leftrightarrow O_2^p$ relative to [53]). In the naive dimensional regularization (NDR) scheme ($\{\gamma^\mu, \gamma^5\} = 0$), taking $\alpha_s(m_Z) = 0.118$ and $m_b = 4.8\,\text{GeV}$, the Wilson coefficients of the operators in Eq. (2.16) are

$$
\begin{aligned}
C_{1-6}(m_b) &= \{1.080\,,\ -0.177\,,\ 0.011\,,\ -0.033\,,\ 0.010\,,\ -0.040\}\\
C_{7-10}(m_b) &= \{4.9\times10^{-4}\,,\ 4.6\times10^{-4}\,,\ -9.8\times10^{-3}\,,\ 1.9\times10^{-3}\}\\
C_{7\gamma,8g}(m_b) &= \{-0.299\,,\ -0.143\}\,.
\end{aligned}
\tag{2.17}
$$

The hierarchy in the magnitudes of these Wilson cefficients is important for phenomenological analyses. We will not attempt, however, to distinguish them parametrically (*i.e.* we count $C_i \sim 1$).

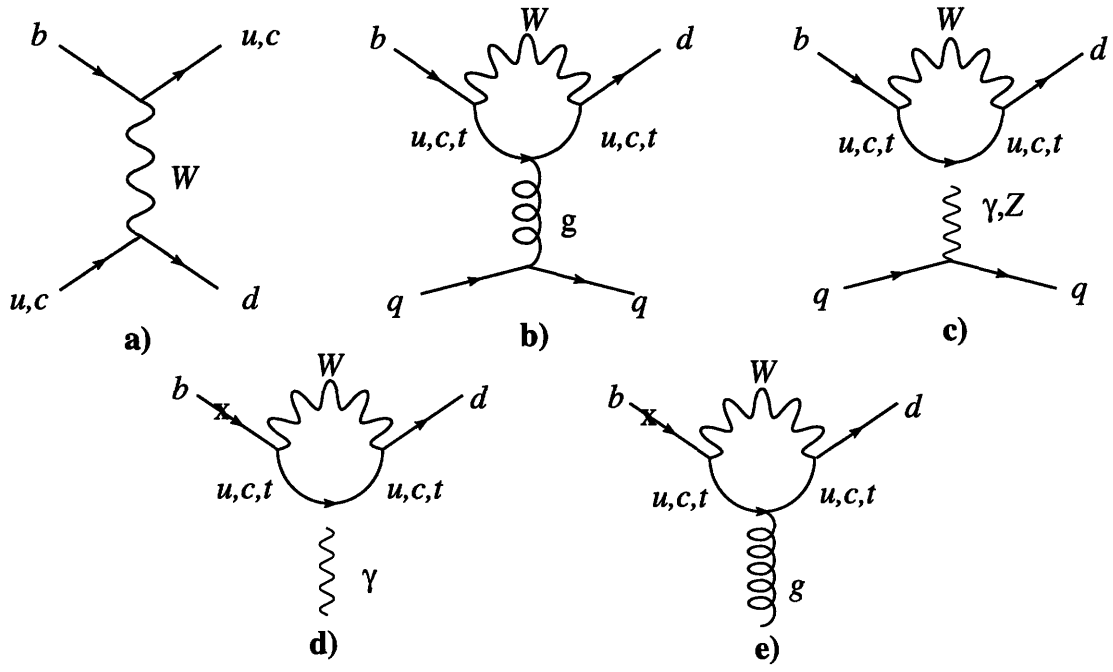

Figure 2-3: Standard Model diagrams contributing to H_W operators in Eq. (2.15). a) Current-current. b) QCD penguin. c) Electroweak penguin. d) Electromagnetic penguin. e) Chromomagnetic penguin. In c) and d), the "$\gamma, (Z)$" attaches to either particle in the loop. In d) and e), "x" is a b-quark mass insertion required to reproduce the chiral structure of the magnetic operators.

Having separated the scales m_W and m_b by matching and running the electroweak Hamiltonian, we turn our attention to the effective theories used to disentangle strong interaction effects at and below m_b.

2.3 Heavy-quark effective theory

In this section we describe the infrared non-perturbative degrees of freedom of a B meson containing a b quark,[3] and their appropriate EFT, the heavy-quark effective theory (HQET) [86, 84, 76]. (See Manohar and Wise [125] for a pedagogical introduction.) This theory separates $m_{b,c}$ from physics at the hadronic/non-perturbative scale $\Lambda \sim \Lambda_{\rm QCD}$ by expanding in inverse powers of the heavy quark masses.

In the B's rest frame, the light constituents – gluons and u, d, s quarks and anti-

[3]This discussion is valid (with obvious substitutions) for any hadron containing a single heavy quark or anti-quark.

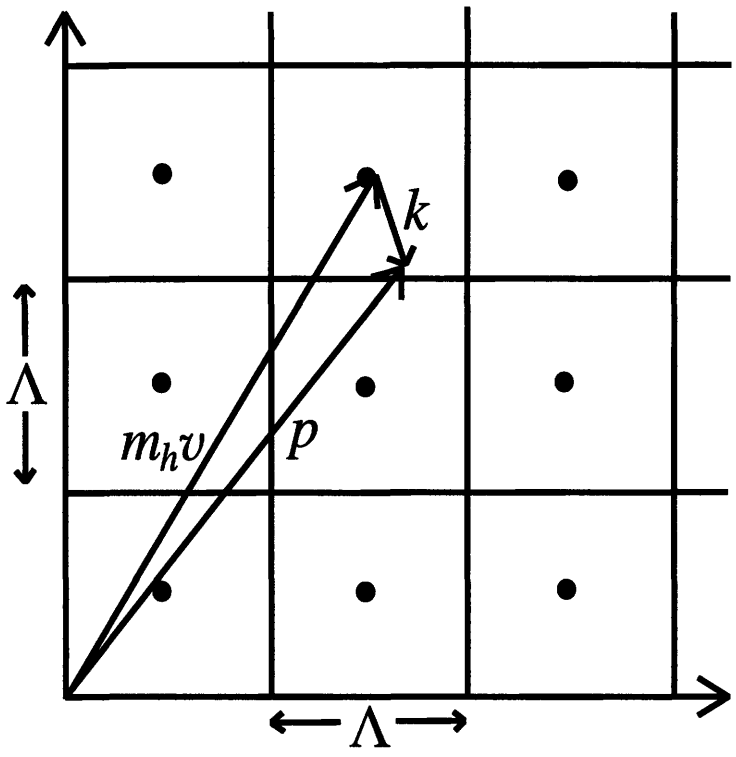

Figure 2-4: Momentum space tiling for HQET.

quarks – have typical momentum components on the order of the non-perturbative scale Λ. The b quark acts as a static color source for this light "brown muck". While the b's momentum changes by $\Delta p \sim \Lambda$ in interactions with the light degrees of freedom, its velocity is unchanged, $\Delta v = \Delta p / m_b \to 0$ in the heavy quark limit $m_b \to \infty$. The anti-quark components present in the full-theory b field should not be included as a dynamical degree of freedom in our low-energy theory of the B since it takes an energy $\sim 2m_b$ to pair produce $b\bar{b}$.

This physical description is formalized by HQET. Let $h(x)$ be the full-theory heavy-quark field for which we wish to derive a low-energy EFT. $h(x)$ both annihilates a heavy quark and creates a heavy anti-quark, with a rapidly varying phase due to the large mass m_h. If we were using a momentum-space-cutoff regulator, h would have momentum-space support over all momenta up to a scale $\Lambda_{\text{cut}} \sim m_h$. To define the EFT, we tile momentum space as in Figure 2-4. Each momentum p is decomposed

into a large and a small piece as

$$p = m_h v + k \tag{2.18}$$

where v is a time-like four-vector with $v^2 = 1$ that labels which box p lies in while $k \sim \Lambda$ indicates the position of p within the box. Similary we decompose $h(x)$ into a sum of fields labeled by the velocity v

$$h(x) = \sum_v e^{-im_h v\cdot x}\left[h_v(x) + \mathfrak{h}_v(x)\right]. \tag{2.19}$$

The labeled fields should be thought of as only having support for momenta $k \lesssim \Lambda$. (Strictly speaking, they have support over all momenta since we do not use cutoff regulators. An EFT, properly defined, however, is regulator-independent. Contributions from the region $k \gtrsim \Lambda$ are removed by renormalization.) The exponential prefactor removes the large momentum $m_h v$. The field h_v satisfies a projection relation $P_v h_v = h_v$ where $P_v = (1 + \not{v})/2$. In the h rest frame, $v = (1, 0, 0, 0)$ and $(1 + \gamma^0)/2$ projects onto the particle degrees of freedom of h. The other labeled field $\mathfrak{h}$ satisfies $P_{-v}\mathfrak{h}_v = \mathfrak{h}_v$.

To obtain the HQET Lagrangian, we start by substituting Eq. (2.19) into the QCD heavy-quark Lagrangian,

$$\begin{aligned}\mathcal{L} &= \bar{h}(i\not{D} - m_h)h \\ &= \sum_v \bar{h}_v(iv\cdot D)h_v - \bar{\mathfrak{h}}_v(iv\cdot D + 2m_h)\mathfrak{h}_v + \bar{h}_v i\not{D}\mathfrak{h}_v + \bar{\mathfrak{h}}_v i\not{D}h_v\,.\end{aligned} \tag{2.20}$$

This has been simplified using the Dirac projection relations. The velocity superselection rule, that $\mathcal{L}$ does not link heavy quarks with different v's, resulted from taking the residual momenta in the labeled fields to scale like Λ. Then label and residual momentum are individually conserved,

$$\int \mathrm{d}^4x\; e^{im_h(v-v')\cdot x} e^{i(k-k')\cdot x} = \delta_{v,v'}\;(2\pi)^4\delta^4(k-k')\,. \tag{2.21}$$

In the Lagrangian Eq. (2.20), the field $\mathfrak{h}_v$ has mass $2m_h$ corresponding to heavy pair production, which need not be included as a dynamic freedom in our low-energy effective theory. Removing $\mathfrak{h}_v$ from Eq. (2.20) using its equation of motion

$$(iv \cdot D + 2m_h)\mathfrak{h}_v = i\not{D} h_v \tag{2.22}$$

is equivalent to integrating $\mathfrak{h}_v$ out at tree level. The result is

$$\mathcal{L}_{\text{HQET}} = \sum_{h=b,c} \sum_{v} \bar{h}_v iv \cdot D h_v + \mathcal{O}(\Lambda/m_h)\,. \tag{2.23}$$

The leading HQET Lagrangian Eq. (2.23) has an $SU(4)$ spin-flavor symmetry that reflects the physical picture of the heavy quark as a static color source for the light constituents of the hadron. This symmetry relates non-perturbative effects from otherwise distinct processes. The mesons B, B^*, D, D^* transform as a spin-flavor multiplet. Up to $1/m_h$ corrections, transition form factors between these mesons can be expressed in terms of a single *Isgur-Wise function* whose normalization is fixed at zero recoil [99]. This can be used to measure $|V_{cb}|$ from the heavy-to-heavy semi-leptonic decay $B \to D^* \ell \nu$. Departures from spin-flavor symmetry are calculable in the effective theory, but require the introduction of additional non-perturbative functions and parameters. In Chapter 5, we use a heavy-quark symmetry relationship between the $BB^*\pi$ and $DD^*\pi$ couplings in heavy-hadron chiral perturbation theory.

2.4 Soft-collinear effective theory I

Our theoretical description of B decays to energetic light hadrons or energetic hadronic jets involves additional partonic degrees of freedom beyond the hard modes of the QCD with $p \sim m_b$ and the soft non-perturbative modes of HQET with typical dynamical momenta $\sim \Lambda$. The constituents of an energetic hadronic state X with $E_X \gg m_X$ are *collinear* quarks and gluons. The relevant EFT is the soft-collinear effective theory [13, 15, 27, 22].

In the "endpoint region" of inclusive decays such as $B \to X_s\gamma$ and $B \to X_u\ell\bar{\nu}$, the hadronic state X has large energy, $E_X \sim Q$ where $Q \sim m_b$ is the "hard" scale, but moderate invariant mass, $m_X \sim \mu_I$ where $\mu_I \sim \sqrt{Q\Lambda}$ is the "intermediate" scale. The theory SCET_I that contains the relevant modes for such hadronic states is obtained from QCD by matching calculations at the hard scale. SCET_I separates the scales Q and $\sqrt{Q\Lambda}$ by expanding in a power-counting parameter $\lambda \sim m_X/E_X \sim \sqrt{\Lambda/Q} \ll 1$. For these decays, we can separate the intermediate scale from the hadronic scale Λ by matching SCET_I onto HQET.

For exclusive decays containing one or more energetic light hadrons, such as $B \to \pi\pi$ (Chapter 4), or $B \to \pi\ell\nu$ in its endpoint region (Chapter 5), the intermediate scale is again important, and SCET_I is used to separate Q and $\sqrt{Q\Lambda}$. In order to separate the hadronic scale in these processes, however, we need *non-perturbative* collinear modes, with $p^2 \sim \Lambda^2$, to interpolate for individual light mesons. These modes are part of an effective field theory SCET_II, described in section 2.5. SCET_II is obtained from SCET_I by matching calculations at the intermediate scale [23]. Therefore we begin with SCET_I.

2.4.1 Degrees of freedom and Lagrangian

Since collinear partons travel near the light-cone, it is convenient to decompose momenta using two light-like auxiliary vectors n and $\bar{n}$ normalized $n \cdot \bar{n} = 2$. Any four-momentum p can be expressed in terms of its light-cone components $(p^+, p^-, p_\perp) = (n \cdot p, \bar{n} \cdot p, p_\perp)$ as

$$p = \bar{n} \cdot p \frac{n}{2} + n \cdot p \frac{\bar{n}}{2} + p_\perp \,, \tag{2.24}$$

in terms of which, $p^2 = p^+p^- + p_\perp^2$. For large momentum in the $+z$ direction, the conventional choice for the auxiliary vectors is $n = (1, 0, 0, 1)$ and $\bar{n} = (1, 0, 0, -1)$. With this choice, boosts in the $+z$ direction simply give multiplicative factors

$$(p^+, p^-, p_\perp) \xrightarrow{\text{boost}} (e^{-\alpha}p^+, e^{\alpha}p^-, p_\perp) \,, \tag{2.25}$$

Type	$(p^+, p^-, p^\perp)$	Fields	Scaling
collinear	$Q(\lambda^2, 1, \lambda)$	$\xi_{n,p}$	λ
		$(A^+_{n,p}, A^-_{n,p}, A^\perp_{n,p})$	$(\lambda^2,1,\lambda)$
usoft	$Q(\lambda^2, \lambda^2, \lambda^2)$	q_{us}, h_v	λ^3
		A^μ_{us}	λ^2

Table 2.1: Power counting for $\mathrm{SCET_I}$ fields.

where α is the rapidity of the boost. n-collinear modes with $p^2 \sim Q^2\lambda^2$ can be thought of as full-theory modes with homogeneous momentum components $\sim Q\lambda$ boosted by $e^\alpha \sim Q/\lambda$ in the n direction. By definition, collinear momenta have light-cone components $(p_c^+, p_c^-, p_c^\perp) \sim Q(\lambda^2, 1, \lambda)$.

$\mathrm{SCET_I}$ contains collinear quarks, anti-quarks, and gluons. In deriving the weak effective Hamiltonian in section 2.2, it was straightforward to reproduce the infrared structure of the full theory, in that case the Standard Model; we simply used the same IR regulators in both theories and kept all particles with mass less than m_W. SCET is more subtle since we are integrating out off-shell modes of massless fields. A collinear parton can interact with an *ultrasoft* (usoft) parton with homogenous momentum components $p_{us} \sim Q\lambda^2$ without changing its virtuality by a parametric amount, and both collinear and usoft gluon modes are required to reproduce the infrared physics of QCD [13]. The field content of $\mathrm{SCET_I}$ is summarized in Table 2.1.

The construction of the collinear Lagrangian proceeds analogously to that of $\mathcal{L}_{\mathrm{HQET}}$. We start by tiling the momentum space of collinear particles as in Figure 2-5. Each momentum p is split into a large piece $\tilde{p} = \bar{n}\cdot\tilde{p}\, n/2 + \tilde{p}_\perp$ that indicates which tile p lies on, while the residual momentum k points to p's location within the tile. Again, it is impractical to use a cutoff regulator that would make this tiling exact. In any regulator, these statements are true in the sense that we assign power countings $\bar{n}\cdot\tilde{p} \sim Q\lambda^0$, $\tilde{p}_\perp \sim Q\lambda^1$, and $k \sim Q\lambda^2$. The large momentum $\tilde{p}$ gives a rapidly varying phase to the n-collinear quark field, $\psi_n(x)$. The large phase is $-i\tilde{p}\cdot x$ when $\psi_n(x)$ annihilates a particle, and $+i\tilde{p}\cdot x$ when it creates an anti-particle. We would like to express the collinear quark field $\psi_n(x)$ as a sum of labeled fields with the large phases removed. We do so as follows. Define a field $\psi^+_{n,p}(x)$ that annihilates

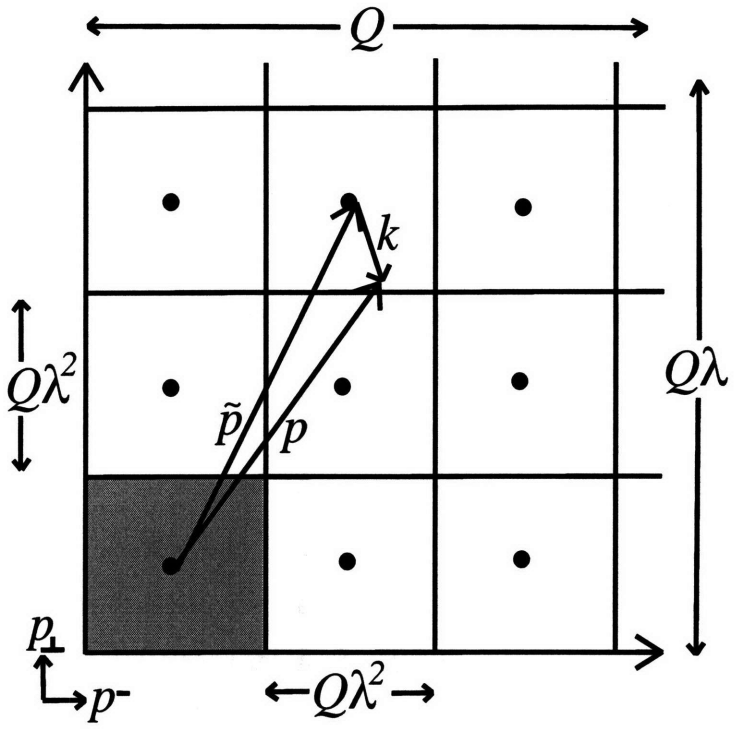

Figure 2-5: Tiling of collinear momentum space. $p = \tilde{p} + k$ where $\tilde{p} = \bar{n} \cdot \tilde{p} \frac{n}{2} + \tilde{p}_\perp$ is the large label momentum and $k \sim Q\lambda^2$ is the residual momentum.

a particle with large momentum $\bar{n} \cdot p$, and a field $\psi^-_{n,p}(x)$ that creates an anti-particle with large momentum $\bar{n} \cdot p$. (Note: These superscripts $\pm$ do *not* refer to light-cone components!) Both of these labeled fields have only residual momentum dependence $k \sim \Lambda = Q\lambda^2$ in their residual x dependence. The collinear quark field can be written as a sum,

$$\begin{aligned}
\psi_n(x) &= \sum_{\tilde{p}\neq 0} \left[e^{-i\tilde{p}\cdot x} \psi^+_{n,p} + e^{+i\tilde{p}\cdot x} \psi^-_{n,p} \right] \\
&= \sum_{\tilde{p}\neq 0} e^{-i\tilde{p}\cdot x} \left[\psi^+_{n,p} + \psi^-_{n,-p} \right] \\
&= \sum_{\tilde{p}\neq 0} e^{-i\tilde{p}\cdot x} \psi_{n,p} \,. \qquad (2.26)
\end{aligned}$$

For notational simplicity we omit the tilde in the subscript. From the definition Eq. (2.26), we see that when $\bar{n} \cdot p$ is positive, $\psi_{n,p}$ annihilates a particle with $\bar{n} \cdot p$ large and positive, and when $\bar{n} \cdot p$ is negative, $\psi_{n,p}$ creates an anti-particle with $-\bar{n} \cdot p$ large

and positive. In other words, when ψ_n interpolates for a final-state anti-quark moving in the $+n$ direction, it is the terms in the sum with *negative* $\bar{n}\cdot p$ that contribute. Similarly, the collinear gluon field is

$$A_n(x) = \sum_{\tilde{p}\neq 0} e^{-i\tilde{p}\cdot x} A_{n,p}(x)\,. \tag{2.27}$$

The hermiticity of $A_n = A_n^*$ implies $A_{n,p}^* = A_{n,-p}$.

The sums over collinear labels in Eqs. (2.26) and (2.27) exclude the "zero bin" $\tilde{p} = 0$, where the momentum is purely residual, since by definition a collinear field carries $(p_c^+, p_c^-, p_c^\perp) \sim Q(\lambda^2, 1, \lambda)$. Partons with homogeneous momentum components $\sim Q\lambda^2$ are included in the theory as a distinct degree of freedom, usoft fields, as mentioned above. The fact that collinear fields do not have support in the zero bin has far-reaching consequences in the effective theory [124]. Zero-bin subtractions motivated by the formula

$$\sum_{p\neq 0} = \sum_{p} - \sum_{p=0} \tag{2.28}$$

render finite seemingly divergent convolutions that appear in processes with exclusive light hadrons. The zero bin does not play a role in Chapters 3 and 5, but it is crucial for the analysis in Chapter 4. We will abstain from further discussion of the zero bin until Chapter 4.

The collinear quark field $\psi_{n,p}$ has two large ("good") components $\xi_{n,p} = P_n\psi_{n,p} \sim \lambda$ and two small ("bad") components $\zeta_{n,p} = P_{\bar{n}}\psi_{n,p} \sim \lambda^2$, where $P_n = \not{n}\bar{\not{n}}/4$ and $P_{\bar{n}} = \bar{\not{n}}\not{n}/4$ are rank-2 Dirac projection matrices with $P_n + P_{\bar{n}} = 1$. The two-component spinors satisfy

$$\begin{aligned} P_n\xi_{n,p} &= \xi_{n,p}\,, \qquad & \not{n}\xi_{n,p} &= 0\,, \\ P_{\bar{n}}\zeta_{n,p} &= \zeta_{n,p}\,, \qquad & \bar{\not{n}}\zeta_{n,p} &= 0\,. \end{aligned} \tag{2.29}$$

The λ scalings for fields are chosen to make their kinetic action, which determines their propagators, scale as $\mathcal{O}(\lambda^0)$. This moves the λ dependence of the action into interactions, and free propagation of fields counts as order unity. Since collinear fields

are equivalent to boosted, power-expanded, full-theory fields we can determine their scalings by examining the full-theory two-point functions. For the quark field,

$$\int \mathrm{d}^4x\, e^{ip\cdot x}\langle 0|T\ \psi_n(x)\bar{\psi}_n(0)|0\rangle = \frac{i\not{p}}{p^2+i\epsilon}\,, \tag{2.30}$$

where T stands for time ordering. We find $\xi_{n,p} \sim \lambda$ and $\zeta_{n,p} \sim \lambda^2$ by projecting Eq. (2.30) using Eq. (2.29), taking p and x to be collinear (*e.g.* $\mathrm{d}^4x_c \sim (Q\lambda)^{-4}$ and $p_c^2 \sim Q^2\lambda^2$), and equating powers of λ on both sides. The two-point function for the gluon field in a generalized covariant (Lorentz) gauge,

$$\int \mathrm{d}^4x\, e^{ip\cdot x}\langle 0|T\ A_n^\mu(x)\bar{A}_n^\nu(0)|0\rangle = \frac{-i}{p^2}\Big(g^{\mu\nu} - \alpha\frac{p^\mu p^\nu}{p^2}\Big)\,, \tag{2.31}$$

indicates that the light-cone components of A_n scale like collinear momenta, $(A_n^+, A_n^-, A_n^\perp) \sim Q(\lambda^2, 1, \lambda)$. The other field scalings in Table 2.1 follow from a similar line of reasoning.

Inserting Eq. (2.26) into the massless QCD quark Lagrangian,[4]

$$\begin{aligned}\mathcal{L} &= \bar{\psi} i\not{D}\psi \\ &= \sum_{\tilde{p},\tilde{p}'} e^{-i(\tilde{p}-\tilde{p}')}\Big[\bar{\xi}_{n,p'}\frac{\not{\bar{n}}}{2}(in\cdot D)\xi_{n,p} + \bar{\zeta}_{n,p'}\frac{\not{n}}{2}(\bar{n}\cdot p + i\bar{n}\cdot D)\zeta_{n,p} \\ &\qquad + \bar{\xi}_{n,p'}(\not{p}_\perp + i\not{D}_\perp)\zeta_{n,p} + \bar{\zeta}_{n,p'}(\not{p}_\perp + i\not{D}_\perp)\xi_{n,p}\Big]\,.\end{aligned} \tag{2.32}$$

This has been simplified using Eq. (2.29). When integrated over all space-time to obtain the action, the large phase factors in $\mathcal{L}$ simply enforce conservation of label momentum. From now on, where there is no chance for confusion we will omit these factors and conserve label momentum as a rule. The small spinor components $\zeta_{n,p}$ can be integrated out at tree level using their equation of motion

$$0 = \frac{\delta\mathcal{L}}{\delta\bar{\eta}_{n,p'}} = \frac{\not{n}}{2}(\bar{n}\cdot p + i\bar{n}\cdot D)\zeta_{n,p} + (\not{p}_\perp + i\not{D}_\perp)\xi_{n,p}\,. \tag{2.33}$$

[4]Light-quark mass effects can be taken into account in SCET [112], but are not considered in this thesis.

giving

$$\mathcal{L} = \sum_{\tilde{p},\tilde{p}'} \bar{\xi}_{n,p'} \Big[in\cdot D + (\not{p}_\perp + i\not{D}_\perp) \frac{1}{\bar{n}\cdot p + i\bar{n}\cdot D} (\not{p}_\perp + i\not{D}_\perp) \Big] \frac{\not{\bar{n}}}{2} \xi_{n,p} \,. \tag{2.34}$$

The covariant derivative D contains both collinear and usoft gluon fields.

The leading-order Lagrangian is obtained by expanding Eq. (2.34) in λ. This expression, and many others in SCET, are greatly simplified by the introduction of a collinear *label operator* $\mathcal{P}^\mu = \bar{\mathcal{P}}\, n^\mu/2 + \mathcal{P}_\perp^\mu$ [27]. $\mathcal{P}$ acts to the right and gives the sum of collinear label momenta of fields minus the sum of the collinear label momenta of conjugate fields (such as $\bar{\psi}_{n,p}$ and $A^*_{n,p}$). $\mathcal{P}^\dagger$ acts to the left and gives *minus* the sum of collinear label momenta of fields *plus* the sum of the collinear label momenta of conjugate fields. For example,

$$\bar{\mathcal{P}}\, \bar{\xi}_{n,p'} A_{n,q} \xi_{n,p} = \big[\bar{n}\cdot(-p'+q+p)\big] \bar{\xi}_{n,p'} A_{n,q} \xi_{n,p} = -\bar{\xi}_{n,p'} A_{n,q} \xi_{n,p}\, \bar{\mathcal{P}}^\dagger \,. \tag{2.35}$$

Expanding Eq. (2.34) and making use of the label operator notation, the leading-order collinear quark Lagrangian is

$$\mathcal{L}^{(0)}_{\xi\xi} = \bar{\xi}_n \Big[in\cdot D_c + \not{D}_c^\perp \frac{1}{i\bar{n}\cdot D_c} i\not{D}_c^\perp \Big] \frac{\not{\bar{n}}}{2} \xi_n \,. \tag{2.36}$$

where $\xi_n = \sum_p \exp(-ip\cdot x)\xi_{n,p}$. The covariant derivative iD_c in Eq. (2.36) has light-cone components

$$\begin{aligned} in\cdot D_c &= in\cdot\partial + g\, n\cdot A_n + g\, n\cdot A_{us} \\ iD_c^\perp &= \mathcal{P}^\perp + g\, A_n^\perp \\ i\bar{n}\cdot D_c &= i\bar{n}\cdot\mathcal{P} + g\,\bar{n}\cdot A_n \,. \end{aligned} \tag{2.37}$$

It is given the subscript c because, acting on collinear fields, its components scale like those of a collinear momentum.[5] Power counting dictates that $n\cdot A_{us}$ and $n\cdot$

[5]Many different covariant derivatives appear in the SCET literature. The definition for $in\cdot D_c$ in Eq. (2.37) is not standard, but its advantage should become clear in section 2.4.2.

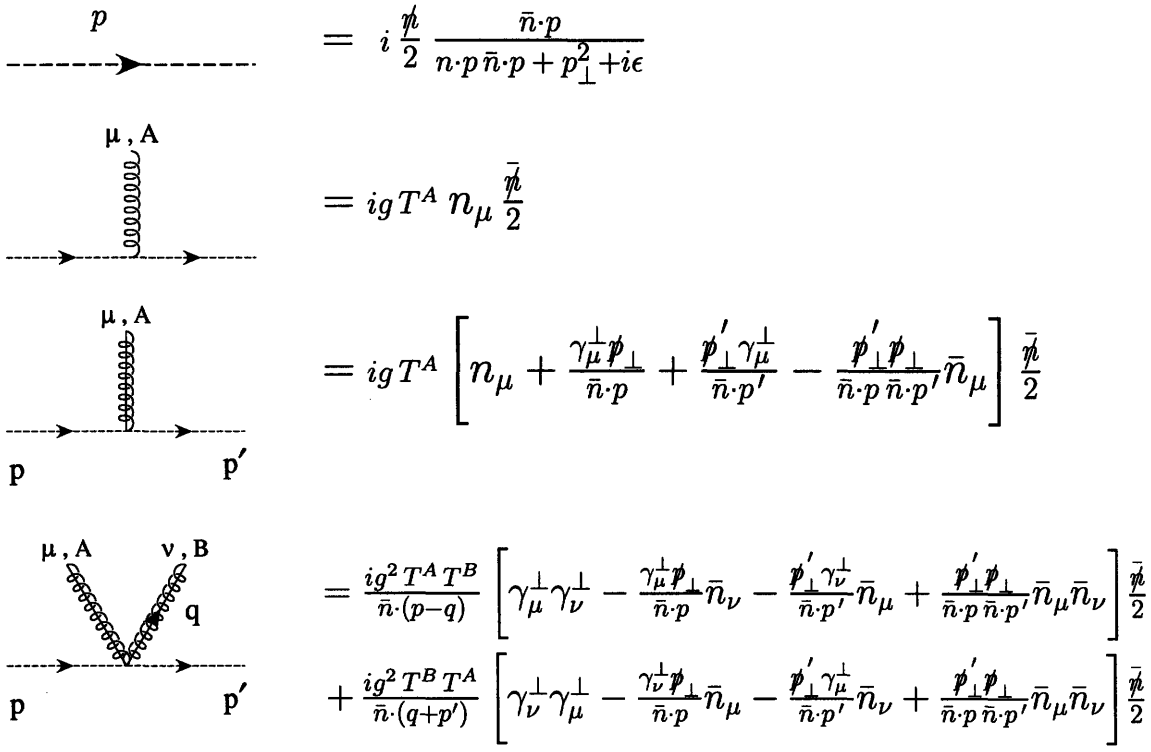

$$= i\frac{\not{n}}{2}\frac{\bar{n}\cdot p}{n\cdot p\,\bar{n}\cdot p + p_\perp^2 + i\epsilon}$$

$$= igT^A n_\mu \frac{\bar{\not{n}}}{2}$$

$$= igT^A\left[n_\mu + \frac{\gamma_\mu^\perp \not{p}_\perp}{\bar{n}\cdot p} + \frac{\not{p}_\perp' \gamma_\mu^\perp}{\bar{n}\cdot p'} - \frac{\not{p}_\perp' \not{p}_\perp}{\bar{n}\cdot p\,\bar{n}\cdot p'}\bar{n}_\mu\right]\frac{\bar{\not{n}}}{2}$$

$$= \frac{ig^2 T^A T^B}{\bar{n}\cdot(p-q)}\left[\gamma_\mu^\perp\gamma_\nu^\perp - \frac{\gamma_\mu^\perp \not{p}_\perp}{\bar{n}\cdot p}\bar{n}_\nu - \frac{\not{p}_\perp' \gamma_\nu^\perp}{\bar{n}\cdot p'}\bar{n}_\mu + \frac{\not{p}_\perp' \not{p}_\perp}{\bar{n}\cdot p\,\bar{n}\cdot p'}\bar{n}_\mu\bar{n}_\nu\right]\frac{\bar{\not{n}}}{2}$$

$$+ \frac{ig^2 T^B T^A}{\bar{n}\cdot(q+p')}\left[\gamma_\nu^\perp\gamma_\mu^\perp - \frac{\gamma_\nu^\perp \not{p}_\perp}{\bar{n}\cdot p}\bar{n}_\mu - \frac{\not{p}_\perp' \gamma_\mu^\perp}{\bar{n}\cdot p'}\bar{n}_\nu + \frac{\not{p}_\perp' \not{p}_\perp}{\bar{n}\cdot p\,\bar{n}\cdot p'}\bar{n}_\mu\bar{n}_\nu\right]\frac{\bar{\not{n}}}{2}$$

Figure 2-6: $\mathcal{L}_{\xi\xi}^{(0)}$ Feynman rules: a dashed line is a collinear quark; a spring is an ultrasoft gluon; a spring with a line is a collinear gluon. $\bar{n}\cdot p$ and $p^\perp$ momenta are label parts only. Figure from Bauer et al. [15].

A_n appear together in the leading-order collinear covariant derivative. The other components of the usoft gauge field are suppressed relative to the label operator and A_n. The inverse covariant derivative in Eq. (2.36) can be interpreted as an expansion in $g\bar{n}\cdot A_c$. A precise definition will be given in the next sub-section (*c.f.* Eq. (2.42)). The manipulations leading to Eq. (2.36) hold at tree level, but in fact this is the most general form for the leading collinear quark Lagrangian consistent with gauge invariance, discussed in the next sub-section, and reparametrization invariance, discussed in section 2.4.4. Some Feynman rules for $\mathcal{L}_{\xi\xi}^{(0)}$ are given in Figure 2-6.

The leading collinear quark Lagrangian is derived in an analogous manner. The result is [22]

$$\mathcal{L}_{cg}^{(0)} = \frac{1}{2g^2}\mathrm{Tr}\left\{\left[iD_c^\mu,\, iD_c^\nu\right]\right\}^2 + \text{g.f.} \tag{2.38}$$

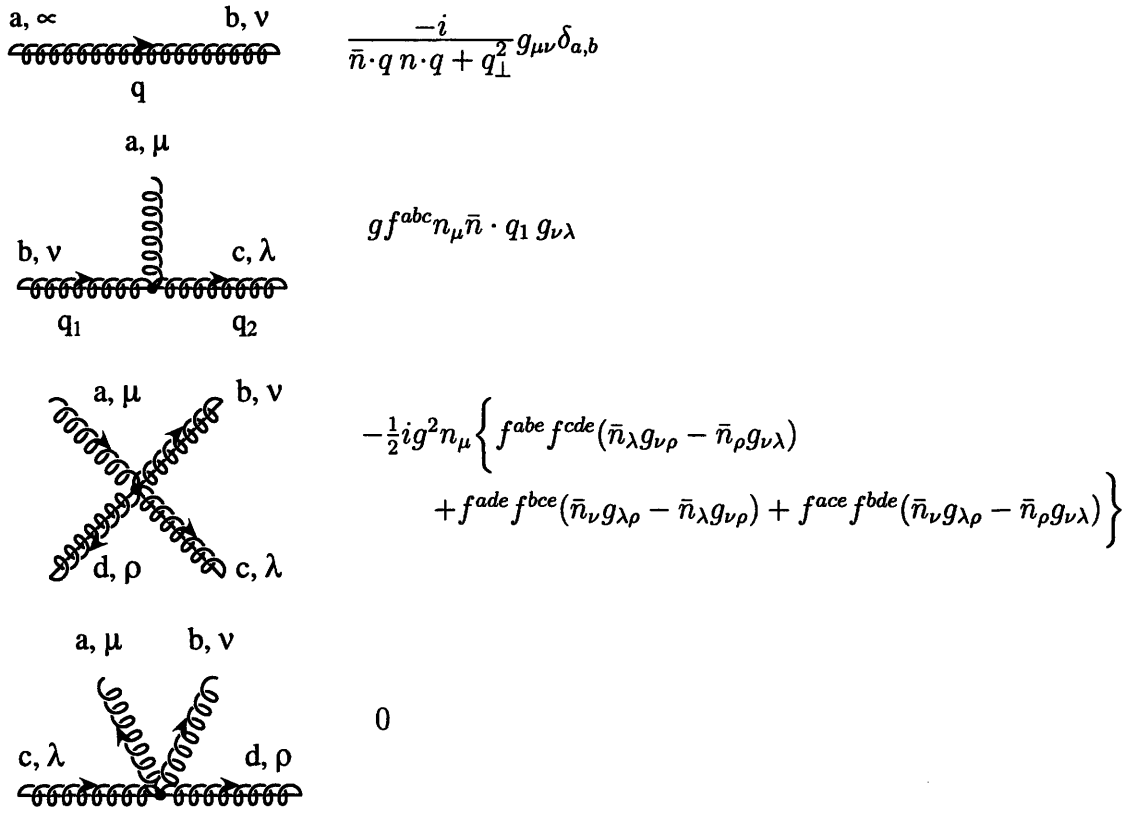

Figure 2-7: $\mathcal{L}_{cg}^{(0)}$ Feynman rules (Eq. (2.38)) in Feynman gauge: a spring is an ultrasoft gluon; a spring with a line is a collinear gluon. $\bar{n}\cdot p$ and $p^\perp$ momenta are label parts only. Figure from Bauer et al. [22]

where the trace is over color indices, the collinear covariant derivative is defined in Eq. (2.37), and g.f. stands for gauge fixing terms. Again, only the $n\cdot A_{us}$ component of the ultrasoft gluon field appears at leading order in the power counting.

The ultrasoft Lagrangian density is the same as in QCD, with appropriate power countings for ultrasoft fields,

$$\mathcal{L}_{us} = \bar{q}_{us} i \not{D}_{us} q_{us} + \frac{1}{2g} \mathrm{Tr}\, \left\{ [D_{us}^\mu,\, D_{us}^\nu] \right\}^2 + \text{g.f.}\,, \tag{2.39}$$

with $iD_{us} = i\partial + g\, A_{us}$ and where g.f. stands for gauge fixing terms.

2.4.2 Gauge invariance

SCET has a rich set of gauge symmetries that severely restricts the allowed form of the effective theory operators [22, 24]. Gauge invariance will be an important consideration for the construction of heavy-to-light current operators in Chapter 3 and flavor-changing weak operators for non-leptonic decays in Chapter 4. In $\mathrm{SCET_I}$ there are both usoft gauge transformations that have $i\partial U_{us} \sim \lambda^2$ and collinear gauge transformations that have support over collinear momenta $(i\partial^+, i\partial^-, i\partial_\perp)U_c \sim (\lambda^2, 1, \lambda)$. We will address the implications of latter type first.

Ultrasoft fields cannot resolve, and therefore do not transform under, the rapid fluctuations induced by a collinear gauge transformation. The collinear quark transforms as one might expect, $\xi_n \to U_c \xi_n$. The collinear gluon transformation requires a bit more thought. The slowly-varying usoft gluon field behaves like a classical color background field for the quantum collinear field. In the presence of this background, A_n transforms in such a way that the combination iD_c, which involves $n \cdot A_{us}$ as in Eq. (2.37), transforms under U_c like one would expect a covariant derivative to transform, *e.g.* $iD_c \xi_n \to U_c iD_c \xi_n$. It is easy to see that leading-order collinear Lagrangians, Eqs. (2.36) and (2.38), whose derivatives and gauge fields only come in this combination, are invariant under collinear gauge transformations.

Power counting allows an arbitrary number of $\bar{n} \cdot A_n \sim \lambda^0$ gluons in any collinear operator. We have already seen an example of this in the inverse covariant derivative $(i\bar{n} \cdot D_c)^{-1}$ in $\mathcal{L}^{(0)}_{\xi\xi}$. Collinear gauge invariance, however, dictates that these gluons always appear in the form of a Wilson line functional $W[\bar{n} \cdot A_n]$ that transforms in such a way that $W^\dagger \xi_n$ is invariant [27]. This collinear Wilson line is

$$\begin{aligned} W &= \Big[\sum_{\text{perms}} \exp\Big(- g \frac{1}{\bar{\mathcal{P}}} \bar{n} \cdot A_n \Big) \Big] \\ &= \sum_{m=0}^{\infty} \sum_{\text{perms}} \frac{(-g)^m}{m!} \frac{\bar{n} \cdot A_{n,q_m} \cdots \bar{n} \cdot A_{n,q_1}}{\bar{n} \cdot q_1 \, \bar{n} \cdot (q_1 + q_2) \cdots \bar{n} \cdot (\sum_{i=1}^m q_i)} \,. \end{aligned} \tag{2.40}$$

In the second line, there is an implied large phase factor and sum on labels q_i. In both lines, "perms" refers to all permutations of the gluon fields. The Wilson line

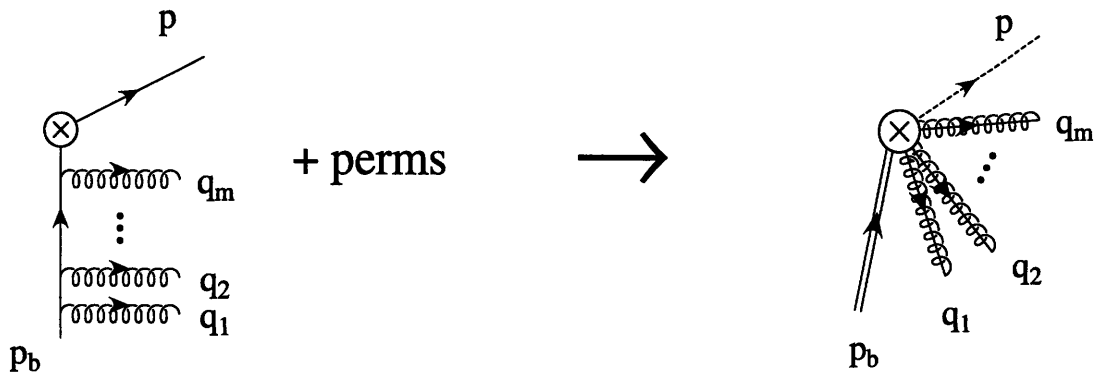

Figure 2-8: Generation of the collinear Wilson line W in the leading-order heavy-to-light current matching. Left: full-theory. Right: SCET. Figure from Bauer et al. [15].

satisfies $W^\dagger W = 1$ and

$$(i\bar{n}\cdot D_c)^n = W\bar{\mathcal{P}}^n W^\dagger \tag{2.41}$$

With this, the leading collinear-quark Lagrangian is

$$\mathcal{L}^{(0)}_{\xi\xi} = \bar{\xi}_n\Big[in\cdot D_c + i\not{D}_c^\perp W\frac{1}{\bar{\mathcal{P}}}W^\dagger i\not{D}_c^\perp\Big]\frac{\not{\bar{n}}}{2}\xi_n\,. \tag{2.42}$$

Power counting also allows the Wilson coefficient of a collinear operator to be an arbitrary function of $\bar{n}\cdot p \sim \lambda^0$ label momenta. Gauge symmetry, however, restricts Wilson coefficients to only depend on the large label of gauge-invariant combinations of fields. A simple application of these concepts is the leading-order heavy-to-light usoft-collinear current $J^{(0)} = \bar{\xi}_n W\Gamma h_v$, where Γ is the Dirac structure in the full-theory current. The Wilson line W, required for collinear gauge invariance, is built up by full-theory diagrams in which the heavy quark goes off-shell by emitting one or more $\bar{n}\cdot A_n$ gluons, as shown in Figure 2-8. At tree level, the Wilson coefficient of $J^{(0)}$ is unity. Beyond tree level, the current is

$$J^{(0)} = \bar{\xi}_n W\, C(\bar{\mathcal{P}}^\dagger)\Gamma h_v\,. \tag{2.43}$$

The coefficient function C depends on the large label momentum of the gauge-invariant product $\bar{\xi}_n W$, picked out by $\bar{\mathcal{P}}^\dagger$.

Ultrasoft gauge invariance contrains the form of purely ultrasoft interactions as well as usoft-collinear interactions. Under a usoft gauge transformation, usoft fields behave as one might expect them to, *e.g.* $h_v \to U_{us} h_v$ and $iD_{us}\, q_{us} \to U_{us}\, iD_{us}\, q_{us}$. For rapidly-varying collinear fields, the usoft gauge transformation is like a global color rotation, *e.g.* $\xi_n \to U_{us}\xi_n$ and $A_n \to U_{us} A_{us} U_{us}^\dagger$. It is easy to see that the leading-order collinear Lagrangians, as well as the leading heavy-to-light current, are both usoft gauge invariant. Just as the collinear Wilson line W simplifies collinear gauge symmetry considerations, it is useful to define a light-like ultrasoft Wilson line

$$Y(x) \equiv \tilde{\mathrm{P}} \exp\left(i\, g \int_{s_0}^{0} \mathrm{d}s\; n\cdot A_{us}(x + s\, n) \right), \tag{2.44}$$

where $\tilde{P}$ can stand for either path ordering, P, or anti-path ordering, $\bar{P}$, and the reference point s_0 can be taken as $+$ or $-\infty$. The conventional choice, the one we make unless otherwise stated, is $\tilde{P} = P$ and $s_0 = -\infty$. We comment on these choices in section 2.4.5. The differential line element, $\mathrm{d}s \sim \lambda^{-2}$, scales like a residual x dependence and so $Y \sim \lambda^0$. This ultrasoft Wilson line transforms as $Y \to U_{us} Y$ and satisfies $Y^\dagger Y = 1$ and $Y^\dagger in\cdot D_{us} Y = in\cdot\partial$.

The BPS collinear field redefinition [22]

$$\xi_{n,p}(x) \to Y(x)\xi_{n,p}(x)\,, \qquad A_{n,q}(x) \to Y(x) A_{n,q}(x) Y^\dagger(x)\,, \tag{2.45}$$

removes usoft gluons from the leading-order collinear Lagrangian since

$$in\cdot D_c \to in\cdot\partial + g\, n\cdot A_n\,. \tag{2.46}$$

(Note that in the literature, the right-hand side of Eq. (2.46) is usually what is meant by $in\cdot D_c$.) In this thesis, $in\cdot D_c$ can either contain $n\cdot A_{us}$ or not, depending on the context, *i.e.* pre- or post- Eq. (2.45), respectively. After the redefinition, all usoft-collinear interactions are contained in factors of Y in operators, giving a simple statement of usoft-collinear factorization. For example, the leading heavy-to-light current $J^{(0)} \to \bar{\xi}_n W \Gamma Y^\dagger h_v$. Post-BPS-redefinition collinear fields no longer transform

under usoft gauge transformations.

In constructing operator bases, we will use the following structures, which are both collinear and usoft gauge invariant:

$$\chi_n \equiv W^\dagger \xi_n, \qquad \mathcal{H}_v \equiv Y^\dagger h_v, \qquad \mathcal{D}_c \equiv W^\dagger D_c W\,, \qquad \mathcal{D}_{us} \equiv Y^\dagger D_{us} Y\,, \tag{2.47}$$

as well as the $\mathcal{P}$ label momentum operator. The fields in Eq. (2.47) are all post-BPS redefinition. It is convenient to be able to switch the collinear derivatives for field strengths, for which we use

$$\begin{aligned} i\mathcal{D}_c^{\perp\mu} &= \mathcal{P}_\perp^\mu + ig\mathcal{B}_\perp^\mu\,, & i\overleftarrow{\mathcal{D}}_c^{\perp\mu} &= -\mathcal{P}_\perp^{\dagger\mu} - ig\mathcal{B}_\perp^\mu\,, \\ in\!\cdot\!\mathcal{D}_c &= in\!\cdot\!\partial + ign\!\cdot\!\mathcal{B}\,, & in\!\cdot\!\overleftarrow{\mathcal{D}}_c &= in\!\cdot\!\overleftarrow{\partial} - ign\!\cdot\!\mathcal{B}\,. \end{aligned} \tag{2.48}$$

Here the field strength tensors are

$$ig\mathcal{B}_\perp^\mu \equiv \Big[\frac{1}{\overline{\mathcal{P}}}[i\bar{n}\cdot\mathcal{D}_c, i\mathcal{D}_c^{\perp\mu}]\Big]\,, \qquad ign\cdot\mathcal{B} \equiv \Big[\frac{1}{\overline{\mathcal{P}}}[i\bar{n}\cdot\mathcal{D}_c, in\cdot\mathcal{D}_c]\Big], \tag{2.49}$$

where the label operators and derivatives act only on fields inside the outer square brackets. For convenience we will also use the shorthand notation

$$\begin{aligned} \bar{\chi}_{n,\omega} &\equiv \Big[\bar{\chi}_n\,\delta(\omega - n\cdot v\overline{\mathcal{P}}^\dagger)\Big]\,, \\ (ig\mathcal{B}_\perp^\mu)_\omega &\equiv \Big[ig\mathcal{B}_\perp^\mu\,\delta(\omega - n\cdot v\overline{\mathcal{P}}^\dagger)\Big]\,, \\ (ign\cdot\mathcal{B})_\omega &\equiv \Big[ign\cdot\mathcal{B}\,\delta(\omega - n\cdot v\overline{\mathcal{P}}^\dagger)\Big]\,, \end{aligned} \tag{2.50}$$

so that $\bar{\chi}_{n,\omega}$ corresponds to the gauge invariant combination of fields $(\bar{\xi}_n W)$ carrying large $\mathcal{O}(\lambda^0)$ momentum ω. In a Feynman diagram, ω goes in the same direction as fermion number, *i.e.* positive along the arrow. An operator built out of several of these components then has multiple labels, $J(\omega_1, \omega_2, \ldots)$, and the Wilson coefficient for the operator will be a function of the same ω_i momentum labels, $C(\omega_1, \omega_2, \ldots)$.

For example, the leading heavy-to-light current in Eq. (2.43) is written as

$$J^{(0)} = \int \mathrm{d}\omega\, C(\omega)\chi_{n,\omega}\Gamma\mathcal{H}_v \tag{2.51}$$

2.4.3 Reduction in spin structures

The number of independent Dirac structures in a quark bilinear is reduced by Dirac projection relations. For heavy-to-light currents $\bar{\chi}_n\Gamma\mathcal{H}_v$ considered in Chapter 3, we can project the Dirac structure onto a four-dimensional basis $\{1, \gamma^5, \gamma_\perp^\alpha\}$ using

$$\Gamma \doteq \mathrm{tr}\left[P_{\bar{n}}\Gamma P_v\right] + \gamma^5\,\mathrm{tr}\left[\gamma^5 P_{\bar{n}}\Gamma P_v\right] + \gamma_\alpha^\perp\,\mathrm{tr}\left[\gamma_\perp^\alpha P_{\bar{n}}\Gamma P_v\right], \tag{2.52}$$

where $\doteq$ indicates that the relation is true between $\bar{\chi}_n$ and $\mathcal{H}_v$. Similarly, in collinear quark bilinears, $\bar{\chi}_n\Gamma\chi_n$, which appear both in sub-leading heavy-to-light currents and in the non-leptonic SCET weak effective Hamiltonian, we can project the Dirac structure onto the four-dimensional basis $\{\not{\bar{n}}, \not{\bar{n}}\gamma^5, \not{\bar{n}}\gamma_\perp^\alpha\}$ using

$$\Gamma \doteq \frac{\not{\bar{n}}}{8}\,\mathrm{tr}\left[\not{n}P_{\bar{n}}\Gamma P_n\right] + \frac{\not{\bar{n}}\gamma^5}{8}\,\mathrm{tr}\left[\gamma^5\not{n}P_{\bar{n}}\Gamma P_n\right] + \frac{\not{\bar{n}}\gamma_\alpha^\perp}{8}\,\mathrm{tr}\left[\gamma_\perp^\alpha\not{n}P_{\bar{n}}\Gamma P_n\right]. \tag{2.53}$$

When χ_n has a definite chirality, $\gamma^5 P_{R,L} = \pm P_{R,L}$ reduces the dimensionality of the space of Dirac structures to two, with spanning set $\{\not{\bar{n}}, \not{\bar{n}}\gamma_\perp^\alpha\}$. In that case the subspace spanned by $\not{\bar{n}}\gamma_\perp^\alpha$ is only one-dimensional, and we can turn any contraction involving $i\epsilon_\perp^{\mu\nu}$ into a contraction with $g_\perp^{\mu\nu}$, where the two-index $\perp$ tensors

$$\begin{aligned}
\epsilon_\perp^{\mu\nu} &= \bar{n}_\rho n_\sigma \epsilon^{\mu\nu\rho\sigma}/2\,, \\
g_\perp^{\mu\nu} &= g^{\mu\nu} - \frac{n^\mu\bar{n}^\nu}{2} - \frac{\bar{n}^\mu n^\nu}{2}\,,
\end{aligned} \tag{2.54}$$

satisfy

$$g_\perp^{\alpha[\mu}\epsilon_\perp^{\nu]\beta} = -g_\perp^{\alpha\beta}\epsilon_\perp^{\mu\nu}\,. \tag{2.55}$$

(Note: Our convention for the ϵ tensor is such that with the usual choice of n and $\bar{n}$, $\epsilon_\perp^{12} = 1$.) For example, $i\epsilon_\perp^{\mu\nu}\bar{\xi}_n^L\not{\bar{n}}\gamma_\nu^\perp\xi_n^R = \bar{\xi}_n^L\not{\bar{n}}\gamma_\perp^\mu\gamma_5\xi_n^R = \bar{\xi}_n^L\not{\bar{n}}\gamma_\perp^\mu\xi_n^R$.

2.4.4 Reparameterization invariance

The theory QCD+H_W, of which SCET is an effective theory, is manifestly Lorentz invariant, and each particle is described by a single four-momentum. This is not the case in SCET. The auxiliary vectors $v, n, \bar{n}$ break manifest Lorentz invariance, and the decomposition of momenta into label and residual pieces is not unique. Lorentz symmetry is restored in the effective theory by requiring invariance under small changes, *reparametrization* (RP), of the auxiliary vectors. The decomposition ambiguity is removed by requiring invariance under shifts between label and residual. The structure of effective theory operators is constrained by these reparameterization invariances (RPIs).

In HQET it is convenient to formulate the RPI constraints to all orders in $1/m$ by constructing RP invariant operators and then expanding them to generate a chain of related operators [118]. These operators start at some fixed order in $1/m$, but once the RP invariant form of this operator is known, all higher terms in the chain are determined. The RP symmetries in SCET are richer and typically the constraints are derived order by order in λ. In this case, higher-order operators in the chain are not fully determined until the appropriate order in λ is considered. RPI constraints in SCET were first considered by Chay and Kim [59]. The complete set of SCET reparametrizations were formulated in Ref. [123] and used to prove that the leading-order (LO) SCET Lagrangian is not renormalized to all orders in perturbation theory.

Recall that the total momentum P^μ of a heavy quark is decomposed as $P^\mu = m_h v^\mu + k^\mu$, where m_h is the quark's mass, v^μ is its velocity, and k^μ is a residual momentum of order $m_h\lambda^2$. Then the simultaneous shifts

$$v^\mu \to v^\mu + \beta^\mu \quad \text{and} \quad k^\mu \to k^\mu - m_h\beta^\mu, \tag{2.56}$$

can have no physical consequences [118]. Here β is an infinitesimal four-velocity that we assign the maximal power counting $\beta \sim \lambda^2$ that preserves $k \sim Q\lambda^2$. We refer to this reparameterization invariance as HQET-RPI. The transformation of the field

$h_v \to h_v + \delta h_v$ induces terms at $\mathcal{O}(\lambda^0)$ and $\mathcal{O}(\lambda^2)$,

$$\delta^{(\lambda^0)} h_v = (i m_h \beta \cdot x) h_v \,, \qquad \delta^{(\lambda^2)} h_v = \frac{\not{\beta}}{2} \, h_v. \tag{2.57}$$

Recall that the total momentum P^μ of a collinear particle is decomposed into the sum of a collinear momentum p^μ, with $(n \cdot p, \bar{n} \cdot p, p_\perp) \sim Q(\lambda^2, 1, \lambda)$, and an ultrasoft momentum k^μ, with $(n \cdot k, \bar{n} \cdot k, k_\perp) \sim Q(\lambda^2, \lambda^2, \lambda^2)$:

$$\begin{aligned} P^\mu &= p^\mu + k^\mu & (2.58) \\ &= \frac{n^\mu}{2} \bar{n} \cdot (p + k) + \frac{\bar{n}^\mu}{2} n \cdot k + (p_\perp + k_\perp). & (2.59) \end{aligned}$$

This decomposition has two types of ambiguity. The first comes from splitting P^μ into large and small components. Operators must be invariant under a transformation that takes

$$\begin{aligned} &\overline{\mathcal{P}} \to \overline{\mathcal{P}} + \bar{n} \cdot \ell \,, \qquad && i\bar{n} \cdot \partial \to i\bar{n} \cdot \partial - \bar{n} \cdot \ell \,, \\ &\mathcal{P}_\perp^\mu \to \mathcal{P}_\perp^\mu + \ell_\perp^\mu \,, \qquad && i\partial_\perp^\mu \to i\partial_\perp^\mu - \ell_\perp^\mu, \end{aligned} \tag{2.60}$$

where all operators and derivatives act on one or more collinear fields, and ℓ^μ is $\mathcal{O}(\lambda^2)$. We refer to this reparameterization invariance as SCET RPI-a. Examples of an infinitesimal transformation on fields and operators are

$$\delta_a^{(\lambda^0)} \chi_n = (i\ell \cdot x) \chi_n \,, \qquad \delta_a^{(\lambda^1)} \mathcal{P}_\perp^\alpha = \ell_\perp^\alpha \,, \qquad \delta_a^{(\lambda^2)} \bar{\mathcal{P}} = \bar{n} \cdot \ell \,, \tag{2.61}$$

where $n \cdot \ell = 0$. Note that $(i\ell \cdot x)$ terms only affect ultrasoft derivatives acting on the fields since RPI constraints are found by evaulating operators at $x = 0$.

The second ambiguity in the decomposition of the momentum of the collinear particles comes from choosing the light-cone vectors n and $\bar{n}$. An infinitesimal change in these vectors that preserves the relations $n^2 = 0$, $\bar{n}^2 = 0$, and $n \cdot \bar{n} = 2$ can have no physical consequences. The most general infinitesimal transformations of n and $\bar{n}$

that preserve these conditions along with the collinear power counting are [123]

$$\text{(I)}\begin{cases} n_\mu \to n_\mu + \Delta_\mu^\perp \\ \bar{n}_\mu \to \bar{n}_\mu \end{cases} \qquad \text{(II)}\begin{cases} n_\mu \to n_\mu \\ \bar{n}_\mu \to \bar{n}_\mu + \varepsilon_\mu^\perp \end{cases} \qquad \text{(III)}\begin{cases} n_\mu \to (1+\alpha)\, n_\mu \\ \bar{n}_\mu \to (1-\alpha)\, \bar{n}_\mu \end{cases} \tag{2.62}$$

where $\{\Delta_\mu^\perp, \epsilon_\mu^\perp, \alpha\} \sim \{\lambda^1, \lambda^0, \lambda^0\}$ are five infinitesimal parameters. ϵ and Δ get the $\perp$ modifier because $\bar{n}\cdot\epsilon^\perp = n\cdot\epsilon^\perp = \bar{n}\cdot\Delta^\perp = n\cdot\Delta^\perp = 0$. Note that ϵ and α are $\mathcal{O}(1)$ but infinitesimal.

In Chapter 3, we will consider higher-order RPI relations for heavy-to-light currents in SCET_I. For processes involving heavy-to-light currents it is often convenient to work in the special frame where $v_\perp = 0$, so that $v^\mu = \bar{n}\cdot v\, n^\mu/2 + n\cdot v\, \bar{n}^\mu/2$ and $n\cdot v\, \bar{n}\cdot v = 1$. If we start in the frame $v_\perp = 0$, then transformations (I) or (II) or (HQET-RPI) take us out of this frame. A certain combined type-I and type-II transformation, however, leaves $v_\perp = 0$ [96]. We refer to this transformation as RPI-$\star$. We can also form a combined HQET and type-II transformation that leaves $v_\perp = 0$, which we refer to as RPI-\$ [2]. These transformations are

$$(\star)\begin{cases} n_\mu \to n_\mu + \Delta_\mu^\perp \\ \bar{n}_\mu \to \bar{n}_\mu - \frac{\Delta_\mu^\perp}{(n\cdot v)^2} \\ v_\mu \to v_\mu \end{cases}, \qquad (\$)\begin{cases} v^\mu \to v^\mu + \beta_T^\mu \\ \bar{n}^\mu \to \bar{n}^\mu + \frac{2}{n\cdot v}\,\beta_\perp^\mu \\ n_\mu \to n_\mu \end{cases}, \tag{2.63}$$

where $\Delta^\perp \sim \lambda$, $\beta \sim \lambda^2$, and $\beta_\perp$ is the $\perp$-part of β_T. In defining the \$ transformation we found that it is more convenient to leave $v_\perp = 0$ by making a transformation on v simultaneously with $\bar{n}$, rather than simultaneously with n. Under the $\star$ transformation the components of a generic four-vector V_μ transform as

$$\begin{aligned} n\cdot V &\xrightarrow{\star} n\cdot V + \Delta^\perp\cdot V^\perp, \\ \bar{n}\cdot V &\xrightarrow{\star} \bar{n}\cdot V - \frac{\Delta^\perp\cdot V^\perp}{(n\cdot v)^2}, \\ V_\mu^\perp &\xrightarrow{\star} V_\mu^\perp + \Delta_\mu^\perp\Big(-\frac{\bar{n}}{2} + \frac{n}{2(n\cdot v)^2}\Big)\cdot V + \Big(-\frac{\bar{n}_\mu}{2} + \frac{n_\mu}{2(n\cdot v)^2}\Big)\Delta^\perp\cdot V^\perp \end{aligned} \tag{2.64}$$

Working to second order in λ, we need the following terms from an RPI-$\star$ transfor-

mation:

$$
\begin{aligned}
\delta_\star^{(\lambda^0)}\mathcal{P}_\perp^\mu &= -\frac{\Delta_\perp^\mu}{2}\,\bar{\mathcal{P}}\,, & \delta_\star^{(\lambda^0)}(ign\cdot\mathcal{B}) &= \Delta_\perp\cdot(ig\mathcal{B}_\perp)\,, \qquad (2.65)\\
\delta_\star^{(\lambda^0)}(ig\mathcal{B}_\perp^\mu) &= 0\,, & \delta_\star^{(\lambda^0)}\bar{\chi}_n &= 0\,,\\
\delta_\star^{(\lambda^1)}\mathcal{P}_\perp^\mu &= (\bar{n}\cdot v)^2 n_T^\mu\,\Delta^\perp\cdot\mathcal{P}_\perp\,, & \delta_\star^{(\lambda^1)}\bar{\chi}_n &= \bar{\chi}_n\,\frac{\not{\bar{n}}\not{\Delta}^\perp}{4}\,,\\
\delta_\star^{(\lambda^1)}(ig\mathcal{B}_\perp^\mu) &= (\bar{n}\cdot v)^2 n_T^\mu\,\Delta^\perp\cdot(ig\mathcal{B}_\perp)\,, & \delta_\star^{(\lambda^2)}\bar{\mathcal{P}} &= -(\bar{n}\cdot v)^2\Delta_\perp\cdot\mathcal{P}_\perp\,,\\
\delta_\star^{(\lambda^2)}\bar{\chi}_n &= -\bar{\chi}_n\Big(ig\not{\mathcal{B}}^\perp+\not{\mathcal{P}}^{\perp\dagger}\Big)\frac{1}{\bar{\mathcal{P}}^\dagger}\frac{\not{\Delta}^\perp}{2(n\cdot v)^2}+\bar{\chi}_n\Big[\frac{1}{(n\cdot v)^2\bar{\mathcal{P}}}\,ig\mathcal{B}^\perp\cdot\Delta^\perp\Big]\,,
\end{aligned}
$$

where n_T is the transverse part of n,

$$
n_T^\mu = n^\mu - n\cdot v\, v^\mu = \frac{n^\mu}{2} - (n\cdot v)^2\frac{\bar{n}^\mu}{2}\,. \qquad (2.66)
$$

We will also need the transformation

$$
\delta_\star^{(\lambda^2)}\delta(\omega - n\cdot v\bar{\mathcal{P}}^\dagger) \;=\; \frac{1}{n\cdot v}\,\Delta_\perp\cdot\mathcal{P}_\perp^\dagger\,\delta'(\omega - n\cdot v\bar{\mathcal{P}}^\dagger)\,. \qquad (2.67)
$$

For the RPI-\$ transformation, working to second order in λ, we will need the following terms:

$$
\begin{aligned}
\delta_\$^{(\lambda^0)}h_v &= (im\beta_T\cdot x)h_v\,, & \delta_\$^{(\lambda^2)}h_v &= \frac{\not{\beta}_T}{2}\,h_v\,, \qquad (2.68)\\
\delta_\$^{(\lambda^2)}\,\delta(\omega - n\cdot v\bar{\mathcal{P}}^\dagger) &= -n\cdot\beta_T\,\bar{\mathcal{P}}^\dagger\,\delta'(\omega - n\cdot v\bar{\mathcal{P}}^\dagger)\,.
\end{aligned}
$$

For the last identity it is straightforward to see that the \$ transformation on $\bar{n}$ does not enter until one order higher. We chose to define the RPI-\$ transformation to be for v and $\bar{n}$ rather than v and n because of the property that terms with $\bar{n}$ are often pushed to higher order, making the relations derived with RPI \$ more orthogonal to those from RPI $\star$. For example, in order to have a simple form for the $\delta_\$\Gamma$'s in Eq. (3.34) below, it is important that it is $\bar{n}$ –not n– that transforms. Finally, we note that since all Dirac structures are $\mathcal{O}(1)$, all RP transformations of Dirac structures have the same power counting as the transformation parameter, in particular, $\delta_\star\Gamma \sim \mathcal{O}(\lambda^1)$

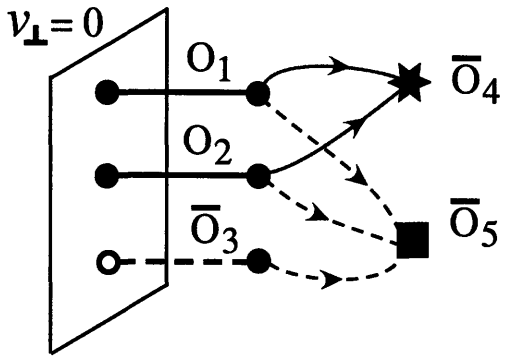

Figure 2-9: Transformation of operators on and off the $v_\perp = 0$ surface. Here $O_{1,2}$ exist for $v_\perp = 0$, while $\overline{O}_{3,4,5}$ vanish on the $v_\perp = 0$ surface.

and $\delta_{\$}\Gamma \sim \mathcal{O}(\lambda^2)$.

Finally, note that we will consider the RPI tranformations of all fields prior to making the BPS field redefinition in Eq. (2.45) so that we do not have to transform Y. However, in order not to have to switch our notation back and forth we will write all equations with the operators obtained after the field redefinition. This implies that results quoted for the transformation of objects involving $\mathcal{H}_v$ should be though of as being made for h_v, with the field redefinition which induces $\mathcal{H}_v$ made only afterwards.

Completeness of Projected RPI

It is natural to ask if for $v_\perp = 0$ the transformations RPI-\$ and RPI-$\star$ in Eq. (2.63) are sufficient to give the complete set of constraints that arise from the original SCET type-I, SCET type-II, and HQET RPI transformations. The set { RPI-\$, RPI-$\star$, SCET-II } forms an equivalent complete grouping related by linear combinations. We addressed this question in [2] by considering a split of all possible operators into two sets, a set $\{O_i\}$ that do not vanish on the $v_\perp = 0$ surface and a set $\{\overline{O}_i\}$ that do. An example is pictured in Fig. 2-9. Constraints are derived by requiring cancellations among the resulting post-transformation set of operators. If we consider an operator O_i then under one of the projected RPI transformations, RPI-\$ or RPI-$\star$, it transforms into the set $\{O_j, \overline{O}_k\}$. On the other hand an operator $\overline{O}_i$ only transforms back into the set $\{\overline{O}_j\}$. This is a special feature of the projected transformations and ensures that relations derived on the $v_\perp = 0$ surface can not be spoiled by operators which

appear away from the surface. It appears that we can neglect the $\overline{\mathrm{O}}_i$ operators since they vanish when we project on the $v_\perp = 0$ plane. However it is still possible that we will miss an additional relation between operators on the surface, so that the surface analysis will not be complete.

There are two possible sources that could lead to additional relations beyond those derived from projected RPI on the surface. First, under the SCET RPI-II transformation $\epsilon_\perp \sim \lambda^0$ is allowed, while in the RPI-$\star$ and RPI-\$ transformations we only have smaller transformations of $\bar{n}$ of $\mathcal{O}(\lambda^1)$ and $\mathcal{O}(\lambda^2)$. Thus we could miss relations from the more restrictive $\epsilon_\perp \sim \lambda^0$ allowed by SCET RPI-II. Note that an SCET RPI-II transformation takes us off the projected surface. Second if we project onto $v_\perp = 0$ then constraints are derived only by enforcing cancellations within the set $\{\mathrm{O}_j\}$. It is possible that an operator $\overline{\mathrm{O}}_4$ exists that is obtained from the transformation of two operators O_1 and O_2 that are *not related by transformations on the surface.* Enforcing the cancellation of $\overline{\mathrm{O}}_4$ then relates O_1 and O_2. This is pictured by the star in Fig. 2-9. A related alternative is an operator like $\overline{\mathrm{O}}_5$ pictured with the box which is obtained from transformations of $\mathrm{O}_{1,2}$ and $\overline{\mathrm{O}_3}$. If $\overline{\mathrm{O}_3}$ is otherwise constrained then this would also constrain $\mathrm{O}_{1,2}$. In cases with multiple operators appearing and multiple transformations we must of course consider the linear independence of combinations of operators. If an $\overline{\mathrm{O}}_i$ contributes and it is not otherwise constrained then this is not of concern, since in the end we discard $\overline{\mathrm{O}}_i$ by projecting onto the $v_\perp = 0$ surface anyway. We will call an operator that vanishes for $v_\perp = 0$ but that generates a relation between operators on the surface a "supplementary projected operator" (SPO).[6] To check for the existence of an SPO we might in general need the full set of $v_\perp \neq 0$ operators. At $\mathcal{O}(\lambda)$ the comparison of the results derived in Ref. [130] in the full space, to those derived in Ref. [96] on the surface $v_\perp = 0$ shows that there are no SPO's at this order.

For the $\mathcal{O}(\lambda^2)$ heavy-to-light operators considered in Chapter 3, we show that there also no SPO's in section 3.2.4. This is done by a careful choice of Dirac basis that makes it simpler to demonstrate that there are no further type-II RPI relations,

[6] In the case of type-II transformations, operators like $\overline{\mathrm{O}_4}$ and $\overline{\mathrm{O}_5}$ need not be in the $\{\overline{\mathrm{O}}_j\}$ class.

and by explicit construction for other possible SPO's. Thus, the analysis on the $v_\perp = 0$ surface is complete for our computation.

2.4.5 Comments on boundary conditions for $Y(x)$

In constructing subleading operators we combine objects that are individually collinear and usoft gauge invariant. The logic which ensures that all subleading operators can be organized in terms of these objects relies on the decoupling of usoft gluons from the leading order collinear Lagrangian by a field redefinition involving the Wilson line Y [22]. In this section, we show that all results are independent of the choice of boundary condition for this Wilson line [2]. Processes described by SCET can depend on the path of Wilson lines, but this path is determined independent of the choice of boundary condition.

We define

$$\begin{aligned} Y(x^\mu) &= \tilde{\mathrm{P}} \exp\left(ig \int_{s_0}^{0} ds\; n\cdot A_{us}(x_s^\mu)\right), \\ Y^\dagger(x^\mu) &= \tilde{\mathrm{P}}' \exp\left(-ig \int_{\bar{s}_0}^{0} ds\; n\cdot A_{us}(x_s^\mu)\right), \end{aligned} \tag{2.69}$$

where $x_s^\mu = x^\mu + sn^\mu$. With respect to the equation of motion, $n\cdot D_{us} Y = 0$, the point s_0 implements a boundary condition at infinity, and $\tilde{\mathrm{P}}$ denotes path ordering P or anti-path ordering $\overline{\mathrm{P}}$. If $Y^\dagger$ is to be the hermitian conjugate of Y one requires that $\bar{s}_0 = s_0^\dagger$ and $\tilde{\mathrm{P}}' = \overline{\tilde{\mathrm{P}}}$. This ensures that $Y^\dagger Y = 1$ and that the field redefinition in Eq. (2.45) causes the usoft gluons to decouple in the collinear Lagrangian. The following definitions will also be useful

$$\begin{aligned} Y_+ &= \mathrm{P}\exp\left(ig\int_{-\infty}^{0} ds\; n\cdot A_{us}(x_s^\mu)\right), \qquad Y_- = \overline{\mathrm{P}}\exp\left(-ig\int_{0}^{\infty} ds\, n\cdot A_{us}(x_s^\mu)\right), \\ Y_-^\dagger &= \overline{\mathrm{P}}\exp\left(-ig\int_{-\infty}^{0} ds\; n\cdot A_{us}(x_s^\mu)\right), \qquad Y_+^\dagger = \mathrm{P}\exp\left(ig\int_{0}^{\infty} ds\; n\cdot A_{us}(x_s^\mu)\right). \end{aligned} \tag{2.70}$$

Here $(Y_\pm)^\dagger = Y_\mp^\dagger$, and the subscript on $Y_\pm^\dagger$ should be read as $(Y^\dagger)_\pm$ rather than $(Y_\pm)^\dagger$.

A common choice for s_0 is the one made in Ref. [22],

$$s_0 = \bar{s}_0 = -\infty\,, \qquad \tilde{\mathrm{P}} = \mathrm{P}\,, \quad \tilde{\mathrm{P}}' = \overline{\mathrm{P}}\,, \tag{2.71}$$

where $Y = Y_+$ and $Y^\dagger = Y_-^\dagger$. In Ref. [16] the choice $s_0 = +\infty$ with $\tilde{\mathrm{P}}' = \mathrm{P}$ was made in order to correspond with particle production, $Y^\dagger = Y_+^\dagger$. A third possible choice is [23]

$$s_0 = -\infty\,\mathrm{sign}(\bar{\mathcal{P}})\,, \quad \bar{s}_0 = -\infty\,\mathrm{sign}(\bar{\mathcal{P}}^\dagger)\,, \quad \begin{cases} \tilde{\mathrm{P}}{=}\mathrm{P}\,, \tilde{\mathrm{P}}'{=}\overline{\mathrm{P}} & \text{for } \bar{\mathcal{P}}, \bar{\mathcal{P}}^\dagger > 0 \\ \tilde{\mathrm{P}}{=}\overline{\mathrm{P}}\,, \tilde{\mathrm{P}}'{=}\mathrm{P} & \text{for } \bar{\mathcal{P}}, \bar{\mathcal{P}}^\dagger < 0 \end{cases}. \tag{2.72}$$

Eq. (2.72) still satisfies $s_0^\dagger = \bar{s}_0$ but corresponds to a different choice for particles and antiparticles.[7] Here $Y = Y_+$, $Y^\dagger = Y_-^\dagger$ for particles, while $Y = Y_-$, $Y^\dagger = Y_+^\dagger$ for antiparticles. To see this recall that

$$\xi_{n,p} = \xi^+_{n,p} + \xi^-_{n,-p}\,, \tag{2.73}$$

and that if the label momentum is positive $\bar{n}{\cdot}p > 0$ we get the field for particles, ξ_n^+, and if the label is negative $\bar{n}{\cdot}p < 0$ we get the field operator for antiparticles, ξ_n^- [27]. Although it is important to make some choice for s_0, if one is careful then in any physical problem the dependence on s_0 cancels. Any path dependence exhibited by a final result can be derived independently of the choice of s_0 that one makes in the field redefinition.

Since the dependence on s_0 sometimes causes confusion, we explore some of the subtleties in this section, in particular, why it is important to remember that factors of Y, $Y^\dagger$ can also be induced in the interpolating fields for incoming and outgoing collinear states, and why a common choice for $s_0 = \bar{s}_0^\dagger$ is sufficient to properly reproduce the $i\epsilon$ prescription in perturbative computations. In many processes (examples being color allowed $B \to D\pi$ and $B \to X_s\gamma$) the s_0 dependence of the Wilson lines cancels and the following considerations are not crucial. In other processes, however,

[7] Note that in this case $s_0 = -\infty\,\mathrm{sign}(\bar{\mathcal{P}})$, is an operator.

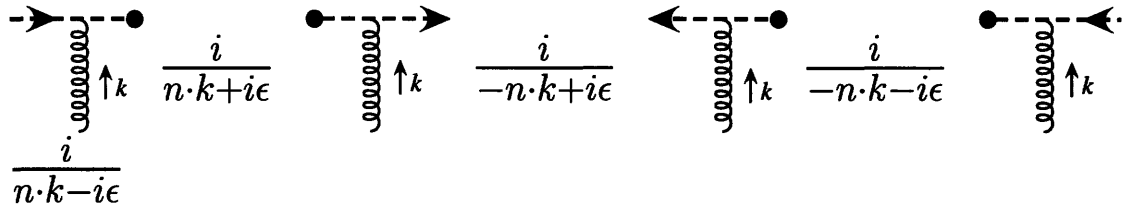

$(Y_+\,\xi_n^+)$ $\qquad$ $(\bar{\xi}_n^+\,Y_+^\dagger)$ $\qquad$ $(\bar{\xi}_n^-\,Y_-^\dagger)$ $\qquad$ $(Y_-\,\xi_n^-)$

Figure 2-10: Eikonal $i\epsilon$ prescriptions for incoming/outgoing quarks and antiquarks and the result that reproduces this with an ultrasoft Wilson line and sterile quark field.

the path for the Wilson line is important for the final result, particularly when these Wilson lines do not entirely cancel. An example of this is jet event shapes as discussed in Refs. [107, 18, 16]. See also the discussion of path dependence in eikonal lines in Refs. [72, 44, 71, 106, 69, 100, 70, 61].

First consider the perturbative computation of attachments of usoft gluons to incoming and outgoing quark and antiquark lines. The results for the eikonal factors for one gluon are summarized in Fig. 2-10, and can be computed directly with the SCET collinear quark Lagrangian (or from an appropriate limit of the QCD propagator). These attachments seem to force one to make a particular choice for s_0 and $\bar{s}_0$, see for example the recent detailed study in Ref. [61]. In our notation it is straightforward to show that this choice corresponds to

$$s_0 = -\infty\,\mathrm{sign}(\bar{\mathcal{P}})\,, \quad \bar{s}_0 = +\infty\,\mathrm{sign}(\bar{\mathcal{P}}^\dagger)\,, \quad \begin{cases} \tilde{\mathrm{P}}=\tilde{\mathrm{P}}'=\mathrm{P}\,, & \text{for } \bar{\mathcal{P}},\bar{\mathcal{P}}^\dagger > 0 \\ \tilde{\mathrm{P}}=\tilde{\mathrm{P}}'=\overline{\mathrm{P}}\,, & \text{for } \bar{\mathcal{P}},\bar{\mathcal{P}}^\dagger < 0 \end{cases} . \tag{2.74}$$

To see this take a quark with label $\bar{n}\cdot p > 0$ and an antiquark with label $\bar{n}\cdot p' < 0$, and

note that

$$Y\xi_{n,p} = \tilde{\mathrm{P}}\exp\left(ig\int_{-\infty}^{0} ds\; n\cdot A_{us}(x_s^\mu)\right)\xi_{n,p}^{+} = \mathrm{P}\exp\left(ig\int_{-\infty}^{0} ds\; n\cdot A_{us}(x_s^\mu)\right)\xi_{n,p}^{+} \equiv Y_{+}\xi_{n,p}^{+}\,, \tag{2.75}$$

$$\bar{\xi}_{n,p}Y^\dagger = \bar{\xi}_{n,p}^{+}\tilde{\mathrm{P}}'\exp\left(-ig\int_{\infty}^{0} ds\; n\cdot A_{us}(x_s^\mu)\right) = \bar{\xi}_{n,p}^{+}\mathrm{P}\exp\left(ig\int_{0}^{\infty} ds\; n\cdot A_{us}(x_s^\mu)\right) \equiv \bar{\xi}_{n,p}^{+}Y_{+}^\dagger\,,$$

$$Y\xi_{n,p'} = \tilde{\mathrm{P}}\exp\left(ig\int_{\infty}^{0} ds\; n\cdot A_{us}(x_s^\mu)\right)\xi_{n,p'}^{-} = \overline{\mathrm{P}}\exp\left(-ig\int_{0}^{\infty} ds\; n\cdot A_{us}(x_s^\mu)\right)\xi_{n,p'}^{-} \equiv Y_{-}\xi_{n,p'}^{-}\,,$$

$$\bar{\xi}_{n,p'}Y^\dagger = \bar{\xi}_{n,p'}^{-}\tilde{\mathrm{P}}'\exp\left(-ig\int_{-\infty}^{0} ds\; n\cdot A_{us}(x_s^\mu)\right) = \bar{\xi}_{n,p'}^{-}\overline{\mathrm{P}}\exp\left(-ig\int_{-\infty}^{0} ds\; n\cdot A_{us}(x_s^\mu)\right) \equiv \bar{\xi}_{n,p'}^{-}Y_{-}^\dagger\,.$$

This is in agreement with the $\tilde{Y} = Y_{-}$, $Y^\dagger = Y_{-}^\dagger$, $Y = Y_{+}$, $\tilde{Y}^\dagger = Y_{+}^\dagger$ used in [61] for the production and annihilation of antiparticles and the annihilation and production of particles respectively. The results in Eq. (2.75) reproduce the natural choice of having incoming quarks/antiquarks enter from $-\infty$, while outgoing quarks/antiquarks extend out to $+\infty$.

Although the choice in Eq. (2.74) agrees with the $i\epsilon$'s in Fig. 2-10 it causes complications in the attachments of usoft gluons to internal collinear propagators. With Eq. (2.74) we have $s_0^\dagger \neq \bar{s}_0$. Now the field redefinition still induces factors of $Y_{+}^\dagger Y_{-} = 1$ and $Y_{-}^\dagger Y_{+} = 1$ in production and annhilation terms in the collinear Lagrangian, but it also induces factors of $Y_{+}^\dagger Y_{+} = Y_\infty$ and $Y_{-}^\dagger Y_{-} = Y_\infty^\dagger$ in quark-quark and antiquark-antiquark terms in the action, where

$$Y_\infty = \mathrm{P}\exp\left(ig\int_{-\infty}^{+\infty} ds\; n\cdot A_{us}(x_s^\mu)\right). \tag{2.76}$$

When usoft gluons attach to a collinear propagator with endpoints x and y we must end up with a finite Wilson line $Y(x,y)$. In the original collinear Lagrangian (prior to the field redefinition) this finite Wilson line is generated by the time ordering of fields in the usoft gluon interaction vertices. If a field redefinition is made with boundary conditions satifying $s_0^\dagger = \bar{s}_0$ then the vertices bordering a collinear propagator induce Wilson lines whose s_0 dependence cancels, leaving this same finite Wilson line. For example, with $s_0 = -\infty$, $Y(-\infty,x)Y(-\infty,0)^\dagger = Y(0,x)$. A choice like that in

Eq. (2.74) is more complicated since it violates hermiticity: $(\xi_n)^\dagger = \xi_n^\dagger$ prior to the field redefinition, but this is no longer true for the ξ_n and $\bar{\xi}_n$ fields after the field redefinition. Correspondingly, the term in the action determining the free propagator depends on Y_∞. Thus, in this case there are Y factors in both the propagators and vertices which must be taken into account in order for the path ordering not to conflict with the result from time ordering, and give the same finite Wilson line.

Let's adopt the choice in Eq. (2.71) rather than Eq. (2.74) and check that the theory with the field redefinition in Eq. (2.45) still correctly reproduces the results in Fig. 2-10 for this case. Here we have $Y = Y_+$, $Y^\dagger = Y_-^\dagger$ for particles and antiparticles. Thus, the correct $i\epsilon$'s are obviously reproduced for the incoming collinear lines as well as intermediate propagator states. On the other hand, the result for an outgoing quark seems to have the wrong factor since $\bar{\xi}_n^+$ comes with a $Y_-^\dagger$ rather than a $Y_+^\dagger$. However, with the standard definition of an outgoing state there is actually an extra Y_∞ induced by the field redefinition on the out-state itself. When we take this factor into account we have $Y_\infty Y_-^\dagger = Y_+^\dagger$ as expected. To see this, recall that an outgoing collinear quark state ${}_{out}\langle \vec{p}|$ is generated by a suitably weighted integral over $\langle 0|\xi_n^+(x_T)$, in the large time limit $T \to \infty$ for $x_T = (T, \vec{x})$. When we make the field redefinition this field, $\xi_n^+(x_T)$ generates an usoft Wilson line which extends from our reference point $s_0 = -\infty$ to the $\bar{n}\cdot x$ point for our asymptotic outgoing state (which is $+\infty$ for $T \to \infty$), namely a factor of Y_∞. A similar argument applies for outgoing antiquark states, where we get $Y_+ Y_\infty^\dagger = Y_-$. The same considerations must also be made for hadronic bound states where they apply to the interpolating quark/antiquark fields used along with the LSZ formula to define the outgoing state. The factors of Y_∞ are universal, independent of which out-state we choose. There are no additional factors for our incoming states since our reference point and $T = -\infty$ coincide, $Y(-\infty, -\infty) = 1$. Once the Y_∞ factors are taken into account, the choice in Eq. (2.71) correctly reproduces the path for outgoing quark and antiquark lines. If we had instead made the choice for s_0 in Eq. (2.72) (which also satisfies $s_0^\dagger = \bar{s}_0$) then we would have $Y_\infty^{(\dagger)}$ factors for incoming antiquark states and outgoing quark states, but the final outcome is the same. Thus the complete result is independent of the s_0

choice.

The above discussion covers usoft interactions from the collinear Lagrangian, but it is also worth remarking on the interactions induced by the field redefinition in (possibly non-local) operators that are not time ordered. We continue to use Eq. (2.71). Here again, the identity $Y^\dagger Y = 1$ is important in order to prove the cancellation of usoft gluon attachments. It is convenient to adopt a convention where one collects the extra factors of Y_∞ induced from outgoing states together with the $Y^\dagger$'s from production fields in these operators. In this case if we consider $J(x) = \bar{\xi}_n^+ \bar{n}\!\!\!/ \xi_n^-$ for the production of a collinear quark and antiquark, then instead of writing only the $Y_-^\dagger$ and Y_+ from the fields we write $J \to \bar{\xi}_n^+ Y_+^\dagger \bar{n}\!\!\!/ Y_- \xi_n^- = \bar{\xi}_n^+ \bar{n}\!\!\!/ \xi_n^-$ which includes the Y's from any out-state this current could produce. Here the usoft interactions in the Y and $Y^\dagger$ lines extend from x to ∞ and cancel. For the annihilation of a quark and antiquark the lines extend from $-\infty$ to x and also cancel, namely $Y_-^\dagger Y_+ = 1$. These two cancellations are often sufficient to ensure the decoupling of usoft gluons. For example, in exclusive processes we must have color singlet combinations to connect to incoming or outgoing collinear hadrons and so we can typically pair up $\bar{\xi}_n^\pm$ and $\xi_n^\mp$ fields in the hard scattering operator and make the cancellations manifest.

If we instead consider an inclusive process like DIS then we have a quark scattered to a quark (we consider generic Bjorken $x < 1$ in the Breit frame). In this case including the Y_∞ from one outgoing quark in the final state gives $\bar{\xi}_n^+ \bar{n}\!\!\!/ \xi_n^+ \to \bar{\xi}_n^+ Y_+^\dagger \bar{n}\!\!\!/ Y_+ \xi_n^+$ where the Wilson lines do not seem to cancel. Here in order for the cancellation of usoft gluons to take place it is important to either a) take into account all factors of Y_∞ from the outgoing proton state, or b) include the Y_∞ from one outgoing quark state but note that we are only matching cut diagrams for this inclusive process. The choice a) or b) depends on whether we want to take the imaginary part at the very end, or from the beginning. For b) the effective theory computation has the imaginary part of the hard computation, but the imaginary part also effects the collinear operator, where we can denote the cut by a vertical line, $|$. With our initial state for the T-matrix taken on the RHS of the cut, the signs are as in Fig. 2-10, but on the LHS we have the complex conjugate of these expressions, and the above computation

becomes

$$(\bar{\xi}_n)\big|(\bar{n}\!\!\!/\xi_n) \to (\bar{\xi}_n Y_-^\dagger)\big|(\bar{n}\!\!\!/ Y_+\xi_n) = \bar{\xi}_n\, \bar{n}\!\!\!/\, \xi_n\,. \tag{2.77}$$

Thus, the usoft gluon interactions also cancel in this case. Alternatively, with a) one must keep track of all the lines in the full forward scattering calculation including $Y_\infty^{(\dagger)}$ factors from all initial and/or final state quarks, and then the Y's in the low energy theory again all cancel. Both ways we arrive at the same final result, $(\mathrm{Im}\, C)\bar{\xi}_n \bar{n}\!\!\!/\xi_n$ (see Refs. [14, 122] for a discussion of DIS in SCET). Similar considerations can be applied to $B \to X_s\gamma$ in the endpoint region. The s_0 dependence cancels, and for this process we are left with a finite usoft Wilson line, $\bar{h}_v(x)Y(x,0)h_v(0)$.

To summarize, keeping careful track of the boundary condition s_0 dependence in the usoft Wilson line Y, a choice satisfying $s_0 = \bar{s}_0^\dagger$ appears to be the most natural (even though there will be additional Y_∞ factors from states). Physical results are independent of the choice made for the s_0 reference point. They may still depend on the path of Wilson lines in the final result, but this is determined by the universal class of processes described by the operator rather than the choice of s_0 in the field redefinition. Similar conclusions hold for the path dependence in collinear Wilson lines W. We note that with respect to the definitions of the gauge invariant structures made in Eq.(2.50), the remaining allowed global color rotations simply correspond to color rotations at the reference point. We will pick the same reference point in W and Y factors. For example, the gauge invariant product of fields $(Y^\dagger h_v)$ carries a color index in the **3** representation, which by convention is acted on by global rotations $U(s_0)$, via $(Y^\dagger h_v) \to U(s_0)(Y^\dagger h_v)$. These color rotations still connect invariant products of collinear and usoft fields.

2.5 Soft-collinear effective theory II

The focus of section 2.4 was $\mathrm{SCET_I}$, which can be used to analyze B decays involving energetic inclusive hadronic jets, such as $B \to X_s\gamma$ and $B \to X_u\ell\bar{\nu}$ in the endpoint

region. SCET is also a powerful theoretical tool for separating scales at and below m_b in B decays to final states with *exclusive* energetic hadrons. The subject of Chapter 4 is the decay $B \to M_1 M_2$ where M_1 and M_2 are light pseudoscalar or vector mesons (π, ρ, K, $K^* \ldots$), and this section is meant to provide the additional necessary background. As in the inclusive case, exclusive B-decay amplitudes are most easily calculated in the B rest frame where non-perturbative modes with typical momenta $\sim \Lambda$ interpolate for the initial state B. In $B \to M_1 M_2$, the final state hadrons M_1 and M_2 are back-to-back with energy $E_M \approx m_B/2 \gg \Lambda_{\rm QCD}$. Collinear fields in the light-like direction n interpolate for one light meson, and collinear fields in the opposite direction $\bar{n}$ interpolate for the other. Unlike the SCET_I collinear modes, which have $p_c^2 \sim Q\Lambda_{\rm QCD}$, these collinear modes are non-perturbative with $p_c^2 \sim \Lambda_{\rm QCD}^2$ since they interpolate for exclusive light hadrons with $m_M \sim \Lambda_{\rm QCD}$. They are contained in an effective theory called SCET_II [23]. We begin by describing the SCET_II degrees of freedom, power counting, and Lagrangian.

2.5.1 Degrees of freedom and Lagrangian

This section parallels the development of the SCET_I degrees of freedom in section 2.4.1, skipping many of the steps presented there, but emphasizing the most important differences between SCET_I and SCET_II. Consider a light meson M with $m_M \sim \Lambda$ where $\Lambda \sim \Lambda_{\rm QCD} \approx 300\text{GeV}$ is the non-perturbative/hadronic scale of QCD. In M's rest frame, $p_M = (m_M, 0, 0, 0)$, the constituent partons of M – gluons and light quarks and anti-quarks – have homogeneous typical momenta $\sim \Lambda$. As in SCET_I, we decompose four-vectors into light-cone components $(p^+, p^-, p^\perp)$ using auxiliary vectors $n = (1, 0, 0, 1)$ and $\bar{n} = (1, 0, 0, -1)$ as in Eq. (2.24). The meson momentum has components $(m_M, m_M, 0)$ and the typical parton momentum is $(\Lambda, \Lambda, \Lambda)$. Now boost M by a factor $e^\alpha = Q/m_M$ in the $+z$ direction, keeping the same n and $\bar{n}$. Then p_M has light-cone components $(m_M^2/Q, Q, 0)$. The constituent partons of the boosted M are described by boosted versions of rest-frame constituent fields. Their typical momenta are

$$(\Lambda, \Lambda, \Lambda) \to (m_M \Lambda/Q, \Lambda Q/m_M, \Lambda) \sim Q(\eta^2, 1, \eta) \tag{2.78}$$

where $\eta \sim \Lambda/Q$ is the SCET_{II} power-counting parameter and we take $m_M \sim \Lambda$. SCET_{II} n-collinear quarks and gluons have $p_n \sim Q(\eta^2, 1, \eta)$ and interpolate for the n-boosted meson M. In $B \to M_1 M_2$ we also need nearly-light-like non-perturbative modes in the opposite direction to interpolate for the other final-state meson. $\bar{n}$-collinear momenta scale like $Q(1, \eta^2, \eta)$. (Technically, we use n_1 and n_2 to mean the physical directions of the light hadrons, information contained in external states. In that case, n and $\bar{n}$ define directions of SCET operators and we sum over all distinct n in the effective theory.) Just like in SCET_{I}, collinear fields in SCET_{II} are labeled by their collinear direction and their large momenta, and the x dependence of the labeled fields carries the residual momentum dependence.

To reproduce the infrared structure of QCD, we will also need to include modes with homogeneous momentum components $\sim \Lambda$, SCET_{II} versions of the ultrasoft modes in SCET_{I}, which will again interpolate for the initial state B. In terms of the SCET_{II} power-counting parameter, however, these modes have typical momenta $\sim Q\eta$ so we call them soft instead of ultrasoft. Soft modes have an $n \cdot p_s \sim Q\eta$ component which is parametrically larger than $n \cdot p_n \sim \eta^2$, and a $\bar{n} \cdot p_s \sim Q\eta$ component which is parametrically larger than $\bar{n} \cdot p_{\bar{n}} \sim \eta^2$. To maintain manifest power counting in the effective theory, we split *soft* momenta up into large label and small residual pieces, much in the same way that we did for collinear momenta. We even introduce a soft label operator that behaves in an analagous manner to the collinear label operator. We use the same symbol $\mathcal{P}$, but it is always clear which label operator is meant by the context.

In contrast to SCET_{I}, all SCET_{II} modes are non-perturbative, $p_n^2 \sim p_{\bar{n}}^2 \sim p_s^2 \sim \Lambda^2$. They are well-separated, however, in a variable

$$\zeta_p \equiv p^-/p^+ . \tag{2.79}$$

The SCET_{II} degrees of freedom needed for $B \to M_1 M_2$ are summarized in Table 2.2 and Figure 2-11.

Recall that in SCET_{I}, an ultrasoft and collinear momentum sum to a collinear

Type	$(p^+, p^-, p^\perp)$	ζ_p	Fields	Scaling
n-collinear	$Q(\eta^2, 1, \eta)$	η^{-2}	$\xi_{n,p}$	η
			$(A^+_{n,p},\ A^-_{n,p},\ A^\perp_{n,p})$	$(\eta^2,1,\eta)$
$\bar{n}$-collinear	$Q(1, \eta^2, \eta)$	η^2	$\xi_{\bar{n},p}$	η
			$(A^+_{\bar{n},p},\ A^-_{\bar{n},p},\ A^\perp_{\bar{n},p})$	$(1,\eta^2,\eta)$
soft	$Q(\eta, \eta, \eta)$	η^0	q_s, h_v	$\eta^{3/2}$
			A^μ_s	$\eta^{3/2}$

Table 2.2: Power counting for $\mathrm{SCET_{II}}$ fields.

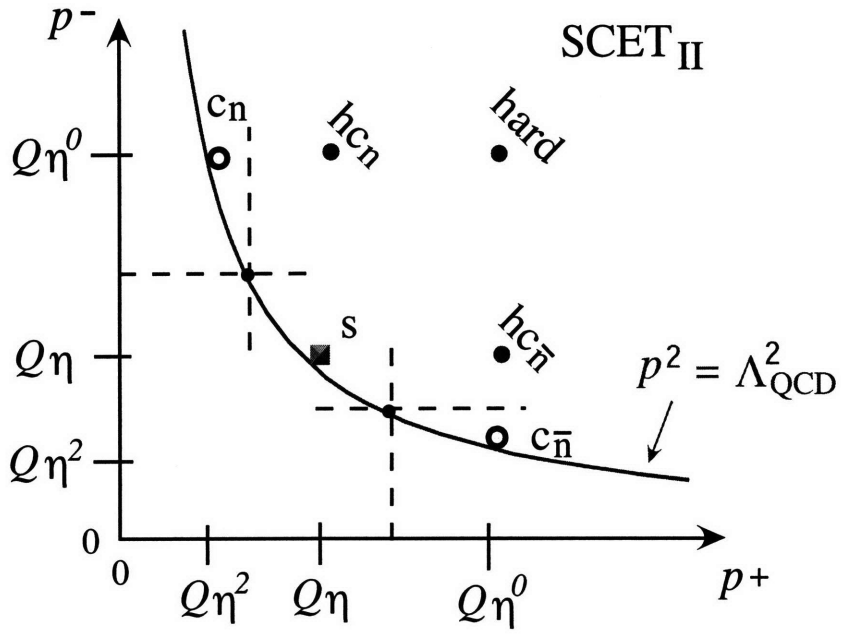

Figure 2-11: Degrees of freedom and momentum regions for $\mathrm{SCET_{II}}$ for $B \to M_1 M_2$: n-collinear (c_n), soft (s), and $\bar{n}$-collinear ($c_{\bar{n}}$). All three lie on the solid (red) curve $p^2 = p^+ p^- = \Lambda^2_{\mathrm{QCD}}$. Also shown (in pink) are three regions of perturbative momenta, two with hard-collinear momenta (hc_n, $hc_{\bar{n}}$) and one where the momenta are hard. Figure from Ref. [124].

momentum $(\lambda^2, 1, \lambda) + (\lambda^2, \lambda^2, \lambda^2) \sim (\lambda^2, 1, \lambda)$. In $\mathrm{SCET_{II}}$, adding a soft and an n-collinear momentum gives a perturbative *n-hard-collinear* momentum, $p_{hc-n} \sim p_s + p_n \sim Q(\eta, 1, \eta)$ with $p^2_{n-hc} \sim Q\Lambda$, that lives *outside* the theory $\mathrm{SCET_{II}}$. This greatly restricts the form of soft-collinear interactions in $\mathrm{SCET_{II}}$, which must conserve both soft and collinear label momenta. All soft-collinear interactions within $\mathrm{SCET_{II}}$ must involve two or more soft fields and two or more collinear fields of the same type. Interactions via perturbative hard-collinear parton exchange are treated

perturbatively in $\mathrm{SCET_I}$, and interactions via perturbative hard parton propagators are treated in the full theory, QCD.

$\mathrm{SCET_{II}}$ for exclusive B decays is obtained by a two-step matching procedure [24]. First, QCD is matched onto $\mathrm{SCET_I}$ at a scale $\mu \sim m_b$, as described in section 2.4. The BPS field redefinition [22], Eq. (2.45), moves all usoft-collinear interactions into ultrasoft Wilson lines Y and $Y^\dagger$ in operators. At the intermediate (hard-collinear) scale $\mu \sim \sqrt{Q\Lambda}$, we perform a perturbative matching of $\mathrm{SCET_I}$ with usoft and collinear fields, onto $\mathrm{SCET_{II}}$ with soft and collinear fields. For local operators, the matching simply means renaming ultrasoft fields soft, and changing the scalings of fields and momenta accordingly. Examples of such a local matching are given in sections 4.3 and 4.5. Matching $\mathrm{SCET_I}$ time-ordered products onto $\mathrm{SCET_{II}}$ is a little trickier. One must contract gauge-invariant blocks of fields in $\mathrm{SCET_I}$ to ensure gauge invariance in the $\mathrm{SCET_{II}}$ operator. An example of this sort of matching is carried out for a class of η-suppressed contributions to the $B \to M_1 M_2$ amplitude in section 4.4.

Chapter 3

Heavy-to-light currents in SCET

3.1 Introduction

Heavy-to-light currents, $J = \bar{q}\Gamma b$, are important for describing a broad range of processes with SCET, including both inclusive semileptonic and radiative decays like $B \to X_u \ell \bar{\nu}$ and $B \to X_s \gamma$ [13, 15, 22, 17, 45, 111, 46, 34, 109, 62], exclusive semileptonic and radiative decays such as $B \to \pi \ell \bar{\nu}$ and $B \to K^* \gamma$ [15, 59, 35, 23, 130, 58, 37, 108, 87, 29], and exclusive hadronic decays like $B \to \pi\pi$ [60, 19, 31, 79]. Here, we consider higher order RPI relations for heavy-to-light currents in SCET_I with ultrasoft and collinear fields.

RPI constraints on subleading Lagrangians and tree-level currents to $\mathcal{O}(\lambda^2)$ were derived in Ref. [35] (and verified in [111] for a basis with $v_\perp \neq 0$). At $\mathcal{O}(\lambda)$, the extension to a complete set of heavy-to-light currents constrained by RPI relations including currents that appear beyond tree-level was made in Ref. [130]. At this order, all Wilson coefficients are constrained by RPI except for one scalar, four vector, and six tensor currents, for which the one-loop matching was done in Ref. [39] and independently in Ref. [28]. For the currents that survive for $v_\perp = 0$, the $\mathcal{O}(\lambda)$ RPI relations were verified in Ref. [96]. To simplify the computation, they considered constraints restricted to the projected $v_\perp = 0$ surface (from the RPI-$\star$ transformation defined earlier in section 2.4.4) since this involves writing down fewer operators. At $\mathcal{O}(\lambda^2)$, the allowed set of field structures for the heavy-to-light currents was deter-

mined in Ref. [34]. Four-quark operator currents first appear at this order.[1] The type-II RPI invariance was extended to include light quark mass effects and provide constraints on certain m_q dependent operators [62].

Our main objective in this chapter is to derive the complete basis of currents at $\mathcal{O}(\lambda^2)$ by constructing a basis that is valid at any order in perturbation theory and including all RPI relations. Results are derived for use in the $v_\perp = 0$ frame (and we take $m_q = 0$ in all currents). For the $\mathcal{O}(\lambda^2)$ heavy-to-light currents, we show that transformations on the projected surface $v_\perp = 0$ give the complete set of relations for currents defined on this surface (see section 3.2.4). By eliminating the field operators we show that it is convenient to consider the RPI relations as constraint equations of the form

$$\sum_{i,k} B_i(\omega_k)\, \Gamma_i^B = \sum_{j,\ell} C_j(\omega_\ell)\, \Gamma_j^C \,, \tag{3.1}$$

where B_i and Γ_i^B are Wilson coefficients and Dirac structures for operators that appear at some fixed order in λ, and C_j and Γ_i^C are terms that appeared in operators from lower orders. By deriving these constraint equations in section 3.2.2 prior to searching for their solutions, it becomes easier to simultaneously consider the restrictions imposed by the five different types of RPI invariance from both SCET and HQET, since each gives a separate constraint. A simple counting procedure is given for determining all possible Dirac structures prior to imposing the RPI conditions. The solution of the constraint equations in section 3.2.3 give relations between the B_i and C_j coefficients and determine the allowed Dirac structures Γ_i^B in terms of Γ_j^C.

[1] In the most common decomposition the Wilson coefficients of the four quark operators start at $\mathcal{O}(\alpha_s^2)$, so these operators are not needed if the basis is restricted to LO in $\alpha_s(m_b)$, such as in Ref. [111].

3.2 Heavy-to-light currents to $\mathcal{O}(\lambda^2)$

To order λ^2, the operators and Wilson coefficients for the heavy-to-light currents can be written as

$$\begin{aligned} J = \quad & J^{(0)} + J^{(1)} + J^{(2)} \\ = \quad & \sum_j \int d\omega\, C_j(\omega, m, \mu) J_j^{(0)}(\omega, \mu) + \sum_{x,j} \int [d\omega_i]\, B_{xj}(\omega_i, m, \mu) J_j^{(1x)}(\omega_i, \mu) \\ & + \sum_{x,j} \int [d\omega_i]\, A_{xj}(\omega_i, m, \mu) J_j^{(2x)}(\omega_i, \mu), \end{aligned} \tag{3.2}$$

where $J^{(kx)}(\omega_i)$ represents the $\mathcal{O}(\lambda^k)$ terms with dependence on convolution parameters ω_i. Here the subscript x distinguishes distinct field structures at a given order, and j sums over distinct Dirac structures. At $\mathcal{O}(\lambda)$ we know that there are at most two relevant convolution parameters $i = 1, 2$, while we will see below that at $\mathcal{O}(\lambda^2)$ there are at most three. We will consider both scalar, vector, and tensor currents (and the simple extension to the pseudoscalar and axial vector cases). When necessary we add an (s), (v), or (t) superscript to the Wilson coefficients in order to distinguish these cases, e.g. $B_{a1}^{(v)}$.

We begin in section 3.2.1 by constructing all consistent field structures for the NNLO currents. In section 3.2.2 we use reparameterization invariance to derive the constraint equations for these currents under different types of RPI invariance on the $v_\perp = 0$ surface. In section 3.2.3 we solve the constraint equations to find the allowed Dirac structures and obtain relations among the Wilson coefficients. Finally, in section 3.2.4 we show that the results from the $v_\perp = 0$ surface are equivalent to those obtained if all relations in the full space were projected onto this plane.

3.2.1 Current field structures at $\mathcal{O}(\lambda^2)$

We first construct a basis of currents that is consistent with gauge invariance and power counting and eliminate structures that are redundant by the equations of mo-

tion and Bianchi identity. At LO and NLO the currents are

$$\begin{aligned} J^{(0)}(\omega) &= \bar{\chi}_{n,\omega}\Gamma\mathcal{H}_v\,, \\ J^{(1a)}(\omega) &= \frac{1}{\omega}\,\bar{\chi}_{n,\omega}\mathcal{P}_\alpha^{\perp\dagger}\Theta_{(a)}^\alpha\mathcal{H}_v \\ J^{(1b)}(\omega_{1,2}) &= \frac{1}{m}\,\bar{\chi}_{n,\omega_1}(ig\mathcal{B}_\alpha^\perp)_{\omega_2}\Theta_{(b)}^\alpha\mathcal{H}_v\,. \end{aligned} \tag{3.3}$$

At NNLO we find that a convenient basis for the set of field structures for the bilinear quark operators is

$$\begin{aligned} J^{(2a)}(\omega) &= \frac{1}{2m}\,\bar{\chi}_{n,\omega}\Upsilon_{(a)}^\sigma iD_{us\,\sigma}^T\mathcal{H}_v\,, \\ J^{(2b)}(\omega) &= -\frac{n\cdot v}{\omega}\,\bar{\chi}_{n,\omega}\,i\bar{n}\cdot\overleftarrow{D}_{us}\Upsilon_{(b)}\mathcal{H}_v\,, \\ J^{(2c)}(\omega) &= -\frac{1}{\omega}\,\bar{\chi}_{n,\omega}i\overleftarrow{D}_{us\,\alpha}^\perp\Upsilon_{(c)}^\alpha\mathcal{H}_v\,, \\ J^{(2d)}(\omega) &= \frac{1}{\omega^2}\,\bar{\chi}_{n,\omega}\mathcal{P}_\alpha^{\perp\dagger}\mathcal{P}_\beta^{\perp\dagger}\Upsilon_{(d)}^{\alpha\beta}\mathcal{H}_v\,, \\ J^{(2e)}(\omega_{1,2}) &= \frac{1}{m(\omega_1+\omega_2)}\,\bar{\chi}_{n,\omega_1}(ig\mathcal{B}_\alpha^\perp)_{\omega_2}\mathcal{P}_\beta^{\perp\dagger}\Upsilon_{(e)}^{\alpha\beta}\mathcal{H}_v\,, \\ J^{(2f)}(\omega_{1,2}) &= \frac{\omega_2}{m(\omega_1+\omega_2)}\,\bar{\chi}_{n,\omega_1}\left(\frac{\mathcal{P}_\beta^\perp}{\omega_2}+\frac{\mathcal{P}_\beta^{\perp\dagger}}{\omega_1}\right)(ig\mathcal{B}_\alpha^\perp)_{\omega_2}\Upsilon_{(f)}^{\alpha\beta}\mathcal{H}_v\,, \\ J^{(2g)}(\omega_{1,2}) &= \frac{1}{m\,n\cdot v}\,\bar{\chi}_{n,\omega_1}\left\{(ign\cdot\mathcal{B})_{\omega_2}+2(ig\mathcal{B}_\perp)_{\omega_2}\cdot\mathcal{P}_\perp^\dagger\frac{1}{\bar{\mathcal{P}}^\dagger}\right\}\Upsilon_{(g)}\mathcal{H}_v\,, \\ J^{(2h)}(\omega_{1,2,3}) &= \frac{1}{m(\omega_2+\omega_3)}\,\bar{\chi}_{n,\omega_1}(ig\mathcal{B}_\beta^\perp)_{\omega_2}(ig\mathcal{B}_\alpha^\perp)_{\omega_3}\Upsilon_{(h)}^{\alpha\beta}\mathcal{H}_v\,, \\ J^{(2i)}(\omega_{1,2,3}) &= \frac{1}{m(\omega_2+\omega_3)}\mathrm{Tr}[(ig\mathcal{B}_\beta^\perp)_{\omega_2}(ig\mathcal{B}_\alpha^\perp)_{\omega_3}]\,\bar{\chi}_{n,\omega_1}\Upsilon_{(i)}^{\alpha\beta}\mathcal{H}_v\,. \end{aligned} \tag{3.4}$$

For a basis of four quark operators we take

$$\begin{aligned} J^{(2j)}(\omega_1,\omega_2,\omega_3) &= \sum_{f=u,d,s}\left[\bar{\chi}_{n,\omega_2}^f\Upsilon_{(j\chi)}\chi_{n,\omega_3}^f\right]\left[\bar{\chi}_{n,\omega_1}\Upsilon_{(j\mathcal{H})}\mathcal{H}_v\right], \\ J^{(2k)}(\omega_1,\omega_2,\omega_3) &= \sum_{f=u,d,s}\left[\bar{\chi}_{n,\omega_2}^f T^A\Upsilon_{(k\chi)}\chi_{n,\omega_3}^f\right]\left[\bar{\chi}_{n,\omega_1}T^A\Upsilon_{(k\mathcal{H})}\mathcal{H}_v\right] \end{aligned} \tag{3.5}$$

where the matrices T^A are generators of SU(3) with an implied sum on A and χ_n^f has a collinear quark with flavor f, whereas χ_n carries the flavor of quark from the full theory current. We impose the RPI type-III invariance in Eq. (2.62) on all operators by multiplying by an appropriate power of $n\cdot v$. The basis in Eqs. (3.3,3.4,3.5) is valid whether or not we take $v_\perp = 0$. The $v_\perp = 0$ choice only effects the basis of Dirac structures.

The 11 operators in Eqs. (3.4,3.5) can be compared with the 15 field structures in the basis of Ref. [34]. We have no analog of their $J^{(2)}_{1,2,3,7}$ currents which have an explicit x^μ because with momentum labels the multipole expansion is performed directly in momentum space [119]. Correspondingly, our $J^{(2b)}$ and $J^{(2c)}$ currents have no analogs in their basis. There is a correspondence, $J^{(2a,2d)} \leftrightarrow J^{(2)}_{4,6}$, $J^{(2e,2f,2g)} \leftrightarrow J^{(2)}_{8,9,10}$, $J^{(2i,2j,2k)} \leftrightarrow J^{(2)}_{13,14,15}$, and our $J^{(2h)}$ encodes their $J^{(2)}_{12}$ and $J^{(2)}_{13}$ currents.

In arriving at Eq. (3.4) we have used Eq. (2.48) to switch to a basis with $\mathcal{P}_\perp$'s, $in\cdot\partial$, and field strengths rather than collinear covariant derivatives in order to give simpler constraints from RPI. The basis with covariant derivatives is more natural from the point of view of tree level matching and the relation between the two is discussed in section 3.3. The prefactors in $J^{(2a-2i)}$ have been chosen with these relationships in mind, in order to make the matching coefficients for the operators simple. The combinations in $J^{(2f,2g)}$ were chosen because they have simpler transformations under RPI.

Structures were also removed from Eq. (3.4) using equations of motion and the Bianchi identity. In the effective field theory this gives a valid basis at any loop order. After decoupling the usoft gluons the LO Lagrangian for collinear quarks is [22]

$$\mathcal{L}_c^{(0)} = \bar\xi_n \frac{\bar n\!\!\!/}{2}\Big(in\cdot D_c + i\not{D}_c^\perp W\frac{1}{\bar{\mathcal{P}}}W^\dagger i\not{D}_c^\perp\Big)\xi_n = \bar\chi_n\frac{\bar n\!\!\!/}{2}\Big(in\cdot\mathcal{D}_c + i\not{D}_c^\perp\frac{1}{\bar{\mathcal{P}}}i\not{D}_c^\perp\Big)\chi_n\,, \quad (3.6)$$

so the equation of motion for χ_n can be written

$$in\cdot\partial\chi_n = -(ign\cdot\mathcal{B})\chi_n - i\not{D}_c^\perp\frac{1}{\bar{\mathcal{P}}}i\not{D}_c^\perp\chi_n\,, \quad (3.7)$$

where using Eq. (2.48) the last term can be written as a sum of terms with either

two $\mathcal{P}_\perp$'s, two $(ig\mathcal{B}_\perp)$'s, or one of each. Eq. (3.7) shows that a a current $\bar{\chi}_n in\cdot\overleftarrow{\partial}\, hc\mathcal{H}_v$ is redundant by the collinear quark equation of motion and need not be included in the list, explaining why we only have $J^{(2b)}$ and $J^{(2c)}$. (Note that $in\cdot\mathcal{D}_{us}\chi_n = in\cdot\partial\chi_n$.) As noted in [34], this makes their $J_5^{(2)}$ current redundant. In $J^{(2a)}$ we have restricted the ultrasoft derivative acting on h_v to be purely transverse since the heavy quark equation of motion is $v\cdot D_{us}\, h_v{=}0$.

One can also consider using the collinear gluon equation of motion. After the field redefinition in Eq. (2.45), the lowest order collinear gluon Lagrangian is the same as in QCD [22], $\mathcal{L}_g^{(0)} = 1/(2g^2)\ \mathrm{tr}\{[iD_c^\mu, iD_c^\nu]\}^2$. Varying $\mathcal{L}_c^{(0)} + \mathcal{L}_g^{(0)}$ with respect to the collinear gluon field $A_{c\mu}^A$ and contracting with $\bar{n}_\mu T^A$ gives

$$0 = \bar{n}_\mu T^A \frac{\delta\mathcal{L}^{(0)}}{\delta A_{c\mu}^A} = \frac{1}{g}\bar{n}_\mu\,[iD_{c\nu}, [iD_c^\mu, iD_c^\nu]] + gT^A \sum_f \bar{\xi}_n^f T^A \frac{\bar{n}\!\!\!/}{2}\xi_n^f\,. \tag{3.8}$$

Next we multiply by $W^\dagger$ on the left and W on the right, use the identity $(W^\dagger T^A W)\otimes T^A = T^A\otimes(WT^AW^\dagger)$, and label by ω_2 to give

$$\begin{aligned} -g^2 T^A \sum_f \big[\bar{\chi}_n^f\, T^A \frac{\bar{n}\!\!\!/}{2}\chi_n^f\big]_{\omega_2} &= \big(\,[i\mathcal{D}_{c\nu}, [i\bar{n}\cdot\mathcal{D}_c, i\mathcal{D}_c^\nu]]\,\big)_{\omega_2} \\ &= \frac{\omega_2^2}{2}(ign\cdot\mathcal{B})_{\omega_2} - \omega_2\mathcal{P}_\nu^\perp(ig\mathcal{B}_\perp^\nu)_{\omega_2} - \sum_{\omega_3}\omega_3\big[(ig\mathcal{B}_\perp^\nu)_{\omega_2-\omega_3}, (ig\mathcal{B}_\nu^\perp)_{\omega_3}\big]\,. \end{aligned} \tag{3.9}$$

Multiplying by $\bar{\chi}_{n,\omega_1}$ on the left and $\Gamma\mathcal{H}_v$ on the right where Γ is some Dirac structure gives

$$\begin{aligned} \frac{\omega_2^2}{2}\,\bar{\chi}_{n,\omega_1}(ign\cdot\mathcal{B})_{\omega_2}\Gamma\mathcal{H}_v &= -g^2\sum_{f,\omega_3}\big[\bar{\chi}_{n,\omega_2-\omega_3}^f T^A\frac{\bar{n}\!\!\!/}{2}\chi_{n,\omega_3}^f\big]\big[\bar{\chi}_{n,\omega_1}T^A\Gamma\mathcal{H}_v\big] \\ &\quad + \omega_2\,\bar{\chi}_{n,\omega_1}\mathcal{P}_\nu^\perp(ig\mathcal{B}_\perp^\nu)_{\omega_2}\Gamma\mathcal{H}_v + \sum_{\omega_3}\omega_3\,\bar{\chi}_{n,\omega_1}\big[(ig\mathcal{B}_\perp^\nu)_{\omega_2-\omega_3}, (ig\mathcal{B}_\nu^\perp)_{\omega_3}\big]\Gamma\mathcal{H}_v\,. \end{aligned} \tag{3.10}$$

This result can be used to eliminate the current $J^{(2g)}(\omega_{1,2})$ in terms of $J^{(2e)}$ and $J^{(2k)}$ if desired. We have chosen not to remove this operator since doing so would induce a tree level matching contribution for $J^{(2k)}$. For listing results it was more convenient to leave all four quark operators with coefficients that start at one-loop order, $\mathcal{O}(\alpha_s^2)$.

Since Eq. (3.10) eliminates a current that will not show up in the constraint equations it does not effect the discussion of RPI relations.

The Bianchi identity in QCD is $D_\mu G_{\nu\sigma} + D_\nu G_{\sigma\mu} + D_\sigma G_{\mu\nu} = 0$. It can be used to eliminate terms proportional to $igB^{\mu\nu}_{\perp\perp} \equiv [iD^\mu_\perp, iD^\nu_\perp]$ or

$$ig\mathcal{B}^{\mu\nu}_{\perp\perp} \equiv \left[\frac{1}{\bar{\mathcal{P}}} W^\dagger igB^{\mu\nu}_{\perp\perp} W\right], \tag{3.11}$$

in terms of factors of $ig\mathcal{B}^\lambda_\perp$ or $igB^\lambda_\perp = [i\bar{n}\cdot D, iD^\lambda_\perp]$. The Bianchi identity gives $[\bar{n}\cdot D, B^{\mu\nu}_{\perp\perp}] = [D^\mu_\perp, B^\nu_\perp] - [D^\nu_\perp, B^\mu_\perp]$ so using Eq. (2.48) we have

$$(ig\mathcal{B}^{\mu\nu}_{\perp\perp}) = \frac{\mathcal{P}^\mu_\perp}{\bar{\mathcal{P}}}(ig\mathcal{B}^\nu_\perp) - \frac{\mathcal{P}^\nu_\perp}{\bar{\mathcal{P}}}(ig\mathcal{B}^\mu_\perp) + \frac{1}{\bar{\mathcal{P}}^2}\left[(ig\mathcal{B}^\mu_\perp), (\bar{\mathcal{P}} ig\mathcal{B}^\nu_\perp)\right] - \frac{1}{\bar{\mathcal{P}}^2}\left[(ig\mathcal{B}^\nu_\perp), (\bar{\mathcal{P}} ig\mathcal{B}^\mu_\perp)\right] \tag{3.12}$$

Thus a heavy-to-light current with $(ig\mathcal{B}^{\mu\nu}_{\perp\perp})$ can be matched onto a linear combination of $J^{(2f,2e)}$ and $J^{(2h)}$ with antisymmetric indices in $\Upsilon^{\alpha\beta}_{(h)}$.

3.2.2 Constraint equations from reparameterization invariance

We derive constraint equations for the allowed subleading currents considering the different types of RPI in turn.

RPI-$\star$ at $\mathcal{O}(\lambda)$

To set the stage we review the constraints at $\mathcal{O}(\lambda)$ from SCET RPI. To ensure that the next-to-leading order current is RPI-$\star$ invariant, we must have

$$\delta^{(\lambda^1)}_\star J^{(0)} + \delta^{(\lambda^0)}_\star J^{(1)} = 0. \tag{3.13}$$

Computing the various terms in this equation gives[2]

$$\begin{aligned}
\delta_\star^{(\lambda^1)} J^{(0)}(\omega) &= \bar{\chi}_{n,\omega}\Big(\frac{1}{4}\not{\bar{n}}\not{\Delta}_\perp\Gamma + \delta_\star^{(\lambda^1)}\Gamma\Big)\mathcal{H}_v\,, \\
\delta_\star^{(\lambda^0)} J^{(1a)}(\omega) &= \frac{1}{\omega}\bar{\chi}_{n,\omega}\Big(-\frac{1}{2}\Delta_\alpha^\perp\overline{\mathcal{P}}^\dagger\Big)\Theta_{(a)}^\alpha\mathcal{H}_v\,, \\
\delta_\star^{(\lambda^0)} J^{(1b)}(\omega_{1,2}) &= 0.
\end{aligned} \tag{3.14}$$

The terms that must cancel all have a common dependence on $\bar{\chi}_{n,\omega}$, $\Delta_\alpha^\perp$, and $\mathcal{H}_v$ which can be factored out. The remaining coefficients and Dirac structures give the constraint equation:

$$\boxed{\sum_j B_{aj}(\omega)\Theta_{(aj)}^\alpha = \sum_j C_j(\omega)\Big(\frac{1}{2}\frac{\not{\bar{n}}}{\bar{n}\cdot v}\gamma_\perp^\alpha\Gamma_{(j)} + 2\delta_\star^\alpha\Gamma_{(j)}\Big)} \tag{3.15}$$

where the index α is $\perp$, j sums over Dirac structures, and $\delta_\star^\alpha\Gamma_{(j)}$ is defined through

$$\delta_\star^{(\lambda^1)}\Gamma_{(j)} = \frac{1}{n\cdot v}\,\Delta_\alpha^\perp\delta_\star^\alpha\Gamma_{(j)}\,. \tag{3.16}$$

RPI-\$ at $\mathcal{O}(\lambda^2)$

The only terms in the current whose transformation under RPI-\$ leaves uncanceled terms are $J^{(0)}$ and $J^{(2a)}$. We must have

$$\delta_\$^{(\lambda^2)} J^{(0)} + \delta_\$^{(\lambda^0)} J^{(2a)} = 0. \tag{3.17}$$

Now,

$$\begin{aligned}
\delta_\$^{(\lambda^2)} J^{(0)}(\omega) &= \bar{\chi}_n\big[-n\cdot\beta_T\,\overline{\mathcal{P}}^\dagger\delta'(\omega - n\cdot v\overline{\mathcal{P}}^\dagger)\big]\Gamma\mathcal{H}_v + \bar{\chi}_{n,\omega}\Big[\delta_\$^{(\lambda^2)}\Gamma + \frac{\Gamma\not{\beta}_T}{2}\Big]\mathcal{H}_v\,, \\
\delta_\$^{(\lambda^0)} J^{(2a)}(\omega) &= \frac{1}{2m}\bar{\chi}_{n,\omega}\Upsilon_{(a)}^\sigma(-m\beta_\sigma^T)\mathcal{H}_v.
\end{aligned} \tag{3.18}$$

[2]Note the remark on our use of notation at the end of section 2.4.4 that explains why we do not include the transformation of Y.

Suppressing the common fields $\bar{\chi}_{n,\omega}$, $\mathcal{H}_v$, and vector β_T^σ leads to the constraint equation

$$\boxed{\sum_j A_{aj}(\omega)\Upsilon^\sigma_{(aj)} = \sum_j \left\{ C_j(\omega)\big(2\delta^\sigma_\$\Gamma_{(j)} + \Gamma_{(j)}\gamma_T^\sigma\big) + 2\omega\frac{d}{d\omega}C_j(\omega)\,\frac{n_T^\sigma}{n\cdot v}\Gamma_{(j)}\right\},} \tag{3.19}$$

where

$$\delta_\$^{(\lambda^2)}\Gamma_{(j)} = \beta_\sigma^T\delta^\sigma_\$\Gamma_{(j)} \qquad \text{and} \qquad \gamma_T^\sigma = \gamma^\sigma - \not{v}v^\sigma. \tag{3.20}$$

SCET RPI-a at $\mathcal{O}(\lambda^2)$

The terms in the current that transform under SCET RPI-a are $J^{(0)}$, $J^{(1a)}$, $J^{(2b)}$, and $J^{(2c)}$. We must have

$$\delta_a^{(\lambda^2)}J^{(0)} + \delta_a^{(\lambda^1)}J^{(1a)} + \delta_a^{(\lambda^0)}J^{(2b)} + \delta_a^{(\lambda^0)}J^{(2c)} = 0. \tag{3.21}$$

Now,

$$\begin{aligned}
\delta_a^{(\lambda^2)}J^{(0)}(\omega) &= \bar{\chi}_n\big[-n\cdot v\,\bar{n}\cdot\ell\,\delta'(\omega - n\cdot v\overline{\mathcal{P}}^\dagger)\big]\Gamma\mathcal{H}_v\,,\\
\delta_a^{(\lambda^1)}J^{(1a)}(\omega) &= \frac{1}{\omega}\,\bar{\chi}_{n,\omega}\,\ell_\alpha^\perp\,\Theta^\alpha_{(a)}\mathcal{H}_v\,,\\
\delta_a^{(\lambda^0)}J^{(2b)}(\omega) &= -\frac{n\cdot v}{\omega}\,\bar{\chi}_{n,\omega}\Upsilon_{(b)}\,\bar{n}\cdot\ell\,\mathcal{H}_v\,,\\
\delta_a^{(\lambda^0)}J^{(2c)}(\omega) &= -\frac{1}{\omega}\,\bar{\chi}_{n,\omega}\Upsilon^\alpha_{(c)}\,\ell_\alpha^\perp\,\mathcal{H}_v\,.
\end{aligned} \tag{3.22}$$

This leads to the a constraint equation between $\mathcal{O}(\lambda^2)$ and $\mathcal{O}(\lambda^0)$

$$\boxed{\sum_j A_{bj}(\omega)\Upsilon_{(bj)} = \sum_j \omega C_j'(\omega)\Gamma_{(j)}} \tag{3.23}$$

and a constraint equation between $\mathcal{O}(\lambda^2)$ and $\mathcal{O}(\lambda)$

$$\boxed{\sum_j A_{cj}(\omega)\Upsilon^\alpha_{(cj)} = \sum_j B_{aj}(\omega)\Theta^\alpha_{(aj)}\,.} \tag{3.24}$$

SCET RPI-$\star$ at $\mathcal{O}(\lambda^2)$

Under RPI-$\star$ we must have

$$\delta^{(\lambda^2)} J^{(0)} + \delta^{(\lambda^1)} J^{(1)} + \delta^{(\lambda^0)} J^{(2)} = 0. \tag{3.25}$$

Many of the currents transform under this form of RPI:

$$\begin{aligned}
\delta_\star^{(\lambda^2)} J^{(0)}(\omega) &= -\bar\chi_n \Big\{ ig\bar{\mathcal{B}}_\perp \not{\Delta}_\perp \frac{(\bar n\cdot v)^2}{2\overline{\mathcal{P}}^\dagger} + \Big[ig\mathcal{B}_\perp\cdot\Delta_\perp \frac{(\bar n\cdot v)^2}{\overline{\mathcal{P}}^\dagger}\Big] + \mathcal{P}_\perp^\dagger \not{\Delta}_\perp \frac{(\bar n\cdot v)^2}{2\overline{\mathcal{P}}^\dagger} \Big\} \delta(\omega - n\cdot v\overline{\mathcal{P}}^\dagger) \\
&\qquad - \Delta_\perp\cdot\mathcal{P}_\perp^\dagger (\bar n\cdot v)\, \delta'(\omega - n\cdot v\overline{\mathcal{P}}^\dagger) \Big\} \Gamma\, \mathcal{H}_v\,, \\
\delta_\star^{(\lambda^1)} J^{(1a)}(\omega) &= \frac{1}{\omega}\,\bar\chi_{n,\omega} \Big\{ \mathcal{P}_\alpha^{\perp\dagger} \Big(\frac{\not{\bar n}\not{\Delta}_\perp}{4}\Theta_{(a)}^\alpha + \delta_\star^{(\lambda^1)}\Theta_{(a)}^\alpha \Big) + (\bar n\cdot v)^2 \Delta_\perp\cdot\mathcal{P}_\perp^\dagger n_\sigma^T \Theta_{(a)}^\sigma \Big\} \mathcal{H}_v\,, \\
\delta_\star^{(\lambda^1)} J^{(1b)}(\omega_{1,2}) &= \frac{1}{m}\bar\chi_{n,\omega_1} \Big\{ ig\mathcal{B}_\alpha^\perp \Big(\frac{\not{\bar n}\not{\Delta}_\perp}{4}\Theta_{(b)}^\alpha + \delta_\star^{(\lambda^1)}\Theta_{(b)}^\alpha \Big) + (\bar n\cdot v)^2\, \Delta_\perp\cdot(ig\mathcal{B}_\perp)\, n_\sigma^T \Theta_{(b)}^\sigma \Big\}_{\omega_2} \mathcal{H}_v\,, \\
\delta_\star^{(\lambda^0)} J^{(2a,2b,2c)} &= 0\,, \\
\delta_\star^{(\lambda^0)} J^{(2d)}(\omega) &= \frac{(\bar n\cdot v)}{\omega}\,\bar\chi_{n,\omega} \Big(-\frac{1}{2}\Delta_\alpha^\perp \mathcal{P}_\beta^{\perp\dagger} - \frac{1}{2}\mathcal{P}_\alpha^{\perp\dagger}\Delta_\beta^\perp \Big) \mathcal{H}_v\,, \\
\delta_\star^{(\lambda^0)} J^{(2e)}(\omega_{1,2}) &= \frac{1}{m(\omega_1+\omega_2)}\,\bar\chi_{n,\omega_1} (ig\mathcal{B}_\alpha^\perp)_{\omega_2} \Big(-\frac{1}{2}\Delta_\beta^\perp \overline{\mathcal{P}}^\dagger \Big) \Upsilon_{(g)}^{\alpha\beta}\, \mathcal{H}_v\,, \\
\delta_\star^{(\lambda^0)} J^{(2f,2g,2h,2i,2j,2k)} &= 0\,.
\end{aligned} \tag{3.26}$$

The terms in Eq. (3.26) can be grouped into two unique field structures, $[\bar\chi_{n,\omega}\Delta_\alpha^\perp \mathcal{P}_\beta^\dagger \cdots \mathcal{H}_v]$ and $[\bar\chi_{n,\omega}\Delta_\alpha^\perp \mathcal{B}_\beta^\dagger \cdots \mathcal{H}_v]$, which must cancel independently. This gives two constraint equations. The terms proportional to $\Delta_\alpha^\perp \mathcal{P}_\beta^{\perp\dagger}$ give

$$\begin{aligned}
\sum_j A_{dj}(\omega)\big(\Upsilon_{(dj)}^{\alpha\beta} + \Upsilon_{(dj)}^{\beta\alpha}\big) &= \sum_j \Big\{ -C_j(\omega)\gamma_\perp^\beta\gamma_\perp^\alpha\Gamma_{(j)} - 2\omega C_j'(\omega) g_\perp^{\alpha\beta}\Gamma_{(j)} \Big\} \\
&\quad + \sum_j B_{aj}(\omega)\Big(\frac{1}{2}\frac{\not{\bar n}}{\bar n\cdot v}\gamma_\perp^\alpha \Theta_{(aj)}^\beta + 2\delta_\star^\alpha \Theta_{(aj)}^\beta + 2g_\perp^{\alpha\beta}\frac{n_\sigma^T}{n\cdot v}\Theta_{(aj)}^\sigma \Big).
\end{aligned} \tag{3.27}$$

From Eq. (3.15) we know that the index σ on $\Theta_{(aj)}^\sigma$ must be $\perp$ so the last term vanishes. Inserting Eq. (3.15) also simplifies the nonvanishing terms. Finally we

know that $\Upsilon^{\alpha\beta}_{dj}$ is symmetric in α and β. With these simplifications we have the constraint equation

$$\sum_j A_{dj}(\omega)\,\Upsilon^{\alpha\beta}_{(dj)} = \sum_j \Big\{ -\frac{1}{2}C_j(\omega)\gamma_\perp^\beta\gamma_\perp^\alpha\Gamma_{(j)} - \omega C_j'(\omega) g_\perp^{\alpha\beta}\Gamma_{(j)} + \frac{1}{2}C_j(\omega)\frac{\bar{n}\!\!\!/}{\bar{n}\cdot v}\gamma_\perp^\alpha\delta_\star^\beta\Gamma_{(j)}\Big\} + \sum_j B_{aj}(\omega)\,\delta_\star^\alpha\Theta^\beta_{(aj)}\,. \tag{3.28}$$

Since the LHS is symmetric in $\alpha\beta$, all terms on the RHS that are not symmetric should cancel. The terms from Eq. (3.26) that are proportional to $\Delta_\alpha^\perp\mathcal{B}_\beta^\perp$ give another constraint

$$\sum_j A_{ej}(\omega_1,\omega_2)\Upsilon^{\beta\alpha}_{(ej)} = -\sum_j C_j(\omega_1+\omega_2)\Big(\frac{m}{\omega_1+\omega_2}\gamma_\perp^\beta\gamma_\perp^\alpha + \frac{2m}{\omega_2}g_\perp^{\alpha\beta}\Big)\Gamma_{(j)} + \sum_j B_{bj}(\omega_1,\omega_2)\Big(\frac{1}{2}\frac{\bar{n}\!\!\!/}{\bar{n}\cdot v}\gamma_\perp^\alpha\Theta^\beta_{(bj)} + 2\delta_\star^\alpha\Theta^\beta_{(bj)} + 2g_\perp^{\alpha\beta}\frac{n_\sigma^T}{n\cdot v}\Theta^\sigma_{(bj)}\Big). \tag{3.29}$$

In Eqs. (3.28) and (3.29), the indices α and β are purely perpendicular. The equation that defines $\delta_\star^\alpha\Theta^\beta$ is the same as Eq. (3.16), just with the Θ^β Dirac structures.

3.2.3 Solutions to the constraint equations

We now find solutions for the $\mathcal{O}(\lambda^2)$ constraints in Eqs. (3.19,3.23,3.24,3.28,3.29). Note that by careful construction of our operator basis we have ensured that each equation gives a constraint on a different NNLO operator.

Eqs. (3.15,3.19,3.28,3.29) have implicit spinor indices, one or two vector indices, and a sum in j over independent structures. Since all of the equations appear between $[\bar{\xi}_n\cdots\mathcal{H}_v]$ they are only valid when the spinor indices are projected onto a 4-dimensional subspace, rather than the full 16-dimensional space of Dirac structures.

It is useful to exploit the following method to determine how many independent Dirac structures we should have for each operator. Start by consider the three minimal structures that appear in the trace reduction formula, Eq. (2.52), namely $\{1,\gamma_5,\gamma_\perp^\alpha\}$. Next for each case write down all possible scalar objects (v^μ, n^μ, $g^{\mu\nu}$, ...) to saturate

the Lorentz vector indices coming from derivatives in the operator and current indices, taking into account any symmetries. To satisfy parity and time reversal with γ_5, we will need to have an ϵ-tensor, such as $i\epsilon_\perp^{\mu\nu}\gamma_5$. As long as the scalar objects are linearly independent these steps give a complete basis.

At $\mathcal{O}(\lambda^0)$, a complete basis of Dirac structures for scalar, vector, and tensor heavy-to-light currents is [15]

$$\Gamma_{(1)} = 1\,, \quad \Gamma^\mu_{(1-3)} = \left\{\gamma^\mu, v^\mu, \frac{n^\mu}{n\cdot v}\right\}, \quad \Gamma^{\mu\nu}_{(1-4)} = \left\{i\sigma^{\mu\nu}, \gamma^{[\mu}v^{\nu]}, \frac{1}{n\cdot v}\gamma^{[\mu}n^{\nu]}, \frac{1}{n\cdot v}n^{[\mu}v^{\nu]}\right\}. \tag{3.30}$$

At $\mathcal{O}(\lambda)$, there is no constraint on $J^{(1b)}$, and Eq. (3.15) constrains the $J^{(1a)}$ currents in terms of $J^{(0)}$. To impose this constraint we need

$$\begin{aligned}
&\delta^\alpha_\star\Gamma_{(1)} = 0\,, && \delta^\alpha_\star\Gamma^\mu_{(1,2)} = 0\,, && \delta^\alpha_\star\Gamma^\mu_{(3)} = g_\perp^{\alpha\mu}\,, \\
&\delta^\alpha_\star\Gamma^{\mu\nu}_{(1,2)} = 0\,, && \delta^\alpha_\star\Gamma^{\mu\nu}_{(3)} = \gamma^{[\mu}g_\perp^{\nu]\alpha}\,, && \delta^\alpha_\star\Gamma^{\mu\nu}_{(4)} = g_\perp^{\alpha[\mu}v^{\nu]}\,.
\end{aligned} \tag{3.31}$$

The constraint equation causes some Dirac structures to always appear in the same combination. We find

$$\begin{aligned}
\Theta^\alpha_{(a1)} &= \frac{1}{2}\frac{\not{n}}{\bar{n}\cdot v}\gamma_\perp^\alpha\,, \qquad \Theta^\alpha_{(b1)} = \gamma_\perp^\alpha\,, \\
\Theta^{\alpha\mu}_{(a1-3)} &= \left\{\frac{1}{2}\frac{\not{n}}{\bar{n}\cdot v}\gamma_\perp^\alpha\{\gamma^\mu, v^\mu\}, \frac{\not{n}}{2}\gamma_\perp^\alpha n^\mu + 2g_\perp^{\alpha\mu}\right\}, \\
\Theta^{\alpha\mu}_{(b1-4)} &= \left\{\gamma_\perp^\alpha\{\gamma^\mu, v^\mu, \frac{n^\mu}{n\cdot v}\}, g_\perp^{\alpha\mu}\right\}, \\
\Theta^{\alpha\mu\nu}_{(a1-4)} &= \left\{\frac{1}{2}\frac{\not{n}}{\bar{n}\cdot v}\gamma_\perp^\alpha\{i\sigma^{\mu\nu}, \gamma^{[\mu}v^{\nu]}\}\,,\ \frac{\not{n}}{2}\gamma_\perp^\alpha\gamma^{[\mu}n^{\nu]} - 2g_\perp^{\alpha[\mu}\gamma^{\nu]}\,,\ \frac{\not{n}}{2}\gamma_\perp^\alpha n^{[\mu}v^{\nu]} + 2g_\perp^{\alpha[\mu}v^{\nu]}\right\}, \\
\Theta^{\alpha\mu\nu}_{(b1-6)} &= \left\{\gamma_\perp^\alpha\Gamma^{\mu\nu}_{(1-4)}\,,\ g_\perp^{\alpha[\mu}\gamma^{\nu]}\,,\ g_\perp^{\alpha[\mu}v^{\nu]}\right\},
\end{aligned} \tag{3.32}$$

where $\Gamma^{\mu\nu}_{(1-4)}$ are given in Eq. (3.30), which is in agreement with Ref. [130]. This basis is equivalent to the one in Ref. [130].[3] We take Θ_{bj} terms with no $\not{n}$ so that this choice

[3]Note that a structure $g_\perp^{\alpha[\mu}n^{\nu]}$ is redundant in 4-dimensions [39, 96].

does not need to be modified if we enlarge the basis for $v_\perp \neq 0$ (see section 3.2.4). With Eq. (3.32), the constraint Eq. (3.15) gives relations for the Wilson coefficients in the $J^{(1a)}$ current

$$B^{(s)}_{a1}(\omega) = C^{(s)}_{1}(\omega), \qquad B^{(v)}_{a1-3}(\omega) = C^{(v)}_{1-3}(\omega), \qquad B^{(t)}_{a1-4}(\omega) = C^{(t)}_{1-4}(\omega)\,. \tag{3.33}$$

These results agree with Refs. [59, 35, 130].

At $\mathcal{O}(\lambda^2)$ we must solve Eqs. (3.19,3.23,3.24,3.28,3.29). From these equations we see that the currents $J^{(2f)}$, $J^{(2g)}$, $J^{(2h)}$, $J^{(2j)}$, and $J^{(2k)}$ are not constrained. The currents $J^{(2a)}$, $J^{(2b)}$, $J^{(2c)}$, and $J^{(2d)}$ are all related to the leading order current $J^{(0)}$. Finally the currents $J^{(2e)}$ are related to the currents $J^{(0)}$ and $J^{(1b)}$.

To solve the equations we will need

$$\begin{aligned}
&\delta^\sigma_{\$}\Gamma_{(1)} = 0\,, \quad \delta^\sigma_{\$}\Gamma^\mu_{(1)} = 0\,, \qquad \delta^\sigma_{\$}\Gamma^\mu_{(2)} = g_T^{\sigma\mu}\,, \qquad \delta^\sigma_{\$}\Gamma^\mu_{(3)} = \bar{n}_T^\sigma n^\mu \\
&\delta^\sigma_{\$}\Gamma^{\mu\nu}_{(1)} = 0\,, \quad \delta^\sigma_{\$}\Gamma^{\mu\nu}_{(2)} = \gamma^{[\mu} g_T^{\nu]\sigma}\,, \quad \delta^\sigma_{\$}\Gamma^{\mu\nu}_{(3)} = \bar{n}_T^\sigma \gamma^{[\mu} n^{\nu]}\,, \quad \delta^\sigma_{\$}\Gamma^{\mu\nu}_{(4)} = \bar{n}_T^\sigma n^{[\mu} v^{\nu]} + \frac{1}{n\cdot v} n^{[\mu} g_T^{\nu]\sigma}\,,
\end{aligned} \tag{3.34}$$

where $\bar{n}_T^\sigma = -(\bar{n}\cdot v)^2 n_T^\sigma$. We will also need

$$\begin{aligned}
&\delta^\alpha_\star \Theta^\beta_{(b1)} = -g_\perp^{\alpha\beta}\, n\cdot v\, \frac{\not{\bar{n}}}{2}\,, \\
&\delta^\alpha_\star \Theta^{\beta\mu}_{(b1,2,3)} = -g_\perp^{\alpha\beta}\, n\cdot v\, \frac{\not{\bar{n}}}{2}\, \Gamma^\mu_{(1,2,3)} + \gamma_\perp^\beta \delta^\alpha_\star \Gamma^\mu_{(1,2,3)}\,, \qquad \delta^\alpha_\star \Theta^{\beta\mu}_{(b4)} = g_\perp^{\alpha\beta} \frac{n_T^\mu}{n\cdot v}\,, \\
&\delta^\alpha_\star \Theta^{\beta\mu\nu}_{(b1,2,3,4)} = -g_\perp^{\alpha\beta}\, n\cdot v\, \frac{\not{\bar{n}}}{2}\, \Gamma^{\mu\nu}_{(1,2,3,4)} + \gamma_\perp^\beta \delta^\alpha_\star \Gamma^{\mu\nu}_{(1,2,3,4)}\,, \qquad \delta^\alpha_\star \Theta^{\beta\mu\nu}_{(b5)} = \frac{1}{n\cdot v}\, g_\perp^{\alpha\beta} n_T^{[\mu} \gamma^{\nu]}\,, \\
&\delta^\alpha_\star \Theta^{\beta\mu\nu}_{(b6)} = \frac{1}{n\cdot v}\, g_\perp^{\alpha\beta} n_T^{[\mu} v^{\nu]}\,,
\end{aligned} \tag{3.35}$$

where $\alpha\beta$ were projected onto $\perp$ directions. Note that $\delta^\alpha_\star \Theta_{(aj)}$ are easily obtained from these. The constraints in Eqs.(3.23,3.24) have a particularly simple solution:

$$A_{bj}(\omega) = \omega C'_j(\omega), \qquad A_{cj}(\omega) = B_{aj}(\omega), \qquad \Upsilon_{(bj)} = \Gamma_{(j)}, \qquad \Upsilon_{(cj)} = \Theta_{(aj)}\,. \tag{3.36}$$

Solutions to the other equations are slightly more involved. We present solutions to

the constraint equations for the scalar, vector, and tensor currents in turn.

Solutions for scalar and pseudoscalar currents at $\mathcal{O}(\lambda^2)$

The RPI constraints do not effect the allowed Dirac structures for scalar currents, so we have the complete sets

$$\Upsilon^{\sigma}_{(a1,2)} = \left\{\gamma^{\sigma}_T, \frac{n^{\sigma}_T}{n\cdot v}\right\}, \qquad \Upsilon_{(b1)} = \Upsilon_{(g1)} = 1\,, \qquad \Upsilon^{\alpha}_{(c1)} = \frac{1}{2}\frac{\bar{n}\!\!\!/}{\bar{n}\cdot v}\gamma^{\alpha}_{\perp}\,,$$
$$\Upsilon^{\alpha\beta}_{(d1)} = g^{\alpha\beta}_{\perp}\,, \qquad \Upsilon^{\alpha\beta}_{(e1,2)} = \Upsilon^{\alpha\beta}_{(f1,2)} = \Upsilon^{\alpha\beta}_{(h1,2)} = \Upsilon^{\alpha\beta}_{(i1,2)} = \left\{2g^{\alpha\beta}_{\perp}, \gamma^{\alpha}_{\perp}\gamma^{\beta}_{\perp}\right\}. \quad (3.37)$$

For the four quark operators, there are three possible Dirac structures in the $\bar{\chi}_n \cdots \chi_n$ bilinear, $\{\bar{n}\!\!\!/, \bar{n}\!\!\!/\gamma_5, \bar{n}\!\!\!/\gamma^{\alpha}_{\perp}\}$. In performing the matching onto SCET at a scale $\sim m_b$, the light quark masses are perturbations, and for matching onto the $\mathcal{O}(\lambda^2)$ four quark operator we can set $m_q = 0$. In this case, chirality rules out the $\bar{n}\!\!\!/\gamma^{\alpha}_{\perp}$ structure which connects right and left handed quarks. A complete set of structures is therefore

$$\left(\Upsilon \otimes \Upsilon\right)_{(j1,j2)} = \left(\Upsilon \otimes \Upsilon\right)_{(k1,k2)} = \left\{\frac{\bar{n}\!\!\!/}{\bar{n}\cdot v} \otimes 1\,,\ \frac{\bar{n}\!\!\!/}{\bar{n}\cdot v}\gamma^5 \otimes \gamma^5\right\}. \quad (3.38)$$

To solve the RPI-\$ constraint, we insert the Dirac structures Eqs. (3.30,3.34,3.37) into Eq. (3.19). Satisfying this constraint requires a relation on the Wilson coefficients

$$A^{(s)}_{a1}(\omega) = C^{(s)}_1(\omega) \qquad A^{(s)}_{a2}(\omega) = 2\omega C^{(s)\prime}_1(\omega)\,. \quad (3.39)$$

The solution for the SCET RPI-a constraint equation in (3.36) gives

$$A^{(s)}_{b1}(\omega) = \omega C^{(s)\prime}_1(\omega) \qquad A^{(s)}_{c1}(\omega) = C^{(s)}_1(\omega). \quad (3.40)$$

To solve the SCET RPI-$\star$ constraints in Eqs. (3.28,3.29), we need the additional Dirac structures in Eqs. (3.32,3.35). On the RHS of Eq. (3.28) we observe that all structures that were not symmetric in $\alpha\beta$ cancel, in agreement with the symmetry of the LHS.

Solving the equations, the relations on the Wilson coefficients are

$$\begin{aligned} A_{d1}^{(s)}(\omega) &= -\omega C_1^{(s)\prime}(\omega)\,, \\ A_{e1}^{(s)}(\omega_{1,2}) &= -\frac{m}{\omega_2}\, C_1^{(s)}(\omega_1+\omega_2)\,, \\ A_{e2}^{(s)}(\omega_{1,2}) &= -\frac{m}{(\omega_1+\omega_2)}\, C_1^{(s)}(\omega_1+\omega_2) - B_{b1}^{(s)}(\omega_{1,2})\,. \end{aligned} \tag{3.41}$$

The following Wilson coefficients of scalar currents are not determined by the RPI constraints

$$A_{f1,2}^{(s)}(\omega_{1,2})\,, \quad A_{g1,2}^{(s)}(\omega_{1,2})\,, \quad A_{h1,2}^{(s)}(\omega_{1,2,3})\,, \quad A_{i1,2}^{(s)}(\omega_{1,2,3})\,, \quad A_{j1,2,k1,2}^{(s)}(\omega_{1,2,3})\,. \tag{3.42}$$

Since the light quark in the full theory current retains its chirality in the effective theory current, the results for the expansion of the pseudoscalar current, $\bar{q}\gamma_5 b$, are simple to extract from those for the scalar case, $\bar{q}\, b$. The Dirac structures for pseudoscalar currents may be obtained by multiplying Eqs. (3.37,3.38) on the left by γ_5 and $1 \otimes \gamma^5$, respectively. The constraints on the Wilson coefficients of these currents are then identical.

Solutions for vector and axial-vector currents at $\mathcal{O}(\lambda^2)$

The analysis for the scalar current can be extended to the vector currents, where the extra Lorentz index makes ensuring that the Dirac basis is complete slightly more difficult. We use the method discussed in section 3.2.3 to count the number of terms in the Dirac basis prior to imposing the RPI constraints. For the case of $\Upsilon_a^{\sigma\mu}$ the index σ is transverse to v and we have

$$1:\ \{g_T^{\sigma\mu}, n_T^\sigma n^\mu, n_T^\sigma v^\mu\}\,, \qquad \gamma_5 : \{i\epsilon_\perp^{\sigma\mu}\}\,, \qquad \gamma_\perp^\sigma : \{n^\mu, v^\mu\}\,, \qquad \gamma_\perp^\mu : \{n_T^\sigma\}\,, \tag{3.43}$$

which has seven elements. The counting for the $\Upsilon_{b,c,g}$ cases are straightforward. For $\Upsilon_d^{\alpha\beta\mu}$ the indices $\alpha\beta$ are $\perp$ and symmetric. We have

$$1:\ \{g_\perp^{\alpha\beta}n^\mu, g_\perp^{\alpha\beta}v^\mu\}\,, \qquad \gamma_5:\{-\}\,, \qquad \gamma_\perp^\mu:\{g_\perp^{\alpha\beta}\}\,, \qquad \gamma_\perp^{\{\alpha}:\{g_\perp^{\beta\}\mu}\}\,, \tag{3.44}$$

so there are four elements in the basis. Finally, for $\Upsilon_{e,f,h,i}^{\alpha\beta\mu}$ we have

$$1:\ \{g_\perp^{\alpha\beta}n^\mu, g_\perp^{\alpha\beta}v^\mu\},\quad \gamma_5:\{i\epsilon_\perp^{\alpha\beta}n^\mu, i\epsilon_\perp^{\alpha\beta}v^\mu\},\quad \gamma_\perp^\mu:\{g_\perp^{\alpha\beta}\},\quad \gamma_\perp^\alpha:\{g_\perp^{\beta\mu}\},\quad \gamma_\perp^\beta:\{g_\perp^{\alpha\mu}\}, \tag{3.45}$$

so the basis has seven elements.

For computations, a different basis choice is slightly more convenient. The independent Dirac structures appearing on the RHS of the constraint equations reduce the basis for $\Upsilon_{\{a1-7\}}^{\sigma\mu}$ by one further element. For the vector currents we find

$$\begin{aligned}
\Upsilon_{(a1-6)}^{\sigma\mu} &= \left\{\gamma^\mu\gamma_T^\sigma, v^\mu\gamma_T^\sigma + 2g_T^{\sigma\mu}, \frac{n^\mu}{n\cdot v}\gamma_T^\sigma, \{\gamma^\mu, v^\mu, \frac{n^\mu}{n\cdot v}\}\frac{n_T^\sigma}{n\cdot v}\right\}, \qquad (3.46)\\
\Upsilon_{(b1-3)}^{\mu} &= \Upsilon_{(g1-3)}^{\mu} = \left\{\gamma^\mu, v^\mu, \frac{n^\mu}{n\cdot v}\right\}, \qquad \Upsilon_{(c1-3)}^{\mu} = \left\{\frac{1}{2}\frac{\bar{n}\!\!\!/}{\bar{n}\cdot v}\gamma_\perp^\alpha\{\gamma^\mu, v^\mu\}, \frac{\bar{n}\!\!\!/}{2}\gamma_\perp^\alpha n^\mu + 2g_\perp^{\alpha\mu}\right\},\\
\Upsilon_{(d1-4)}^{\alpha\beta\mu} &= \left\{g_\perp^{\alpha\beta}\{\gamma^\mu, v^\mu, \frac{n^\mu}{n\cdot v}\}, \frac{1}{2}\frac{\bar{n}\!\!\!/}{\bar{n}\cdot v}\gamma_\perp^{\{\alpha}g_\perp^{\beta\}\mu}\right\},\\
\Upsilon_{(e1-7)}^{\alpha\beta\mu} &= \left\{2g_\perp^{\alpha\beta}\{\gamma^\mu, v^\mu, \frac{n^\mu}{n\cdot v}\}, \gamma_\perp^\alpha\gamma_\perp^\beta\{\gamma^\mu, v^\mu, \frac{n^\mu}{n\cdot v}\}, \frac{1}{2}\frac{\bar{n}\!\!\!/}{\bar{n}\cdot v}\gamma_\perp^\beta g_\perp^{\alpha\mu}\right\},\\
\Upsilon_{(f,h,i1-7)}^{\alpha\beta\mu} &= \left\{2g_\perp^{\alpha\beta}\{\gamma^\mu, v^\mu, \frac{n^\mu}{n\cdot v}\}, \gamma_\perp^\alpha\gamma_\perp^\beta\{\gamma^\mu, v^\mu, \frac{n^\mu}{n\cdot v}\}, \gamma_\perp^\beta g_\perp^{\alpha\mu}\right\}.
\end{aligned}$$

The index symmetrization means $\gamma_\perp^{\{\alpha}g_\perp^{\beta\}\mu} = \gamma_\perp^\alpha g_\perp^{\beta\mu} + \gamma_\perp^\beta g_\perp^{\alpha\mu}$. In Eq. (3.46) we have used Eq. (2.52) to remove redundant structures.

The operators $J^{(2a,2b,2c)}$ bear some similarity to the complete basis of six $1/m$ suppressed heavy-to-light currents in HQET [77, 78]. The differences are due to the fact that for a collinear light quark we have the vector n^μ available to build additional structures and from the fact that working in the $v^\perp = 0$ frame, we do not need operators like $\bar{\chi}_n i\, v\cdot\overleftarrow{\mathcal{D}}^\perp\Upsilon\mathcal{H}_v$.

For the four quark operators, a basis of Dirac structures is

$$(\Upsilon\otimes\Upsilon)^{\mu}_{(j1-6)}=(\Upsilon\otimes\Upsilon)^{\mu}_{(k1-6)}=\Big\{\frac{\not{\bar{n}}}{\bar{n}\cdot v}\otimes\{\gamma^{\mu},v^{\mu},\frac{n^{\mu}}{n\cdot v}\}\,,\ \frac{\not{\bar{n}}}{\bar{n}\cdot v}\gamma^{5}\otimes\gamma^{5}\{\gamma^{\mu},v^{\mu},\frac{n^{\mu}}{n\cdot v}\}\Big\}\,. \tag{3.47}$$

Here the counting of the number of independent structures proceeds in the same way as for the bilinear operators, except that we start by writing down minimal structures for the four quark operator where we impose the correct chirality on the purely collinear fermion bilinear. For $J^{(2j)}$ we start with six structures, $\{\not{\bar{n}}\,,\not{\bar{n}}\gamma_5\}\otimes\{1,\gamma_5,\gamma_\perp^\alpha\}$, and find that only the six terms

$$\not{\bar{n}}\otimes 1:\{v^{\mu},n^{\mu}\},\qquad \not{\bar{n}}\otimes\gamma_\perp^{\mu}:\{1\},\qquad \not{\bar{n}}\gamma_5\otimes\gamma_\perp^{\alpha}:\{i\epsilon_\perp^{\alpha\mu}\},\qquad \not{\bar{n}}\gamma_5\otimes\gamma_5:\{v^{\mu},n^{\mu}\}\,, \tag{3.48}$$

are allowed, which we swap for the basis in Eq. (3.47). The analysis of discrete symmetries for these currents is similar to that of the four quark operators in the HQET Lagrangian [42].

Using Eqs. (3.30,3.34), the relations for the vector current coefficients obtained by solving the RPI-$ constraint in Eq. (3.19) are

$$\begin{aligned} A^{(v)}_{a1-3}(\omega)&=C^{(v)}_{1-3}(\omega)\,, & A^{(v)}_{a4}(\omega)&=2\omega C^{(v)\prime}_{1}(\omega)\,,\\ A^{(v)}_{a5}(\omega)&=2\omega C^{(v)\prime}_{2}(\omega)\,, & A^{(v)}_{a6}(\omega)&=-2C^{(v)}_{3}(\omega)+2\omega C^{(v)\prime}_{3}(\omega)\,, \end{aligned} \tag{3.49}$$

The RPI-a solution in Eq. (3.36) gives

$$A^{(v)}_{b1-3}(\omega)=\omega C^{(v)\prime}_{1-3}(\omega)\,,\qquad A^{(v)}_{c1-3}(\omega)=C^{(v)}_{1-3}(\omega)\,. \tag{3.50}$$

Using in addition Eq. (3.46), we find that solving Eq. (3.28) gives

$$\begin{aligned} A^{(v)}_{d1}(\omega)&=-\omega C^{(v)\prime}_{1}(\omega)\,, & A^{(v)}_{d2}(\omega)&=-\omega C^{(v)\prime}_{2}(\omega)-2C^{(v)}_{3}(\omega)\,,\\ A^{(v)}_{d3}(\omega)&=-\omega C^{(v)\prime}_{3}(\omega)+2C^{(v)}_{3}(\omega)\,, & A^{(v)}_{d4}(\omega)&=C^{(v)}_{3}(\omega)\,. \end{aligned} \tag{3.51}$$

Finally, solving the second RPI-$\star$ constraint in Eq. (3.29) gives

$$
\begin{aligned}
A^{(v)}_{e1}(\omega_{1,2}) &= -\Big(\frac{m}{\omega_2}\Big)C_1(\omega_1+\omega_2) - B_{b3}(\omega_{1,2})\,, \\
A^{(v)}_{e2}(\omega_{1,2}) &= -\Big(\frac{m}{\omega_2}\Big)C_2(\omega_1+\omega_2) - B_{b4}(\omega_{1,2})\,, \\
A^{(v)}_{e3}(\omega_{1,2}) &= -\Big(\frac{m}{\omega_2}\Big)C_3(\omega_1+\omega_2) + B_{b3}(\omega_{1,2}) + B_{b4}(\omega_{1,2})\,, \\
A^{(v)}_{e4}(\omega_{1,2}) &= -\Big(\frac{m}{\omega_1+\omega_2}\Big)C_1(\omega_1+\omega_2) + B_{b1}(\omega_{1,2}) + 2B_{b3}(\omega_{1,2})\,, \\
A^{(v)}_{e5}(\omega_{1,2}) &= -\Big(\frac{m}{\omega_1+\omega_2}\Big)C_2(\omega_1+\omega_2) - 2B_{b1}(\omega_{1,2}) - B_{b2}(\omega_{1,2})\,, \\
A^{(v)}_{e6}(\omega_{1,2}) &= -\Big(\frac{m}{\omega_1+\omega_2}\Big)C_3(\omega_1+\omega_2) - 3B_{b3}(\omega_{1,2})\,, \\
A^{(v)}_{e7}(\omega_{1,2}) &= -2B_{b3}(\omega_{1,2}) + B_{b4}(\omega_{1,2})\,.
\end{aligned}
\tag{3.52}
$$

The following Wilson coefficients of the $\mathcal{O}(\lambda^2)$ vector currents are not determined by the RPI constraints,

$$
A^{(v)}_{f1-7}(\omega_{1,2})\,, \qquad A^{(v)}_{g1-3}(\omega_{1,2})\,, \qquad A^{(v)}_{h1-7,i1-7}(\omega_{1,2,3})\,, \qquad A^{(v)}_{j1-6,k1-6}(\omega_{1,2,3})\,. \tag{3.53}
$$

The Dirac structures for axial-vector currents which expand $\bar{u}\gamma_5\gamma^\mu b$ may be obtained by multiplying the Dirac structures in Eq. (3.46) by γ_5 on the left and in Eq. (3.47) by $1 \otimes \gamma^5$. The relations for their Wilson coefficients are then the same as the vector currents.

Solutions for tensor currents at $\mathcal{O}(\lambda^2)$

The counting of the number of independent terms proceeds just as in the vector case but now with antisymmetric indices $\mu\nu$. For $J^{(2a)}$, the index σ is transverse to v and there are ten structures

$$
\begin{aligned}
1 &: \{v^{[\mu}n^{\nu]}n^\sigma, g_\perp^{\sigma[\mu}v^{\nu]}, g_\perp^{\sigma[\mu}n^{\nu]}\}\,, & \gamma_5 &: \{i\epsilon_\perp^{\mu\nu}n^\sigma, i\epsilon_\perp^{\sigma[\mu}n^{\nu]}, i\epsilon_\perp^{\sigma[\mu}v^{\nu]}\}\,, \\
\gamma_\perp^{[\mu} &: \{v^{\nu]}n^\sigma, n^{\nu]}n^\sigma, g_\perp^{\nu]\sigma}\}\,, & \gamma_\perp^\sigma &: \{v^{[\mu}n^{\nu]}\}\,.
\end{aligned}
\tag{3.54}
$$

The bases for $J^{(2b,2g)}$ are simple, while for $J^{(2c)}$ we have six terms

$$1 : \{g_\perp^{\alpha[\mu} v^{\nu]}, g_\perp^{\alpha[\mu} n^{\nu]}\}, \quad \gamma_5 : \{i\epsilon_\perp^{\alpha[\mu} n^{\nu]}, i\epsilon_\perp^{\alpha[\mu} v^{\nu]}\}, \quad \gamma_\perp^{[\mu} : \{g_\perp^{\nu]\sigma}\}, \quad \gamma_\perp^{\alpha} : \{v^{[\mu} n^{\nu]}\}. \quad (3.55)$$

We also have six terms for $J^{(2d)}$

$$1 : \{g_\perp^{\alpha\beta} n^{[\mu} v^{\nu]}\}, \quad \gamma_5 : \{i\epsilon_\perp^{\mu\nu} g_\perp^{\alpha\beta}\}, \quad \gamma_\perp^{[\mu} : \{n^{\nu]} g_\perp^{\alpha\beta}, v^{\nu]} g_\perp^{\alpha\beta}\}, \quad \gamma_\perp^{\{\alpha} : \{g_\perp^{\beta\}[\mu} n^{\nu]}, g_\perp^{\beta\}[\mu} v^{\nu]}\}, \quad (3.56)$$

where the identity $g_\perp^{\alpha[\mu}\epsilon_\perp^{\nu]\beta} = -g_\perp^{\alpha\beta}\epsilon_\perp^{\mu\nu}$ leaves only one term for γ_5. Finally for $J^{(2e,2f,2h,2i)}$ we count ten terms

$$1 : \{g_\perp^{\alpha\beta} n^{[\mu} v^{\nu]}, g_\perp^{\alpha[\mu} g_\perp^{\nu]\beta}\}, \quad \gamma_5 : \{i\epsilon_\perp^{\mu\nu} g_\perp^{\alpha\beta}, i\epsilon_\perp^{\alpha\beta} n^{[\mu} v^{\nu]}\}, \quad \gamma_\perp^{[\mu} : \{n^{\mu]} g_\perp^{\alpha\beta}, v^{\mu]} g_\perp^{\alpha\beta}\},$$
$$\gamma_\perp^{\alpha} : \{g_\perp^{\beta[\mu} n^{\nu]}, g_\perp^{\beta[\mu} v^{\nu]}\}, \qquad \gamma_\perp^{\beta} : \{g_\perp^{\alpha[\mu} n^{\nu]}, g_\perp^{\alpha[\mu} v^{\nu]}\}. \quad (3.57)$$

Again only $J^{(2a)}$ has its basis of Dirac structures further restricted by the RPI-\$ constraint in Eq. (3.19), which reduces the basis by two terms (since only eight linearly independent Wilson coefficients appear in Eq. (3.60) below). For the complete set of Dirac structures for tensor currents we find

$$\Upsilon^{\sigma\mu\nu}_{(a1-8)} = \Big\{ i\sigma^{\mu\nu}\gamma_T^\sigma \,,\; \gamma^{[\mu} v^{\nu]}\gamma_T^\sigma - 2g_T^{\sigma[\mu}\gamma^{\nu]} \,,\; \frac{1}{n\cdot v}\gamma^{[\mu} n^{\nu]}\gamma_T^\sigma \,,\; \frac{1}{n\cdot v} n^{[\mu} v^{\nu]}\gamma_T^\sigma - 2g_T^{\sigma[\mu} n^{\nu]} \,,$$
$$\Gamma^{\mu\nu}_{(1-4)}\frac{n_T^\sigma}{n\cdot v}\Big\}, \qquad \Upsilon^{\mu\nu}_{(b,g1-4)} = \Big\{\Gamma^{\mu\nu}_{(1-4)}\Big\},$$
$$\Upsilon^{\alpha\mu\nu}_{(c1-4)} = \Big\{ \frac{1}{2}\frac{\not{\bar{n}}}{\bar{n}\cdot v}\gamma_\perp^\alpha\{i\sigma^{\mu\nu}, \gamma^{[\mu} v^{\nu]}\} \,,\; \frac{\not{\bar{n}}}{2}\gamma_\perp^\alpha\gamma^{[\mu} n^{\nu]} - 2g_\perp^{\alpha[\mu}\gamma^{\nu]} \,,\; \frac{\not{\bar{n}}}{2}\gamma_\perp^\alpha n^{[\mu} v^{\nu]} + 2g_\perp^{\alpha[\mu} v^{\nu]}\Big\},$$
$$\Upsilon^{\alpha\beta\mu\nu}_{(d1-6)} = \Big\{ g_\perp^{\alpha\beta}\Gamma^{\mu\nu}_{(1-4)} \,,\; \frac{1}{4}\frac{\not{\bar{n}}}{\bar{n}\cdot v}\gamma_\perp^{\{\alpha} g_\perp^{\beta\}[\mu}\gamma^{\nu]} \,,\; \frac{1}{4}\frac{\not{\bar{n}}}{\bar{n}\cdot v}\gamma_\perp^{\{\alpha} g_\perp^{\beta\}[\mu} v^{\nu]}\Big\},$$
$$\Upsilon^{\alpha\beta\mu\nu}_{(e1-10)} = \Big\{ 2g_\perp^{\alpha\beta}\Gamma^{\mu\nu}_{(1-4)} \,,\; \gamma_\perp^\alpha\gamma_\perp^\beta\Gamma^{\mu\nu}_{(1-4)} \,,\; \frac{1}{2}\frac{\not{\bar{n}}}{\bar{n}\cdot v}\gamma_\perp^\beta g_\perp^{\alpha[\mu}\gamma^{\nu]} \,,\; \frac{1}{2}\frac{\not{\bar{n}}}{\bar{n}\cdot v}\gamma_\perp^\beta g_\perp^{\alpha[\mu} v^{\nu]}\Big\},$$
$$\Upsilon^{\alpha\beta\mu\nu}_{(f,h,i1-10)} = \Big\{ 2g_\perp^{\alpha\beta}\Gamma^{\mu\nu}_{(1-4)} \,,\; \gamma_\perp^\alpha\gamma_\perp^\beta\Gamma^{\mu\nu}_{(1-4)} \,,\; \gamma_\perp^\beta g_\perp^{\alpha[\mu}\gamma^{\nu]} \,,\; \gamma_\perp^\beta g_\perp^{\alpha[\mu} v^{\nu]}\Big\}, \quad (3.58)$$

where $g_T^{\alpha\beta} = g^{\alpha\beta} - v^\alpha v^\beta$. Similarly, for the tensor four quark operator currents, a

complete basis is

$$
\begin{aligned}
(\Upsilon \otimes \Upsilon)^{\mu\nu}_{(j1-10)} &= (\Upsilon \otimes \Upsilon)^{\mu\nu}_{(k1-10)} \\
&= \left\{ \frac{\not{\bar{n}}}{\bar{n}\cdot v} \otimes \Gamma^{\mu\nu}_{(1-4)} \,,\; \frac{\not{\bar{n}}}{\bar{n}\cdot v}\gamma^5 \otimes \gamma^5 \Gamma^{\mu\nu}_{(1-4)} \,,\; i\sigma^{\mu\nu} \otimes 1 \,,\; i\sigma^{\mu\nu}\gamma_5 \otimes \gamma_5 \right\}, \qquad (3.59)
\end{aligned}
$$

where just as for the vector case we have made use of chirality.

The relations for tensor Wilson coefficients obtained by solving the RPI-\$ constraint equation are:

$$
\begin{aligned}
A^{(t)}_{a1}(\omega) &= C_1(\omega)\,, & A^{(t)}_{a2}(\omega) &= C_2(\omega)\,, \qquad (3.60)\\
A^{(t)}_{a3}(\omega) &= C_3(\omega)\,, & A^{(t)}_{a4}(\omega) &= C_4(\omega)\,,\\
A^{(t)}_{a5}(\omega) &= 2\omega C_1'(\omega)\,, & A^{(t)}_{a6}(\omega) &= 2\omega C_2'(\omega)\,,\\
A^{(t)}_{a7}(\omega) &= -2C_3(\omega) + 2\omega C_3'(\omega)\,, & A^{(t)}_{a8}(\omega) &= -2C_4(\omega) + 2\omega C_4'(\omega)\,.
\end{aligned}
$$

The relations for Wilson coefficients from the RPI-a constraint equations are

$$
A^{(t)}_{b1-4}(\omega) = \omega C^{(t)\prime}_{1-4}(\omega), \qquad A^{(t)}_{c1-4}(\omega) = C^{(t)}_{1-4}(\omega). \qquad (3.61)
$$

Finally, solving the RPI-$\star$ constraint in Eq. (3.28) for the tensor case gives

$$
\begin{aligned}
A^{(t)}_{d1}(\omega) &= -\omega C^{(t)\prime}_1(\omega)\,, & A^{(t)}_{d2}(\omega) &= -\omega C^{(t)\prime}_2(\omega) - 2C^{(t)}_3(\omega)\,,\\
A^{(t)}_{d3}(\omega) &= -\omega C^{(t)\prime}_3(\omega) + 2C^{(t)}_3(\omega)\,, & A^{(t)}_{d4}(\omega) &= -\omega C^{(t)\prime}_4(\omega) + 2C^{(t)}_4(\omega)\,,\\
A^{(t)}_{d5}(\omega) &= -2C^{(t)}_3(\omega)\,, & A^{(t)}_{d6}(\omega) &= 2C^{(t)}_4(\omega)\,. \qquad (3.62)
\end{aligned}
$$

while the constraint in Eq. (3.29) has the solution

$$
\begin{aligned}
A^{(t)}_{e1}(\omega_{1,2}) &= -\Big(\frac{m}{\omega_2}\Big)C^{(t)}_1(\omega_1+\omega_2) - 2B^{(t)}_{b3}(\omega_{1,2})\,,\\
A^{(t)}_{e2}(\omega_{1,2}) &= -\Big(\frac{m}{\omega_2}\Big)C^{(t)}_2(\omega_1+\omega_2) - B^{(t)}_{b4}(\omega_{1,2}) + B_{b5}(\omega_{1,2})\,,\\
A^{(t)}_{e3}(\omega_{1,2}) &= -\Big(\frac{m}{\omega_2}\Big)C^{(t)}_3(\omega_1+\omega_2) - B^{(t)}_{b3}(\omega_{1,2}) - B^{(t)}_{b5}(\omega_{1,2})\,,\\
A^{(t)}_{e4}(\omega_{1,2}) &= -\Big(\frac{m}{\omega_2}\Big)C^{(t)}_4(\omega_1+\omega_2) - 2B^{(t)}_{b3}(\omega_{1,2}) + B^{(t)}_{b4}(\omega_{1,2}) + B^{(t)}_{b6}(\omega_{1,2})\,,\\
A^{(t)}_{e5}(\omega_{1,2}) &= -\Big(\frac{m}{\omega_1+\omega_2}\Big)C^{(t)}_1(\omega_1+\omega_2) - B^{(t)}_{b1}(\omega_{1,2}) + 4B^{(t)}_{b3}(\omega_{1,2})\,,\\
A^{(t)}_{e6}(\omega_{1,2}) &= -\Big(\frac{m}{\omega_1+\omega_2}\Big)C^{(t)}_2(\omega_1+\omega_2) - 2B^{(t)}_{b1}(\omega_{1,2}) + B^{(t)}_{b2}(\omega_{1,2}) + 2B^{(t)}_{b4}(\omega_{1,2})\,,\\
A^{(t)}_{e7}(\omega_{1,2}) &= -\Big(\frac{m}{\omega_1+\omega_2}\Big)C^{(t)}_3(\omega_1+\omega_2) + 3B^{(t)}_{b3}(\omega_{1,2})\,,\\
A^{(t)}_{e8}(\omega_{1,2}) &= -\Big(\frac{m}{\omega_1+\omega_2}\Big)C^{(t)}_4(\omega_1+\omega_2) + 6B^{(t)}_{b3}(\omega_{1,2}) - 3B^{(t)}_{b4}(\omega_{1,2})\,,\\
A^{(t)}_{e9}(\omega_{1,2}) &= -2B^{(t)}_{b3}(\omega_{1,2}) + B^{(t)}_{b5}(\omega_{1,2})\,,\\
A^{(t)}_{e10}(\omega_{1,2}) &= 4B^{(t)}_{b3}(\omega_{1,2}) - 2B^{(t)}_{b4}(\omega_{1,2}) + B^{(t)}_{b6}(\omega_{1,2})\,.
\end{aligned}
\tag{3.63}
$$

The following Wilson coefficients of the $\mathcal{O}(\lambda^2)$ tensor currents are not determined by the RPI constraints

$$
A^{(t)}_{f1-10}(\omega_{1,2})\,,\qquad A^{(t)}_{g1-4}(\omega_{1,2,3})\,,\qquad A^{(t)}_{h,i1-10}(\omega_{1,2})\,,\qquad A^{(t)}_{j,k1-10}(\omega_{1,2,3})\,. \tag{3.64}
$$

3.2.4 Absence of supplementary projected operators at $\mathcal{O}(\lambda^2)$

Here we show that the analysis above on the surface $v_\perp = 0$ is complete by showing that there are no supplementary projected operators as defined in section 2.4.4. The analysis of the proceeding section makes this simpler, since a complete set of relations have been derived for all currents $J_j^{(2b-2e)}$. Thus, we only need to worry about supplementary projected operators generated by transforming the currents $J_j^{(2a,2f-2k)}$. To simplify our proof we first swap all factors of $\bar{n}\cdot v$ for $1/(n\cdot v)$.

First consider the SCET RPI-II transformation at $\mathcal{O}(\lambda^0)$ for these $J^{(2)}$ currents. At this order we have

$$\bar{n}^\mu \to \bar{n}^\mu + \epsilon_\perp^\mu\,, \qquad \gamma_\perp^\mu \to \gamma_\perp^\mu - \frac{n^\mu}{2}\not{\epsilon}_\perp - \frac{\epsilon_\perp^\mu}{2}\not{n}\,, \qquad v_\perp^\mu \to -\frac{n^\mu}{2}\,\epsilon_\perp\cdot v_\perp - \frac{\epsilon_\perp^\mu}{2}\,n\cdot v\,,$$
$$\mathcal{P}_\perp^\mu \to \mathcal{P}_\perp^\mu - \frac{n^\mu}{2}\,\epsilon_\perp\cdot\mathcal{P}_\perp\,, \qquad \mathcal{B}_\perp^\mu \to \mathcal{B}_\perp^\mu - \frac{n^\mu}{2}\,\epsilon_\perp\cdot\mathcal{B}_\perp\,. \tag{3.65}$$

We use the convention where all indices $\alpha\beta$ are $\perp$ for the field structures and Dirac structures in $J_j^{(2f-2k)}$. Now due to the contractions of the α and β indices only the transformations on $\bar{n}^\mu$ and $\gamma_\perp^\mu$ can contribute for these operators (there are no $\bar{n}$'s or $\perp$'s in the $J^{(2a)}$ case). The transformation related to their labels ω_i is $\mathcal{O}(\lambda)$ and need not be considered and the field transformations cancel. Thus, the only terms that appear in an RPI-II relation are those whose Dirac structure transforms, $\delta_{\rm II}^\lambda \Upsilon_{(a,f,g,h,i,j,k)} \neq 0$. However, with our choice of the complete basis of Dirac structures on the $v_\perp = 0$ surface, the structures for these currents all have zero transformations. In this regard it was important to take a basis with no factors of $\not{n}$. Away from this surface we must add to our basis of Dirac structure by including additional $v_\perp$ dependent terms and it is only these terms that can have additional relations. For example, factors of $v_\perp$ are induced when we reduce a basis that includes factors of $\not{n}$ using the trace formula in Eq. (2.52). The same is true with our choice of the basis of $J_j^{(1b)}$ currents.

Finally consider whether the transformations RPI-$\star$ and RPI-\$ induce SPO's or equivalently SCET RPI-I and HQET RPI. Since the $\bar{n}$ transformation in RPI-\$ did not enter at the order we are working it is apparent that there are no SPO's from the HQET RPI. Examining the results of the RPI-I transformations we find that none of the $J_j^{(2a,2f-2k)}$ currents have $\mathcal{O}(\lambda^0)$ transformations (since the Dirac structures transform at $\mathcal{O}(\lambda)$ and the field structures that do transform all cancel out).

Thus the results derived in the previous section give the complete set of RPI relations for the $\mathcal{O}(\lambda^2)$ currents when $v_\perp = 0$.

3.3 Change of Basis and Comparison with Tree Level Results

In expanding the heavy-to-light currents, two different bases of operators are useful. At tree level it is convenient to write the result for the currents in terms of collinear covariant derivatives, giving one basis. For the derivation of RPI relations and factorization theorems, a basis such as the one in Eq. (3.4) is more useful.

The tree level matching of the full theory current $\bar{q}\overline{\Gamma}b$ onto SCET currents was done to subsubleading order in Ref. [35]. In deriving Feynman rules we find the momentum space version more convenient so we use the equivalent result from [111]

$$\bar{\psi}^q\overline{\Gamma}\psi^b \to \overline{J}^{(0)}+\overline{J}^{(1a)}+\overline{J}^{(1b)}+\overline{J}^{(2a)}+\overline{J}^{(2b)}+\overline{J}^{(2c)}+\overline{J}^{(2d)}+\overline{J}^{(2d)}+\overline{J}^{(2f)}\,, \tag{3.66}$$

where

$$\overline{J}^{(0)}(\omega) = \bar{\chi}_{n,\omega}\overline{\Gamma}\mathcal{H}_v\,, \tag{3.67}$$

$$\overline{J}^{(1a)}(\omega) = \frac{1}{\omega}\big(\bar{\chi}_n\, i\overleftarrow{\mathcal{D}}^{\alpha}_{c\perp}\big)_{\omega}\overline{\Theta}_{(a)\,\alpha}\,\mathcal{H}_v\,, \qquad \overline{J}^{(1b)}(\omega_{1,2}) = \frac{-1}{m}\,\bar{\chi}_{n,\omega_1}(ig\mathcal{B}^{\alpha}_{c\perp})_{\omega_2}\,\overline{\Theta}_{(b)\,\alpha}\,\mathcal{H}_v\,.$$

$$\overline{J}^{(2a)}(\omega) = \frac{1}{2m}\,\bar{\chi}_{n,\omega}\,\overline{\Upsilon}_{(a)\,\alpha}\,i\overrightarrow{\mathcal{D}}^{T\,\alpha}_{us}\,\mathcal{H}_v\,, \qquad \overline{J}^{(2b)}(\omega) = \frac{1}{\omega}\,\bar{\chi}_{n,\omega}\,\overline{\Upsilon}_{(b)\,\alpha}\,i\overleftarrow{\mathcal{D}}^{\perp\,\alpha}_{us}\,\mathcal{H}_v\,,$$

$$\overline{J}^{(2c)}(\omega) = -\Big(\bar{\chi}_n\frac{\bar{n}\cdot v}{\bar{\mathcal{P}}}\,\frac{ign\cdot\mathcal{B}_c}{n\cdot v}\Big)_{\omega}\overline{\Upsilon}_{(c)}\,\mathcal{H}_v\,, \qquad \overline{J}^{(2d)}(\omega_{1,2}) = \frac{-1}{m}\bar{\chi}_{n,\omega_1}\Big(\frac{ign\cdot\mathcal{B}_c}{n\cdot v}\Big)_{\omega_2}\overline{\Upsilon}_{(d)}\,\mathcal{H}_v\,,$$

$$\overline{J}^{(2e)}(\omega_{1,2}) = \frac{-1}{m\,\omega_1}\big(\bar{\chi}_n i\overleftarrow{\mathcal{D}}^{\alpha}_{c\perp}\big)_{\omega_1}(ig\mathcal{B}^{\beta}_{c\perp})_{\omega_2}\overline{\Upsilon}_{(e)\,\alpha\beta}\,\mathcal{H}_v\,,$$

$$\overline{J}^{(2f)}(\omega_{1,2}) = \frac{-1}{m}\bar{\chi}_{n,\omega_1}\Big(\frac{1}{n\cdot v\,\bar{\mathcal{P}}}i\mathcal{D}^{\alpha}_{c\perp}\,ig\mathcal{B}^{\beta}_{c\perp}\Big)_{\omega_2}\overline{\Upsilon}_{(f)\,\alpha\beta}\,\mathcal{H}_v\,.$$

The $\overline{\Gamma}$ in $\overline{J}^{(0)}$ is simply the Dirac structure of the full theory current. The Dirac structures that appear in the subleading currents are

$$\overline{\Theta}_{(a)\,\alpha} = \gamma^{\perp}_{\alpha}\frac{\not{\bar{n}}}{2\bar{n}\cdot v}\overline{\Gamma}\,, \qquad \overline{\Theta}_{(b)\,\alpha} = \overline{\Gamma}\frac{\not{n}}{2n\cdot v}\gamma^{\perp}_{\alpha} \tag{3.68}$$

and

$$\overline{\Upsilon}_{(a)\,\alpha} = \overline{\Gamma}\gamma_\alpha^T\,, \qquad \overline{\Upsilon}_{(b)\,\alpha} = \gamma_\alpha^\perp \frac{\not{\bar{n}}}{2\bar{n}\cdot v}\overline{\Gamma}\,, \qquad \overline{\Upsilon}_{(c)} = \overline{\Gamma}\,,$$
$$\overline{\Upsilon}_{(d)} = \overline{\Gamma}\frac{\not{v}\not{\bar{n}}\not{v}}{4}\,, \qquad \overline{\Upsilon}_{(e)\,\alpha\beta} = \gamma_\alpha^\perp \frac{\not{v}}{2}\overline{\Gamma}\frac{\not{\bar{n}}}{2}\gamma_\beta^\perp\,, \qquad \overline{\Upsilon}_{(f)\,\alpha\beta} = \overline{\Gamma}\gamma_\alpha^\perp\gamma_\beta^\perp\,. \tag{3.69}$$

Each of the operators $\overline{J}$ has unit Wilson coefficient at tree level. By re-expressing these operators in the basis of operators presented in this chapter, we determine the tree-level Wilson coefficients of our currents. This provides a check of the RPI relations.

3.3.1 Conversion

In terms of our basis, the leading order tree level current $\overline{J}^{(0)}$ is given by

$$\int \mathrm{d}\omega\, \overline{J}^{(0)}(\omega) = \int \mathrm{d}\omega\, J_1^{(0)}(\omega)\,. \tag{3.70}$$

This result holds for all five Lorentz types, $\overline{\Gamma} = \{1\,, \gamma^5\,, \gamma^\mu\,, \gamma^5\gamma^\mu, i\sigma^{\mu\nu}\}$. For the remainder of this section, we will suppress the explicit ω-dependence of our basis $J(\omega)$'s as well as the appropriate integrals $\int[\mathrm{d}\omega_i]$ whenever results hold equally well as integrals or as densities. For example, Eq. (3.70) would be written simply as $\overline{J}^{(0)} = J_1^{(0)}$. If the Lorentz type (s,p,v,a,t) of the current is not specified, the same result holds for all five types as above.

For the $\mathcal{O}(\lambda)$ currents, the relations differ for the scalar, vector, and tensor cases,

$$\int d\omega_1\, \overline{J}_{s,p}^{(1a)}(\omega_1) = \int d\omega_1\, J_1^{(1a)}(\omega_1) - \int d\omega_{1,2}\, \frac{m}{\omega_1+\omega_2} J_1^{(1b)}(\omega_1,\omega_2)\,, \tag{3.71}$$
$$\int d\omega_1\, \overline{J}_{v,a}^{(1a)}(\omega_1) = \int d\omega_1\, J_1^{(1a)}(\omega_1) + \int d\omega_{1,2}\, \frac{m}{\omega_1+\omega_2}\left[J_1^{(1b)}(\omega_1,\omega_2) - 2J_2^{(1b)}(\omega_1,\omega_2)\right],$$
$$\int d\omega_1\, \overline{J}_{t}^{(1a)}(\omega_1) = \int d\omega_1\, J_1^{(1a)}(\omega_1) + \int d\omega_{1,2}\, \frac{m}{\omega_1+\omega_2}\left[-J_1^{(1b)}(\omega_1,\omega_2) - 2J_2^{(1b)}(\omega_1,\omega_2)\right],$$
$$\overline{J}_{s,p}^{(1b)} = 0\,, \qquad \overline{J}_{v,a}^{(1b)} = -J_3^{(1b)}\,, \qquad \overline{J}_{t}^{(1b)} = 2J_1^{(1b)} + J_3^{(1b)} + 2J_4^{(1b)} + 2J_5^{(1b)}\,.$$

The last line of relations are true as integrals or as densities. For example $J^{(1b)}_{v,a}(\omega_{1,2}) = -J^{(1b)}_3(\omega_{1,2})$. At $\mathcal{O}(\lambda^2)$ the relations between the two forms of subleading currents are the same for all $\overline{J}^{(2a,2b,2c)}$ currents

$$\overline{J}^{(2a)} = J^{(2a)}_1\,, \quad \overline{J}^{(2b)} = J^{(2c)}_1\,, \quad \int d\omega_1\, \overline{J}^{(2c)} = \int d\omega_{1,2}\, \frac{m}{\omega_2}\Big[-J^{(2e)}_1 + J^{(2g)}_1\Big]\,, \tag{3.72}$$

where in the last relation the arguments of $\overline{J}^{(2c)}(\omega_1)$ and $J^{(2e,2g)}_1(\omega_{1,2})$ are implicit. The remaining currents come in different combinations depending on the Dirac structure. For $\overline{J}^{(2d)}$ we have

$$\overline{J}^{(2d)}_{s,p} = 0\,, \qquad \overline{J}^{(2d)}_{v,a} = J^{(2e)}_3 - J^{(2g)}_3\,, \qquad \overline{J}^{(2d)}_t = -J^{(2e)}_3 + J^{(2g)}_3\,. \tag{3.73}$$

For the scalar $\overline{J}^{(2e)}$ currents,

$$\int d\omega_{1,2}\, \overline{J}^{(2e)}_{s,p} = \int d\omega_{1,2}\, \Big[J^{(2e)}_1 - J^{(2e)}_2\Big] + \int d\omega_{1,2}\Big[e \to f\Big] + \int d\omega_{1,2,3}\, \frac{\omega_2+\omega_3}{\omega_1+\omega_2}\Big[e \to h\Big] \tag{3.74}$$

with similar relations for the vector and tensor cases (suppressing the integrals for convenience),

$$\begin{aligned}
\overline{J}^{(2e)}_{v,a} &= \Big[J^{(2e)}_1 - J^{(2e)}_3 - J^{(2e)}_4 + J^{(2e)}_6 + 2J^{(2e)}_7\Big] + \Big[J^{(2f)}_1 - J^{(2f)}_3 - J^{(2f)}_4 + J^{(2f)}_6 - 2J^{(2f)}_7\Big] \\
&\quad + \frac{\omega_2+\omega_3}{\omega_1+\omega_2}\Big[J^{(2h)}_1 - J^{(2h)}_3 - J^{(2h)}_4 + J^{(2h)}_6 - 2J^{(2h)}_7\Big]\,, \\
\overline{J}^{(2e)}_t &= \Big[-J^{(2e)}_1 - J^{(2e)}_3 + J^{(2e)}_5 + J^{(2e)}_7\Big] + \Big[e \to f\Big] + \frac{\omega_2+\omega_3}{\omega_1+\omega_2}\Big[e \to h\Big]\,.
\end{aligned} \tag{3.75}$$

Finally for $\overline{J}^{(2f)}$,

$$\begin{aligned}
\overline{J}^{(2f)}_{s,p} &= \Big[-J^{(2e)}_1 + J^{(2e)}_2\Big] - \frac{\omega_1}{\omega_2}\Big[e \to f\Big] - \Big[e \to h\Big]\,, \\
\overline{J}^{(2f)}_{v,a} &= \Big[-J^{(2e)}_3 - J^{(2e)}_4 + 2J^{(2e)}_6\Big] - \frac{\omega_1}{\omega_2}\Big[e \to f\Big] - \Big[e \to h\Big]\,, \\
\overline{J}^{(2f)}_t &= \Big[-J^{(2e)}_1 - J^{(2e)}_3 + J^{(2e)}_5 + 2J^{(2e)}_7\Big] - \frac{\omega_1}{\omega_2}\Big[e \to f\Big] - \Big[e \to h\Big]\,,
\end{aligned} \tag{3.76}$$

where the suppressed integrals are the same as for $\overline{J}^{(2e)}$.

3.3.2 Wilson coefficients at tree level

Inserting Eqs. (3.70-3.76) into Eq. (3.66), we can read off the tree level Wilson coefficients of our basis. For example, since $\overline{J}^{(0)}$ is the only term at leading order we have $C_1^{(d)}(\omega) = 1$ and $C_{j\neq 1}^{(d)}(\omega) = 0$ for $d = s, p, v, a, t$.

For scalar currents, the non-vanishing tree-level Wilson coefficients are

$$C_1^{(s)}(\omega) = 1\,, \qquad B_{a1}^{(s)}(\omega) = 1\,, \qquad B_{b1}^{(s)}(\omega_{1,2}) = \frac{-m}{\omega_1+\omega_2}\,, \tag{3.77}$$

and at $\mathcal{O}(\lambda^2)$

$$\begin{aligned} &A_{a1}^{(s)}(\omega) = 1\,, && A_{c1}^{(s)}(\omega) = 1\,, \\ &A_{e1}^{(s)}(\omega_{1,2}) = -\frac{m}{\omega_2}\,, && A_{f1}^{(s)}(\omega_{1,2}) = 1 + \frac{\omega_1}{\omega_2}\,, \\ &A_{f2}^{(s)}(\omega_{1,2}) = -1 - \frac{\omega_1}{\omega_2}\,, && A_{g1}^{(s)}(\omega_{1,2}) = \frac{m}{\omega_2}\,, \\ &A_{h1}^{(s)}(\omega_{1,2}) = \frac{\omega_1+2\omega_2+\omega_3}{\omega_1+\omega_2}\,, && A_{h2}^{(s)}(\omega_{1,2,3}) = -\frac{\omega_1+2\omega_2+\omega_3}{\omega_1+\omega_2}\,. \end{aligned} \tag{3.78}$$

The same results hold for the pseudoscalar currents. To $\mathcal{O}(\lambda^2)$, the values of the Wilson coefficients for vector currents that do not vanish at tree-level are

$$\begin{aligned} &C_1^{(v)}(\omega) = 1\,, && B_{a1}^{(v)}(\omega) = 1\,, \\ &B_{b1}^{(v)}(\omega_{1,2}) = \frac{m}{\omega_1+\omega_2}\,, && B_{b2}^{(v)}(\omega_{1,2}) = \frac{-2m}{\omega_1+\omega_2}\,, \qquad B_{b3}^{(v)}(\omega_{1,2}) = -1\,, \end{aligned} \tag{3.79}$$

and

$$
\begin{aligned}
&A^{(v)}_{a1}(\omega) = 1\,, && A^{(v)}_{c1}(\omega) = 1\,,\\
&A^{(v)}_{e1}(\omega_{1,2}) = 1 - \frac{m}{\omega_2}\,, && A^{(v)}_{e3}(\omega_{1,2}) = -1\,,\\
&A^{(v)}_{e4}(\omega_{1,2}) = -2\,, && A^{(v)}_{e6}(\omega_{1,2}) = 3\,,\\
&A^{(v)}_{e7}(\omega_{1,2}) = 2\,, && A^{(v)}_{f1}(\omega_{1,2}) = 1\,,\\
&A^{(v)}_{f3}(\omega_{1,2}) = -1 + \frac{\omega_1}{\omega_2}\,, && A^{(v)}_{f4}(\omega_{1,2}) = -1 + \frac{\omega_1}{\omega_2}\,,\\
&A^{(v)}_{f6}(\omega_{1,2}) = 1 - \frac{2\omega_1}{\omega_2}\,, && A^{(v)}_{f7}(\omega_{1,2}) = -2\,,\\
&A^{(v)}_{g1}(\omega_{1,2}) = \frac{m}{\omega_2}\,, && A^{(v)}_{g3}(\omega_{1,2}) = -1\,,\\
&A^{(v)}_{h1}(\omega_{1,2,3}) = \frac{\omega_2+\omega_3}{\omega_1+\omega_2}\,, && A^{(v)}_{h3}(\omega_{1,2,3}) = \frac{\omega_1-\omega_3}{\omega_1+\omega_2}\,,\\
&A^{(v)}_{h4}(\omega_{1,2,3}) = \frac{\omega_1-\omega_3}{\omega_1+\omega_2}\,, && A^{(v)}_{h6}(\omega_{1,2,3}) = \frac{-2\omega_1-\omega_2+\omega_3}{\omega_1+\omega_2}\,,\\
&A^{(v)}_{h7}(\omega_{1,2,3}) = -2\,\frac{\omega_2+\omega_3}{\omega_1+\omega_2}\,. &&
\end{aligned}
\tag{3.80}
$$

The same results hold for the axial vector currents. Finally, for the $\mathcal{O}(\lambda^2)$ tensor currents we have nonvanishing coefficients

$$
\begin{aligned}
&C^{(t)}_1(\omega) = 1\,, \quad B^{(t)}_{a1}(\omega) = 1\,, \quad B^{(t)}_{b1}(\omega_{1,2}) = 2 - \frac{m}{\omega_1+\omega_2}\,, \quad B^{(t)}_{b2}(\omega_{1,2}) = \frac{-2m}{\omega_1+\omega_2}\,,\\
&B^{(t)}_{b3}(\omega_{1,2}) = 1\,, \quad B^{(t)}_{b4}(\omega_{1,2}) = 2\,, \quad B^{(t)}_{b5}(\omega_{1,2}) = 2\,,
\end{aligned}
\tag{3.81}
$$

and

$$
\begin{aligned}
&A^{(t)}_{a1}(\omega) = 1\,, && A^{(t)}_{c1}(\omega) = 1\,,\\
&A^{(t)}_{e1}(\omega_{1,2}) = -2 - \frac{m}{\omega_2}\,, && A^{(t)}_{e3}(\omega_{1,2}) = -3\,,\\
&A^{(t)}_{e5}(\omega_{1,2}) = 2\,, && A^{(t)}_{e7}(\omega_{1,2}) = 3\,,\\
&A^{(t)}_{f1}(\omega_{1,2}) = -1 + \frac{\omega_1}{\omega_2}\,, && A^{(t)}_{f3}(\omega_{1,2}) = -1 + \frac{\omega_1}{\omega_2}\,,\\
&A^{(t)}_{f5}(\omega_{1,2}) = 1 - \frac{\omega_1}{\omega_2}\,, && A^{(t)}_{f7}(\omega_{1,2}) = 1 - \frac{2\omega_1}{\omega_2}\,,\\
&A^{(t)}_{g1}(\omega_{1,2}) = \frac{m}{\omega_2}\,, && A^{(t)}_{g3}(\omega_{1,2}) = 1\,,\\
&A^{(t)}_{h1}(\omega_{1,2,3}) = \frac{\omega_1-\omega_3}{\omega_1+\omega_2}\,, && A^{(t)}_{h3}(\omega_{1,2,3}) = \frac{\omega_1-\omega_3}{\omega_1+\omega_2}\,,\\
&A^{(t)}_{h5}(\omega_{1,2,3}) = \frac{-\omega_1+\omega_3}{\omega_1+\omega_2}\,, && A^{(t)}_{h7}(\omega_{1,2,3}) = \frac{-2\omega_1-\omega_2+\omega_3}{\omega_1+\omega_2}\,.
\end{aligned}
\tag{3.82}
$$

It is straightforward to check that these results all satisfy the RPI relations from section 3.2.3, providing a cross-check on those results.

3.3.3 One-Loop Results

The relations from section 3.2.3 apply at any order in perturbation theory, so they can also be used to determine one-loop values for certain coefficients. For the LO

currents the one-loop coefficients in $\overline{\rm MS}$ at $\mu = m$ are [15]

$$
\begin{aligned}
C_1^{(s)}(\hat\omega) &= 1 - \frac{\alpha_s(m)C_F}{4\pi}\left\{2\ln^2(\hat\omega) + 2{\rm Li}_2(1-\hat\omega) - \frac{2\ln(\hat\omega)}{1-\hat\omega} + \frac{\pi^2}{12}\right\},\\
C_1^{(v)}(\hat\omega) &= 1 - \frac{\alpha_s(m)C_F}{4\pi}\left\{2\ln^2(\hat\omega) + 2{\rm Li}_2(1-\hat\omega) + \ln(\hat\omega)\Big(\frac{3\hat\omega-2}{1-\hat\omega}\Big) + \frac{\pi^2}{12} + 6\right\},\\
C_1^{(t)}(\hat\omega) &= 1 - \frac{\alpha_s(m)C_F}{4\pi}\left\{2\ln^2(\hat\omega) + 2{\rm Li}_2(1-\hat\omega) + \ln(\hat\omega)\Big(\frac{4\hat\omega-2}{1-\hat\omega}\Big) + \frac{\pi^2}{12} + 6\right\},\\
C_2^{(v)}(\hat\omega,1) &= \frac{\alpha_s(m)C_F}{4\pi}\left\{\frac{2}{(1-\hat\omega)} + \frac{2\hat\omega\ln(\hat\omega)}{(1-\hat\omega)^2}\right\}, \qquad C_2^{(t)}(\hat\omega) = 0\,,\\
C_3^{(v)}(\hat\omega) &= \frac{\alpha_s(m)C_F}{4\pi}\left\{\frac{(1-2\hat\omega)\hat\omega\ln(\hat\omega)}{(1-\hat\omega)^2} - \frac{\hat\omega}{1-\hat\omega}\right\},\\
C_3^{(t)}(\hat\omega) &= \frac{\alpha_s(m)C_F}{4\pi}\left\{\frac{-2\hat\omega\ln(\hat\omega)}{1-\hat\omega}\right\}, \qquad C_4^{(t)}(\hat\omega) = 0\,,
\end{aligned}
\tag{3.83}
$$

where $\hat\omega = \omega/m$ and $C_F = 4/3$ for color $SU(3)$. The quark-gluon-antiquark operators $J^{(1b)}$ have coefficients that are not fixed by RPI, and these were determined by a one-loop matching in [39, 28]. Thus all $\mathcal{O}(\lambda^{0,1})$ currents are known at one-loop order. The expressions are fairly lengthy, and so we do not repeat them here. Using their results and our Eqs. (3.39-3.41), (3.49-3.52), and (3.60-3.63), the coefficients of the currents $J^{(2a,2b,2c,2d,2e)}$ are also determined at one-loop order.

We give the scalar current case as an example. For the scalar current, the coefficient at $\mu = m$ is [39, 28]

$$
\begin{aligned}
B_{(b1)}^{(s)}(\hat\omega_{1,2},1) &= -\frac{1}{\hat\omega} + \frac{\alpha_s C_F}{4\pi}\left[\frac{-2}{\hat\omega_2}\left\{\ln^2\hat\omega - \ln^2\hat\omega_1 - \ln\Big(\frac{\hat\omega}{\hat\omega_1}\Big)\right\} + \Big(\frac{4}{\hat\omega} + \frac{2}{1-\hat\omega}\Big)\ln\hat\omega\right.\\
&\quad -\frac{2}{\hat\omega_1}\Big(\frac{\ln\hat\omega}{1-\hat\omega} - \frac{\ln\hat\omega_2}{1-\hat\omega_2}\Big) - \frac{\hat\omega_2\ln\hat\omega_2}{(1-\hat\omega_2)^2} + \frac{2(1-\hat\omega_1)}{\hat\omega_1\hat\omega_2}\big\{{\rm Li}_2(1-\hat\omega) - {\rm Li}_2(1-\hat\omega_1)\big\}\\
&\quad \left. -\frac{2}{\hat\omega_1\hat\omega_2}\Big\{{\rm Li}_2(1-\hat\omega_2) - \frac{\pi^2}{6}\Big\} - \frac{4}{\hat\omega} - \frac{1}{1-\hat\omega_2}\right]\\
&\quad -\frac{\alpha_s C_A}{4\pi}\left[\frac{-1}{\hat\omega_2}\left\{\ln^2\hat\omega - \ln^2\hat\omega_1 - \ln\Big(\frac{\hat\omega}{\hat\omega_1}\Big)\right\} + \frac{1}{\hat\omega_1}\ln\Big(\frac{\hat\omega}{\hat\omega_2}\Big) + \frac{\ln\hat\omega_2}{1-\hat\omega_2}\right.\\
&\quad \left. +\frac{1-\hat\omega_1}{\hat\omega_1\hat\omega_2}\big\{{\rm Li}_2(1-\hat\omega) - {\rm Li}_2(1-\hat\omega_1)\big\} - \frac{1}{\hat\omega_1\hat\omega_2}\Big\{{\rm Li}_2(1-\hat\omega_2) - \frac{\pi^2}{6}\Big\}\right]\\
&\quad +\frac{\alpha_s C_F}{4\pi}\frac{1}{\hat\omega}\left[2\ln^2(\hat\omega) + 2{\rm Li}_2(1-\hat\omega) - \frac{2\ln(\hat\omega)}{1-\hat\omega} + \frac{\pi^2}{12}\right],
\end{aligned}
\tag{3.84}
$$

where $C_A = 3$, $\hat{\omega}_{1,2} = \omega_{1,2}/m$, $\hat{\omega} = \hat{\omega}_1 + \hat{\omega}_2$, and we have transformed to our basis. We will also need the derivative of the LO scalar currents coefficient

$$\frac{d}{d\omega} C_1^{(s)}(\hat{\omega}, 1) = -\frac{\alpha_s(m) C_F}{2\pi m} \left\{ \frac{-1 + \hat{\omega} + (2 - 4\hat{\omega} + \hat{\omega}^2) \ln \hat{\omega}}{\hat{\omega}(1-\hat{\omega})^2} \right\}. \tag{3.85}$$

Now in section IIIC we derived the following results for the $\mathcal{O}(\lambda^2)$ currents

$$\begin{aligned}
&A_{a1}^{(s)}(\omega) = C_1^{(s)}(\omega), && A_{a2}^{(s)}(\omega) = 2\omega C_1^{(s)\prime}(\omega), \\
&A_{b1}^{(s)}(\omega) = \omega C_1^{(s)\prime}(\omega), && A_{c1}^{(s)}(\omega) = C_1^{(s)}(\omega), \quad A_{d1}^{(s)}(\omega) = -\omega C_1^{(s)\prime}(\omega), \\
&A_{e1}^{(s)}(\omega_{1,2}) = -\frac{m}{\omega_2} C_1^{(s)}(\omega_1+\omega_2), && A_{e2}^{(s)}(\omega_{1,2}) = -\frac{m}{(\omega_1+\omega_2)} C_1^{(s)}(\omega_1+\omega_2) - B_{b1}^{(s)}(\omega_{1,2}).
\end{aligned} \tag{3.86}$$

Combined with Eqs.(3.83-3.85), these relations determine the coefficients at one-loop order. The results for the $J_j^{(2a-2e)}$ vector and tensor currents at one-loop order are easily obtained in the same manner.

To summarize, in this chapter we derived a complete basis of scalar, vector, and tensor heavy-to-light currents in the soft-collinear effective theory I at next-to-next-to-leading order in the power counting, $\mathcal{O}(\lambda^2)$. Building on the approach in Ref. [96] where one takes $v_\perp = 0$ from the start, we considered the full set of RPI relations that leave us on this surface. The completeness of deriving RPI relations projected on a surface was analyzed in Chapter 2. With a careful choice of Dirac structures in our analysis of heavy-to-light currents at $\mathcal{O}(\lambda^2)$, it was demonstrated that the projected RPI gives the full set of constraints.

A simple method for counting the number of Dirac structures in the basis for any operator with $d = 4$ was given.[4] Several types of reparameterization invariance provide restrictions on the structure of these currents. We formulated RPI as constraint equations on the allowed Dirac structures and Wilson coefficients as given in Eqs. (3.15), (3.19), (3.23), (3.24), (3.28), and (3.29). We expect that a similar setup with constraint equations and projected surfaces will be useful in deriving RPI

[4]We did not consider the complication that occurs if one uses dimensional regularization where there can be additional evanescent $\mathcal{O}(\lambda^2)$ operators that vanish for $d = 4$. In SCET this type of operator has been studied for the $\mathcal{O}(\lambda)$ currents in Ref. [28].

relations at higher orders in λ and in deriving results for non-heavy-to-light currents.

Our main results are contained in the solution of the constraint equations as given in Eqs. (3.37-3.41), (3.46-3.52), and (3.58-3.63). These results determine the coefficients of five of the eleven NNLO operators, $J_j^{(2a,2b,2c,2d,2e)}$, for various Dirac structures indicated by j and at any order in perturbation theory, in terms of the coefficients of NLO and LO operators. This determines 7, 23, and 32 Wilson coefficients for the scalar, vector, and tensor heavy-to-light currents respectively. Results at tree-level and one-loop order were discussed in sections 3.3.2 and 3.3.3. Finally, the operators $J^{(2f,2g,2h,2i,2j,2k)}$ defined in Eqs. (3.4,3.5) together with the Dirac structures in Eqs. (3.37,3.38,3.46,3.47,3.58,3.59) were shown to not be constrained by reparameterization invariance.

Chapter 4

B decays to two light mesons in SCET

4.1 Introduction

The nonleptonic charmless decay channels $B \to M_1 M_2$ provide a wealth of information about the Standard Model, including the study of CP violation and the strong interactions. An interesting experimental observable is the relative "strong" phase between Standard Model amplitudes multiplying the CKM factors $V_{ub}V_{uf}^*$ and $V_{cb}V_{cf}^*$ $(f = d, s)$, since these phases are measured to be large in the $B \to \pi\pi$ and $B \to K\pi$ channels [55]. Since many amplitudes for these decays are loop dominated, it is possible for new physics to give a significant contribution. Except for the simplest observables, however, testing for new physics requires an understanding of the Standard Model background.

The theory of nonleptonic B decays underwent important progress in the last few years. Factorization theorems for $B \to MM'$ decays have been proven to all orders in α_s at leading order in Λ/Q, for decays when M is a light (charmless) meson and M' is either charmed or charmless [31, 32, 21, 57, 60, 126, 19]. Here $Q \sim m_b \sim m_c \sim E_M$ is the "hard" scale and $\Lambda \sim \Lambda_{\rm QCD} \sim 500\,{\rm MeV}$ denotes a typical hadronic scale. An important difference between the various approaches to making predictions for the charmless $B \to M_1 M_2$ decay rates [68, 67, 31, 103, 102, 117, 32, 33, 66, 40, 19, 26]

is how certain $\mathcal{O}(\Lambda/Q)$ power suppressed corrections are treated. In particular, it was observed that so-called annihilation diagrams, in which the initial state "spectator" quark is Wick-contracted with a quark field in the effective Hamiltonian (as in Fig. 4-2), give rise to divergent convolution integrals if one attempts calculating them using conventional factorization techniques [103]. In the KLS (or pQCD) approach [103], these are rendered finite by $k_\perp$ dependences, which effectively cut off the endpoints of the meson distribution functions. KLS found large imaginary parts from the jet scale, $\sqrt{m_b\Lambda}$, from propagators via $\mathrm{Im}\,[xm_b^2-k_\perp^2+i\epsilon]^{-1} = -\pi\delta(xm_b^2-k_\perp^2)$ [115]. They also found that for the physical value of m_b the power suppression of these terms relative to the leading contributions was not very significant. In the BBNS (or QCDF) approach [31, 32, 33, 40], the divergent convolutions are interpreted as signs of infrared sensitive contributions, and are modeled by complex parameters, $X_A = \int_0^1 dy/y = (1+\rho_A e^{i\varphi_A})\ln(m_B/\Lambda)$, with $\rho_A \leq 1$ and an unrestricted strong phase φ_A. In Ref. [79], annihilation diagrams were investigated in the soft-collinear effective theory [13, 15, 27, 22] and parameterized by a complex amplitude. When annihilation is considered in $SU(3)$ flavor analyses a complex parameter is also used [9, 64, 139, 120]. In the absence of a factorization theorem for annihilation contributions, a dimensional analysis based parameterization with Λ/m_b magnitude and unrestricted strong phases is a reasonable way of estimating the uncertainty. In order not to introduce model-dependent correlations, a new parameter could be used for each independent channel.

It was recently shown by Manohar and Stewart [124] that properly separating the physics at different momentum scales removes the divergences, giving well defined results for convolution integrals through a new type of factorization which separates modes in their invariant mass and rapidity. The analysis involves a minimal subtraction with the zero-bin method to avoid double counting rapidity regions, and with the regulation and subtraction of divergences for large p^+ and p^- momenta that behave like ultraviolet divergences. Additional subtractions would correspond to scheme dependent terms, so the minimal subtraction is the usual and simplest choice. We refer to this as MS factorization. In this chapter we classify annihilation contributions

to $B \to M_1 M_2$ decays. We restrict our discussion to non-isosinglet mesons ($M_i = \pi$, K, ρ, ...), which can not be produced solely by gluons, for which the annihilation amplitudes are power suppressed by $\sim \Lambda/Q$. Our notation follows that of Ref. [19] where factorization theorems for the leading order $B \to M_1 M_2$ amplitudes were derived. We demonstrate how rapidity factorization works for the leading terms of order $\mathcal{O}[\alpha_s(m_b)\Lambda/m_b]$ that had previously been addressed with other approaches to factorization. These leading-order annihilation contributions are real despite the presence of endpoint divergences. We also classify which terms can involve a nonperturbative complex hadronic parameter, and demonstrate that they first show up for annihilation at higher order in perturbation theory, $\mathcal{O}[\alpha_s^2(\sqrt{m_b\Lambda})\,\Lambda/m_b]$. Our analysis demonstrates that while certain annihilation contributions are only sensitive to the hard short-distance scale $\mu^2 \sim m_b^2$ (local annihilation), there exist other annihilation contributions that start at the same order in α_s and $1/m_b$ and are sensitive to the intermediate scale $\mu^2 \sim m_b\Lambda$ (hard-collinear annihilation terms) that had not been addressed previously in the literature. The leading local annihilation terms involve f_B and twist-2 distribution functions, while the leading hard-collinear terms have twist-3 meson distributions.

An interesting set of power corrections are those proportional to μ_P where $\mu_\pi = m_\pi^2/(m_u + m_d)$ and $\mu_K = m_K^2/(m_u + m_s)$ [132]. For kaons and pions $\mu_P \sim 2\,\mathrm{GeV}$, so corrections proportional to μ_P/m_b can be sizable, and were labeled "chirally enhanced" in Refs. [31, 32, 33, 40]. In the chiral limit $\mu_P \propto \Lambda_\chi$, where Λ_χ is the chiral symmetry breaking scale, so the enhancement is not parametric, and comes from the fact that $\Lambda_\chi > \Lambda_{\rm QCD}$. In the BBNS approach these Λ^2/m_b^2 annihilation power corrections are included along with the leading-order terms, and when they multiply divergent convolutions they are described by complex parameters. Below we show that, much like the lowest-order annihilation contributions, these terms are also real and factorizable.

In section 4.2 we review the leading order factorization theorem, and classify power corrections to $B \to M_1 M_2$, with a focus on annihilation amplitudes. In section 4.3 a factorization theorem is derived for local annihilation amplitudes at order Λ/m_b for

final states not involving isosinglets (given in Eq. (4.20)). These amplitudes start at $\mathcal{O}(\alpha_s(m_b))$ and involve f_B and twist-2 meson distributions. In section 4.4, we consider the leading hard-collinear annihilation amplitudes, which start at the same power and perturbative order as local annihilation. The extension to chirally enhanced local annihilation terms is considered in section 4.5. In section 4.6 we study annihilation amplitudes from time-ordered products, and classify complex contributions generated at the hard scale m_b, the intermediate scale $\sqrt{m_b\Lambda}$, and the nonperturbative scale Λ. Our results give absolute predictions for the annihilation amplitudes in $B \to PP$, PV, VV channels, given the meson distribution functions as inputs, which are studied in Section 4.7. This section also discusses the implications of our results for models of annihilation used in the literature, and a numerical analysis of the annihilation amplitudes in $\bar{B} \to K\pi$ and $\bar{B} \to K\bar{K}$. Appendix A gives the derivation of a two-dimensional convolution formula with overlapping zero-bin subtractions.

4.2 Annihilation Contributions in SCET

The relevant scales in $B \to M_1 M_2$ decays are m_W, m_b, $E \approx m_B/2$, m_c, the jet scale $\sqrt{E\Lambda}$, and the nonperturbative scale Λ. Here E is the energy of the light mesons, which is much greater than their masses, $m_{M_{1,2}} \sim \Lambda$. To simplify notation, we denote by m_b hereafter the expansion in all hard scales, $\{m_b, E, m_c\}$. The decays $B \to M_1 M_2$ are mediated by the non-leptonic $\Delta B = 1$ weak effective Hamiltonian, Eq. (2.15).

To define what we mean by annihilation amplitudes we use the contraction amplitudes A_1, A_2, P_3, $P_3^{\rm GIM}$ in the full electroweak theory from Ref. [54] (which thus includes penguin annihilation). These amplitudes are scheme and scale independent and correspond to Feynman diagrams with a Wick contraction between the spectator flavor in the initial state and a quark in the operators O_i. Using SCET these annihilation amplitudes can be proven to be suppressed by Λ/m_b to all orders in α_s [19]. These contributions differ from emission-annihilation amplitudes, EA_1 and EA_2, which involve at least one isosinglet meson. As demonstrated in Refs. [40, 137], $EA_{1,2}$ occur at leading order in the power expansion. We focus on isodoublet and

isotriplet final states, so ignore the $EA_{1,2}$ amplitudes hereafter.

To separate the mass scales occurring below m_b we need to match H_W onto operators in SCET. The nonperturbative degrees of freedom are soft quarks and gluons for the B-meson, n-collinear quarks and gluons for one light meson, and $\bar{n}$-collinear fields for the other light meson, as discussed in section 2.5.1. Expanding in Λ/m_b gives

$$\begin{aligned}\langle M_1 M_2|H_W|B\rangle &= A^{(0)} + A_{c\bar{c}} + A^{(1)}_{ann} + A^{(1)}_{rest} + \dots \\ &= \frac{G_F m_B f_{M_1} f_{M_2} f_B}{\sqrt{2}\,\Lambda_0}\Big[\hat{A}^{(0)} + \hat{A}_{c\bar{c}} + \hat{A}^{(1)}_{ann} + \hat{A}^{(1)}_{rest} + \dots\Big]\,. \end{aligned} \tag{4.1}$$

In the second line we switched to dimensionless amplitudes $\hat{A}$ by pulling out a prefactor with the correct $\Lambda^{5/2} m_b^{1/2}$ scaling. Here $\Lambda_0 = 500\,\mathrm{MeV}$ represents a B-meson scale that is $\mathcal{O}(\Lambda_{\mathrm{QCD}})$. Taking $\eta = \Lambda/m_b$ we have the leading order amplitude $\hat{A}^{(0)} = \mathcal{O}(\eta^0)$, and the subleading amplitude $\hat{A}^{(1)} = \hat{A}^{(1)}_{ann} + \hat{A}^{(1)}_{rest} = \mathcal{O}(\eta^1)$, which we have split into the annihilation amplitude $\hat{A}^{(1)}_{ann}$ and the remainder $\hat{A}^{(1)}_{rest}$. The amplitude $\hat{A}_{c\bar{c}}$ in Eq. (4.1), denotes contributions from long-distance charm effects in all amplitudes, while perturbative charm loops contribute in the amplitudes $A^{(0)}$ and $A^{(1)}$.[1]

There are two formally large scales, $m_b \gg \sqrt{m_b\Lambda} \gg \Lambda$, which we will refer to as the hard scale $\mu_h \sim m_b$, and intermediate or hard-collinear scale $\mu_i \sim \sqrt{m_b\Lambda}$. These scales can be integrated out one-by-one [23] with effective theories $\mathrm{SCET_I}$ and $\mathrm{SCET_{II}}$. Integrating out m_b requires matching the O_i onto a series of operators in $\mathrm{SCET_I}$, $Q^{(j)} \sim \lambda^j$ where the $\mathrm{SCET_I}$ power counting parameter $\lambda = \eta^{1/2} = \sqrt{\Lambda/m_b}$. To obtain contributions to $B \to M_1 M_2$, we require an odd number of ultrasoft (usoft) light quarks q_{us}, two or more n-collinear fields, and two or more $\bar{n}$-collinear fields, where $n^2 = \bar{n}^2 = 0$.

We briefly review results from Refs. [57, 60, 19] for the leading amplitude $A^{(0)}$ for

[1] $\hat{A}_{c\bar{c}}$ has the c-fields in $O^c_{1,2}$ and O_{3-10} replaced by nonrelativistic fields [19], and is suppressed by at least their relative velocity, $v \sim 0.3 - 0.5$. The possibility of large nonperturbative charm loop contributions was first discussed in Refs. [67, 66], and the size of these terms remains controversial [30, 20].

$B \to M_1 M_2$. Here we have weak operators $Q^{(0)}_{1d-6d} \sim \lambda^6$, $Q^{(1)}_{1d-8d} \sim \lambda^7$ with no q_{us}'s, taken in time-ordered products with an usoft-collinear quark Lagrangian, $\mathcal{L}^{(j)}_{\xi q} \sim \lambda^j$ for $j = 1, 2$, which has one q_{us}. We denote other subleading Lagrangians by $\mathcal{L}^{(j)}$, and list the $\mathcal{O}(\lambda^7)$ and $\mathcal{O}(\lambda^8)$ time-ordered products for $A^{(0)}$ in Table 4.1. Matching these time-ordered products onto $\mathrm{SCET_{II}}$ gives the leading $\mathcal{O}(\eta^6)$ operators.[2] When combined with the $\eta^{-7/2}$ from the states this yields a matrix element of order $\eta^{5/2}$, in agreement with the prefactor in Eq. (4.1). Examples of the weak operators in $\mathrm{SCET_I}$ are

$$\begin{aligned} Q^{(0)}_{1d} &= \left[\bar{u}_{n,\omega_1} \bar{n}\!\!\!/ P_L b_v\right] \left[\bar{d}_{\bar{n},\omega_2} n\!\!\!/ P_L u_{\bar{n},\omega_3}\right], \\ Q^{(1)}_{1d} &= \left[\bar{u}_{n,\omega_1} ig \mathcal{B}^{\perp}_{n,\omega_4} P_L b_v\right] \left[\bar{d}_{\bar{n},\omega_2} n\!\!\!/ P_L u_{\bar{n},\omega_3}\right], \end{aligned} \tag{4.2}$$

where other $Q^{(0,1)}_{id}$ have different flavor structures. The "quark" fields with subscripts n and $\bar{n}$ contain a collinear quark field and Wilson line with large momenta labels ω_i, such as

$$\bar{u}_{n,\omega} = \left[\bar{\xi}^{(u)}_n W_n \, \delta(\omega - \bar{n} \cdot \mathcal{P}^\dagger)\right]. \tag{4.3}$$

Here $\bar{\xi}_n$ creates a n-collinear quark, or annihilates an antiquark, $W_n = W[\bar{n} \cdot A_n]$ is the standard SCET collinear Wilson line built from the $\bar{n}$ component of n-collinear gluons, $\bar{n} \cdot \mathcal{P}^\dagger$ is an operator that picks out the large $\bar{n} \cdot p$ label momentum of the fields it acts on, and $ig\mathcal{B}^{\perp\mu}_{n,\omega} = \left[1/\bar{\mathcal{P}} \, W_n^\dagger [i\bar{n}\cdot D_{c,n}, iD^\mu_{n,\perp}] W_n \delta(\omega - \bar{\mathcal{P}}^\dagger)\right]$. The b_v is an HQET b-quark field.

The leading order factorization theorem from $\mathrm{SCET_I}$ is [19]

$$A^{(0)} = \frac{G_F m_B^2 f_{M_1}}{\sqrt{2}} \left[\int_0^1 du\, dz\, T_{1J}(u,z) \zeta_J^{BM_2}(z) \phi^{M_1}(u) + \int_0^1 du\, T_{1\zeta}(u) \zeta^{BM_2} \phi^{M_1}(u) \right] + \{M_1 \leftrightarrow M_2\}. \tag{4.4}$$

Here T_{1J} and $T_{1\zeta}$ contain contributions from the hard scales m_b, and ϕ^M is the non-perturbative twist-2 light-cone distribution function. The terms ζ^{BM} and $\zeta_J^{BM}(z)$ contain contributions from both the intermediate scale $\mu_i \sim \sqrt{m_b \Lambda}$ and the scale Λ,

[2] Recall that to derive the η^6, we note that $\lambda^8 = \eta^4$, and changing the scaling $\lambda \to \eta$ for four collinear quark fields in matching $\mathrm{SCET_I} \to \mathrm{SCET_{II}}$ gives the extra η^2. The λ^7 term gains an extra λ from the change in scaling to a collinear $D_\perp$.

and are defined by $\mathrm{SCET_I}$ matrix elements between B and M states. In particular their scaling is

$$\zeta^{BM}(E),\ \zeta_J^{BM}(z,E) \sim \left(\frac{\Lambda}{m_b}\right)^{3/2} \left[\alpha_s(\mu_i) + \dots\right], \tag{4.5}$$

explaining the $\alpha_s(\mu_i)$ entry in the $A^{(0)}$ rows of Table 4.1. The ζ^{BM} functions occur in both semileptonic decays and nonleptonic decays ($E \approx m_B/2$). Integrating out the scale $\sqrt{m_b\Lambda}$ to all orders in α_s by matching onto $\mathrm{SCET_{II}}$ gives [19, 124]

$$\begin{aligned}
\zeta_J^{BM}(z,E) &= \frac{f_B f_M m_B}{4E^2} \int dx \int dk^+\, J(z,x,k_+,E)\, \phi^M(x)\, \phi_+^B(k^+)\,, \\
\zeta^{BM}(E) &= \frac{f_B f_M m_B}{4E^2} \sum_{a,b} \int dx_1 dx_2 \int dk_1^+ dk_2^+\, J_{ab}(x_i,k_j^+,E)\, \phi_a^M(x_i)\, \phi_b^B(k_j^+)\,,
\end{aligned} \tag{4.6}$$

where the ϕ_a^M and ϕ_b^B's are twist-2 and twist-3, two and three parton distributions and we pulled out $f_B f_M$ for convenience. The jet functions J, J_{ab} occur due to the time-ordered product structure in $\mathrm{SCET_I}$ and contain contributions from the scale $\sqrt{m_b\Lambda}$. Using the result for ζ_J^{BM} at order $\alpha_s(\mu_i)$, this result agrees with the BBNS approach (where expressing ζ^{BM} in terms of the full theory form factor generates an additional ζ_J^{BM} term). The result for ζ^{BM} is from Ref. [124] and required the MS factorization with zero-bin subtractions. The set of contributing functions (indices a,b) is determined by the complete set of $\mathrm{SCET_{II}}$ operators derived in Ref. [108]. The power counting in $\alpha_s(\mu_i)$ for the $\mathrm{SCET_I}$ functions ζ^{BM} and ζ_J^{BM} agree with that derived in pQCD [114].

Next we classify the contributions to the power suppressed $B \to M_1 M_2$ amplitudes $A^{(1)}$. In $\mathrm{SCET_I}$ we need to study operators and time-ordered products with scaling up to $\mathcal{O}(\lambda^{10})$. These have one or three light usoft quark fields. The relevant terms are listed in Table 4.1, where $Q_i^{(j)} \sim \lambda^{6+j}$ and our notation for the Lagrangians up to second order is taken from Ref. [24]. All the listed terms have an odd number of soft light quark fields. A basis for the $Q_i^{(4)}$ operators is constructed in section 4.3, for the $Q_i^{(2)}\mathcal{L}_{\xi q}^{(1)}$ terms in section 4.4, and for the $Q_i^{(5)}$ terms in section 4.5. A basis is not yet known for the remaining $Q_i^{(2)}$ operators, for $Q_i^{(3)}$, and for the $\mathcal{L}_{\xi q}^{(3,4)}$ and

Λ/m_b order	T-ordered products in $\mathrm{SCET_I}$	Perturbative order Annhilation	Perturbative order Other	Dependence in $\mathrm{SCET_{II}}$	Properties
$A^{(0)}$	$Q_i^{(0)}\mathcal{L}_{\xi q}^{(1)}$	—	$\alpha_s(\mu_i)$	$\phi_i^B\phi_j^M\phi^{M'}$	Real
	$Q_i^{(0)}\mathcal{L}_{\xi q}^{(2)}$	—	$\alpha_s(\mu_i)$	$\phi_i^B\phi_j^M\phi^{M'}$	Real
	$Q_i^{(0)}\mathcal{L}_{\xi q}^{(1)}\mathcal{L}^{(1)}$	—	$\alpha_s(\mu_i)$	$\phi_i^B\phi_j^M\phi^{M'}$	Real
	$Q_i^{(1)}\mathcal{L}_{\xi q}^{(1)}$	—	$\alpha_s(\mu_i)$	$\phi_+^B\phi^M\phi^{M'}$	Real
$A^{(1)}$	$Q_i^{(j'=0,1)}\mathcal{L}_{\xi q}^{(j\le 4)}\,\Pi_i\,\mathcal{L}^{(k_i)}$	—	$\alpha_s(\mu_i)$		Complex
	$Q_i^{(4)}$	$\alpha_s(\mu_h)$	—	$f_B\,\phi^M\phi^{M'}$	Real
	$Q_i^{(2)}\mathcal{L}_{\xi q}^{(1)}$	$\alpha_s(\mu_h)$	$\alpha_s(\mu_i)$	$\phi^B\phi^{3M}\phi^{M'}$	Real
	$Q_i^{(0)}\big[\mathcal{L}_{\xi q}^{(1)}\big]^3$	$\frac{\alpha_s^2(\mu_i)}{\pi}$	$\frac{\alpha_s^2(\mu_i)}{\pi}$	$S_j(k_{1,2}^+,k_3^-)\ldots$	Complex
	$Q_i^{(0)}\big[\mathcal{L}_{\xi q}^{(1)}\big]^3\mathcal{L}^{(1)}$	$\frac{\alpha_s^2(\mu_i)}{\pi}$	$\frac{\alpha_s^2(\mu_i)}{\pi}$	$S_j(k_{1,2}^+,k_3^-)\ldots$	Complex
	$Q_i^{(0)}\big[\mathcal{L}_{\xi q}^{(1)}\big]^2\mathcal{L}_{\xi q}^{(2)}$	$\frac{\alpha_s^2(\mu_i)}{\pi}$	$\frac{\alpha_s^2(\mu_i)}{\pi}$	$S_j(k_{1,2}^+,k_3^-)\ldots$	Complex
	$Q_i^{(1)}\big[\mathcal{L}_{\xi q}^{(1)}\big]^3$	$\frac{\alpha_s^2(\mu_i)}{\pi}$	$\frac{\alpha_s^2(\mu_i)}{\pi}$	$S_j(k_{1,2}^+,k_3^-)\ldots$	Complex
	$Q_i^{(2)}\big[\mathcal{L}_{\xi q}^{(1)}\big]^2$	—	$\frac{\alpha_s^2(\mu_i)}{\pi}$		Complex
	$Q_i^{(2)}\mathcal{L}_{\xi q}^{(1)}\mathcal{L}^{(1)}$	$\frac{\alpha_s(\mu_h)\alpha_s(\mu_i)}{\pi}$	$\alpha_s(\mu_i)$		Complex
	$Q_i^{(2)}\mathcal{L}_{\xi q}^{(2)}$	$\frac{\alpha_s(\mu_h)\alpha_s(\mu_i)}{\pi}$	$\alpha_s(\mu_i)$		Complex
	$Q_i^{(3)}\mathcal{L}_{\xi q}^{(1)}$	$\frac{\alpha_s(\mu_h)\alpha_s(\mu_i)}{\pi}$	$\alpha_s(\mu_i)$		Complex
$A^{(2)}$	$Q_i^{(5)}$	$\alpha_s(\mu_h)$	—	$f_B\,\mu_M\phi_{pp}^M\phi^{M'}$	Real

Table 4.1: All contributions to $B\to M_1M_2$ amplitudes at leading order ($A^{(0)}$) and at order Λ/m_b ($A^{(1)}$), besides $A_{c\bar{c}}$. In the first $A^{(1)}$ line $j'+j+\sum k_i\le 4$. The terms with — are absent or higher order when matched onto $\mathrm{SCET_{II}}$. The dependence in $\mathrm{SCET_{II}}$ column lists the known dependence on nonperturbative parameters. The properties column shows whether at least one of the nonperturbative parameters is complex. For $A^{(2)}$, suppressed by Λ^2/m_b^2, only the local chirally enhanced annihilation operator is shown.

$\mathcal{L}^{(3)}$ Lagrangians, but they do not contribute at $\mathcal{O}(\alpha_s)$, and only general properties of these operators are required for our analysis. Dashes in Table 4.1 indicate terms that are absent to all orders in α_s for reasons to be explained below. To determine the perturbative order listed in the table we count the number of hard $\alpha_s(\mu_h)$ factors from the matching onto $\mathrm{SCET_I}$, and the number of intermediate scale $\alpha_s(\mu_i)$ factors from matching onto $\mathrm{SCET_{II}}$. The dependence in $\mathrm{SCET_{II}}$ column lists the nonperturbative quantities that appear in the factorization theorem for the leading order result described above, and from the factorization theorems we will derive in sections 4.3, 4.4 and 4.5 below. The properties column lists whether the nonperturbative distribution functions are complex or real as described in detail in section 4.6, and has implications for strong phase information in the power corrections. The results in Table 4.1 imply the following power counting (for amplitudes not involving $A_{c\bar{c}}$),

$$\begin{aligned}
&\mathrm{Re}\big[\hat{A}^{(0)}\big] \sim \alpha_s(\mu_i)\,, && \mathrm{Im}\big[\hat{A}^{(0)}\big] \sim \alpha_s(\mu_i)\,\alpha_s(\mu_h)\,,\\
&\mathrm{Re}\big[\hat{A}^{(1)}_{ann}\big] \sim \big[\alpha_s(\mu_h) + \alpha_s^2(\mu_i)\big]\,\frac{\Lambda}{m_b}\,, && \mathrm{Im}\big[\hat{A}^{(1)}_{ann}\big] \sim \alpha_s^2(\mu_i)\,\frac{\Lambda}{m_b}\,,\\
&\mathrm{Re}\big[\hat{A}^{(1)}_{rest}\big] \sim \alpha_s(\mu_i)\,\frac{\Lambda}{m_b}\,, && \mathrm{Im}\big[\hat{A}^{(1)}_{rest}\big] \sim \alpha_s(\mu_i)\,\frac{\Lambda}{m_b}\,.
\end{aligned} \tag{4.7}$$

To facilitate the discussion we divide the annihilation amplitudes into local annihilation contributions, $A^{(1,2)}_{Lann}$ from the operators $Q_i^{(4,5)}$ that are insensitive to the jet scale, and into the remaining annihilation amplitudes, $A^{(1)}_{Tann}$, which are from time-ordered products in $\mathrm{SCET_I}$. Thus,

$$A^{(1)}_{ann} = A^{(1)}_{Lann} + A^{(1)}_{Tann}\,. \tag{4.8}$$

In the literature [103, 102, 32, 33, 101], only local annihilation amplitudes have been studied, and their matrix elements were parameterized by complex amplitudes. In SCET, $Q_i^{(4)}$ is a six-quark operator with one usoft quark, such as

$$\big(\bar{d}_s \Gamma_s b_v\big)\big(\bar{u}_{\bar{n},\omega_2}\Gamma_{\bar{n}} q_{\bar{n},\omega_3}\big)\big(\bar{q}_{n,\omega_1}\Gamma_n u_{n,\omega_4}\big)\,, \tag{4.9}$$

where other $Q_i^{(4)}$ operators have different flavor structures. To derive the power counting for this operator, start with $Q^{(0)} \sim \lambda^6$, then note that switching a collinear quark to an usoft quark costs λ^2, and adding a ξ_n and $\xi_{\bar{n}}$ from a hard gluon also costs λ^2. This yields $Q_i^{(4)} \sim \mathcal{O}(\alpha_s(\mu_h)\lambda^{10})$. In matching onto $\mathrm{SCET_{II}}$ we simply replace $Q_i^{(4)} \to O_i^{(1L)} \sim \eta^7$, with the operator having an identical form. $\mathrm{SCET_I}$ operators $Q_i^{(4)}$ that do not have the form in Eq. (4.9) exist, but they must be taken in time-ordered products with a subleading Lagrangian and so do not contribute to $A^{(1)}$. For this reason all local operator contributions to $A^{(1)}$ contribute in the annihilation terms and not in $A_{rest}^{(1)}$. Since the matching onto $O_i^{(1L)}$ is local, it appears as in Fig. 4.2a with an $\alpha_s(\mu_h)$, but with no jet function. Thus this contribution to $A_{ann}^{(1)}$ is of order $\alpha_s(\mu_h)/\alpha_s(\mu_i)\,\Lambda/m_b$ relative to $A^{(0)}$. In section 4.3 we construct a complete basis of $Q_i^{(4)}$ operators and show that their matrix elements are factorizable in SCET at any order in perturbation theory, and do not generate strong phases at $\mathcal{O}(\alpha_s(\mu_h))$. We prove a similar theorem for chirally enhanced terms in the set $Q_i^{(5)}$ in section 4.5.

The annihilation amplitudes and other Λ/m_b suppressed amplitudes also occur through time-ordered products. Two examples are shown by Figs. 4.2b and 4.2c. A subset of these terms were considered in Ref. [79], including the diagram in Fig. 4.2c, and the phenomenological impact of these power corrections was studied. So far no attempt has been made to work out the strong phase properties and perturbative orders in α_s of the time-ordered products, a task we take up here. A complete classification of time-ordered products for the leading power corrections to $B \to M_1 M_2$ is listed in Table 4.1. A subset of these terms contribute to the annihilation amplitudes. To see which, we note that terms with a $Q_i^{(0,1)}$ and only one $\mathcal{L}_{\xi q}^{(1)}$ do not contribute to annihilation at either leading or next-to-leading order; the weak operator is not high enough order in λ to contain an extra n–$\bar{n}$ pair, and there are not enough $\mathcal{L}_{\xi q}$'s to produce the pair through a soft quark exchange. To rule out these terms it was important that we are not considering isosinglet final states, which receive emission annihilation contributions already at leading order. The term $Q_i^{(2)}[\mathcal{L}_{\xi q}^{(1)}]^2$ does not contribute to annihilation because we find that all annihilation type contractions are further power suppressed when matched onto $\mathrm{SCET_{II}}$.

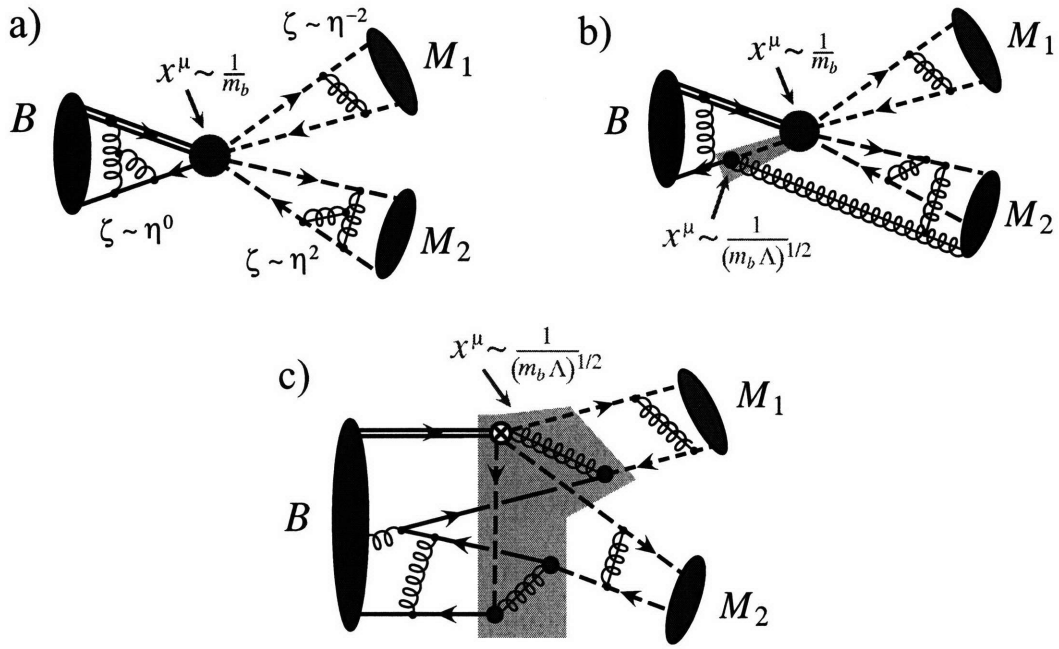

Figure 4-1: Three types of factorization contributions to annihilation amplitudes which are the same order in $\eta = \Lambda_{\rm QCD}/m_b$. a) shows $Q_i^{(4)}$ which has ≥ 1 hard gluon and factorizes at the scale m_b. The rapidity parameter, $\zeta = p^-/p^+$, controls the MS-factorization between soft momenta (B), n-collinear momenta (M_2), and $\bar{n}$-collinear momenta (M_1). b) shows the time-ordered product $Q_i^{(2)}\mathcal{L}_{\xi q}^{(1)}$, which involves factorization at m_b and $\sqrt{m_b\Lambda}$. c) shows the time-ordered product $Q_i^{(1)}[\mathcal{L}_{\xi q}^{(1)}]^3$, which factorizes at the scale $\sqrt{m_b\Lambda}$ and does not need a hard gluon. Graphs a) and b) are of order $\alpha_s(\mu_h)$, while c) is $\alpha_s(\mu_i)^2$.

Time-ordered products with either a $Q^{(j\geq 2)}$ or with three $\mathcal{L}_{\xi q}$'s do contribute to annihilation. Examples of these two types are shown in Figs. 4.2b and 4.2c. Compared to the local annihilation amplitude from $Q_i^{(4)}$, only the time-ordered product $Q^{(2)}\mathcal{L}_{\xi q}^{(1)}$ contributes at the same order in α_s. To demonstrate this, note that for terms with three $\mathcal{L}_{\xi q}$'s all graphs have at least two contracted hard-collinear gluons and so are $\mathcal{O}(\alpha_s^2(\mu_i))$. Graphs with a $Q^{(2,3)}$ start with one $\alpha_s(\mu_h)$, and will also have an additional $\alpha_s(\mu_i)$ from a hard collinear gluon, unless it remains uncontracted in matching onto $\mathrm{SCET_{II}}$. The uncontracted gluon costs an additional λ in the matching onto $\mathrm{SCET_{II}}$, so only the time-ordered product $Q^{(2)}\mathcal{L}_{\xi q}^{(1)}$ can have a leading, $\mathcal{O}(\alpha_s(m_b))$, contribution. Fig. 4.2b gives an example of a diagram occurring from this time-ordered product. The resulting amplitude involves the three-parton distribution, ϕ_{3M_2}. As shown in section 4.4 it also involves the twist-2 distribution ϕ_B^+, and its leading order convolution integrals converge.

The time-ordered products with three $\mathcal{L}_{\xi q}$'s are suppressed by $\alpha_s^2(\mu_i)/\alpha_s(\mu_h)$ relative to $Q_i^{(4)}$, and can be proven to involve a complex nonperturbative function, as labeled in Table 4.1 (an example is shown in Fig. 4.2c). Thus, if perturbation theory converges rapidly at the scale μ_i, then complex annihilation amplitudes are highly suppressed. If perturbation theory at μ_i is poorly convergent then the time-ordered product contribution could be important numerically; comparable or even larger than the leading local annihilation amplitude from $Q_i^{(4)}$. Local annihilation contributions are discussed in detail in sections 4.3 and 4.5, while strong phase properties of the amplitudes and the time-ordered product contributions are taken up in section 4.6.

4.3 Local six-quark operators in $\mathrm{SCET_{II}}$

In this section we construct a complete basis of $O_i^{(1L)}$ operators in $\mathrm{SCET_{II}}$ (the $Q_i^{(4)}$ terms in $\mathrm{SCET_I}$) and derive a factorization theorem for their contributions to $B \to M_1 M_2$. To find a complete basis we consider color, spin, and flavor structures that could appear when matching at any order in α_s. Color is simple, the six-quark operator must have $\Gamma_s \otimes \Gamma_{\bar{n}} \otimes \Gamma_n = 1 \otimes 1 \otimes 1$. Although operators with a T^A in

one or more bilinears are allowed at this order, with the factorization properties of the leading Lagrangians and $\langle M_n M_{\bar{n}}|O|B_s\rangle = \langle 0|\ldots|B_s\rangle\langle M_{\bar{n}}|\ldots|0\rangle\langle M_n|\ldots|0\rangle$, the terms with T^A's give vanishing matrix element between the color singlet hadronic states [21].

For spin we start by looking at chirality which is preserved by the matching at m_b. Since there is no jet function, the soft spectator quark that interpolates for the B-meson must come from the original operator in H_W, and we Fierz this $\bar{\psi}$ field next to the b-quark field. To be definite, we take the other $\bar{\psi}$ field from H_W to go in the $\bar{n}$ direction (in the SCET Hamiltonian we sum over $n \leftrightarrow \bar{n}$). This implies that the pair-produced quark is in the n direction. For $O_{1-4,9,10}$ the allowed chiral structures induced in SCET by matching are $(LH)(LL)(LL)$ and $(LH)(LR)(RL)$ where L and R correspond to the handedness for the light quarks in the bilinears in the order shown in Eq. (4.9). We cannot assign a handedness to the heavy quark denoted here by H. For O_{5-8} we can have $(LH)(RL)(LR)$, $(LH)(RR)(RR)$, $(RH)(LL)(LR)$, and $(RH)(LR)(RR)$. A complete basis of Dirac structures for the individual bilinears is:

$$\Gamma_s = \gamma^\alpha\,, \qquad \Gamma_{\bar{n}} = \{\not{\bar{n}}, \not{\bar{n}}\gamma_\perp^\nu\}\,, \qquad \Gamma_n = \{\not{n}, \not{n}\gamma_\perp^\mu\}\,. \tag{4.10}$$

Structures with γ_5 are not needed because we have specified the handedness. Here $\not{\bar{n}}\gamma_\perp^\mu$ and $\not{n}\gamma_\perp^\nu$ connect left and right-handed quarks, while $\not{\bar{n}}$ and $\not{n}$ connect quarks of the same handedness. From the basis in Eq. (4.10) we must construct an overall scalar using the tensors v^μ, n^μ, $\bar{n}^\mu$, $g_\perp^{\mu\nu}$, and $\epsilon_\perp^{\mu\nu} \equiv \epsilon^{\mu\nu\alpha\beta}\bar{n}_\alpha n_\beta/2$. We take $\epsilon^{0123} = 1$, and work in a frame where $v_\perp^\mu = 0$ and $n\cdot v = \bar{n}\cdot v = 1$, which makes the set $\{n, \bar{n}, v\}$ redundant. For reasons that will become apparent we pick v^μ and $(n^\mu - \bar{n}^\mu)$ as our basis in this section. The definite handedness allows us to turn any contraction involving $i\epsilon_\perp^{\mu\nu}$ into a contraction with $g_\perp^{\mu\nu}$, for example $i\epsilon_\perp^{\mu\nu}\bar{\xi}_n^L \not{\bar{n}}\gamma_\nu^\perp \xi_n^R = \bar{\xi}_n^L \not{\bar{n}}\gamma_\perp^\mu \gamma_5 \xi_n^R = \bar{\xi}_n^L \not{\bar{n}}\gamma_\perp^\mu \xi_n^R$. The $(LH)(LR)(RL)$ and $(LH)(RL)(LR)$ structures can be ruled out since

$$\not{n}\gamma_\perp^\mu P_R \otimes \not{\bar{n}}\gamma_\mu^\perp P_L = \not{n}\gamma_\perp^\mu P_L \otimes \not{\bar{n}}\gamma_\mu^\perp P_R = 0\,. \tag{4.11}$$

Noting that $\not{v} h_v = h_v$ this leaves four allowed spin structures

$$\Gamma_s \otimes \Gamma_{\bar{n}} \otimes \Gamma_n = \left\{ 1 \otimes \not{n} \otimes \not{\bar{n}},\ (\not{\bar{n}} - \not{v}) \otimes \not{n} \otimes \not{\bar{n}},\ \gamma_\perp^\alpha \otimes \not{n} \otimes \not{\bar{n}} \gamma_\alpha^\perp,\ \gamma_\perp^\alpha \otimes \not{n} \gamma_\alpha^\perp \otimes \not{\bar{n}} \right\}. \quad (4.12)$$

The last two structures have $\bar{q}_s \gamma_\perp^\alpha b_v$ and vanish identically for B-meson decays (they would contribute for B^*'s). Furthermore, the local annihilation operators are not sensitive to the k^+ momentum of the soft spectator quark. Thus in taking the matrix element we can use

$$\langle 0 | \bar{q}_s \gamma_5 h_v | B \rangle = -i m_B f_B\,, \qquad \langle 0 | \bar{q}_s \gamma_5 (\not{\bar{n}} - \not{v}) h_v | B \rangle = 0\,. \quad (4.13)$$

Here f_B is the decay constant in the heavy quark limit. The fact that we can match onto a basis of local SCET operators of the form in Eq. (4.9) demonstrates to all orders in α_s that the local annihilation contributions are proportional to f_B. Using Eq. (4.13) the second Dirac structure in Eq. (4.12) is eliminated, so we do not list operators with $(\not{\bar{n}} - \not{v})$ in the soft bilinears below.

Next we consider the allowed flavor structures. From the operators $O_{1,2}$ we have $(\bar{u}b)(\bar{d}q)(\bar{q}u)$, $(\bar{d}b)(\bar{u}q)(\bar{q}u)$, from $O_{1-6,7\gamma,8g}$ we have $(\bar{d}b)(\bar{q}'q)(\bar{q}q')$, $(\bar{q}'b)(\bar{d}q)(\bar{q}q')$, and O_{7-10} give a combination of these. Here the $q\bar{q}$ are the pair produced n and $\bar{n}$ pair,

while the $q'\bar{q}'$ appeared in the weak operators. Thus a basis for B-decay operators is

$$
\begin{aligned}
O_{1d}^{(1L)} &= \frac{2}{m_b^3}\sum_q \left[\bar{d}_s P_R b_v\right]\left[\bar{u}_{\bar{n},\omega_2}\bar{n}\!\!\!/ P_L\, q_{\bar{n},\omega_3}\right]\left[\bar{q}_{n,\omega_1}\bar{n}\!\!\!/ P_L u_{n,\omega_4}\right], \\
O_{2d}^{(1L)} &= \frac{2}{m_b^3}\sum_q \left[\bar{u}_s P_R b_v\right]\left[\bar{d}_{\bar{n},\omega_2}\bar{n}\!\!\!/ P_L\, q_{\bar{n},\omega_3}\right]\left[\bar{q}_{n,\omega_1}\bar{n}\!\!\!/ P_L u_{n,\omega_4}\right], \\
O_{3d}^{(1L)} &= \frac{2}{m_b^3}\sum_{q,q'} \left[\bar{d}_s P_R b_v\right]\left[\bar{q}'_{\bar{n},\omega_2}\bar{n}\!\!\!/ P_L\, q_{\bar{n},\omega_3}\right]\left[\bar{q}_{n,\omega_1}\bar{n}\!\!\!/ P_L q'_{n,\omega_4}\right], \\
O_{4d}^{(1L)} &= \frac{2}{m_b^3}\sum_{q,q'} \left[\bar{q}'_s P_R b_v\right]\left[\bar{d}_{\bar{n},\omega_2}\bar{n}\!\!\!/ P_L\, q_{\bar{n},\omega_3}\right]\left[\bar{q}_{n,\omega_1}\bar{n}\!\!\!/ P_L q'_{n,\omega_4}\right], \\
O_{5d}^{(1L)} &= \frac{2}{m_b^3}\sum_q \left[\bar{d}_s P_R b_v\right]\left[\bar{u}_{\bar{n},\omega_2}\bar{n}\!\!\!/ P_R\, q_{\bar{n},\omega_3}\right]\left[\bar{q}_{n,\omega_1}\bar{n}\!\!\!/ P_R\, u_{n,\omega_4}\right], \\
O_{6d}^{(1L)} &= \frac{2}{m_b^3}\sum_q \left[\bar{u}_s P_R b_v\right]\left[\bar{d}_{\bar{n},\omega_2}\bar{n}\!\!\!/ P_R\, q_{\bar{n},\omega_3}\right]\left[\bar{q}_{n,\omega_1}\bar{n}\!\!\!/ P_R\, u_{n,\omega_4}\right], \\
O_{7d}^{(1L)} &= \frac{2}{m_b^3}\sum_{q,q'} \left[\bar{d}_s P_R b_v\right]\left[\bar{q}'_{\bar{n},\omega_2}\bar{n}\!\!\!/ P_R\, q_{\bar{n},\omega_3}\right]\left[\bar{q}_{n,\omega_1}\bar{n}\!\!\!/ P_R\, q'_{n,\omega_4}\right], \\
O_{8d}^{(1L)} &= \frac{2}{m_b^3}\sum_{q,q'} \left[\bar{q}'_s P_R b_v\right]\left[\bar{d}_{\bar{n},\omega_2}\bar{n}\!\!\!/ P_R\, q_{\bar{n},\omega_3}\right]\left[\bar{q}_{n,\omega_1}\bar{n}\!\!\!/ P_R\, q'_{n,\omega_4}\right]. \qquad (4.14)
\end{aligned}
$$

Here we integrated out c and b quarks in the sum over flavors, so the remaining sums are over $q = u, d, s$ and $q' = u, d, s$. For the $\Delta S = 0$ effective Hamiltonian with Wilson coefficients $a_i^{(d)}(\omega_j)$ we use the notation

$$
H_W = \frac{4G_F}{\sqrt{2}}\sum_{n,\bar{n}}\int [d\omega_1 d\omega_2 d\omega_3 d\omega_4] \sum_{i=1-8} a_i^d(\omega_j)\, O_{id}^{(1L)}(\omega_j)\,. \qquad (4.15)
$$

To pull the CKM structures out of the SCET Wilson coefficients we write

$$
a_i^d(\omega_j) = \begin{cases} \lambda_u^{(d)}\, a_{iu}(\omega_j) + \lambda_c^{(d)}\, a_{ic}(\omega_j) & [i = 1,2,3,4]\,, \\ (\lambda_u^{(d)} + \lambda_c^{(d)})\, a_i(\omega_j) & [i = 5,6,7,8]\,, \end{cases} \qquad (4.16)
$$

where $\lambda_p^{(d)} = V_{pb}V_{pd}^*$. Identical definitions for a_i^s are made by replacing $\lambda_u^{(d)} \to \lambda_u^{(s)}$ and $\lambda_c^{(d)} \to \lambda_c^{(s)}$. For $i = 5,6,7,8$ only penguin operators contribute.

Next we take the $B \to M_1 M_2$ matrix element of H_W. The factorization properties

M_1M_2	$H(x,y)$
$\pi^-\pi^+$, $\pi^-\rho^+$, $\rho^-\pi^+$, $\rho^-\rho^+$	$-\tilde{a}_1^d(x,y) - \tilde{a}_4^d(y,x) - \tilde{a}_3^d(x,y) - \tilde{a}_3^d(y,x)$
$\pi^-\pi^0$, $\rho^-\pi^0$ $\pi^-\rho^0$, $\rho_\parallel^-\rho_\parallel^0$	$\frac{1}{\sqrt{2}}\big[\tilde{a}_2^d(x,y) + \tilde{a}_4^d(x,y) - \tilde{a}_2^d(y,x) - \tilde{a}_4^d(y,x)\big]$
$\pi^0\pi^0$, $\pi^0\rho^0$, $\rho^0\rho^0$	$\big[\frac{1}{2}\tilde{a}_1^d(x,y) + \tilde{a}_3^d(x,y) + \frac{1}{2}\tilde{a}_4^d(x,y)\big] + \big[x \leftrightarrow y\big]$
$K^{(*)-}K^{(*)+}$	$-\tilde{a}_1^d(x,y) - \tilde{a}_3^d(x,y) - \tilde{a}_3^d(y,x)$
$\bar{K}^{(*)0}K^{(*)0}$	$\tilde{a}_3^d(x,y) + \tilde{a}_3^d(y,x) + \tilde{a}_4^d(x,y)$
$K^{(*)-}K^{(*)0}$	$\tilde{a}_2^d(x,y) + \tilde{a}_4^d(x,y)$
$\pi^-\bar{K}^{(*)0}$, $\rho^-\bar{K}^{(*)0}$	$\tilde{a}_2^s(x,y) + \tilde{a}_4^s(x,y)$
$\pi^0\bar{K}^{(*)-}$, $\rho^0K^{(*)-}$	$-\frac{1}{\sqrt{2}}\big[\tilde{a}_2^s(x,y) + \tilde{a}_4^s(x,y)\big]$
$\pi^0\bar{K}^{(*)0}$, $\rho^0\bar{K}^{(*)0}$	$\frac{1}{\sqrt{2}}\,\tilde{a}_4^s(x,y)$
$\pi^+K^{(*)-}$, $\rho^+K^{(*)-}$	$-\tilde{a}_4^s(x,y)$

Table 4.2: Hard functions for $\bar{B}^0$ and B^- decays for the annihilation amplitude $A_{Lann}^{(1)}$ in Eq. (4.20). For each pair of mesons in the table, the first is M_1 and the second M_2.

of SCET yield

$$\langle M_1M_2|O_{1d}^{(1L)}|B\rangle = \frac{2}{m_b^3}\sum_q \langle M_1|\bar{u}_{\bar{n},\omega_2}\bar{n}\!\!\!/P_L\, q_{\bar{n},\omega_3}|0\rangle\langle M_2|\bar{q}_{n,\omega_1}\bar{n}\!\!\!/P_L u_{n,\omega_4}|0\rangle\langle 0|\bar{d}_s P_R b_v|B\rangle + \big\{M_1 \leftrightarrow M_2\big\}\,, \tag{4.17}$$

with similar results for the other $O_{id}^{(1L)}$ terms. Here the $\{M_1 \leftrightarrow M_2\}$ indicates terms where the flavor quantum numbers of the M_2 state match those of the $\bar{n}$-collinear operator. The matrix elements in Eq. (4.17) are zero for transversely polarized vector mesons in agreement with the helicity counting in Ref. [101]. Equation (4.17) can be evaluated using Eq. (4.13) and

$$\begin{aligned}
\langle P_{n_1}(p)|\bar{q}_{n,\omega}^{(f)}\bar{n}\!\!\!/P_{L,R}\,q_{n,\omega'}^{(f')}|0\rangle &= \frac{\pm i\,f_P}{2}\,c_{Pff'}\,\delta_{nn_1}\,\delta(\bar{n}\cdot p-\omega+\omega')\,\phi_P(y)\,,\\
\langle V_{n_1}(p,\varepsilon)|\bar{q}_{n,\omega}^{(f)}\bar{n}\!\!\!/P_{L,R}\,q_{n,\omega'}^{(f')}|0\rangle &= \frac{if_V m_V \bar{n}\cdot\varepsilon}{2\,\bar{n}\cdot p}\,c_{Vff'}\,\delta_{nn_1}\,\delta(\bar{n}\cdot p-\omega+\omega')\,\phi_{V_\parallel}(y)\,.
\end{aligned} \tag{4.18}$$

Here f, f' are flavor indices, $\phi_P(y)$ and $\phi_{V_\parallel}(y)$ are the twist-2 light-cone distribution functions for pseudoscalars and vectors, $y = \omega/\bar{n}\cdot p = \omega/m_b$, and $c_{Pff'}$, $c_{Vff'}$ are Clebsch-Gordan coefficients. For the M_2 mesons, P_{n_2} and V_{n_2}, we have the same equation with $n \leftrightarrow \bar{n}$, and $y \to x$. Since the $P_{L,R}$ only induce $\pm$ signs in the pseudoscalar matrix element, it is convenient to define

M_1M_2	$H(x,y)$
$\pi^-K^{(*)+}$, $\rho^-K^{(*)+}$	$-\tilde{a}_4^d(y,x)$
$\pi^0K^{(*)0}$, $\rho^0K^{(*)0}$	$\frac{1}{\sqrt{2}}\,\tilde{a}_4^d(y,x)$
$\pi^-\pi^+$, $\pi^-\rho^+$, $\rho^-\pi^+$, $\rho^-\rho^+$	$-\tilde{a}_1^s(x,y)-\tilde{a}_3^s(x,y)-\tilde{a}_3^s(y,x)$
$\pi^0\pi^0$, $\pi^0\rho^0$, $\rho^0\rho^0$	$\big[\frac{1}{2}\tilde{a}_1^s(x,y)+\tilde{a}_3^s(x,y)\big]+\big[x\leftrightarrow y\big]$
$K^{(*)-}K^{(*)+}$	$-\tilde{a}_1^s(x,y)-\tilde{a}_4^s(y,x)-\tilde{a}_3^s(x,y)-\tilde{a}_3^s(y,x)$
$\bar{K}^{(*)0}K^{(*)0}$	$\tilde{a}_3^s(x,y)+\tilde{a}_3^s(y,x)+\tilde{a}_4^s(y,x)$

Table 4.3: Hard functions for $\bar{B}_s$ decays for the annihilation amplitude $A^{(1)}_{Lann}$ in Eq. (4.20).

$$\tilde{a}_1^d = a_1^d + \kappa a_5^d\,, \qquad \tilde{a}_2^d = a_2^d + \kappa a_6^d\,, \qquad \tilde{a}_3^d = a_3^d + \kappa a_7^d\,, \qquad \tilde{a}_4^d = a_4^d + \kappa a_8^d\,, \quad (4.19)$$

with similar definitions for $\tilde{a}_i^s$. Here $\kappa = +1$ for PP, VV, and $\kappa = -1$ for PV channels. Using these results, the $\mathcal{O}(\Lambda/m_b)$ local annihilation amplitudes are

$$A^{(1)}_{Lann}(\bar{B}\to M_1M_2) = \frac{G_F f_B f_{M_1} f_{M_2}}{\sqrt{2}} \int_0^1 dx\,dy\,H(x,y)\,\phi^{M_1}(y)\phi^{M_2}(x)\,. \qquad (4.20)$$

Here $H(x,y)$ are perturbatively calculable hard coefficients determined by the SCET Wilson coefficients $\tilde{a}_i(\omega_j)$. Results for different final states are listed in Table 4.2 for $\bar{B}^0$ and B^- decays, and in Table 4.3 for $\bar{B}_s$ decays. Our derivation of the local annihilation amplitude in Eq. (4.20) is valid to all orders in α_s, and provides a proof of factorization for this term.

Matching at tree level involves computing the $\mathcal{O}(\alpha_s(m_b))$ graphs in Fig. 4-2 and comparing them with matrix elements of the SCET operators $Q_i^{(4)}$. Doing so we find

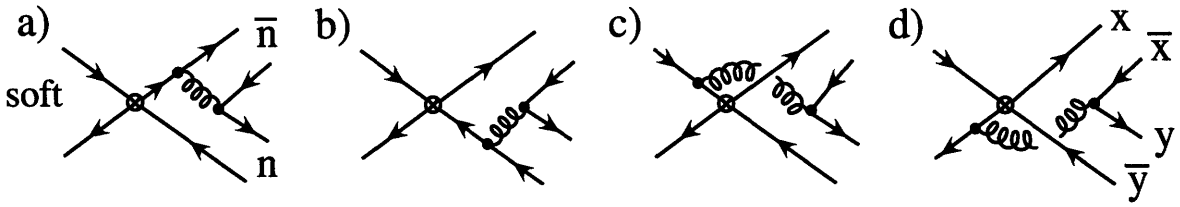

Figure 4-2: Tree level annihilation graphs for $B \to M_1 M_2$ decays. Here soft, n, $\bar{n}$ denote quarks that are soft, n-collinear, and $\bar{n}$-collinear respectively.

that the Wilson coefficients $a_i(x,y)$ are

$$
\begin{aligned}
a_{1u} &= \frac{C_F\pi\alpha_s(\mu_h)}{N_c^2} F(x,y)\left(C_1 + \frac{3}{2}C_{10}\right), \quad a_{1c} = \frac{C_F\pi\alpha_s(\mu_h)}{N_c^2} F(x,y)\left(\frac{3}{2}C_{10}\right), \\
a_{2u} &= \frac{C_F\pi\alpha_s(\mu_h)}{N_c^2} F(x,y)\left(C_2 + \frac{3}{2}C_9\right), \quad a_{2c} = \frac{C_F\pi\alpha_s(\mu_h)}{N_c^2} F(x,y)\left(\frac{3}{2}C_9\right), \\
a_{3u} &= \frac{C_F\pi\alpha_s(\mu_h)}{N_c^2} F(x,y)\left(C_4 - \frac{1}{2}C_{10}\right), \quad a_{3c} = \frac{C_F\pi\alpha_s(\mu_h)}{N_c^2} F(x,y)\left(C_4 - \frac{1}{2}C_{10}\right), \\
a_{4u} &= \frac{C_F\pi\alpha_s(\mu_h)}{N_c^2} F(x,y)\left(C_3 - \frac{1}{2}C_9\right), \quad a_{4c} = \frac{C_F\pi\alpha_s(\mu_h)}{N_c^2} F(x,y)\left(C_3 - \frac{1}{2}C_9\right), \\
a_5 &= \frac{C_F\pi\alpha_s(\mu_h)}{N_c^2} F(\bar{y},\bar{x})\left(\frac{3}{2}C_8\right), \qquad a_6 = 0, \\
a_7 &= \frac{C_F\pi\alpha_s(\mu_h)}{N_c^2} F(\bar{y},\bar{x})\left(C_6 - \frac{1}{2}C_8\right), \qquad a_8 = 0,
\end{aligned}
\tag{4.21}
$$

where $\mu_h \sim m_b$, $\bar{x} = 1-x$, $\bar{y} = 1-y$, with quark momentum fractions x and y as defined in Eq. (4.18) and shown in Fig. 4-2. The function F is

$$
F(x,y) = \left[\frac{1}{\bar{x}^2 y} - \frac{1}{y(x\bar{y}-1)}\right]_{\emptyset} + \frac{d(\mu_-)\,\delta'(\bar{x})}{y}, \tag{4.22}
$$

where the $\emptyset$-notation and term involving the Wilson coefficient $d(\mu_-)$ are discussed below. The function $F(\bar{y},\bar{x})$ will involve $d(\mu_+)$. Note that the coefficients $a_{3u,3c,4u,4c,7,8}$ are polluted in the sense of Ref. [19], meaning that $\mathcal{O}(\alpha_s^2)$ matching results proportional to the large coefficients $C_{1,2}$ could compete numerically. The others are not polluted: $a_{1u,2u}$ involve $C_{1,2}$ at $\mathcal{O}(\alpha_s)$, while $a_{1c,2c,5,6}$ only get contributions from electroweak penguins. Our results for the diagrams in Fig. 4-2 agree with Refs. [103, 33]. This includes the appearance of the combinations of momentum fractions in the func-

tions $F(x,y)$ and $F(\bar{y},\bar{x})$, up to $\emptyset$-distribution and d-term. For later convenience we define moment parameters which convolute the hard coefficients with the meson distributions

$$\beta_{iu}^{M_1M_2} = \int_0^1 dx\, dy\, [a_{iu}(x,y)+\kappa a_{i+4}(x,y)]\, \phi^{M_1}(y)\phi^{M_2}(x)\,,$$
$$\beta_{ic}^{M_1M_2} = \int_0^1 dx\, dy\, [a_{ic}(x,y)+\kappa a_{i+4}(x,y)]\, \phi^{M_1}(y)\phi^{M_2}(x)\,. \tag{4.23}$$

In Eq. (4.22) the subscript $\emptyset$ denotes the fact that singular terms in convolution integrals are finite in SCET due to the MS-factorization which involves convolution integrals such as

$$\sum_{x,x'\neq 0} \int dx_r\, dx_r'\, \delta(1-x-x')\, \frac{\phi_M(x,x',\mu)}{\bar{x}^2}\,, \tag{4.24}$$

where $x^{(\prime)}$ and $x_r^{(\prime)}$ correspond to label and residual momenta [124]. Implementing $x \neq 0$ and $x' \neq 0$ in the MS-factorization scheme requires zero-bin subtractions and divergences in the rapidity must also be regulated. The δ-function sets $x' = 1-x$, so $x' \neq 0$ enforces $x \neq 1$. With the usual assumption that $\phi_M(x)$ vanishes at its endpoints with a power-like fall-off slower than quadratic, only integrals over $1/\bar{x}^2$ in $F(x,y)$ and $1/y^2$ in $F(\bar{y},\bar{x})$ require special care,

$$\left\langle \bar{x}^{-2}\right\rangle^M = \int_0^1 dx\, \frac{\phi_M(x,\mu)}{(\bar{x}^2)_\emptyset}\,, \qquad \left\langle y^{-2}\right\rangle^M = \int_0^1 dy\, \frac{\phi_M(x,\mu)}{(y^2)_\emptyset}\,. \tag{4.25}$$

The resulting moments $\langle \bar{x}^{-2}\rangle^M$ and $\langle y^{-2}\rangle^M$ should be considered hadronic parameters, for which we use the minimal subtraction scheme. Their value depends on μ and $\mu_\pm$ and are scheme dependent beyond the usual $\overline{\rm MS}$ scheme for ϕ_M. In order to derive a result that makes it easy to model these moments we follow Ref. [124] and assume there is no interference between the rapidity renormalization and invariant

mass renormalization, which gives

$$\langle \bar{x}^{-2} \rangle^M = \int_0^1 dx \, \frac{\phi_M(x,\mu) + \bar{x}\phi'_M(1,\mu)}{\bar{x}^2} - \phi'_M(1,\mu) \ln\Big(\frac{\bar{n}\cdot p_M}{\mu_-}\Big) ,$$
$$\langle y^{-2} \rangle^M = \int_0^1 dy \, \frac{\phi_M(y,\mu) - y\phi'_M(0,\mu)}{y^2} + \phi'_M(0,\mu) \ln\Big(\frac{n\cdot p_M}{\mu_+}\Big) . \qquad (4.26)$$

Here $\phi'_M(1)$ is generated by a zero-bin subtraction which avoids double counting the region where $\bar{x} \to 0$. When $\bar{x} \to 0$ the corresponding outgoing quark becomes soft, and this contribution is taken into account by a time-ordered product term in Table 4.1. To obtain the renormalized $\langle \bar{x}^{-2} \rangle^M$ result in Eq. (4.26) requires $1/\epsilon_{\rm UV}$ counterterms which correspond to operators with the $\bar{n}$-collinear bilinears in Eq. (4.14), $[\bar{u}_{\bar{n},\omega_2} \not{\bar{n}} \gamma_5 q_{\bar{n},\omega_3}]$ etc., which can be written as [124]

$$O_{ct} = \frac{\partial}{\partial \omega_3} (\bar{\xi}_{\bar{n}} W)_{\omega_2} \not{\bar{n}} \gamma_5 (W^\dagger \xi_{\bar{n}})_{\omega_3} \Big|_{\omega_3 \to 0} . \qquad (4.27)$$

The matrix element of these terms is taken prior to performing the partial derivative and the limit $\omega_3 \to 0$, and gives $\phi'_M(1,\mu)$. These terms do not have a $\omega_3 \neq 0$ restriction, and consistency of the renormalization procedure used to obtain Eq. (4.26) demands that the fields here are $\bar{n}$-collinear. An analogous set of terms are required for $\phi'_M(0,\mu)$. These terms are real at any scale, which follows from the requirements discussed in section 4.6 for an $\mathrm{SCET_{II}}$ operator to be able to generate a physical strong phase. The dependences on $\mu_\pm$ in Eq. (4.26) are canceled by the leading dependences on these scales, $d(\mu_-) = \ln(p_M^-/\mu_-) + \kappa$ and $d(\mu_+) = \ln(p_M^+/\mu_+) + \kappa$, which appeared in Eq. (4.22). Here κ can be fixed by a matching computation. The $d(\mu_\pm)$ correspond to the renormalized coefficients of the O_{ct}, and must be included for consistency at this order [110]. In the rough numerical analysis we do later on, we will treat the contributions from these coefficients as part of the uncertainty.

Note that in deriving the result in Eq. (4.22) we have dropped $i\epsilon$ factors from the propagators. If these terms were kept, the second term in $F(x,y)$ would be

$$\frac{1}{(y + i\epsilon)\,(x\bar{y} - 1 + i\epsilon)} . \qquad (4.28)$$

The $i\epsilon$'s yield imaginary contributions with $\delta(y)$ and $\delta(x\bar{y}-1)$. They contribute for $y=0$ or for $x=\bar{y}=1$, so these contributions occur in zero-bins, which are excluded from the convolution integrals in the factorization theorem we have derived with SCET. The zero-bins correspond to degrees of freedom that are soft, and including these regions would induce a double counting, so the correct factorization theorem in QCD does not include them. Factors analogous to $x \neq 0$ and $x' \neq 0$ in Eq. (4.24) ensure that there is no contribution to the integral from any zero-bin momentum, and we find that the δ-function terms give zero. This remains true for more singular distributions yielding $\delta^{(n)}(x)$, and so also applies to the first term in $F(x,y)$. Thus it is correct to drop the $i\epsilon$ factors from the start. This should be compared with the approach in KLS where the $i\epsilon$ factors generate a strong phase from the tree level diagrams from a $k_\perp^2$ dependent δ-function. In our derivation any such $k_\perp^2$ imaginary terms could only occur at higher orders in Λ/m_b.

Thus at order $\alpha_s(\mu_h)$ the lowest order annihilation factorization theorem is determined by the convolutions

$$\begin{aligned}
&\int_0^1 dx\, dy\, F(x,y)\phi^{M_1}(y)\phi^{M_2}(x) \qquad (4.29)\\
&\quad = \langle \bar{x}^{-2}\rangle^{M_2}\langle y^{-1}\rangle^{M_1} - \langle [y(x\bar{y}-1)]^{-1}\rangle^{M_1M_2} + d(\mu_-)\phi'_{M_2}(1)\langle y^{-1}\rangle^{M_1}\,,\\
&\int_0^1 dx\, dy\, F(\bar{y},\bar{x})\phi^{M_1}(y)\phi^{M_2}(x)\\
&\quad = \langle y^{-2}\rangle^{M_1}\langle \bar{x}^{-1}\rangle^{M_2} - \langle [\bar{x}(x\bar{y}-1)]^{-1}\rangle^{M_1M_2} - d(\mu_+)\phi'_{M_1}(0)\langle \bar{x}^{-1}\rangle^{M_2}\,.
\end{aligned}$$

Here we use Eq. (4.26), and

$$\langle y^{-1}\rangle^M = \int_0^1 dy\, \frac{\phi^M(y,\mu)}{y}\,, \quad \langle f(x,y)\rangle^{M_1M_2} = \int_0^1 dx \int_0^1 dy\, f(x,y)\, \phi^{M_1}(y,\mu)\, \phi^{M_2}(x,\mu). \qquad (4.30)$$

These results do not have a complex phase because the right-hand side of Eq. (4.29) is real.

We have shown that the convolution formula in Eq. (4.20) for the local contribu-

tions $O_i^{(1L)}$ yields a well-defined annihilation amplitude. At order $\alpha_s(m_b)$ the result is real, so $A_{Lann}^{(1)}$ is real up to perturbative corrections. Order $\alpha_s^2(m_b)$ corrections to the a_i will produce perturbative strong phases in $A_{Lann}^{(1)}$. Further discussion on strong phases is given in section 4.6, while phenomenological implications are taken up in section 4.7.

4.4 Three-body annihilation

In this section we compute the leading term in the perturbative expansion of $A_{\rm hard-col}^{(1ann)}$, which has the form

$$A_{\rm hard-col}^{(1ann)} \sim \alpha_s(m_b) \frac{H(x_1,y_1,y_2)}{k} \otimes f_B \phi_B^+(k)\, f_{M_1}\phi_{M_1}(x_1)\, f_{3M_2}\phi_{3M_2}(y_1,y_2)\,. \qquad (4.31)$$

Here H is a calculable hard-scattering kernel, ϕ_{3M} is a three-parton twist-3 distribution, and f_{3M} is the corresponding decay constant. The amplitude in Eq. (4.31) occurs at the same order in $1/m_b$ and $\alpha_s(m_b)$ as $A_{\rm hard}^{(1ann)}$ and should be included for a complete leading order annihilation amplitude. Unlike $A_{\rm hard}^{(1ann)}$ its convolution integrals converge without using rapidity factorization. Furthermore, the LO annihilation involves B-meson information beyond f_B, thus demonstrating that annihilation is more complicated than the short distance picture leading to a scaling $\sim f_B/m_b$ that is often used in parametric estimates [43].

Most of the flavor-changing operators in H_W in Eq. (2.15) have spin $(V-A)\otimes(V-A)$, such as $O_1^u = (\bar{u}b)_{V-A}\,(\bar{d}u)_{V-A}$. We will prove below that all such operators give vanishing contribution to Eq. (4.31), so that only O_{5-8} are relevant for our analysis. The Wilson coefficients of these penguin operators are considerably smaller than $C_1(m_b) = 1.08$ and $C_2(m_b) = -0.18$, but can give important contributions in penguin observables because $C_{1,2}$ only contribute through loops [33].

The calculation of $A_{hard-col}^{(1ann)}$ involves finding $\mathrm{SCET_I}$ operators of the form

$$Q_{id}^{(2)} \propto \left[\bar{q}'_{n',\omega_5}\Theta_{us}b_v\right]\left[\bar{d}_{\bar{n},\omega_2}\Theta_{\bar{n}}q_{\bar{n},\omega_3}\right]\left[\bar{q}_{n,\omega_1}\Theta_n q'_{n,\omega_4}\right], \qquad (4.32)$$

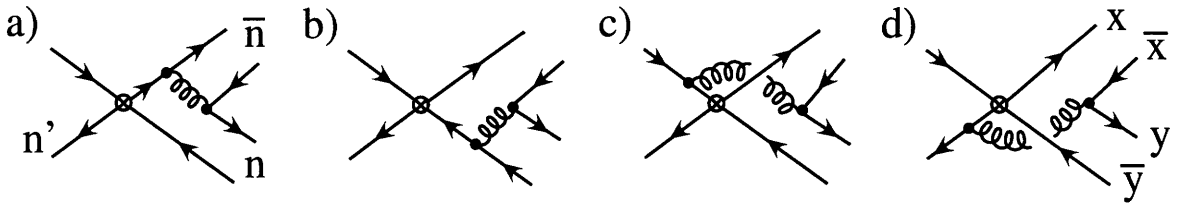

Figure 4-3: Tree-level annihilation graphs for $B \to M_1 M_2$ decays. The gluon and the fermion propagator connecting it to the weak vertex are both offshell by $p^2 \sim m_b$. Matching on to $\mathrm{SCET_I}$, these graphs give rise to the six-quark operators $Q^{(2)}$, the filled circle at the center of Fig. 4.2b.

where $\Theta_{us} \otimes \Theta_{\bar{n}} \otimes \Theta_n$ are color and spin structures, q and q' are flavors, and the collinear direction $n' = n$ or $\bar{n}$. The fermion fields are gauge invariant with large label momenta specified by the subscripts ω, for example $q_{n,\omega_1} = \delta(\omega_1 - \bar{n}\cdot\mathcal{P}) W_n^\dagger \xi_n^{(q)}$ where W_n is a Wilson line. At tree level these operators arise from the full-theory diagrams in Fig. 4-3 with three light n'-collinear quarks and two collinear in the other direction, $\bar{n}'$. They have Wilson coefficients of $\mathcal{O}(\alpha_s(m_b))$. We identify n as the collinear direction of the pair-produced quark of flavor q and sum over all n in the $\mathrm{SCET_I}$ weak Hamiltonian. We will see shortly that the flavor structure is as in Eq. (4.32), and that the matching requires T^A color structures for two of the Θ's.

To finalize our description of the calculation we consider matching the time-ordered product $T[Q^{(2)}\mathcal{L}^{(1)}_{\xi q}]$ onto $\mathrm{SCET_{II}}$ with diagrams as shown in Figure 4.2b. $Q^{(2)}$ has an excess of n'-collinear fermions since only two are needed to interpolate for a collinear meson. The subleading Lagrangian [36] $\mathcal{L}^{(1)}_{\xi q} = \bar{q}'_{us} ig \not{\mathcal{B}}^\perp_{n'} q'_{n'}$ removes an n'-collinear fermion and provides the soft field that interpolates for the light anti-quark in the B meson. Here $ig\,\mathcal{B}^{\perp\mu}_{n',\omega} = \big[1/(\bar{n}'\cdot\mathcal{P})\, W^\dagger_{n'}[i\bar{n}\cdot D_{n'}, iD^\mu_{n',\perp}] W_{n'} \delta(\omega - \bar{n}'\cdot\mathcal{P}^\dagger)\big]$, and the form of the $\mathrm{SCET_{II}}$ operators is

$$O^{(1T)}_{id} \propto \frac{1}{n'\cdot k} \left[\bar{q}'_{s,n'k}\Gamma_s b_v\right]\left[\bar{d}_{\bar{n}}\Gamma_{\bar{n}} q_{\bar{n}}\right]\left[\bar{q}_n \Gamma_n q'_n\right] ig\mathcal{B}^{\perp\beta}_{n'}\,, \tag{4.33}$$

with $\Gamma_s \otimes \Gamma_{\bar{n}} \otimes \Gamma_n$ containing spin and color structures. The collinear gluon field strength $ig\mathcal{B}^\perp_{n'} \sim \eta$, interpolates for gluons in a final state meson, so there is no perturbative suppression from the factor of g. At tree level, integrating out the hard-collinear quark propagator in Fig. 4.2g induces an inverse factor $1/(n'\cdot k)$ of the soft

momentum which will be convoluted with the B-distribution, $\phi_B^+(n'\cdot k)$. In Eq. (4.33) this compensates the η suppression from $ig\mathcal{B}_{n'}^\perp$ to make $O^{(1T)}$ the same order as the six-quark operators for the hard annihilation, which is $\mathcal{O}(\eta^7)$. We have checked that operators with more $ig\mathcal{B}_{n'}^\perp$'s or with soft gluon field strengths do not occur at this order in $1/m_b$ and $\alpha_s(m_b)$.

Note that SCET_{II} time-ordered products (T-products) do not contribute at $\mathcal{O}(\eta^7)$. To see this, recall that our process has a soft initial state and n and $\bar{n}$-collinear final states. An example of an SCET_{II} Lagrangian that connects these sectors [97] has two-collinear quarks and two-soft quarks [126], $\bar{q}_s q_s \bar{\xi}_n \xi_n \sim \eta$. In these operators the two n-collinear particles conserve the large $p^- \sim \eta^0$ momenta, and the two soft particles conserve the $p^+ \sim \eta$ momenta. Thus this operator, as well as analogous operators with gluons, only support scattering, $ns \to ns$, and not annhilation such as $nn \to ss$ or $ss \to nn$. Another example is $\mathcal{L}_{\text{II}} \sim \bar{\xi}_n A_n A_{\bar{n}} \xi_{\bar{n}} \sim \eta^2$, where analogous statements hold for n and $\bar{n}$. Weak operators, like $O_{id}^{(1T)}$, that have the same n-$\bar{n}$-s structure as the initial and final states are already $\mathcal{O}(\eta^7)$, so T-products with them are power suppressed. The above considerations rule out the majority of T-products. An example of an annihilation T-product in SCET_{II} that survives these criteria is $\mathcal{L}_{\text{II}}$, with a weak operator with fields $(\bar{q}_s h_v \bar{\xi}_n \xi_{\bar{n}}) \sim \eta^5$. These T-products involve at least one loop momentum ℓ^μ where, due to the double multipole expansion, $\ell^\pm$ must be smaller than the conserved p^- and p^+, see Eq.(25) of Ref. [135]. As a contour integral in ℓ^+ or ℓ^- we have ≥ 2 poles that are all on the same side of the axis, and therefore the loop gives zero. At $\mathcal{O}(\eta^7)$ this is sufficient to rule out possible annihilation T-products, including those with more than one SCET_{II} Lagrangian. Note that in Ref. [126] a T-product contribution was identified for $\bar{B}^0 \to D^0\pi^0$, however in that scattering process the integral did not satisfy the same pole criteria as we find here.

Constructing the operator bases

Next we construct a full basis for the operators $Q^{(2)}$ and $O^{(1T)}$ in the SCET_{I} and SCET_{II} weak effective Hamiltonians, respectively. General symmetry arguments allow us to reduce the operator bases to the small subset relevant to our calculation of

$A^{(1ann)}_{\text{hard-col}}$, and for this reason it is convenient to construct the bases for SCET_I and SCET_II simultaneously. First consider spin in SCET_I. For light fermion fields of definite handedness, a complete basis of Dirac structures for the individual bilinears in Eq. (4.32) is

$$\Theta_{us/n'} = \{1, \gamma_\perp^\alpha\}\,, \qquad \Theta_{\bar{n}} = \{\not{\bar{n}}, \not{\bar{n}}\gamma_\perp^\mu\}\,, \qquad \Theta_n = \{\not{n}, \not{n}\gamma_\perp^\mu\}\,. \tag{4.34}$$

Using these bases, we must construct a complete set of $Q^{(2)}$ spin structures with chiralities inherited in perturbative matching from the full-theory fields in O_{1-10} and the produced $q\bar{q}$ pair. To make a Lorentz scalar, the spin structure must have zero $\gamma_\perp$'s or two $\gamma_\perp$'s contracted with $g_\perp^{\alpha\beta} = g^{\alpha\beta} - n^\alpha\bar{n}^\beta/2 - n^\beta\bar{n}^\alpha/2$. Note that contracting with $\epsilon_\perp^{\alpha\beta} = \bar{n}^\rho n^\sigma \epsilon^{\alpha\beta\rho\sigma}/2$ does not yield an independent operator since for example $i\epsilon_\perp^{\mu\nu}\bar{\xi}_n^L \not{\bar{n}}\gamma_\nu^\perp \xi_n^R = \bar{\xi}_n^L \not{\bar{n}}\gamma_\perp^\mu \gamma_5 \xi_n^R = \bar{\xi}_n^L \not{\bar{n}}\gamma_\perp^\mu \xi_n^R$. For $O_{1-4,9,10}$ the only allowed chiral structure is $(LH)(LL)(LL)$ where L and R refer to the handedness for the light quarks in the bilinears in the order shown in Eq. (4.32). We cannot assign a handedness to the heavy quark denoted here by H. This chiral structure is realized as the spin structures

$$\Theta_{us/n} \otimes \Theta_{\bar{n}} \otimes \Theta_n = 1 \otimes \not{\bar{n}} \otimes \not{n}\,, \qquad \Theta_{us/\bar{n}} \otimes \Theta_{\bar{n}} \otimes \Theta_n = 1 \otimes \not{n} \otimes \not{\bar{n}}\,. \tag{4.35}$$

We have ruled out the chirality $(LH)(LR)(RL)$ corresponding to a spin structure $1 \otimes \not{\bar{n}}\gamma_\perp^\alpha \otimes \not{n}\gamma_\alpha^\perp$ by using $P_R \not{n}' \gamma_\perp^\alpha \otimes P_L \not{\bar{n}}' \gamma_\alpha^\perp = 0$. This equation encodes the helicity flip argument of Ref. [101]. Similarly, for O_{5-8} the chirality $(LH)(RR)(RR)$ is also realized as the spin structures Eq. (4.35), whereas $(LH)(RL)(LR)$ is not allowed since $P_L \not{n}\gamma_\perp^\alpha \otimes P_R \not{\bar{n}}\gamma_\alpha^\perp = 0$. We will show momentarily, however, that using SCET_II the terms in Eq. (4.35) are not needed to compute $A^{(1ann)}_{hard-col}$. For O_{5-8} we can also have

$$\Theta_{us/n} \otimes \Theta_{\bar{n}} \otimes \Theta_n = \gamma_\perp^\alpha \otimes \not{\bar{n}} \otimes \not{n}\gamma_\alpha^\perp\,, \quad \Theta_{us/\bar{n}} \otimes \Theta_{\bar{n}} \otimes \Theta_n = \gamma_\perp^\alpha \otimes \not{\bar{n}}\gamma_\alpha^\perp \otimes \not{n}\,, \tag{4.36}$$

corresponding to chiralities $(RH)(LL)(LR)$ and $(RH)(LR)(RR)$, respectively, and thus the flavor structure shown in Eq. (4.32), namely $(\bar{q}'b)(\bar{d}q)(\bar{q}q')$. The second structure in Eq. (4.35) is related to the second structure in Eq. (4.36) by a Fierz

transformation swapping $\bar{d}_{\bar{n}}$ and $\bar{q}'_{\bar{n}}$ quarks and we will choose the latter for our operator basis. The complete set of spin structures in Eqs. (4.35) and (4.36) contains neither $\Theta_{us/n} \otimes \Theta_{\bar{n}} \otimes \Theta_n = \gamma_\perp^\alpha \otimes \not{n} \gamma_\alpha^\perp \otimes \not{\bar{n}}$ nor $\Theta_{us/\bar{n}} \otimes \Theta_{\bar{n}} \otimes \Theta_n = \gamma_\perp^\alpha \otimes \not{n} \otimes \not{\bar{n}} \gamma_\alpha^\perp$. These possibilities are excluded by the projection relation $\Theta_{us/n'} \doteq \not{\bar{n}}' \not{n}' \Theta_{us/n'} \not{\bar{n}}/4$ and the helicity flip equation.

Now consider spin and chirality in $\mathrm{SCET_{II}}$. The allowed $O^{(1T)}$ spin structures must respect the handedness inherited from the $\mathrm{SCET_I}$ fields in the perturbative matching of $T[Q^{(2)}\mathcal{L}_{\xi q}^{(1)}]$. For $n' = \bar{n}$ in $Q^{(2)}$, taking either one of the $\bar{n}$-collinear anti-quark fields soft yields an annihilation operator. For $n' = n$, however, the field $\bar{q}_n$ in the third bilinear was pair produced and does not contribute to the annihilation amplitude when made soft by $\mathcal{L}_{\xi q}^{(1)}$. So given the $\mathrm{SCET_I}$ spin structures Eqs. (4.35) and (4.36) corresponding to chiralities described in the text, we need to consider $O^{(1T)}$ chiralities $(LH)(LL)(LL)$, $(LH)(RR)(RR)$, $(RH)(LL)(LR)$, and $(RH)(LR)(RR)$ with bilinears in the order shown in Eq. (4.33), *i.e.* soft $-\ \bar{n} - n$. With the first bilinear purely soft, a complete basis of Dirac structures for the individual bilinears is

$$\Gamma_s = \{\not{n}, \not{\bar{n}}, \gamma_\perp^\alpha\}\,, \qquad \Gamma_{\bar{n}} = \{\not{n}, \not{n}\gamma_\perp^\mu\}\,, \qquad \Gamma_n = \{\not{\bar{n}}, \not{\bar{n}}\gamma_\perp^\mu\}\,. \tag{4.37}$$

A Lorentz scalar $O^{(1T)}$ has an odd number of $\gamma_\perp$'s since one must be contracted into the $n-$ or $\bar{n}-$collinear field strength $\mathcal{B}_\perp^\beta$. For chiralities $(LH)(LL)(LL)$ and $(LH)(RR)(RR)$ the allowed Dirac structure is

$$(\Gamma_s \otimes \Gamma_{\bar{n}} \otimes \Gamma_n)\mathcal{B}_{n',\perp}^\beta = (\gamma_\beta^\perp \otimes \not{n} \otimes \not{\bar{n}})\mathcal{B}_{n',\perp}^\beta \tag{4.38}$$

with $n' = n$ or $\bar{n}$, but the corresponding operators $O^{(1T)}$ have $\bar{q}_s \gamma_\perp^\mu b_v$ and do not contribute for B decays. Since $(LH)(LL)(LL)$ is the only $O^{(1T)}$ chirality corresponding to the $(V-A)(V-A)$ operators $O_{1-4,9,10}$, this proves that only O_{5-8} can contribute to Eq. (4.31). Furthermore since all (LH) terms are ruled out, the soft quark can only be q', and not a d-quark.

This leaves the $(RH)(LL)(LR)$ and $(RH)(LR)(RR)$ structures from O_{5-8} with

soft quark flavor q', for which we have the additional spin structures,

$$\begin{aligned} n' = n: &\qquad \Gamma_s \otimes \Gamma_{\bar{n}} \otimes \Gamma_n \mathcal{B}^\beta_{n,\perp} = \left\{ \not{n} \otimes \not{n} \otimes \not{\bar{n}} \not{\mathcal{B}}_{n,\perp},\ \not{n} \otimes \not{n} \gamma^\perp_\beta \otimes \not{\bar{n}} \mathcal{B}^\beta_{n,\perp} \right\}, \\ n' = \bar{n}: &\qquad \Gamma_s \otimes \Gamma_{\bar{n}} \mathcal{B}^\beta_{\bar{n},\perp} \otimes \Gamma_n = \left\{ \not{\bar{n}} \otimes \not{n} \not{\mathcal{B}}_{\bar{n},\perp} \otimes \not{\bar{n}},\ \not{\bar{n}} \otimes \not{n} \mathcal{B}^\beta_{\bar{n},\perp} \otimes \not{\bar{n}} \gamma^\perp_\beta \right\}, \end{aligned} \tag{4.39}$$

plus those with $\not{n} \leftrightarrow \not{\bar{n}}$ in Γ_s. While these eight are all allowed by chirality and Lorentz invariance, six can be ruled out by considering the spin and factorization properties of our time-ordered product. The matching from $\mathrm{SCET_I}$ to $\mathrm{SCET_{II}}$ does not affect the spin and color structure of the $\bar{n}'$-collinear bilinear at this order in the power expansion, since once a jet direction is chosen the collinear fields in the opposite direction are decoupled. Here $\bar{n}'$ is the opposite of n'. From Eqs. (4.35) and (4.36) the allowed $\Theta_{\bar{n}'}$ structures have no $\gamma_\perp$'s, and therefore the second structure on each line of Eq. (4.39) does not appear at any order in the perturbative matching. Also, the allowed structures Eqs. (4.35) and (4.36) are invariant under $\Theta_{us} \to \Theta_{us} \not{\bar{n}}'/2$ and only power-suppressed interactions couple the $b-$quark to the n' sector. Therefore, Γ_s should not vanish under $\Gamma_s \to \Gamma_s \not{\bar{n}}'/2$, and the operators with $\not{n} \leftrightarrow \not{\bar{n}}$ mentioned below Eq. (4.39) are ruled out. In perturbation theory this just corresponds to the appearance of an $\not{n}'$ from the n'-collinear propagator next to the b-quark. This leaves only the operators with a $\not{\mathcal{B}}_\perp$ in Eq. (4.39).

Finally consider color. In $\mathrm{SCET_I}$ the operators $Q^{(2)}$ are color singlets, but each bilinear on its own could be singlet or octet. A complete set of color structures includes

$$\begin{aligned} \Theta_{us/n'} \otimes \Theta_{\bar{n}} \otimes \Theta_n = \big\{ & T^a \otimes 1 \otimes T^a,\ T^a \otimes T^a \otimes 1,\ 1 \otimes 1 \otimes 1, \\ & 1 \otimes T^a \otimes T^a,\ T^a \otimes T^b \otimes T^c f^{abc},\ T^a \otimes T^b \otimes T^c d^{abc} \big\}. \end{aligned} \tag{4.40}$$

Once again we can reduce this set using the factorization properties of $\mathrm{SCET_I}$. As argued for spin, an $\mathrm{SCET_I}$ operator with color structure $\Theta_{\bar{n}'}$ matches onto a $\mathrm{SCET_{II}}$ operator with the same structure $\Gamma_{\bar{n}'}$ in its $\bar{n}'$ bilinear. So $\Theta_{\bar{n}'}$ cannot be a color octet,

and the allowed structures are

$$\Theta_{us/n} \otimes \Theta_{\bar{n}} \otimes \Theta_n = \{1 \otimes 1 \otimes 1,\, T^a \otimes 1 \otimes T^a\}$$
$$\Theta_{us/\bar{n}} \otimes \Theta_{\bar{n}} \otimes \Theta_n = \{1 \otimes 1 \otimes 1,\, T^a \otimes T^a \otimes 1\}\,. \tag{4.41}$$

In $\mathrm{SCET_{II}}$ each of the three bilinears interpolates for a color singlet meson and therefore each bilinear must seperately be a color singlet, $\Gamma_s \otimes \Gamma_{\bar{n}} \otimes \Gamma_n = 1 \otimes 1 \otimes 1$.

Matching onto $\mathrm{SCET_I}$ and $\mathrm{SCET_{II}}$

We now present the matching from H_W in Eq. (2.15) onto the $\mathrm{SCET_I}$ operators $Q^{(2)}$ and then the matching of the $\mathrm{SCET_I}$ time-ordered product $T[Q^{(2)}\mathcal{L}^{(1)}_{\xi q}]$ onto $\mathrm{SCET_{II}}$ operators $O^{(1T)}_{id}$. The hadronic matrix elements of $O^{(1T)}_{id}$ will give the factorization formula for $A^{(1ann)}_{\mathrm{hard-col}}$. From the arguments presented above, the complete basis of $\mathrm{SCET_I}$ operators $Q^{(2)}$ is

$$Q^{(2)}_{1d} = \frac{2}{m_b^3} \sum_{q,q'} \left[\bar{q}'_{n,\omega_5} P_L \gamma_\perp^\alpha T^a b_v\right] \left[\bar{d}_{\bar{n},\omega_2} \not{n} P_L\, q_{\bar{n},\omega_3}\right] \left[\bar{q}_{n,\omega_1} \not{\bar{n}}\, \gamma_\alpha^\perp T^a P_R\, q'_{n,\omega_4}\right],$$
$$Q^{(2)}_{2d} = \frac{2}{m_b^3} \sum_{q,q'} \left[\bar{q}'_{\bar{n},\omega_5} P_L \gamma_\perp^\alpha T^a b_v\right] \left[\bar{d}_{\bar{n},\omega_2} \not{n} \gamma_\alpha^\perp T^a\, P_R\, q_{\bar{n},\omega_3}\right] \left[\bar{q}_{n,\omega_1} \not{\bar{n}} P_R\, q'_{n,\omega_4}\right],$$
$$Q^{(2)}_{3d,4d} = Q^{(2)}_{1d,2d}\, \frac{3e_{q'}}{2}, \tag{4.42}$$

with sums over $q, q' = u, d, s$, plus analogous operators $Q^{(2)}_{5d-8d}$ which have color structure $1 \otimes 1 \otimes 1$. The electroweak penguin operators $O_{7,8}$ induce the two operators $Q^{(2)}_{3d,4d}$, which have the same spin and flavor structures as $O^{(2)}_{1d,2d}$, but with a factor of the quark electric charge $e_{q'}$ included under the summation. Combining the pieces in $\mathrm{SCET_{II}}$, a complete basis for the $\mathcal{O}(\eta^7)$ operators with one $ig\mathcal{B}^\beta_\perp$ that contribute to

B decays is

$$
\begin{aligned}
O_{1d}^{(1T)} &= \frac{1}{m_b^3\, k^+} \sum_{q,q'} \left[\bar{q}'_{s,-k^+} P_L \not{n}\, S_n^\dagger b_v\right] \left[\bar{d}_{\bar{n},\omega_2} \not{n} P_L\, q_{\bar{n},\omega_3}\right] \left[\bar{q}_{n,\omega_1} \not{\bar{n}}\, (ig \not{\mathcal{B}}_\perp)_{n,\omega_5} P_R\, q'_{n,\omega_4}\right], \\
O_{2d}^{(1T)} &= \frac{1}{m_b^3\, k^-} \sum_{q,q'} \left[\bar{q}'_{s,-k^-} P_L \not{\bar{n}}\, S_{\bar{n}}^\dagger b_v\right] \left[\bar{d}_{\bar{n},\omega_2} \not{n}\, (ig \not{\mathcal{B}}_\perp)_{\bar{n},\omega_5} P_R\, q_{\bar{n},\omega_3}\right] \left[\bar{q}_{n,\omega_1} \not{\bar{n}} P_R\, q'_{n,\omega_4}\right], \\
O_{3-4d}^{(1T)} &= O_{1-2d}^{(1T)}\, \frac{3e_{q'}}{2}\,.
\end{aligned}
\tag{4.43}
$$

Here $\bar{q}'_{s,-k^+} = (\bar{q}'_s S_n)\delta(k^+ + n\cdot\mathcal{P}^\dagger)$ and $\bar{q}'_{s,-k^-} = (\bar{q}'_s S_{\bar{n}})\delta(k^- + \bar{n}\cdot\mathcal{P}^\dagger)$ and the direction for the soft Wilson lines S_n and $S_{\bar{n}}$ are determined by the matching from $\mathrm{SCET_I}$. Just like the local annihilation operators, we see that the $O_i^{(1T)}$'s can not create transversly polarized vector mesons. The basis for $\Delta S = 1$ decays, $O_{is}^{(1T)}$ switches $\bar{d}_{\bar{n}} \to \bar{s}_{\bar{n}}$.

Next, we carry out the perturbative matching onto the bases in Eqs. (4.42) and (4.43), and derive the factorization theorem. The $\mathrm{SCET_I}$ weak Hamiltonian with Wilson coefficients a_i^{hc} for the operators $Q_{id}^{(2)}$ is

$$
H_W = \frac{4G_F}{\sqrt{2}} (\lambda_u^{(d)} + \lambda_c^{(d)}) \sum_{n,\bar{n}} \int [d\omega_1 d\omega_2 d\omega_3 d\omega_4 d\omega_5] \sum_{i=1-8} a_i^{hc}(\omega_j)\, Q_{id}^{(2)}(\omega_j)\,. \tag{4.44}
$$

Since only the penguin operators O_{5-8} contribute, we pulled out the common CKM factor with $\lambda_u^{(d)} = V_{ub}V_{ud}^*$ and $\lambda_c^{(d)} = V_{cb}V_{cd}^*$. The analogous result for $\Delta S = 1$ has the same a_i^{hc} coefficients. To match onto the a_i^{hc} at tree level we first do a spin Fierz on the full theory O_{5-8} operators to obtain spin structures $P_L \otimes P_R$, and then compute the graphs in Fig. 4-3. Only graphs c) and d) are nonzero and we find [at $\mu = m_b$]

$$
\begin{aligned}
a_1^{hc}(x,y,\bar{y}) &= \frac{\pi\alpha_s(m_b)}{N_C} \left\{ \frac{2C_F\, C_5 + C_6}{y[x(1-y)-1]} + \frac{(2C_F - C_A)C_5 + C_6}{(1-x)y(1-\bar{y})} \right\}, \\
a_2^{hc}(x,\bar{x},y) &= \frac{\pi\alpha_s(m_b)}{N_C} \left\{ -\frac{(2C_F - C_A)C_5 + C_6}{\bar{x}[(1-\bar{x})(1-y)-1]} - \frac{2C_F\, C_5 + C_6}{\bar{x}y(1-x)} \right\}.
\end{aligned}
\tag{4.45}
$$

The coefficients $a_{3,4}^{hc}$ are identical to $a_{1,2}^{hc}$ respectively with the replacements $C_{5,6} \to C_{7,8}$. a_{5-8}^{hc} also begin at $\mathcal{O}(\alpha_s(m_b))$ but give $\alpha_s(\mu_i)$-suppressed contributions when matched onto $\mathrm{SCET_{II}}$, so we do not list their values. These coefficients are "polluted" in that one-loop $\mathcal{O}(\alpha_s(m_b)^2)$ contributions proportional to $C_{1,2}$ could compete

numerically with the results in Eq. (4.45). Here $x, \bar{x}, y$, and $\bar{y}$ are defined in Fig. 4-3, namely $y = \omega_1/m_b$, $\bar{y} = -\omega_4/m_b$, $x = \omega_2/m_b$, $\bar{x} = -\omega_3/m_b$. For $n' = n$ as in $a_{1,3}$, we have $\bar{x} = 1-x$, but $\bar{y} \neq 1-y$ since the momentum is shared between three $n-$collinear partons. Likewise, for $n' = \bar{n}$ as in $a^{hc}_{2,4}$ we have $\bar{y} = 1 - y$ but $\bar{x} \neq 1 - x$.

Having constructed the operators $Q^{(2)}$ and determined their Wilson coefficients, it is straightforward to match the time-ordered products $T[Q^{(2)}\mathcal{L}^{(1)}_{\xi q}]$ onto the SCET_{II} operators O^{1T}_i. For odd indices i and even indices i' we find that integrating out the hard-collinear quark propagator, shown as the dashed line inside the gray region in Fig. 4.2b, gives

$$\begin{aligned} i\int d^4x\, T[Q^{(2)}_{id}(\omega_j)](0)\mathcal{L}^{(1)}_{\xi q}(x) &= \frac{-1}{N_c}\int dk^+\, O^{(1T)}_{id}(k^+,\omega_j)\,, \\ i\int d^4x\, T[Q^{(2)}_{i'd}(\omega_j)](0)\mathcal{L}^{(1)}_{\xi q}(x) &= \frac{-1}{N_c}\int dk^-\, O^{(1T)}_{i'd}(k^-,\omega_j)\,. \end{aligned} \tag{4.46}$$

At $\mathcal{O}(\alpha_s^2)$ in perturbation theory this matching would include non-trivial jet functions. For example, in the first line a $\int d\omega'_{1,4} J(k^+, \omega'_{1,4}, \omega_{1,4})$ with $\omega'_{1,4}$ taking the place of $\omega_{1,4}$ in $O^{(1T)}_{id}$. However at this order additional time-ordered products and non-perturbative functions become relevant so we stick to $\mathcal{O}(\alpha_s)$ in our analysis. Together Eqs. (4.45) and (4.46) complete the tree-level matching. Now take the matrix element of $O^{(1T)}_{id}$ using Eq. (4.18) and the three-body distributions

$$\langle \pi^+_{n_1}(p)|\, \bar{u}_{n,\omega_1}\, \bar{n}\!\!\!/\, (ig\mathcal{B}\!\!\!/_\perp)_{n,\omega_5} P_R\, d_{n,\omega_4}\, |0\rangle = \frac{if_{3P}}{\omega_5}\, \delta_{nn_1}\, \delta(\bar{n}\cdot p - \omega_1 - \omega_5 + \omega_4)\, \phi_{3P}(y,\bar{y}), \tag{4.47}$$

$$\langle \rho^+_{n_1}(p,\varepsilon)|\, \bar{u}_{n,\omega_1}\, \bar{n}\!\!\!/\, (ig\mathcal{B}\!\!\!/_\perp)_{n,\omega_5} P_R\, d_{n,\omega_4}\, |0\rangle = \frac{if_{3V} m_V \bar{n}\cdot\varepsilon}{\omega_5\, \bar{n}\cdot p}\, \delta_{nn_1}\, \delta(\bar{n}\cdot p - \omega_1 - \omega_5 + \omega_4)\, \phi_{3V}(y,\bar{y})\,.$$

Our convention for the vector meson matrix element has been chosen to simplify the final result for the amplitude and is related to that of [92] by $f_{3V} = m_V f_V^T$ and $\phi_{3V} = -\mathcal{T}/2$. Permutations in the flavors give the definitions for other meson

$B \to M_1 M_2$	H_{hc1}	H_{hc2}
$\pi^0\pi^-$, $\rho^0\pi^-$ $\pi^0\rho^-$	$-\frac{1}{\sqrt{2}}\,a_1^{hc} - \frac{1}{\sqrt{2}}\,a_3^{hc}$	$\frac{1}{\sqrt{2}}\,a_2^{hc} + \frac{1}{\sqrt{2}}\,a_4^{hc}$
$\pi^-\pi^0$, $\rho^-\pi^0$ $\pi^-\rho^0$	$\frac{1}{\sqrt{2}}\,a_1^{hc} + \frac{1}{\sqrt{2}}\,a_3^{hc}$	$-\frac{1}{\sqrt{2}}\,a_2^{hc} - \frac{1}{\sqrt{2}}\,a_4^{hc}$
$\pi^+\pi^-$, $\pi^+\rho^-$, $\rho^+\pi^-$	$-a_1^{hc} + \frac{1}{2}a_3^{hc}$	$a_2^{hc} - \frac{1}{2}a_4^{hc}$
$\pi^0\pi^0$, $\rho^0\pi^0$	$a_1^{hc} - \frac{1}{2}\,a_3^{hc}$	$-a_2^{hc} + \frac{1}{2}\,a_4^{hc}$
$\bar{K}^0 K^{(*)0}$, $\bar{K}^{(*)0} K^0$	$a_1^{hc} - \frac{1}{2}a_3^{hc}$	$-a_2^{hc} + \frac{1}{2}a_4^{hc}$
$K^- K^{(*)0}$, $K^{(*)-} K^0$	$a_1^{hc} + a_3^{hc}$	$-a_2^{hc} - a_4^{hc}$
$\pi^-\bar{K}^{(*)0}$, $\rho^-\bar{K}^0$	$a_1^{hc} + a_3^{hc}$	$-a_2^{hc} - a_4^{hc}$
$\pi^0 K^{(*)-}$, $\rho^0 K^-$	$-\frac{1}{\sqrt{2}}\,a_1^{hc} - \frac{1}{\sqrt{2}}\,a_3^{hc}$	$\frac{1}{\sqrt{2}}\,a_2^{hc} + \frac{1}{\sqrt{2}}\,a_4^{hc}$
$\pi^0\bar{K}^{(*)0}$, $\rho^0\bar{K}^0$	$\frac{1}{\sqrt{2}}\,a_1^{hc} - \frac{1}{2\sqrt{2}}\,a_3^{hc}$	$-\frac{1}{\sqrt{2}}\,a_2^{hc} + \frac{1}{2\sqrt{2}}\,a_4^{hc}$
$\pi^+ K^{(*)-}$, $\rho^+ K^-$	$-a_1^{hc} + \frac{1}{2}a_3^{hc}$	$a_2^{hc} - \frac{1}{2}a_4^{hc}$
$B_s \to M_1 M_2$	H_{hc1}	H_{hc2}
$K^+\pi^-$, $K^{*+}\pi^-$, $K^+\rho^-$	$-a_1^{hc} + \frac{1}{2}a_3^{hc}$	$a_2^{hc} - \frac{1}{2}a_4^{hc}$
$K^0\pi^0$, $K^{*0}\pi^0$, $K^0\rho^0$	$\frac{1}{\sqrt{2}}\,a_1^{hc} - \frac{1}{2\sqrt{2}}\,a_3^{hc}$	$-\frac{1}{\sqrt{2}}\,a_2^{hc} + \frac{1}{2\sqrt{2}}\,a_4^{hc}$
K^+K^-, $K^{*+}K^-$, K^+K^{*-}	$-a_1^{hc} + \frac{1}{2}a_3^{hc}$	$a_2^{hc} - \frac{1}{2}a_4^{hc}$
$K^0\bar{K}^0$, $K^{*0}\bar{K}^0$, $K^0\bar{K}^{*0}$	$a_1^{hc} - \frac{1}{2}a_3^{hc}$	$-a_2^{hc} + \frac{1}{2}a_4^{hc}$

Table 4.4: Hard functions for the annihilation amplitude $A_{Tann}^{(1)}$ in Eq. (4.49) for $\bar{B}^0$, B^-, and $\bar{B}_s$ decays. The result for $B^- \to \pi^0\pi^-$ is obtained by adding the results using the entries from the first two rows, and so vanishes in the isospin limit.

channels, and we use the phase convention in [88]. The soft matrix element is

$$\langle 0|\bar{q}^{(f)}_{s,-n'\cdot k} P_L \not{n}' S^\dagger_{n'} b_v|\bar{B}\rangle = i\frac{f_B\, m_B}{2}\phi_B^+(n'\cdot k)\,. \tag{4.48}$$

Combining these pieces the factorization theorem with tree-level jet functions is

$$\begin{aligned} A^{(1ann)}_{\text{hard}-\text{collin}} = {} & \frac{G_F f_B m_B}{\sqrt{2}\, m_b N_c}\,(\lambda_u^{(d)} + \lambda_c^{(d)}) \int_0^\infty dk\, \frac{\phi_B^+(k)}{k} \\ & \times \Bigg\{ f_{3M_1} f_{M_2} \int_0^1 dx \int_0^1 dy \int_0^{1-y} d\bar{y}\, \frac{H_{hc1}^{M_1M_2}(x,y,\bar{y})}{1-y-\bar{y}}\, \phi_{3M_1}(y,\bar{y})\phi_{M_2}(x) \\ & + \eta_{M_1} f_{M_1} f_{3M_2} \int_0^1 dy \int_0^1 dx \int_0^{1-x} d\bar{x}\, \frac{H_{hc2}^{M_1M_2}(x,\bar{x},y)}{1-x-\bar{x}}\, \phi_{M_1}(y)\phi_{3M_2}(x,\bar{x}) \Bigg\}, \end{aligned} \tag{4.49}$$

where $\eta_M = -1$ or $+1$ for a pseudoscalar or vector meson, respectively. The hard coefficients $H_{hc1}^{M_1M_2}$ and $H_{hc2}^{M_1M_2}$ for different $B \to M_1M_2$ channels are listed in Table 4.4 in terms of coefficients in the SCET_I weak Hamiltonian. The amplitude contains the three-body distribution function as promised. The convolutions in Eq. (4.49) are

real, and assuming the standard endpoint behavior for the distribution functions they converge without the rapidity factorization of [124].

For the parametric and numerical analysis in section 4.7, it will be useful to define moment parameters

$$\beta_{hc1}^{M_1M_2},\, \beta_{hc3}^{M_1M_2} = \int dx dy d\bar{y}\, \frac{a_{1,3}^{hc}(x,y,\bar{y})}{1-y-\bar{y}}\, \phi_{3M_1}(y,\bar{y})\phi_{M_2}(x)\,, \tag{4.50}$$

$$\beta_{hc2}^{M_1M_2},\, \beta_{hc4}^{M_1M_2} = \int dy dx d\bar{x}\, \frac{a_{2,4}^{hc}(x,\bar{x},y)}{1-x-\bar{x}}\, \phi_{M_1}(y)\phi_{3M_2}(x,\bar{x})\,, \qquad \beta_B = \frac{1}{3}\int \frac{dk}{k}\phi_B^+(k)\,,$$

where $\beta_B = \lambda_B^{-1}/3$ has mass dimension -1.

4.5 Chirally Enhanced Local Annihilation Contributions

At order $\alpha_s(\mu_h)\mu_M\Lambda/m_b^2$ there are contributions from chirally enhanced operators that could compete with the $\alpha_s(\mu_h)\Lambda/m_b$ terms [33]. In SCET we define these contributions as the set of SCET_{II} operators analogous to $O_i^{(1L)}$ but with an extra $\not{\mathcal{P}}_\perp$ between collinear quarks fields. We start by constructing a complete basis for local operators at this order with a $\mathcal{P}_\perp^\beta$, calling them $O_i^{(2L)}$. These operators have the same color and flavor structures as Eq. (4.14). The chiral structures induced from the operators O_{1-10} and the initial basis of Dirac structures shown in Eq. (4.10) are also the same, and allow us to eliminate many possibilities.

The complete set of Dirac structures from matching the operators $O_{1-4,9,10}$ include

$$\begin{aligned}\Gamma_s \otimes \Gamma_{\bar{n}} \otimes \Gamma_n \mathcal{P}_\perp^\beta = \big\{ &\gamma_\beta^\perp \otimes \not{n} \otimes \not{\bar{n}}\mathcal{P}_\perp^\beta,\ \gamma_\perp^\alpha \otimes \not{n}\gamma_\alpha^\perp \otimes \not{\bar{n}}\gamma_\beta^\perp \mathcal{P}_\perp^\beta, \\ &\gamma_\beta^\perp \otimes \not{n}\gamma_\perp^\alpha \otimes \not{\bar{n}}\gamma_\alpha^\perp \mathcal{P}_\perp^\beta,\ \gamma_\perp^\alpha \otimes \not{n}\gamma_\beta^\perp \otimes \not{\bar{n}}\gamma_\alpha^\perp \mathcal{P}_\perp^\beta \big\}\,,\end{aligned} \tag{4.51}$$

plus the analogous set $\Gamma_s \otimes \Gamma_{\bar{n}}\mathcal{P}_\perp^\beta \otimes \Gamma_n$. Our basis does not include operators with $\mathcal{P}_\perp^\dagger$, because the mesons M_i have zero $\perp$-momenta, so we can integrate these terms by parts to put them in the form in Eq. (4.51). The third term in Eq. (4.51) has

chiral structure $(LH)(LR)(RL)$ and vanishes by Eq. (4.11). The terms in Eq. (4.51) all have $\bar{q}_s \gamma_\perp^\mu b_v$, and so do not contribute for B-decays. The same holds if we replace $\mathcal{P}_\perp^\beta$ by $ig\mathcal{B}_\perp^\beta$. Thus, at any order in perturbation theory the only $\mathcal{O}(\eta^8)$ local operator contributions from $O_{1-4,9,10}$ are those with a D_s^μ in the soft bilinear.

For O_{5-8} we have the structures in Eq. (4.51), and when the q' flavor is a soft quark with $P_L \otimes P_R$ Dirac structure from O_i we also have

$$\begin{aligned}
\Gamma_s \otimes \Gamma_{\bar{n}} \otimes \Gamma_n \mathcal{P}_\perp^\beta &= \left\{ 1 \otimes \not{n} \otimes \not{\bar{n}} \not{\mathcal{P}}_\perp,\ 1 \otimes \not{n} \gamma_\beta^\perp \otimes \not{\bar{n}} \mathcal{P}_\perp^\beta \right\}, \\
\Gamma_s \otimes \Gamma_{\bar{n}} \mathcal{P}_\perp^\beta \otimes \Gamma_n &= \left\{ 1 \otimes \not{n} \mathcal{P}_\perp^\beta \otimes \not{\bar{n}} \gamma_\beta^\perp,\ 1 \otimes \not{n} \not{\mathcal{P}}_\perp \otimes \not{\bar{n}} \right\},
\end{aligned} \tag{4.52}$$

plus operators with 1 replaced by $\not{\bar{n}} - \not{n}$, which vanish due to Eq. (4.13). The operators in Eq. (4.52) contribute to B-decays. In particular, they yield both transverse and longitudinal polarization in $B \to VV$. A complete basis for the local $\mathcal{O}(\eta^8)$ operators with one $\mathcal{P}_\perp^\beta$ is

$$\begin{aligned}
O_{1d}^{(2L)} &= \frac{1}{m_b^4} \sum_{q,q'} \left[\bar{q}_s' P_L b_v \right] \left[\bar{d}_{\bar{n},\omega_2} \not{n} P_L\, q_{\bar{n},\omega_3} \right] \left[\bar{q}_{n,\omega_1} \not{\bar{n}} \not{\mathcal{P}}_\perp P_R\, q'_{n,\omega_4} \right], \\
O_{2d}^{(2L)} &= \frac{1}{m_b^4} \sum_{q,q'} \left[\bar{q}_s' P_L b_v \right] \left[\bar{d}_{\bar{n},\omega_2} \not{n} \not{\mathcal{P}}_\perp P_R\, q_{\bar{n},\omega_3} \right] \left[\bar{q}_{n,\omega_1} \not{\bar{n}} P_R\, q'_{n,\omega_4} \right], \\
O_{3d}^{(2L)} &= \frac{1}{m_b^4} \sum_{q,q'} \left[\bar{q}_s' P_L b_v \right] \left[\bar{d}_{\bar{n},\omega_2} \not{n} \gamma_\beta^\perp P_R\, q_{\bar{n},\omega_3} \right] \left[\bar{q}_{n,\omega_1} \not{\bar{n}} P_R\, \mathcal{P}_\perp^\beta q'_{n,\omega_4} \right], \\
O_{4d}^{(2L)} &= \frac{1}{m_b^4} \sum_{q,q'} \left[\bar{q}_s' P_L b_v \right] \left[\bar{d}_{\bar{n},\omega_2} \not{n} P_L\, \mathcal{P}_\perp^\beta q_{\bar{n},\omega_3} \right] \left[\bar{q}_{n,\omega_1} \not{\bar{n}} \gamma_\beta^\perp P_R\, q'_{n,\omega_4} \right], \\
O_{5d-8d}^{(2L)} &= O_{1d-4d}^{(2L)}\, \frac{3 e_{q'}}{2},
\end{aligned} \tag{4.53}$$

with sums over $q, q' = u, d, s$. Note that the flavor structure of these operators is identical to $O_{4d}^{(1L)}$. For the the electroweak penguin operators $O_{7,8}$ an additional four operators $O_{5d-8d}^{(2L)}$ are needed, which have the same spin-flavor structures as $O_{1d-4d}^{(2L)}$, but with an $e_{q'}$ charge factor, $\sum_{q,q'} 3e_{q'}/2$. Again we caution that we have not considered the complete set of local Λ^2/m_b^2 operators, since our basis does not include three-body terms with an $ig\mathcal{B}_\perp^\mu$, nor terms with an extra D_s soft covariant derivative. We have also not considered $\mathcal{O}(\mu_{M_1}\mu_{M_2}\Lambda/m_b^3)$ terms. All these terms are real, and it would

be interesting to calculate them in the future.

The weak Hamiltonian with Wilson coefficients for the operators $O_{id}^{(2L)}$ is

$$H_W = \frac{4G_F}{\sqrt{2}} (\lambda_u^{(d)} + \lambda_c^{(d)}) \sum_{n,\bar{n}} \int [d\omega_1 d\omega_2 d\omega_3 d\omega_4] \sum_{i=1-8} a_i^{\chi}(\omega_j)\, O_{id}^{(2L)}(\omega_j)\,. \tag{4.54}$$

Since only the penguin operators O_{5-8} contribute, we pulled out the common CKM factor. Matching at tree level onto the operators $O_{id}^{(2L)}$ by keeping terms linear in the $\perp$-momenta in Fig. 4-2, we find

$$\begin{aligned}
a_1^{\chi}(x,y) &= \frac{4C_F\pi\alpha_s(\mu_h)}{N_c} \left[\Big(C_6 + \frac{C_5}{N_c}\Big) F_1(x,y) + \frac{C_5}{N_c} F_2(x,y) \right]_{\emptyset}, \\
a_2^{\chi}(x,y) &= \frac{4C_F\pi\alpha_s(\mu_h)}{N_c} \left[-\Big(C_6 + \frac{C_5}{N_c}\Big) F_1(\bar{y},\bar{x}) + \frac{C_5}{N_c} F_2(\bar{y},\bar{x}) \right]_{\emptyset}, \\
a_3^{\chi}(x,y) &= \frac{4C_F\pi\alpha_s(\mu_h)}{N_c} \left[-\Big(C_6 + \frac{C_5}{N_c}\Big) F_3(x,y) - \frac{C_5}{N_c} F_2(x,y) \right]_{\emptyset}, \\
a_4^{\chi}(x,y) &= \frac{4C_F\pi\alpha_s(\mu_h)}{N_c} \left[\Big(C_6 + \frac{C_5}{N_c}\Big) F_3(x,y) - \frac{C_5}{N_c} F_2(\bar{y},\bar{x}) \right]_{\emptyset}, \\
a_{5-8}^{\chi}(x,y) &= a_{1-4}^{\chi}(x,y) \quad \text{with } C_5 \to C_7,\ C_6 \to C_8\,,
\end{aligned} \tag{4.55}$$

where x and y are defined in Fig. 4-2 and

$$\begin{aligned}
F_1(x,y) &= \left[\frac{1+\bar{x}}{y^2\,\bar{y}\,\bar{x}^2}\right]_{\emptyset} + d_1(\mu_-)\delta'(\bar{x})\left[\frac{1}{y^2\bar{y}}\right]_{\emptyset} + d_2(\mu_+)\delta'(y)\left[\frac{1+\bar{x}}{\bar{x}^2}\right]_{\emptyset} + d_3(\mu_\pm)\delta'(\bar{x})\delta'(y)\,, \\
F_2(x,y) &= \left[\frac{1}{(1-x\bar{y})\bar{x}y^2}\right]_{\emptyset}, \\
F_3(x,y) &= \left[\frac{1}{y^2\,\bar{x}^2}\right]_{\emptyset} + d_4(\mu_-)\delta'(\bar{x})\left[\frac{1}{y^2}\right]_{\emptyset} + d_5(\mu_+)\delta'(y)\left[\frac{1}{\bar{x}^2}\right]_{\emptyset} + d_6(\mu_\pm)\delta'(\bar{x})\delta'(y)\,.
\end{aligned} \tag{4.56}$$

Here d_{1-6} play the same role as d in Eq. (4.22). The coefficients a_{1-8}^{χ} are polluted in the sense of Ref. [19], meaning that $\mathcal{O}(\alpha_s^2)$ matching results proportional to the large coefficients $C_{1,2}$ could compete numerically. This makes the computation of these $\mathcal{O}(\alpha_s^2)$ corrections important.

For decays involving a pseudoscalar in the final state, the operators $O_{1d}^{(2L)}$ and

$O_{2d}^{(2L)}$ generate so-called "chirally enhanced" terms, proportional to μ_M. Time-ordered products of $\mathrm{SCET_I}$ operators also generate μ_M terms, but only at $\mathcal{O}(\alpha_s^2)$. It is not clear that the chirally enhanced terms are larger numerically than other power corrections. In particular three-body distributions from operators with $\bar{\xi}_n(ig\mathcal{B}_\perp^\mu)\Gamma\xi_n$ are parametrically (and sometimes numerically as well) of similar importance [63]. The distributions are related by [92]

$$\begin{aligned} f_P\mu_P\left[\phi_\sigma^{P\prime}(x)+\frac{(2x-1)}{x(1-x)}\,\phi_\sigma^P(x)\right] &= -6f_{3P}\left[\frac{G_{P_z}^{(t)}(x)}{x}+\frac{G_{P_y}^{(t)}(x)}{1-x}\right], \\ f_P\mu_P\left[\phi_p^P(x)-\frac{1}{6x(1-x)}\,\phi_\sigma^P(x)\right] &= -f_{3P}\left[\frac{G_{P_z}^{(t)}(x)}{x}-\frac{G_{P_y}^{(t)}(x)}{1-x}\right], \end{aligned} \tag{4.57}$$

where $G_{P_z}^{(t)}(x)$ and $G_{P_y}^{(t)}(x)$ are integrals over the three-parton distribution, ϕ_{3P}. These relations allow certain chirally enhanced terms with $\mu_P f_P$ to be traded for non-chirally enhanced terms with f_{3P}. Thus it is clear that the chirally enhanced terms dominate over the three-body operators only in the special case when the linear combinations in the square brackets on the left-hand side of Eq. (4.57) are numerically suppressed. Solving with these linear combinations set to zero determines the two-body distributions ϕ_σ^P and ϕ_p^P in the Wandzura-Wilczek (WW) approximation [136]. Thus in order to uniquely specify the μ_P dependent terms, the WW approximation was needed in Ref. [33].

In contrast, in SCET we are not forced to assume a numerical dominance of the μ_P terms to uniquely identify them. We can instead define local chirally enhanced annihilation terms to be the matrix elements of the operators $O_{1d}^{(2L)}$ and $O_{2d}^{(2L)}$ for final states with a pseudoscalar. With a minimal basis of operators, the matrix elements of these terms are unique. The remaining terms involve other operators, and we postpone discussing them to future work. We proceed to work out the factorization formula for $O_{1d}^{(2L)}$ and $O_{2d}^{(2L)}$ with steps analogous to Eqs. (4.17) through (4.20). To take the matrix element we need Eq. (4.18) and the result

$$\langle P_{n_1}(p)|\,\bar{q}_{n,\omega}^{(f)}\,\bar{n}\!\!\!/\,\mathcal{P}\!\!\!/_\perp P_R\,q_{n,\omega'}^{(f')}\,|0\rangle = -\frac{i}{6}\,c_{Pff'}\,\delta_{nn_1}\,\delta(\bar{n}\cdot p-\omega-\omega')\,f_P\mu_P\,\phi_{pp}^P(y)\,. \tag{4.58}$$

Here $c_{Pff'}$ are Clebsch-Gordan factors, $y = \omega/\bar{n}\cdot p$, and we have not written the ω' dependence in the distribution due to the δ-function. The distribution $\phi_{pp}^P(y)$ is related to more standard twist-3 two-parton and three-parton distributions by [92, 124]

$$\phi_{pp}^P(y) = 3y\left[\phi_p^P(y) + \frac{1}{6}\phi_\sigma^{P\prime}(y) + \frac{2\,f_{3P}}{f_P\mu_P}\int\frac{dy'}{y'}\,\phi_{3P}(y-y',y)\right]. \tag{4.59}$$

Note that in $\mu_P\phi_{pp}^P$, the ϕ_{3P} term does not have the chiral enhancement factor μ_P. There will be additional terms proportional to ϕ_{3P} generated by three-body operators. We choose the ϕ_{pp}^P and ϕ_{3P} basis of twist-three distributions, keeping in mind the relations in Eq. (4.57). For decays involving one or more pseudoscalars in the final state we find the chirally enhanced local annihilation amplitudes

$$A_{Lann}^{(2)} = \frac{G_F f_B f_{M_1} f_{M_2}}{6\sqrt{2}\,m_b}\,(\lambda_u^{(d)} + \lambda_c^{(d)})\int_0^1 dx\,dy\Big[\mu_{M_1}H_{\chi 1}(x,y)\,\phi_{pp}^{M_1}(y)\phi^{M_2}(x) + \mu_{M_2}H_{\chi 2}(x,y)\phi^{M_1}(y)\phi_{pp}^{M_2}(x)\Big], \tag{4.60}$$

where $\mu_\rho = \mu_{K^*} = 0$ and using isospin $\mu_\pi = m_\pi^2/(m_u+m_d)$, $\mu_K = m_K^2/(m_s+m_u) = m_K^2/(m_s+m_d)$. Terms with ϕ_{3P} or terms of the same order with a D_s^μ in their soft matrix elements have not been included in our $A_{Lann}^{(2)}$, though they also give local annihilation contributions to $A^{(2)}$. Furthermore, we focused on the pseudoscalar matrix element in Eq. (4.58) to derive the contribution in Eq. (4.60). The $O_{1d,2d}^{(2L)}$ operators in Eq. (4.53) will contribute additional terms for decays to longitudinal vector mesons involving distributions $h_\parallel^{(s)\prime}$ and $h_\parallel^{(t)}$ (our notation for these distributions follows Ref. [92]). The operators $O_{3d,4d}^{(2L)}$ will produce decays to two transverse vectors with distributions from among $\phi_\perp$, F, $\mathcal{V}$, $\mathcal{A}$. It would be straightforward to work out a factorization theorem from the operators $O_{id}^{(2L)}$ in terms of these distributions, though we will not do so here.

Results for the hard coefficients $H_{\chi 1}$ and $H_{\chi 2}$ in terms of the Wilson coefficients a_i^χ are given in Table 4.5 for $\bar{B}^0$ and B^- decays and in Table 4.6 for $\bar{B}_s$ decays. Note that there are no chirally enhanced annihilation contributions for the $\bar{B}_s \to \pi\pi$ or $\bar{B}_s \to \rho\pi$ channels, so B_s decays could potentially be used to separate annihilation contributions

M_1M_2	$H_{\chi 1}(x,y)$	$H_{\chi 2}(x,y)$
$\pi^0\pi^-$, $\rho^0\pi^-$ $\pi^0\rho^-$	$-\frac{1}{\sqrt{2}}\,a_1^\chi(x,y)-\frac{1}{\sqrt{2}}\,a_5^\chi(x,y)$	$\frac{1}{\sqrt{2}}\,a_2^\chi(x,y)+\frac{1}{\sqrt{2}}\,a_6^\chi(x,y)$
$\pi^-\pi^0$, $\rho^-\pi^0$ $\pi^-\rho^0$	$\frac{1}{\sqrt{2}}\,a_1^\chi(x,y)+\frac{1}{\sqrt{2}}\,a_5^\chi(x,y)$	$-\frac{1}{\sqrt{2}}\,a_2^\chi(x,y)-\frac{1}{\sqrt{2}}\,a_6^\chi(x,y)$
$\pi^+\pi^-$, $\pi^+\rho^-$, $\rho^+\pi^-$	$-a_1^\chi(x,y)+\frac{1}{2}a_5^\chi(x,y)$	$a_2^\chi(x,y)-\frac{1}{2}a_6^\chi(x,y)$
$\pi^0\pi^0$, $\rho^0\pi^0$	$a_1^\chi(x,y)-\frac{1}{2}\,a_5^\chi(x,y)$	$-a_2^\chi(x,y)+\frac{1}{2}\,a_6^\chi(x,y)$
$K^-K^{(*)+}$, $K^{(*)-}K^+$	—	—
$\bar{K}^0K^{(*)0}$, $\bar{K}^{(*)0}K^0$	$a_1^\chi(x,y)-\frac{1}{2}a_5^\chi(x,y)$	$-a_2^\chi(x,y)+\frac{1}{2}a_6^\chi(x,y)$
$K^-K^{(*)0}$, $K^{(*)-}K^0$	$a_1^\chi(x,y)+a_5^\chi(x,y)$	$-a_2^\chi(x,y)-a_6^\chi(x,y)$
$\pi^-\bar{K}^{(*)0}$, $\rho^-\bar{K}^0$	$a_1^\chi(x,y)+a_5^\chi(x,y)$	$-a_2^\chi(x,y)-a_6^\chi(x,y)$
$\pi^0K^{(*)-}$, ρ^0K^-	$-\frac{1}{\sqrt{2}}\,a_1^\chi(x,y)-\frac{1}{\sqrt{2}}\,a_5^\chi(x,y)$	$\frac{1}{\sqrt{2}}\,a_2^\chi(x,y)+\frac{1}{\sqrt{2}}\,a_6^\chi(x,y)$
$\pi^0\bar{K}^{(*)0}$, $\rho^0\bar{K}^0$	$\frac{1}{\sqrt{2}}\,a_1^\chi(x,y)-\frac{1}{2\sqrt{2}}\,a_5^\chi(x,y)$	$-\frac{1}{\sqrt{2}}\,a_2^\chi(x,y)+\frac{1}{2\sqrt{2}}\,a_6^\chi(x,y)$
$\pi^+K^{(*)-}$, ρ^+K^-	$-a_1^\chi(x,y)+\frac{1}{2}a_5^\chi(x,y)$	$a_2^\chi(x,y)-\frac{1}{2}a_6^\chi(x,y)$

Table 4.5: Hard functions for the annihilation amplitude $A^{(2)}_{Lann}$ in Eq. (4.60) for $\bar{B}^0$ and B^- decays. The result for $B^-\to\pi^0\pi^-$ is obtained by adding the results using the entries from the first two rows, and so vanishes in the isospin limit.

M_1M_2	$H_{\chi 1}(x,y)$	$H_{\chi 2}(x,y)$
$K^+\pi^-$, $K^{*+}\pi^-$, $K^+\rho^-$	$-a_1^\chi(x,y)+\frac{1}{2}a_5^\chi(x,y)$	$a_2^\chi(x,y)-\frac{1}{2}a_6^\chi(x,y)$
$K^0\pi^0$, $K^{*0}\pi^0$, $K^0\rho^0$	$\frac{1}{\sqrt{2}}\,a_1^\chi(x,y)-\frac{1}{2\sqrt{2}}\,a_5^\chi(x,y)$	$-\frac{1}{\sqrt{2}}\,a_2^\chi(x,y)+\frac{1}{2\sqrt{2}}\,a_6^\chi(x,y)$
K^+K^-, $K^{*+}K^-$, K^+K^{*-}	$-a_1^\chi(x,y)+\frac{1}{2}a_5^\chi(x,y)$	$a_2^\chi(x,y)-\frac{1}{2}a_6^\chi(x,y)$
$K^0\bar{K}^0$, $K^{*0}\bar{K}^0$, $K^0\bar{K}^{*0}$	$a_1^\chi(x,y)-\frac{1}{2}a_5^\chi(x,y)$	$-a_2^\chi(x,y)+\frac{1}{2}a_6^\chi(x,y)$

Table 4.6: Hard functions for the annihilation amplitude $A^{(2)}_{Lann}$ in Eq. (4.60) for $\bar{B}_s$ decays.

from $A^{(1)}_{Lann}$ and $A^{(2)}_{Lann}$. For later convenience we define moment parameters

$$\begin{aligned}\beta^{M_1M_2}_{\chi 1,\chi 5}&=\frac{1}{6}\int_0^1 dx\,dy\,a^\chi_{1,5}(x,y)\,\phi^{M_1}_{pp}(y)\phi^{M_2}(x)\,,\\ \beta^{M_1M_2}_{\chi 2,\chi 6}&=\frac{1}{6}\int_0^1 dx\,dy\,a^\chi_{2,6}(x,y)\phi^{M_1}(y)\phi^{M_2}_{pp}(x)\,.\end{aligned}\tag{4.61}$$

Neglecting ϕ_{3P} in the WW approximation yields $\phi^P_{pp}(y)=6y(1-y)$. At order $\alpha_s(\mu_h)$ our results for $\beta_{\chi 1}$ and $\beta_{\chi 2}$, taken with the WW approximation, agree with the convolutions derived in this limit in Refs. [33, 40]. Ignoring the $\emptyset$-distributions we would find that these convolution integrals diverge. The zero-bin avoided double counting in our convolutions, and yields a finite and real result for the chirally enhanced annihilation amplitude.

Let's see how the convolutions work out at order $\alpha_s(\mu_h)$ following Ref. [124]. We need two standard convolutions involving zero-bin subtractions,

$$\int_0^1 dx\,dy \left[\frac{1+\bar{x}}{y^2\,\bar{y}\,\bar{x}^2}\right]_\emptyset \phi_{pp}^{M_1}(y)\phi^{M_2}(x) = \left\langle y^{-2}\,\bar{y}^{-1}\right\rangle_{pp}^{M_1}\left(\left\langle \bar{x}^{-2}\right\rangle^{M_2} + \left\langle \bar{x}^{-1}\right\rangle^{M_2}\right),$$
$$\int_0^1 dx\,dy \left[\frac{1+y}{y^2\,x\,\bar{x}^2}\right]_\emptyset \phi^{M_1}(y)\phi_{pp}^{M_2}(x) = \left\langle \bar{x}^{-2}\,x^{-1}\right\rangle_{pp}^{M_2}\left(\left\langle y^{-2}\right\rangle^{M_1} + \left\langle y^{-1}\right\rangle^{M_1}\right). \quad (4.62)$$

Here we model the y^{-2}, y^{-1} moments as in Eq. (4.26) and Eq. (4.30), and for the remaining convolution we find

$$\left\langle y^{-2}\,\bar{y}^{-1}\right\rangle_{pp}^{M_1} = \int_0^1 dy \left[\frac{\phi_{pp}^{M_1}(y,\mu)}{y^2(1-y)} - \frac{y\phi_{pp}^{M_1\prime}(0,\mu)}{y^2}\right] + \phi_{pp}^{M_1\prime}(0,\mu)\,\ln\left(\frac{n\cdot p_{M_1}}{\mu_+}\right). \quad (4.63)$$

The $\mu_\pm$ dependence is canceled by tree level logarithmic dependence in the coefficients, $d_{1,4}(\mu_-) = \ln(p_M^-/\mu_-)$, $d_{2,5}(\mu_+) = \ln(p_M^+/\mu_+)$, $d_{3,6}(\mu_\pm) = \ln(p_M^-/\mu_-)\ln(p_M^+/\mu_+)$. The kernels in Eq. (4.55) also involve two more complicated convolutions that are derived in Appendix A,

$$\begin{aligned}
\left\langle[(1-x\bar{y})\bar{x}y^2]^{-1}\right\rangle_{pp}^{M_1M_2} &= \int_0^1 dx\,dy\left[\frac{1}{(1-x\bar{y})\bar{x}y^2}\right]_\emptyset \phi_{pp}^{M_1}(y)\phi^{M_2}(x) \\
&= \int_0^1 dx\int_0^1 dy\left[\frac{\phi_{pp}^{M_1}(y)\phi^{M_2}(x)}{(\bar{x}+y-\bar{x}y)\bar{x}y^2} - \frac{\phi_{pp}^{M_1\prime}(0)\,\phi^{M_2}(x)}{(\bar{x}+y)\bar{x}y}\right] - \phi_{pp}^{M_1\prime}(0)\int_0^1 dx\,\frac{\phi^{M_2}(x)\,\ln(2-x)}{(1-x)^2}, \\
\left\langle[(1-x\bar{y})\bar{x}^2y]^{-1}\right\rangle_{pp}^{M_2M_1} &= \int_0^1 dx\,dy\left[\frac{1}{(1-x\bar{y})\bar{x}^2y}\right]_\emptyset \phi^{M_1}(y)\phi_{pp}^{M_2}(x) \qquad (4.64) \\
&= \int_0^1 dy\int_0^1 dx\left[\frac{\phi^{M_1}(y)\,\phi_{pp}^{M_2}(x)}{(\bar{x}+y-\bar{x}y)\bar{x}^2y} + \frac{\phi^{M_1}(y)\,\phi_{pp}^{M_2\prime}(1)}{(\bar{x}+y)\bar{x}y}\right] + \phi_{pp}^{M_2\prime}(1)\int_0^1 dy\,\frac{\phi^{M_1}(y)\,\ln(1+y)}{y^2}.
\end{aligned}$$

As promised, the minimal subtraction scheme yields a well defined result for $A_{Lann}^{(2)}$. The scheme dependence cancels order by order in α_s between the matrix element and perturbative corrections to the kernels obtained by matching. In any scheme the result at order $\alpha_s(\mu_h)$ is real.

4.6 Generating Strong Phases

In this section we derive results for the order at which strong phases occur in the power suppressed amplitudes $A^{(1)}$. It is convenient to classify complex contributions to the $B \to M_1 M_2$ amplitudes according to the distance scale at which they are generated. We use the terminology hard, jet, and nonperturbative to refer to imaginary contributions from the scales m_b, $\sqrt{m_b \Lambda}$, and Λ^2 respectively. We will not attempt to classify strong phases generated by charm loops, since a complete understanding of factorization for these terms order by order in a power counting expansion is not yet available.

For a matrix element to have a physical complex phase it must contain information about both final state mesons. Generically, terms in the factorized power expansion of $B \to M_1 M_2$ amplitudes involve only vacuum to meson matrix elements, so strong phase information can be contained in the Wilson coefficients or the factorized operators, but not in the states. This provides tight constraints on the source of strong phases. Nonperturbative strong phases will occur if matrix elements of these factorized operators give complex distribution functions. A sufficient condition to generate a nonperturbative phase, is to have a factorized operator that is sensitive to the directions of two or more final state mesons [126], information that can be carried by Wilson lines. Physically, this is a manifestation of soft rescattering of final states. In processes like ours where soft-collinear and collinear(n)-collinear($\bar{n}$) factorization are relevant, and there is only one hadron in any given light cone direction, this criterion implies that all strong phases reside in the soft matrix elements, where the directional information from collinear hadrons is retained in soft Wilson lines, S_r, with direction r^μ. Since $S_r^\dagger S_r = 1$ these Wilson lines often cancel, but for many of the power suppressed terms listed in Table 4.1 the cancellation is not complete. This mechanism for generating a strong phase was first observed for $\bar{B}^0 \to D^0 \pi^0$ [126], where a nonperturbative soft matrix element occurs through four-quark operators depending on n and v' (which are null and time-like vectors for the final state light and charmed mesons, respectively).

For the $B \to M_1 M_2$ decays with two energetic light mesons, a nonperturbative strong phase requires a soft matrix element depending on the S_n and $S_{\bar{n}}$ Wilson lines in $\mathrm{SCET_{II}}$. The simplest way to obtain the Wilson lines for the soft operators is to match $\mathrm{SCET_I}$ onto $\mathrm{SCET_{II}}$ [23]. In $\mathrm{SCET_I}$ one first uses the decoupling field redefinition on collinear fields [22], $\xi_n \to Y_n \xi_n$, $\xi_{\bar{n}} \to Y_{\bar{n}} \xi_{\bar{n}}$, $A_n \to Y_n A_n Y_n^\dagger$ and $A_{\bar{n}} \to Y_{\bar{n}} A_{\bar{n}} Y_{\bar{n}}^\dagger$, which generates the Wilson lines and factorizes usoft and collinear fields. The fields of a given type are then grouped together by Fierz rearrangements. Matching the resulting operators or time-ordered products onto $\mathrm{SCET_{II}}$ gives $Y_r \to S_r$, and we can read off which soft Wilson lines are present. Because of the properties of the subleading $\mathrm{SCET_I}$ operators, we will not have an S_n and $S_{\bar{n}}$ in the final $\mathrm{SCET_{II}}$ operator unless we have a subleading $\mathrm{SCET_I}$ Lagrangian with an n-collinear field and usoft fields, and one with $\bar{n}$-collinear fields and usoft fields. We used this property to determine which entries are real or complex, and listed the results in the last column of Table 4.1. The complex entries with multiple $\mathcal{L}_{\xi q}^{(j)}$'s [35] also have at least two hard-collinear gluons, and so generate contributions that start at $\alpha_s(\mu_i)^2$ when matched onto $\mathrm{SCET_{II}}$.

To determine the perturbative order of the complex contributions, we must also classify which hard and jet coefficients give complex phases. In general any hard coefficient generated by matching at ≥ 1 loop will give imaginary contributions, since these loops involve fields for both final state mesons, as pointed out for the general case in Ref. [31, 32] and for charm loops in Ref. [12]. Since all leading order contributions in Table 4.1 have at least one $\alpha_s(\mu_i)$, the hard imaginary contributions for $A^{(0)}$ are $\mathcal{O}[\alpha_s(\mu_i)\alpha_s(\mu_h)/\pi]$. At order Λ/m_b all annihilation contributions but $Q_i^{(4)}$ have at least one $\alpha_s(\mu_i)$, and for these terms the hard complex contributions involve $\alpha_s(\mu_i)\alpha_s(\mu_h)$ and thus are smaller than the nonperturbative terms proportional to $\alpha_s(\mu_i)^2$. For $Q_i^{(4)}$ the amplitude is real at the leading perturbative order, $\alpha_s(\mu_h)$, as demonstrated in section 4.3, and so hard complex contributions start at $\alpha_s^2(\mu_h)$. In contrast for the amplitude $A_{rest}^{(1)}$ a complex amplitude is generated at order $\alpha_s(\mu_i)\,\Lambda/m_b$, which is only suppressed by Λ/m_b compared to $A^{(0)}$.

Finally, we should examine complex contributions from the jet scale. At leading

order there is a unique jet function J [19]. J also contributes to the heavy-to-light form factors and only knows about the n-collinear direction. Thus $A^{(0)}$ does not get imaginary contributions at any order in the $\alpha_s(\mu_i)$ expansion (which has been demonstrated explicitly to $\alpha_s^2(\mu_i)$ [28]). At next-to-leading order in the power expansion, there is no known relation of the power suppressed jet functions with analogous jet functions in the form factors. However, the subleading jet functions also depend only on one collinear direction, and do not carry information about both final state mesons that could generate a physical strong phase. We demonstrate this fact more explicitly by examining the calculation at $\mathcal{O}(\alpha_s(\mu_i))$, which is sufficient to see that the amplitudes are real up to the order where a nonperturbative phase first occurs. At this order the jet functions are generated by matching tree level SCET_I diagrams onto SCET_II. A typical example is

$$\frac{1}{(x+i\epsilon)\,(k^+ + i\epsilon)}\,, \tag{4.65}$$

where x is a momentum fraction that will be convolved with a collinear distribution function, and the k^+ will be convolved with a soft distribution function. These jet functions are real if and only if we can drop the $i\epsilon$ factors. However, just as in section 4.3, the $i\epsilon$ terms can be dropped because the zero-bin subtractions [124] ensure that this does not change the convolution.[3] Thus factorization gives real $\mathcal{O}(\alpha_s(\mu_i))$ jet functions.

This demonstrates that complex contributions in the power suppressed annihilation amplitudes are suppressed,

$$\text{Im}\left[\frac{A_{ann}^{(1)}}{A^{(0)}}\right] = \mathcal{O}\left(\frac{\alpha_s(\mu_i)}{\pi}\,\frac{\Lambda}{m_b}\right) + \mathcal{O}\left(\frac{\Lambda^2}{m_b^2}\right). \tag{4.66}$$

On general grounds one might have expected $\mathcal{O}(\Lambda/m_b)$ suppressed strong phases, which we have demonstrated are absent in $A_{ann}^{(1)}$, though they do occur in $A_{rest}^{(1)}$.

We close this section by giving two examples of time-ordered products generat-

[3] A equivalent physical argument for dropping the $i\epsilon$ factors was given in Ref. [126], where it was needed to prove that certain long-distance contributions are absent in color suppressed decays.

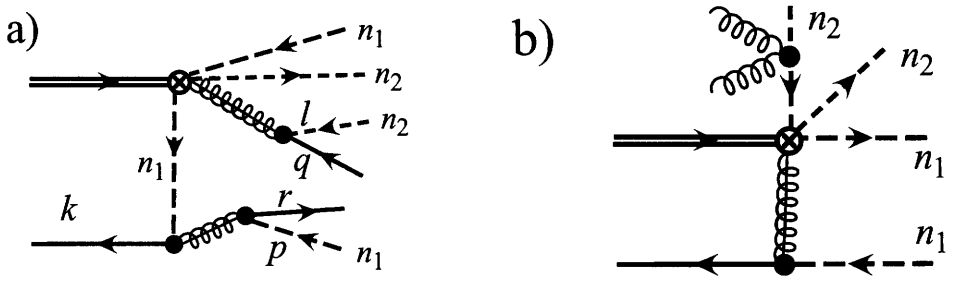

Figure 4-4: Graphs which generate a strong phase in lowest order matching of $\mathrm{SCET_I}$ operators onto $\mathrm{SCET_{II}}$: a) has a $Q^{(1)}$, two $\mathcal{L}^{(1)}_{\xi_{n_1}q}$, and one $\mathcal{L}^{(1)}_{\xi_{n_2}q}$ and contributes to the annihilation amplitude at $\mathcal{O}(\alpha_s^2(\mu_i))$; and b) has a $Q^{(1)}$, one $\mathcal{L}^{(1)}_{\xi_{n_1}q}$, and one $\mathcal{L}^{(2)}_{\xi_{n_2}\xi_{n_2}}$ and contributes to non-annihilation amplitudes at $\mathcal{O}(\alpha_s(\mu_i))$. Dashed quark lines are n_1 or n_2 collinear, and solid quark lines are soft.

ing the nonperturbative strong phases discussed above. We consider a time-ordered product with three $\mathcal{L}^{(1)}_{\xi q}$ insertions contributing to annihilation. When matching onto $\mathrm{SCET_{II}}$ we integrate out the hard-collinear modes, leading to an eight-quark operator. Figure 4-4a shows the order $\alpha_s^2(\mu_i)$ contribution to this matching. The soft quark lines remain open as their contraction leads to an on-shell line which must be treated nonpertrubatively. The resulting $\mathrm{SCET_{II}}$ operator has the generic form

$$\begin{aligned} O^{II} &= J(n_2\cdot p, n_1\cdot l, n_1\cdot r, n_2\cdot q, n_1\cdot k) \\ &\quad\times (\bar{q}_s S_{n_1})_{n_1\cdot r}\,\Gamma^{(1)}(S^\dagger_{n_2} q_s)_{n_2\cdot q}\,(\bar{q}_s S_{n_2})_{n_1\cdot k}\,\Gamma^{(2)}(S^\dagger_{n_1} h_v)\,(\bar{q}_{n_1,l}\Gamma^{(3)} q_{n_1,l'})\,(\bar{q}_{n_2,p'}\Gamma^{(4)} q_{n_2,p}) \end{aligned} \tag{4.67}$$

where we use the shorthand subscript notation, $(S^\dagger_{n_i} q_s)_{n_i\cdot q} \equiv [\delta(n_i\cdot q - n_i\cdot\mathcal{P}) S^\dagger_{n_i} q_s]$. We took the jet directions to be n_1 and n_2, rather than n and $\bar{n}$, to emphasize that the soft operator is sensitive to the relative directions of the jets. The functions S_i shown in Table 4.1 are defined by the matrix element of this type of operator

$$S_i(n_1\cdot k, n_1\cdot r, n_2\cdot q,) \equiv \langle 0|(\bar{q}_s S_{n_1})_{n_1\cdot r}\,\Gamma^{(1)}_i(S^\dagger_{n_2} q_s)_{n_2\cdot q}\,(\bar{q}_s S_{n_2})_{n_1\cdot k}\,\Gamma^{(2)}_i(S^\dagger_{n_1} h_v)|B(v)\rangle\,, \tag{4.68}$$

where i runs over color, Dirac, and flavor structures. To count the factors of π in these amplitudes, note that the hard-collinear contractions give g^4, and that the matrix element of the resulting four-quark operator, $\langle 0|(\bar{q}\ldots q)(\bar{q}\ldots b_v)|B\rangle$, is suppressed by

$1/(4\pi)^2$ relative to $\langle 0|(\bar{q}\ldots b_v)|B\rangle$. (The four-quark operator has an extra loop with no extra couplings.) This demonstrates that nonperturbative complex contributions first occur at order $[\alpha_s(\mu_i)^2/\pi](\Lambda/m_b)$, i.e., suppressed by $[\alpha_s(\mu_i)/\pi](\Lambda/m_b)$ compared to the leading amplitudes. The phases arising from the type of matrix element shown in Eq. (4.68) play a crucial role in explaining the observed strong phases which arise in color suppressed decays [126]. Their resulting operators predict the equality of amplitudes and strong phases between decays involving D and D^* mesons and have been confirmed in the data [129]. This type of diagrams also have long-distance contributions of the same order, which arise from time-ordered products in $\mathrm{SCET_{II}}$ and can also be complex. To see this note that the hard-collinear quark propagator in Fig. 4-4a could also be on-shell (i.e., have $\mathcal{O}(\Lambda^2)$ virtuality), in which case it would remain open until the matrix element is taken at the low scale. By opening that line we see that this contribution corresponds to the time-ordered product of a four-quark operator and a six-quark operator, both of which are generated when matching onto $\mathrm{SCET_{II}}$. A long-distance part is the same order in $\alpha_s(\mu_i)$ and does not change our conclusions about these terms. In Fig. 4-4b we show a non-annihilation contribution to $\hat{A}^{(1)}_{rest}$ which is of order $\alpha_s(\mu_i)\Lambda/m_b$. This term is generated by the time-ordered product of $Q^{(1)}$, an insertion of the n_1-collinear $\mathcal{L}^{(1)}_{\xi q}$, and an operator with n_2-collinear quarks and usoft gluons,

$$\mathcal{L}^{(2)}_{\xi\xi} = (\bar{\xi}_n W)\, Y^\dagger_{n_2} i\not{D}^\perp_{us}\, i\not{D}^\perp_{us} Y_{n_2}\, \frac{\not{\bar{n}}}{2\bar{\mathcal{P}}}\, (W^\dagger \xi_n)\,. \tag{4.69}$$

4.7 Applications

4.7.1 Phenomenological Implications

To understand the implications of the experimental data, it is crucial to know which contributions to the $B \to M_1 M_2$ amplitudes can be complex. The best sensitivity to non-SM physics is via interference phenomena, where new interactions enter linearly (instead of quadratically), such as CP-violating observables. The sensitivity to such effects depends on how well we understand the dominant and subdominant SM am-

plitudes, including their strong phases. The existence of strong phases in B decays is experimentally well established (e.g., the $B \to D\pi$ and $B \to \pi\pi$ rates, the CP asymmetry $A_{K^+\pi^-}$, the transversity analysis in $B \to J/\psi K^*$, etc.).

One example of how strong phase information can be useful is the method for determining γ from $B \to \pi\pi$ proposed in Ref. [25]. The method uses isospin, the factorization prediction that $\mathrm{Im}(C/T) \sim \mathcal{O}\big(\alpha_s(m_b), \Lambda/m_b\big)$, and does not require data on the poorly measured direct CP asymmetry $C_{\pi^0\pi^0}$.[4] The phases in $A^{(0)}$ at $\alpha_s(m_b)\alpha_s(\mu_i)$ are calculable and partially known [31, 32, 38]. The current $B \to \pi\pi$ data is in mild conflict (at the $\sim 2\sigma$ level) with the SM CKM fit [90]. More precise measurements are needed to understand how well the theoretical expectations are satisfied, and to decipher whether there might be a hint for new physics. Obviously further information about power corrections in $\mathrm{Im}(C/T)$ could help to clarify the situation.

In all factorization-based approaches to charmless B decays, several parameters are fit from the data or are allowed to vary in certain ranges. The choice and ranges of these parameters should be determined by the power counting. This motivated keeping the charm penguin amplitudes, $A_{c\bar{c}}$ as free parameters in SCET [19], as was done earlier in Ref. [67, 66]. In the BBNS approach these are argued to be factorizable [31, 32]. A fit to the data using this parameterization found large power suppressed effects [55] including annihilation amplitudes, which might be interpreted as a breakdown of the Λ/m_b expansion. In QCD sum rules, the annihilation amplitude was found to be of the expected magnitude and to have a sizable strong phase [104].

Channels like $B \to K\pi$ and $B \to K\bar{K}$ are sensitive to new physics, but by the same token are dominated by penguin amplitudes, which can have charm penguin, annihilation, and other standard model contributions. Since there are possible large nonperturbative c-loop contributions in $A_{c\bar{c}}$ that have the same $SU(3)$ flavor transformation properties as annihilation terms, they cannot be easily distinguished by simple fits to the data. However, in a systematic analysis based on SCET these correspond

[4] Here C and T are isospin amplitudes defined in the t-convention, where λ_t is eliminated from the amplitudes in favor of λ_c and λ_u.

to different operators' matrix elements, so it is possible to disentangle the various contributions and determine their expected size. The factorization theorems for annihilation amplitudes derived here only involve distributions that already occurred at leading order. This means that we can compare the size of annihilation amplitudes to experimental data without further ambiguities from additional hadronic parameters. We take up this comparison in section 4.7.2 below.

As an explicit example of how to assemble our results in sections 4.3, 4.4, and 4.5, we derive the annihilation amplitude for $\bar{B}^0 \to K^-\pi^+$. From Table 4.2 we can read off the result for this channel, $H(x,y) = -a_4^s(x,y) - a_8^s(x,y)$, from Table 4.4, $H_{hc1} = -a_1^{hc} + a_3^{hc}/2$ and $H_{hc1} = a_2^{hc} - a_4^{hc}/2$, and from Table 4.5, $H_{\chi 1} = -a_1^\chi(x,y) + 1/2\, a_5^\chi(x,y)$ and $H_{\chi 2} = a_2^\chi(x,y) - 1/2\, a_6^\chi(x,y)$. With the lowest order matching results in Eqs. (4.21), (4.45) and (4.55) we can set $a_8 = 0$ and $a_{4u} = a_{4c}$, which inserted into Eqs. (4.20) (4.49) and (4.60) gives

$$
\begin{aligned}
A^{(1)}_{Lann}(K^-\pi^+) &= \frac{G_F f_B f_\pi f_K}{\sqrt{2}} (\lambda_c^{(s)} + \lambda_u^{(s)}) \int dx\, dy\, (-1) a_{4u}(x,y) \phi^\pi(y) \phi^K(x) \qquad (4.70)\\
&= -\frac{G_F f_B f_\pi f_K}{\sqrt{2}} (\lambda_c^{(s)} + \lambda_u^{(s)})\, \beta_{4u}^{\pi K}\,,\\
A^{(1)}_{Tann}(K^-\pi^+) &= \frac{G_F f_B m_B}{\sqrt{2} m_b N_c} (\lambda_u^{(s)} + \lambda_c^{(s)})\, 3\beta_B \big[-f_{3\pi} f_K \beta_{hc1}^{\pi K} - f_{3K} f_\pi \beta_{hc2}^{\pi K} \big]\\
A^{(2)}_{Lann}(K^-\pi^+) &= \frac{G_F f_B f_\pi f_K}{6\sqrt{2}} (\lambda_c^{(s)} + \lambda_u^{(s)}) \int dx\, dy \Big[\frac{\mu_\pi}{m_b} \Big\{ -a_1^\chi(x,y) + \frac{1}{2} a_5^\chi(x,y) \Big\} \phi_{pp}^\pi(y) \phi^K(x)\\
&\qquad + \frac{\mu_K}{m_b} \Big\{ a_2^\chi(x,y) - \frac{1}{2} a_6^\chi(x,y) \Big\} \phi^\pi(y) \phi_{pp}^K(x) \Big]\\
&= \frac{G_F f_B f_\pi f_K}{\sqrt{2}} (\lambda_c^{(s)} + \lambda_u^{(s)}) \Big[\frac{\mu_\pi}{m_b} \Big\{ -\beta_{\chi 1}^{\pi K} + \frac{1}{2} \beta_{\chi 5}^{\pi K} \Big\} + \frac{\mu_K}{m_b} \Big\{ \beta_{\chi 2}^{\pi K} - \frac{1}{2} \beta_{\chi 6}^{\pi K} \Big\} \Big]\,.
\end{aligned}
$$

Thus, both the leading order annihilation amplitude $A^{(1)}_{Lann} + A^{(1)}_{Tann}$, and the chirally enhanced annihilation amplitude $A^{(2)}_{Lann}$ are determined by the β's defined in Eqs. (4.23), (4.50), and (4.61). Other $K\pi$ channels have similar expressions with different Clebsch-Gordan coefficients. For the local annihilation, which involves zero-bin subtractions, to see explicitly what the β's involve we insert the $\mathcal{O}(\alpha_s)$ values of

$a_{3u}(x,y)$, $a_1^\chi(x,y)$, and $a_2^\chi(x,y)$ to give

$$
\begin{aligned}
A_{Lann}(K^-\pi^+) &= \frac{G_F f_B f_{M_1} f_{M_2}}{\sqrt{2}}(\lambda_c^{(s)}+\lambda_u^{(s)})\frac{4\pi\alpha_s(\mu_h)}{9} \\
&\times\Bigg\{\Big(\frac{C_9}{6}-\frac{C_3}{3}\Big)\Big[\langle\bar{x}^{-2}\rangle^K\langle y^{-1}\rangle^\pi-\langle[y(x\bar{y}-1)]^{-1}\rangle^{\pi K}+d(\mu_-)\phi_K'(1)\langle y^{-1}\rangle^\pi\Big] \\
&\quad-\frac{2\mu_\pi}{3m_b}\Big(C_6-\frac{C_8}{2}+\frac{C_5}{3}-\frac{C_7}{6}\Big)\Big[\langle y^{-2}\bar{y}^{-1}\rangle_{pp}^\pi\big(\langle\bar{x}^{-2}\rangle^K+\langle\bar{x}^{-1}\rangle^K\big)+d_1(\mu_-)\phi_K'(1)\langle y^{-2}\bar{y}^{-1}\rangle_{pp}^\pi \\
&\qquad-d_2(\mu_+)\phi_\pi'(0)\big(\langle\bar{x}^{-2}\rangle^K+\langle\bar{x}^{-1}\rangle^K\big)-d_3(\mu_\pm)\phi_K'(1)\phi_\pi'(0)\Big] \\
&\quad-\frac{2\mu_\pi}{3m_b}\Big(\frac{C_5}{3}-\frac{C_7}{6}\Big)\langle[(1-x\bar{y})\bar{x}y^2]^{-1}\rangle_{pp}^{\pi K}+\frac{2\mu_K}{3m_b}\Big(\frac{C_5}{3}-\frac{C_7}{6}\Big)\langle[(1-x\bar{y})\bar{x}^2y]^{-1}\rangle_{pp}^{K\pi} \\
&\quad-\frac{2\mu_K}{3m_b}\Big(C_6-\frac{C_8}{2}+\frac{C_5}{3}-\frac{C_7}{6}\Big)\Big[\big(\langle y^{-2}\rangle^\pi+\langle y^{-1}\rangle^\pi\big)\langle x^{-1}\bar{x}^{-2}\rangle_{pp}^K-d_1(\mu_+)\phi_\pi'(0)\langle\bar{x}^{-2}x^{-1}\rangle_{pp}^K \\
&\qquad+d_2(\mu_-)\phi_K'(1)\big(\langle y^{-2}\rangle^\pi+\langle y^{-1}\rangle^\pi\big)-d_3(\mu_\pm)\phi_\pi'(0)\phi_K'(1)\Big]\Bigg\}. \qquad (4.71)
\end{aligned}
$$

Here results for the convolutions denoted by brackets $\langle\cdots\rangle$ can be found in Eqs. (4.26), (4.30), (4.63), and (4.64) in the minimal subtraction scheme. Results for the leading hard-collinear annihilation are similar, but simpler since they do not require zero-bin subtractions. Results for other channels can be assembled in a similar fashion. Corrections to $A_{Lann}+A^{(1ann)}_{\rm hard-collin}$ are suppressed by $\mathcal{O}[\alpha_s^2(\mu_i)/(\pi\alpha_s(m_b))]$, while we caution that additional $\alpha_s(\mu_h)\Lambda/m_b$ terms without a μ_π or μ_K will be present in the last two lines of Eq. (4.71). In the next subsection we derive results for all of these channels using a simple model for the distribution functions, and study numerically the size of the annihilation amplitudes.

Annihilation contributions have been claimed to play important roles in several observables [103, 102, 33, 40, 101], in particular in generating large strong phases in $B\to K\pi$ decays [103, 102]. The $B\to\pi\pi$ and $K\pi$ data indicate that the latter decays are dominated by penguin amplitudes, and the pattern of rates and CP asymmetries is not in good agreement with some predictions. In particular, it is not easy in the BBNS analysis to accommodate the measured CP asymmetry, $A_{K^+\pi^-}=-0.108\pm 0.017$ [91], except in the S3 and S4 models of Ref. [40]. In these models the annihilation contributions are included by using asymptotic distributions, and divergent integrals are parameterized as $\int_0^1 dx/x\to X_A$ and $\int_0^1 dx\ln x/x\to -X_A^2/2$, with $X_A=(1+$

$\varrho_A e^{i\varphi_A}) \ln(m_B/500\,\mathrm{MeV})$. Model S3 postulates $\varrho_A = 1$, $\varphi_A = -45°$ for all final states, while in the S4 scenario $\varrho_A = 1$ and $\varphi_A = -55°$, $-20°$, $-70°$ for the PP, PV, VP channels, respectively. Thus

$$S3:\ X_A = 4.0 - 1.7i\,, \qquad S4:\ X_A = \{3.7 - 1.9i\,,\ 4.6 - 0.8i\,,\ 3.2 - 2.2i\}\,. \quad (4.72)$$

In addition, $\alpha_s(\mu)$ and the Wilson coefficients are evaluated at the μ_i intermediate scale [40].

Our result for the factorization of annihilation contributions derived in Sec. 4.3 constrains models of annihilation. Equation (4.20) gives a well defined and real amplitude at leading order, which depends on twist-2 distributions, ϕ_M. It does not involve model parameters ϱ_A and φ_A. For $A^{(1)}_{Lann}$ using Eq. (4.26) and the asymptotic form of the meson distributions, we find a correspondence

$$\text{“}X_A\text{”} = 1 + \int_0^1 dx\, \frac{\phi_\pi(x)}{6\,(x^2)_\emptyset} = \ln\left(\frac{m_b}{\mu_+}\right). \quad (4.73)$$

Clearly, X_A is real. The asymptotic distributions $\sim 6x(1-x)$ are more accurate for large scales, and at the matching scale where $\mu_+ \sim m_b$, X_A is not enhanced by a large logarithm. We estimate $|X_A| \lesssim 1$. Thus, the modeling of annihilation contributions with complex X_A in the BBNS approach (including the phenomenologically favored S3 and S4 scenarios) are in conflict with the heavy quark limit, and should be constrained to give smaller real X_A's.

In the KLS [103] treatment of annihilation, complex amplitudes are generated from dynamics at the intermediate scale from the $i\epsilon$ in propagators. The MS-factorization used in the derivation of our annihilation amplitudes demonstrates that including the $i\epsilon$ term in collinear factorization would induce a double counting. Thus we expect such contributions to physical strong phases to be realized by operators with soft exchange that occur at higher order in Λ/m_b and therefore to be small.

Annihilation contributions were also argued to play an important role in explaining the large transverse polarization fraction in $B \to \phi K^*$ [101]. It was shown that factorization implies $R_T = \mathcal{O}(1/m_b^2)$, where R_T denotes the transverse polarization

fraction [101]. Subsequently, it was shown using SCET that R_T is power suppressed unless a long-distance charm penguin amplitude $A_{c\bar{c}}$ spoils this result [19, 137]. Experimentally, one finds $R_T(B \to \phi K^*) \approx 0.5$ [91], while $R_T(B \to \rho\rho)$ is at the few percent level. It has been argued that the large $R_T(B \to \phi K^*)$ may provide a hint of new physics in the $b \to s\bar{s}s$ channel. In Ref. [101] it was suggested that Standard Model annihilation contributions may account for the observed large value of $R_T(B \to \phi K^*)$. Our analysis in Sec. 4.5 agrees with [101] in that annihilation contributions to the transverse polarization amplitude at first order in α_s are suppressed by not one, but two powers of Λ/m_b. However, we do not find a numerical enhancement of these terms (which in [101] is partly due to the large sensitivity of the $(2X_A - 3)(1 - X_A)$ function to ϱ_A in the BBNS parameterization). The operators in Eq. (4.53) give rise to transverse polarization, but since MS-factorization renders the naively divergent convolutions finite, these power suppressed amplitudes do not receive sizable enhancements. Although we have not derived explicit results for the $B \to \phi K^*$ annihilation amplitudes (since ϕ is an isosinglet), our results make it unlikely that local annihilation can explain the $R_T(B \to \phi K^*)$ data. We have not explored whether the time-ordered products at $\mathcal{O}(\alpha_s^2(\mu_i)\Lambda/m_b)$ could give rise to transverse polarization, and it would be interesting to do so.

4.7.2 Annihilation with simple models for ϕ^M, ϕ^{3M} and ϕ^M_{pp}

In this section we derive numerical results for the annihilation amplitudes in various channels using a simple model for the distributions. We begin by examining the local annihilation amplitude. It is convenient to write the $\Delta S = 0$ amplitude as

$$A_{Lann}(\bar{B} \to M_1 M_2) = \frac{G_F f_B f_{M_1} f_{M_2}}{\sqrt{2}} \Big\{ \lambda_u^{(d)} h_u(\bar{B} \to M_1 M_2) + \lambda_c^{(d)} h_c(\bar{B} \to M_1 M_2) + (\lambda_u^{(d)} + \lambda_c^{(d)}) \Big[\frac{\mu_{M_1}}{m_b} h_{\chi 1}(\bar{B} \to M_1 M_2) + \frac{\mu_{M_2}}{m_b} h_{\chi 2}(\bar{B} \to M_1 M_2) \Big] \Big\} . \tag{4.74}$$

For $\Delta S = 1$ decays we replace $\lambda_{u,c}^{(d)} \to \lambda_{u,c}^{(s)}$. The coefficients h_u, h_c, $h_{\chi 1}$, and $h_{\chi 2}$ are equal to linear combinations of β_{iu}, β_{ic}, $\beta_{\chi 1}$, $\beta_{\chi 2}$, $\beta_{\chi 5}$, and $\beta_{\chi 6}$ with Clebsch-Gordan coefficients determined from Tables 4.2, 4.3, 4.5, 4.6. The combinations are simply determined by the replacements

$$\begin{aligned}
h_u &= \big(H(x,y) \text{ with } \tilde{a}_i^{d,s}(x,y) \to \beta_{iu}^{M_1 M_2},\ \tilde{a}_i^{d,s}(y,x) \to \beta_{iu}^{M_2 M_1}\big)\,, \\
h_c &= \big(H(x,y) \text{ with } \tilde{a}_i^{d,s}(x,y) \to \beta_{ic}^{M_1 M_2},\ \tilde{a}_i^{d,s}(y,x) \to \beta_{ic}^{M_2 M_1}\big)\,, \\
h_{\chi 1} &= \big(H_{\chi 1}(x,y) \text{ with } a_{1,5}^{\chi}(x,y) \to \beta_{\chi 1,\chi 5}\big)\,, \\
h_{\chi 2} &= \big(H_{\chi 2}(x,y) \text{ with } a_{2,6}^{\chi}(x,y) \to \beta_{\chi 2,\chi 6}\big)\,.
\end{aligned} \tag{4.75}$$

For the coefficients $a_{3u,3c,4u,4c,7,8}$ and the a_i^{χ}'s, the $\mathcal{O}(\alpha_s^2 C_{1,2})$ matching corrections could be comparable numerically with the $\mathcal{O}(\alpha_s C_{3-10})$ corrections considered here. This should be kept in mind when examining numbers quoted below for the corresponding β's.

Results for the coefficients β_{iu}, β_{ic}, and $\beta_{\chi i}$, can be found in Eqs. (4.23) and (4.61). To derive numerical results we need to model the meson distribution functions. We take the C_i from Eq. (2.17), use

$$\begin{aligned}
&\alpha_s(\mu_h) = 0.22\,, && \mu_\pi(\mu_h) = 2.3\,\text{GeV}\,, && \mu_K(\mu_h) = 2.7\,\text{GeV}\,, \\
&f_K = 0.16\,\text{GeV}, && f_\pi = 0.13\,\text{GeV}, && f_B = 0.22\,\text{GeV},
\end{aligned} \tag{4.76}$$

where $\mu_h = m_b = 4.7\,\text{GeV}$, f_B comes from a recent lattice determination [85]. For the ϕ's we take simple models with parameters a_i^M and a_{ipp}^M which we consider specified at the high scale μ_h,

$$\begin{aligned}
\phi^M(x) &= 6x(1-x)\big[1 + a_1^M(6x-3) + 6a_2^M(1-5x+5x^2)\big]\,, \\
\phi_{pp}^P(x) &= 6x(1-x)\big[1 + a_{1pp}^P(6x-3) + 6a_{2pp}^P(1-5x+5x^2)\big]\,.
\end{aligned} \tag{4.77}$$

Based on recent lattice data for moments of the π and K distributions [52] we take $a_2^{\pi,K} = 0.2 \pm 0.2$, where the lattice error was doubled to give some estimate for higher

moments. For the π we set $a_1^\pi = a_{1pp}^\pi = 0$, while for the K we use [52] $a_1^K = 0.05 \pm 0.02$. We also take $w_{3\pi,K} = -3 \pm 1$, $a_{2pp}^{\pi,K} = 0 \pm 0.4$ and $a_{1pp}^K = 0.0 \pm 0.2$. Note that the range for our parameters is similar to those used in the BBNS models [33, 40] and light-cone sum rules [10]. Since the uncertainties in the model parameters are large and not significantly affected by variation of the $\mu_\pm$ scales we keep these fixed at m_b, where the logs in the $d_i(\mu_\pm)$ terms drop out and the constant under the logs are neglected. A scan over models with parameters in these limits gives predictions for the annihilation coefficients. For the $\bar{B} \to K\pi$ channels we find

$$\begin{aligned}
&\beta_{2u}^{\pi K} = 1.8 \pm 1.2, \quad \beta_{4u}^{\pi K} = \beta_{4c}^{\pi K} = -0.15 \pm 0.10, \quad \beta_{2c}^{\pi K} = 0.14 \pm 0.09\,, \\
&\beta_{hc1}^{\pi K} = 0.09 \pm 0.33, \quad \beta_{hc2}^{\pi K} = -0.29 \pm 0.09, \quad \beta_{hc3}^{\pi K} = -0.012 \pm 0.002, \quad \beta_{hc4}^{\pi K} = 0.002 \pm 0.01\,, \\
&\beta_{\chi 1}^{\pi K} = 0.0 \pm 6.5, \quad \beta_{\chi 2}^{\pi K} = 0.0 \pm 5.8, \quad \beta_{\chi 5}^{\pi K} = 0.0 \pm 0.094, \quad \beta_{\chi 6}^{\pi K} = 0.0 \pm 0.11\,.
\end{aligned} \tag{4.78}$$

Using these numbers we can compare the size of the local annihilation amplitudes to the $\bar{B} \to K^-\pi^+$ data,

$$\begin{aligned}
R_A(K^-\pi^+) &= \frac{|A_{Lann}^{(1)}(K^-\pi^+) + A_{Lann}^{(2)}(K^-\pi^+)|}{|A_{Expt.Penguin}(K\pi)|} = 0.11 \pm 0.09\,, \\
R_A(\bar{K}^0\pi^-) &= \frac{|A_{Lann}^{(1)}(\bar{K}^0\pi^-) + A_{Lann}^{(2)}(\bar{K}^0\pi^-)|}{|A_{Expt.Penguin}(K\pi)|} = 0.12 \pm 0.09\,.
\end{aligned} \tag{4.79}$$

For the numerator we did a Gaussian scan using the values from Eq. (4.78), and determined the error by the standard deviation. For the denominator we used the experimental penguin amplitude determined by a fit to the $B \to K\pi$ data in Ref. [26]. Numerical results for annihilation amplitudes with three-body distribution functions will be considered later in this section. Although they are similar in size to $A_{Lann}^{(1)}$ they cause only a $\sim 10\%$ change in the value of $R_A(K^-\pi^+)$ in Eq. (4.79). The values of R_A indicate that a fairly small portion of the measured penguin amplitude is from annihilation. We do not quote values for the ratio $A_{Lann}^{(2)}/A_{Lann}^{(1)}$, since each of the numerator and denominator can vanish and the parametric uncertainties are very large. For typical values of the parameters in the $K\pi$ channels we find that the $A_{Lann}^{(2)}$

is comparable or even larger than $A^{(1)}_{Lann}$ in agreement with Ref. [33]. The size of the annihilation amplitudes in Eq. (4.79) are consistent with our expectation for these power corrections. For $B \to \bar{K}K$ we find

$$\begin{aligned}
&\beta^{\bar{K}K}_{1u} = -9.6 \pm 6.2, && \beta^{\bar{K}K}_{2u} = 1.7 \pm 1.1, && \beta^{\bar{K}K}_{3u} = \beta^{\bar{K}K}_{3c} = 0.63 \pm 0.37, \\
&\beta^{\bar{K}K}_{4u} = \beta^{\bar{K}K}_{4c} = -0.14 \pm 0.09, && \beta^{\bar{K}K}_{1c} = -0.03 \pm 0.02, && \beta^{\bar{K}K}_{2c} = 0.13 \pm 0.08, \\
&\beta^{K\bar{K}}_{3u} = \beta^{K\bar{K}}_{3c} = 0.63 \pm 0.37, && \beta^{\bar{K}K}_{\chi 1} = 0.0 \pm 6.5, && \beta^{\bar{K}K}_{\chi 2} = 0.0 \pm 5.5 \\
&\beta^{\bar{K}K}_{\chi 5} = 0.0 \pm 0.095, && \beta^{\bar{K}K}_{\chi 6} = 0.0 \pm 0.11\,. &&
\end{aligned} \tag{4.80}$$

Using these results to determine the $\lambda_c^{(d)}$ annihilation contributions to $B \to \bar{K}K$ and comparing this to the experimental penguin amplitude from Ref. [26] gives

$$R_A(K^-K^0) = \frac{|A^{(1)}_{Lann}(K^-K^0) + A^{(2)}_{Lann}(K^-K^0)|}{|A_{Expt.Penguin}(\bar{K}K)|} = 0.15 \pm 0.11\,. \tag{4.81}$$

This is similar in size to the ratios $R_A(K^-\pi^+)$, $R_A(\bar{K}^0\pi^-)$ and so also consistent with a power correction.

We conclude our simple phenomenological analysis by comparing the leading hard-collinear annihilation amplitude numerically and parametrically to $A^{(1ann)}_{\rm hard}$ and $A^{(2ann)}_{\rm hard}$. First we compare the leading-power annihilation amplitudes in $\bar{B} \to \pi^+K^-$. Dropping terms proportional to the tiny Wilson coefficients C_{7-8}, we have

$$R_1(\pi^+K^-) \equiv \frac{A^{(1ann)}_{\rm hard-col}(\pi^+K^-)}{A^{(1ann)}_{\rm hard}(\pi^+K^-)} = \frac{\frac{G_F f_B m_B}{\sqrt{2} m_b N_c}(\lambda_u^{(s)} + \lambda_c^{(s)})\, 3\beta_B \left[-f_{3\pi} f_K \beta^{K\pi}_{hc1} - f_{3K} f_\pi \beta^{\pi K}_{hc2}\right]}{\frac{G_F f_B}{\sqrt{2}}(\lambda_u^{(s)} + \lambda_c^{(s)}) f_\pi f_K \left[-\beta^{\pi K}_{4u}\right]}\,. \tag{4.82}$$

Parametrically, the moments in R_1 have $\beta_{4u} \sim \beta_{hci} \sim \mathcal{O}(\alpha_s(m_b))$, and the power counting of the prefactor is $f_{3K}\beta_B/f_K \sim 1$. Also there is no suppression from the hierarchy in the C_i's since β_{4u} involves C_3, and $C_3 \approx C_5 \approx C_6$. Thus, we have shown that for consistency in the α_s and $1/m_b$ expansion, the contributions $A^{(1ann)}_{hard-col}$ need to be included with the local contributions $A^{(1ann)}_{hard}$ in the leading annihilation amplitude. Similarly we can compare the new hard-collinear annihilation amplitude

to the chirally enhanced annihilation contribution in $\bar{B}^0 \to \pi^+ K^-$. Isolating the terms proportional to the large coefficients C_5 and C_6 we have

$$R_2(\pi^+K^-) \equiv \frac{A^{(1ann)}_{\rm hard-col}(\pi^+K^-)}{A^{(2ann)}_{\rm hard}(\pi^+K^-)} = \frac{\frac{G_F f_B m_B}{\sqrt{2} m_b N_c}(\lambda_u^{(s)}+\lambda_c^{(s)})\, 3\beta_B\big[-f_{3\pi} f_K \beta^{\pi K}_{hc1} - f_\pi f_{3K} \beta^{\pi K}_{hc2}\big]}{\frac{G_F f_B}{\sqrt{2} m_b}(\lambda_u^{(s)}+\lambda_c^{(s)}) f_\pi f_K \big[-\mu_\pi \beta^{\pi K}_{\chi 1} + \mu_K \beta^{\pi K}_{\chi 2}\big]}. \tag{4.83}$$

Parametrically $\beta_\chi \sim \beta_{hc} \sim \alpha_s(m_b)$, and $R(\pi^+K^-) \sim m_B \beta_B f_{3\pi}/(f_\pi \mu_\pi) \sim m_b/\mu_\pi \sim m_b/\Lambda$ as expected.

We conclude with a brief numerical analysis of the ratios R_1 and R_2. The C_i's are quoted in Eq. (2.17), and the strong coupling and decay constants in Eq. (4.76). The three-body decay constants $f_{3K} \simeq 4.5 \times 10^{-3}\,\mathrm{GeV}^2$ and $f_{3\pi} \simeq 4.5 \times 10^{-3}\,\mathrm{GeV}^2$ come from QCD sum rules [10] and $\beta_B \simeq 1/(.4\,\mathrm{GeV})$ was determined in a fit to nonleptonic data [26]. To model the nonperturbative meson distributions we truncate the conformal partial wave expansions [141] as

$$\begin{aligned} \phi^M(x) &= 6x(1-x)\big[1 + a_1^M(6x-3) + 6a_2^M(1-5x+5x^2)\big]\,, \\ \phi_{3M}(x,\bar{x}) &= 360 x\bar{x}(1-x-\bar{x})^2\big[1 + \frac{w_{3M}}{2}\{7(1-x-\bar{x})-3\}\big]\,. \end{aligned} \tag{4.84}$$

Eq. (4.50) has convergent convolution integrals for these distribution functions. To estimate the moments β and the ratios R we vary the coefficients in Eq. (4.84) in a conservative range inferred from recent lattice results [52] for the a_i^M's and QCD sum rules [10] for the w_{3M}'s. Specifically we take $a_1^\pi = 0$, $a_1^K = 0.05 \pm 0.02$, $a_2^{\pi,K} = 0.2 \pm 0.2$, and $w_3^{\pi,K} = -1 \pm 1$. A Gaussian scan of the model parameters gives

$$\begin{aligned} &\beta^{\bar{K}K}_{hc1} = -1.4 \pm 0.4, \quad \beta^{\bar{K}K}_{hc2} = 0.3 \pm 0.1, \quad R_1(\pi^+K^-) = 0.3 \text{ to } 1.2\,, \\ &\beta^{\pi K}_{hc1} = -1.4 \pm 0.5, \quad \beta^{\pi K}_{hc2} = 0.1 \pm 0.1, \quad R_2(\pi^+K^-) = -0.1 \text{ to } 0.1\,. \end{aligned} \tag{4.85}$$

The denominators of Eq. (4.82) and (4.83) can vanish, giving large departures from Gaussian statistics. So for R_1 and R_2 we quote the range that contains an equivalent number of points as one standard deviation for a Gaussian distribution. Eq. (4.85)

demonstrates that numerically the three-parton contributions to $A^{(1ann)}$ could be of the same size or larger than the local piece $A_{hard}^{(1ann)}$. Numerically, $m_B\beta_B f_{3\pi}/(f_\pi\mu_\pi) \sim 0.2$ causing some suppression in $R_2(\pi^+K^-)$. It would be interesting to examine the size of these three-parton contributions in the k_T-approach of Ref. [103].

In this chapter, we demonstrated how a new factorization in SCET renders annihilation and "chirally enhanced" annihilation contributions finite in charmless non-leptonic $B \to M_1M_2$ decays to non-isosinglet mesons. We constructed a complete basis of SCET_{II} operators for local annihilation contributions as well as factorization theorems valid to all orders in α_s. By matching the full QCD diagrams onto SCET_{II} operators we showed that their matrix elements are real at leading order in Λ/m_b and $\alpha_s(m_b)$. The lowest order local annihilation contributions depend on f_B and twist-2 distributions $\phi^{M_{1,2}}$ with dependence on rapidity cutoffs. We also computed the final missing term of the leading-order annihilation amplitude in $B \to M_1M_2$ decays. These terms involve a three-parton distribution and need to be included for a complete analysis of annihilation. Chirally enhanced local annihilation contributions depend in addition on $\phi_{pp}^{M_{1,2}}$. The annihilation contributions can only have an unsuppressed complex part at $\mathcal{O}(\Lambda/m_b)$ if perturbation theory at the intermediate scale, $\sqrt{\Lambda m_b}$, breaks down.

In the previous literature models for the power-suppressed annihilation corrections were often found to give enhanced contributions with large strong phases, and such assumptions have been important in some fits to the data. Considering all power suppressed amplitudes not involving charm loops, we proved that complex annihilation contributions only occur suppressed by $\alpha_s(\sqrt{\Lambda m_b})\,\Lambda_{\text{QCD}}/m_b$ compared to the leading amplitudes. We anticipate that our results will guide future fits to the vast amount of data on charmless B decays, and yield a better understanding of what this data means.

Chapter 5

$|V_{ub}|$ from $B \to \pi \ell \bar{\nu}$

5.1 Introduction

The remarkable success of the B-factories has led to a new era for precision results in the CKM sector of the standard model. For $|V_{ub}|$, inclusive and exclusive measurements from semi-leptonic decays should yield a precise value, but must surmount the now dominant theoretical uncertainties. For inclusive decays, measuring $|V_{ub}|$ is more difficult than $|V_{cb}|$ because cuts make observables either sensitive to a structure function that demands input from radiative decays or require neutrino reconstruction. The Heavy Flavor Averaging Group (HFAG)'s average from inclusive decays based on theoretical techniques in Ref. [109] is $10^3|V_{ub}| = 4.52 \pm 0.4$ [91]. For $|V_{ub}|$ from $B \to \pi \ell \bar{\nu}$, model-independent form factor information relies on precision lattice QCD.

Recently, the Fermilab/MILC [127] and HPQCD [133, 73] groups have presented unquenched lattice results for $B \to \pi$ form factors. Uncertainties in the discretization restrict the kinematics to pions that are not too energetic $E_\pi \lesssim 1\,\mathrm{GeV}$, for which the invariant mass of the lepton pair is $15\,\mathrm{GeV}^2 \lesssim q^2 \leq 26.4\,\mathrm{GeV}^2$. Unfortunately, since the phase space goes as $|\vec{p}_\pi|^3$, there are fewer events and more experimental uncertainty in this region. For $\bar{B}^0 \to \pi^+ \ell \bar{\nu}$

$$d\Gamma/dq^2 \;=\; \frac{G_F^2}{24\pi^3}\,|V_{ub}|^2\,|\vec{p}_\pi|^3\,|f_+(q^2)|^2\,, \tag{5.1}$$

For example, Belle [1] found

$$10^3\,|V_{ub}|_{q^2\geq 16} = \begin{cases} 3.87 \pm 0.70 \pm 0.22^{+0.85}_{-0.51}\ \text{(FNAL)} \\ 4.73 \pm 0.85 \pm 0.27^{+0.74}_{-0.50}\ \text{(HPQCD)} \end{cases} \tag{5.2}$$

where the errors are statistical, systematic, and theoretical. In quadrature this is an uncertainty of $\sim 25\%$.

HFAG averages the BaBar, CLEO, and Belle results for the total $B \to \pi\ell\bar{\nu}$ branching ratio finding [95],

$$\text{Br}(\bar{B} \to \pi\ell\bar{\nu}) = (1.39 \pm 0.12) \times 10^{-4}\,. \tag{5.3}$$

This uses isospin to combine the charged and neutral B-decay rates, and expresses the result as a B^0 rate. Equation (5.3) would yield $|V_{ub}|$ at the $\simeq 5\%$ level if the normalization of the relevant $B \to \pi$ form factor were known precisely. So far, extractions of $|V_{ub}|$ from the total Br rely on QCD sum rules [11] and quark models for input. For example, HFAG reports results on $\text{Br}(B \to \{\pi, \rho, \omega\}\ell\bar{\nu})$ that lead to central values $10^3|V_{ub}| = 3.4$ to 4.0 [91]. Due to the uncertainty they do not currently average over exclusive extractions of $|V_{ub}|$.

In this chapter we present a model-independent exclusive method for determining the entire $B \to \pi$ form factor $f_+(q^2)$ and thus $|V_{ub}|$. A total uncertainty $\delta|V_{ub}| \simeq 13\%$ is achieved by combining 1) the unquenched lattice results [133, 127, 73], 2) a constraint at $q^2 = 0$ derived from SCET [19] and $B \to \pi\pi$ data, which determines $|V_{ub}|f_+(0)$, and 3) dispersion relations and analyticity, which allow us to interpolate over the entire region of q^2 by bounding the shape of $f_+(q^2)$ between input points. The SCET constraint induces an additional implicit functional dependence on $|V_{ub}|$ in the form factors. Our first analysis uses just the total Br, yielding an analytic formula for $|V_{ub}|$. The second includes q^2-spectra with a χ^2 minimization which allows the experimental data to constrain the theoretical uncertainty. A different approach for including the q^2-spectra was developed in [81] based on the Lellouch distribution method [113].

5.2 Analyticity Bounds

The QCD matrix element governing semi-leptonic $B \to \pi$ decay can be expressed in terms of form factors as

$$\begin{aligned}\langle \pi(p')|J^\mu(0)|B(p)\rangle &= (p+p')^\mu f_+(q^2) + q^\mu f_-(q^2) \\ &= (p+p' - \frac{m_B^2 - m_\pi^2}{q^2} q)^\mu f_+(q^2) + \frac{m_B^2 - m_\pi^2}{q^2} q^\mu f_0(q^2)\,, \end{aligned} \tag{5.4}$$

where J^μ is the vector part of the appropriate left-handed weak quark current. The "kinematic contraint"

$$f_+(0) = f_0(0) \tag{5.5}$$

ensures there is no singularity at $q^2 = 0$. We briefly review how analyticity constrains the $B \to \pi$ form factors, f_+ and f_0, referring to [47, 48, 49, 51] for more detail. Our notation follows [51], and we set $t_\pm = (m_B \pm m_\pi)^2$. Suitable derivatives of a time ordered product of currents, $\Pi^{\mu\nu}(q^2) = i \int d^4x\, e^{iqx} \langle 0|T J^\mu(x) J^{\dagger\nu}(0)|0\rangle$ can be computed with an operator product expansion (OPE) in QCD and are related by a dispersion relation to moments of a positive definite sum over exclusive states

$$\mathrm{Im}\,\Pi^{\mu\nu} = \int [\text{p.s.}]\, \delta(q - p_{B\pi}) \langle 0|J^{\dagger\nu}|\bar{B}\pi\rangle\langle\bar{B}\pi|J^\mu|0\rangle + \ldots \tag{5.6}$$

Keeping this first term bounds a weighted integral over $t_+ \le t \le \infty$ of the squared $B\pi$ production form factor. Using analyticity and crossing symmetry this constrains the shape in $t = q^2$ of the form factors for $B \to \pi$ in the physical semi-leptonic region $m_\pi^2 \le t \le t_-$. The results are simple to express by writing each of $f_+(t)$, $f_0(t)$ as a series

$$f(t) = \frac{1}{P(t)\phi(t,t_0)} \sum_{k=0}^{\infty} a_k(t_0)\, z(t,t_0)^k\,, \tag{5.7}$$

with coefficients a_k that parameterize different allowed functional forms. As shown in Figure 5.2, the variable

$$z(t,t_0) = \frac{\sqrt{t_+ - t} - \sqrt{t_+ - t_0}}{\sqrt{t_+ - t} + \sqrt{t_+ - t_0}}, \tag{5.8}$$

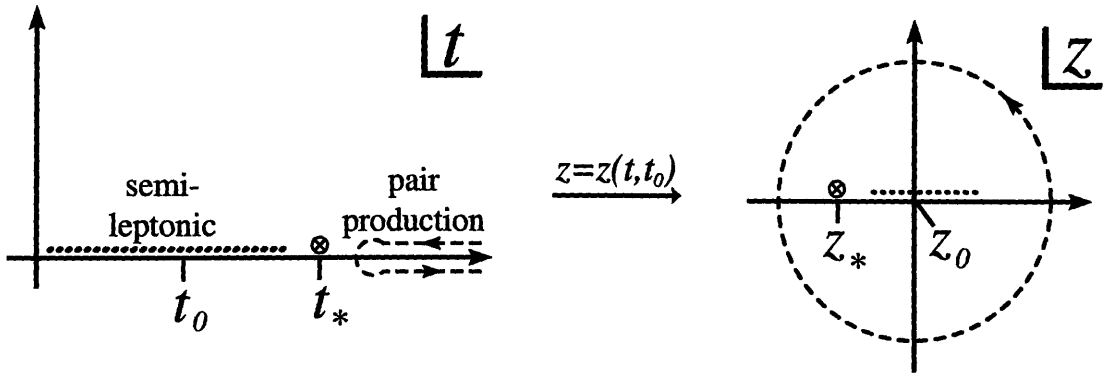

Figure 5-1: Conformal mapping $z(t, t_0)$ (Eq. (5.8)) of the cut complex t plane onto the unit disc $|z| \leq 1$. The dotted line is the physical semi-leptonic region $m_\pi^2 \leq t \leq t_+$. The dashed line is a contour integral around the $B\pi$-pair-production branch cut, $t_+ \leq t < \infty$. The diagrams are not drawn to scale. The form factors are analytic away from the branch cut, except for a simple pole in f_+ at the sub-threshold B^* resonance at $t_* = m_{B^*}^2$, marked by "$\otimes$".

maps the contour around the $B\pi$-pair-production branch cut $t_+ < t < \infty$ onto the unit circle $|z| = 1$ and $-\infty < t < t_+$ onto $z \in [-1, 1]$. t_0 is a free parameter that can be chosen to attain the tightest possible bounds, and it defines $z(t_0, t_0) = 0$. We take $t_0 = 0.65\, t_-$ giving $-0.34 \leq z \leq 0.22$ for the $B \to \pi \ell \bar{\nu}$ range. In Eq. (5.7) the "Blaschke" factor $P(t)$ eliminates sub-threshold poles, such that the product $P f \phi$ is analytic in the unit disc $|z| < 1$, justifying the series expansion. Specifically, $P(t) = 1$ for f_0, while $P(t) = z(t; m_{B^*}^2)$ for f_+ due to the B^* pole. Note that since $z(t, t_0)$ maps $t > t_0$ onto the unit circle, $|P(t)| = 1$ for t in the pair-production region. So we are free to insert a factor of $P * P$ in the dispersive integral Eq. (5.6) and derive constraints on Pf instead of f alone. Finally, the "outer" function is given by

$$\phi(t, t_0) = \sqrt{\frac{n_I}{K \chi_J^{(0)}}} \left(\sqrt{t_+ - t} + \sqrt{t_+ - t_0}\right) \frac{(t_+ - t)^{(a+1)/4}}{(t_+ - t_0)^{1/4}} \times \left(\sqrt{t_+ - t} + \sqrt{t_+}\right)^{-(b+3)} \left(\sqrt{t_+ - t} + \sqrt{t_+ - t_-}\right)^{a/2}, \tag{5.9}$$

where $n_I = 3/2$ and for f_+: $(K = 48\pi, a = 3, b = 2)$, while for f_0: $(K = 16\pi/(t_+ t_-), a = 1, b = 1)$. Here $\chi_J^{(0)}$ corresponds to the lowest moment of $\Pi(q^2)$ computed with an OPE. At two loops, in terms of the pole mass and condensates, and taking

$\mu = m_b$ [82, 113],

$$\chi_{f_+}^{(0)} = \frac{3\big[1+1.140\,\alpha_s(m_b)\big]}{32\pi^2 m_b^2} - \frac{\overline{m}_b\,\langle\bar{u}u\rangle}{m_b^6} - \frac{\langle\alpha_s G^2\rangle}{12\pi m_b^6}\,,$$
$$\chi_{f_0}^{(0)} = \frac{\big[1+0.751\,\alpha_s(m_b)\big]}{8\pi^2} + \frac{\overline{m}_b\,\langle\bar{u}u\rangle}{m_b^4} + \frac{\langle\alpha_s G^2\rangle}{12\pi m_b^4}\,, \tag{5.10}$$

with $\overline{m}_b\langle\bar{u}u\rangle \simeq -0.076\,\mathrm{GeV}^4$, $\langle\alpha_s G^2\rangle \simeq 0.063\mathrm{GeV}^4$. We use $m_b^{\rm pole} = 4.88\,\mathrm{GeV}$ as a central value. With Eq. (5.7) the dispersive bound gives a constraint on the coefficients

$$\sum_{k=0}^{Q} a_k^2 \le 1\,, \tag{5.11}$$

for any choice of Q.

Eqs. (5.7) and (5.11) give only a weak constraint on the normalization of the form factor f_+. In particular, data favors $a_0 \sim 0.02$, so $a_0^2 \ll 1$. The main power of analyticity is that if we fix $f_+(q^2)$ at n_A input points then it constrains the q^2 shape between these points. With $Q = 5$, the error from the bounds is negligible relative to other uncertainties, as we will see below. Our analysis is also insensitive to the exact values of $\chi_J^{(0)}$ or m_b. The bounds can be strengthened using heavy quark symmetry or higher moments of $\Pi(q^2)$ [48, 49], but since this uncertainty is very small we do not use these improvements.

5.3 Input Points

A constraint at $q^2 = 0$ is useful in pinning down the form factor in the small q^2 region. Here we implement a constraint at $q^2 = 0$ on $|V_{ub}|f_+(0)$ that follows from a $B \to \pi\pi$ factorization theorem derived with SCET [19]. The result holds in QCD and uses isospin symmetry and data to eliminate effects due to the relative magnitude and strong phase of penguin contributions. Manipulating formulas in [19] we can write

the result in terms of observables

$$|V_{ub}|f_+(0) = \left[\frac{64\pi}{m_B^3 f_\pi^2}\frac{\overline{B}r(B^- \to \pi^0\pi^-)}{\tau_{B^-}|V_{ud}|^2 G_F^2}\right]^{1/2} \times \left[\frac{(C_1+C_2)t_c - C_2}{C_1^2 - C_2^2}\right]\left[1 + \mathcal{O}\Big(\alpha_s(m_b), \frac{\Lambda_{\rm QCD}}{m_b}\Big)\right], \tag{5.12}$$

where $C_1 = 1.08$ and $C_2 = -0.177$ are Wilson coefficients in the electroweak effective Hamiltonian Eq. (2.15) at $\mu = m_b$ (we drop the tiny $C_{3,4}$), and t_c is a hadronic parameter whose deviation from 1 measures the size of color suppressed amplitudes. In terms of the angles β, γ of the unitarity triangle and CP-asymmetries $S_{\pi^+\pi^-}$ and $C_{\pi^+\pi^-}$ in $B \to \pi^+\pi^-$,

$$t_c = \sqrt{\overline{R}_c \frac{(1 + B_{\pi^+\pi^-}\cos 2\beta + S_{\pi^+\pi^-}\sin 2\beta)}{2\sin^2\gamma}}, \tag{5.13}$$

with $\overline{R}_c = [\overline{B}r(B^0 \to \pi^+\pi^-)\tau_{B^-}]/[2\overline{B}r(B^- \to \pi^0\pi^-)\tau_{B^0}]$, and $B_{\pi^+\pi^-} = (1 - C^2_{\pi^+\pi^-} - S^2_{\pi^+\pi^-})^{1/2}$. Equations (5.12) and (5.13) improve on relations between $B \to \pi\pi$ and $B \to \pi\ell\bar{\nu}$ derived earlier, such as in Ref. [32], because they do not rely on expanding in $\alpha_s(\sqrt{m_b\Lambda})$ or require the use of QCD sum rules for input parameters to calculate t_c.

Equation (5.12) gives our $q^2 = 0$ form factor input

$$f_{\rm in}^0 = |V_{ub}|f_+(0) = (7.2 \pm 1.8) \times 10^{-4}. \tag{5.14}$$

This estimate of 25% uncertainty accounts for the 10% experimental uncertainty, and $\sim 20\%$ theory uncertainty from perturbative and power corrections. The experimental uncertainty includes $\gamma = 70^\circ \pm 15^\circ$, which covers the range from global fits and that preferred by the SCET based $B \to \pi\pi$ method from Ref. [25]. As noted in [19], the dependence of $|V_{ub}|f_+(0)$ on γ is mild for larger γ's. Estimates for perturbative and power corrections to Eq. (5.12) are each at the $\sim 10\%$ level even when "chirally enhanced" terms are included [32, 20].

Next we consider lattice QCD input points, $f_{\rm in}^k$, which are crucial in fixing the

form factor normalization. Technically, using staggered fermions might add model dependence from the $(\det M)^{1/4}$ trick. We take the remarkable agreement in [74] as an indication that this model dependence is small. Using the unquenched MILC configurations, Refs [133, 127, 73] find consistent results with different heavy quark actions. As our default we use the Fermilab results since they have a point at larger q^2:

$$\begin{aligned} f_{\rm in}^1 &= f_+(15.87) = 0.799 \pm 0.058 \pm 0.088\,, \\ f_{\rm in}^2 &= f_+(18.58) = 1.128 \pm 0.086 \pm 0.124\,, \\ f_{\rm in}^3 &= f_+(24.09) = 3.262 \pm 0.324 \pm 0.359\,. \end{aligned} \tag{5.15}$$

The first errors in (5.15) are statistical, $\pm\sigma_i$, and the second are 11% systematic errors, $\pm y f_{\rm in}^i$, with $y = 0.11$. For the lattice error matrix, we use $E_{ij} = \sigma_i^2\delta_{ij} + y^2 f_{\rm in}^i f_{\rm in}^j$, which takes σ_i uncorrelated and includes 100% correlation in the systematic error. Of the eleven reported lattice points we use only three at separated q^2. This maximizes the shape information while minimizing additional correlations that may occur in neighboring points, for example from the chiral extrapolation.

Chiral perturbation theory (ChPT) gives model independent input for f_+ (and f_0) when $E_\pi \sim m_\pi$, namely

$$f_+\big(q^2(E_\pi)\big) = \frac{g f_B m_B}{2 f_\pi (E_\pi + m_{B^*} - m_B)}\Big[1 + \mathcal{O}\Big(\frac{E_\pi}{\Delta}\Big)\Big], \tag{5.16}$$

where g is the $B^*B\pi$ coupling and f_B the decay constant. Possible pole contributions from the low lying $J^\pi = 0^+, 1^+, 2^+$ states vanish by parity and angular momentum conservation. The first corrections scale as E_π/Δ, where $\Delta \sim 600\,\text{MeV}$ is the mass splitting to the first radially excited 1^- state above the B^*. We take $g = 0.5$. This is compatible with D^* decays using heavy quark symmetry. Updating the ChPT fit in [134] by including both $\Gamma(D^{*+})$ and D^* Br-ratios, gives $g_{D^*D\pi} \simeq 0.51$ (at an order where there are no counterterm operators and no $1/m_c$ corrections absorbed in g).

For the lattice average Hashimoto [94] gives $f_B = 189\,\text{MeV}$. Thus,

$$f_{\text{in}}^4 = f_+(26.42) = 10.38 \pm 3.63\,, \tag{5.17}$$

where this fairly conservative 35% error is from uncertainty in gf_B, and from the $m_\pi/\Delta \sim 23\%$ corrections.

5.4 Determining f_+

To determine $f_+(t)$ we drop $a_{k\geq 6}$ in Eq. (5.7), and take $a_5 \to a_5(1-z^2)^{-1/2}$ which properly bounds the truncation error [50]. The f^{0-4} input points then fix a_{0-4} as functions of a_5. Functions that bound $f_+(t)$ are determined from the maximum and minimum values of a_5 satisfying (5.11) with $Q = 5$. Thus we solve

$$\begin{aligned}
&18.3a_0 + 3.96a_1 + 0.857a_2 + 0.185a_3 + 0.0401a_4 \\
&\quad + 0.00887a_5 = f^0/|V_{ub}|\,, \\
&37.8a_0 + 0.960a_1 + 0.0244a_2 + 0.000619a_3 + 1.57\times10^{-5}a_4 \\
&\quad + 4.00\times10^{-7}a_5 = f^1\,,\ \ldots\,, \\
&304.0a_0 - 103.6a_1 + 35.3a_2 - 12.0a_3 + 4.10a_4 - 1.49a_5 = f^4, \\
&a_0^2 + a_1^2 + a_2^2 + a_3^2 + a_4^2 + a_5^2 = 1\,.
\end{aligned} \tag{5.18}$$

In Eq. (5.7) this yields two solutions, $F_\pm$, with parameters

$$f_+(t) = F_\pm(t, \{f_0/|V_{ub}|, f_1, f_2, f_3, f_4\})\,. \tag{5.19}$$

To see how well these solutions bound the form factor we fix $|V_{ub}| = 3.6 \times 10^{-3}$, $f^i = f_{\text{in}}^i$ and plot the bounds as the two black solid lines in Fig. 5-2. The curves lie on top of each other. For comparison we show dashed lines for the bounds on f_+ and f_0 obtained using four lattice points (shown as dots). With these inputs the constraint $f_+(0) = f_0(0)$ is less effective than using the SCET point.

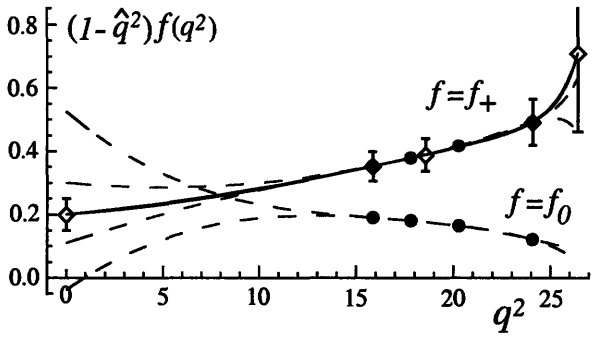

Figure 5-2: Upper and lower bounds on the form factors from dispersion relations, where $\hat{q}^2 = q^2/m_{B^*}^2$ and the $(1-\hat{q}^2)$ factor removes the B^* pole. The overlapping solid black lines are bounds $F_\pm$ derived with the SCET point, 3 lattice points, and the ChPT point (diamonds with error bars). The dashed lines are the bounds derived using instead four lattice points (shown by the dots). Input point errors are not included in these lines, and are analyzed in the text.

5.5 $|V_{ub}|$ from total Br fraction

Equating Eq. (5.3) with the theoretical rate obtained using Eqs. (5.19) gives an analytic equation for $|V_{ub}|$. With $f^i = f^i_{\rm in}$ the solution is

$$|V_{ub}| = (4.13 \pm 0.21 \pm 0.58) \times 10^{-3}\,. \tag{5.20}$$

The first error is experimental, 5.2%, propagated from Eq.(5.3). The second error, 14%, is from theory and is broken down in Table 5.1. It is dominated by the input points. The bound uncertainty from the choice of solution is $< 1\%$ (but would grow to $\pm 12\%$ without the SCET point). The error from m_b and the order in the OPE and are very small because shifts in the normalization through $\chi^{(0)}_{f_+}$ are compensated by shifts in the a_n coefficients, except for the last term a_5 which gives a small contribution. To ensure consistency with the dispersion bounds the input point uncertainty is calculated using the Lellouch-method of generating random points from Gaussians [113], giving $10^3|V_{ub}| = (3.96 \pm 0.20 \pm 0.56)$. Our distributions were determined using Eqs. (5.14,5.15,5.17) and the correlation matrix E_{ij}. Taken individually the SCET and ChPT points give $\sim 5\%$ error, so the lattice uncertainty dominates.

Type of Error	Variation From	$\delta\|V_{ub}\|^{\rm Br}$	$\delta\|V_{ub}\|^{q^2}$
Input Points	1-σ correlated errors	$\pm 14\%$	$\pm 12\%$
Bounds	F_+ versus F_-	$\pm 0.6\%$	$\pm 0.04\%$
$m_b^{\rm pole}$	4.88 ± 0.40	$\pm 0.1\%$	$\pm 0.2\%$
OPE order	2 loop $\rightarrow$ 1 loop	-0.2%	$+0.3\%$

Table 5.1: Summary of theoretical uncertainties on $|V_{ub}|$. Results are shown for an analysis from the total branching fraction, $\delta|V_{ub}|^{\rm Br}$, and from using the $d\Gamma/dq^2$ spectrum, $\delta|V_{ub}|^{q^2}$. For the input point error we quote the average from $F_\pm$.

5.6 $|V_{ub}|$ from q^2 spectra

Results for partial branching fractions, $({\rm Br}_i^{\rm exp} \pm \delta{\rm Br}_i)$, over different bins in q^2 are also available. Cleo [6] and Belle [1] present results for 3 bins with untagged and π^+ semileptonic tags respectively. Babar [75] recently presented total rates from hadronic & leptonic π^+ and π^0 tags as well as π^+ semileptonic tagged data in 3-bins and untagged data over 5-bins. By fitting to these 17 pieces of data with Minuit we exploit the q^2 shape information. To do this we define

$$\chi^2 = \sum_{i=1}^{17} \frac{[{\rm Br}_i^{\rm exp} - {\rm Br}_i(V_{ub}, F_\pm)]^2}{(\delta{\rm Br}_i)^2} + \frac{[f_{\rm in}^0 - f^0]^2}{(\delta f^0)^2} + \frac{[f_{\rm in}^4 - f^4]^2}{(\delta f^4)^2} + \sum_{i,j=1}^{3} [f_{\rm in}^i - f^i][f_{\rm in}^j - f^j](E^{-1})_{ij}\,, \tag{5.21}$$

and minimize χ^2 as a function of $|V_{ub}|$ and f^{0-4}. χ^2 contains both experimental and theoretical errors, with E^{-1} the inverse error matrix. By allowing f^{0-4} in $F_\pm$ to move away from $f_{\rm in}^{0-4}$ the theoretical rate is allowed to adjust itself based on the experimental q^2 shape.

Minimizing (5.21) gives $\chi^2/(dof) = 1.04$ and

$$|V_{ub}| = (3.54 \pm 0.47) \times 10^{-3}\,. \tag{5.22}$$

Results for $f_+(q^2)$ and $d\Gamma/dq^2$ are shown by the black solid curves in Figs. 5-3 and 5-4. Eq. (5.22) has a total error of 13%. If we fix $f^{0-4} = f_{\rm in}^{0-4}$ then the experimental error is 4.9%, ie. $\delta|V_{ub}| = \pm 0.17$. The remainder, $\delta|V_{ub}| = \pm 0.44$ is from the input points,

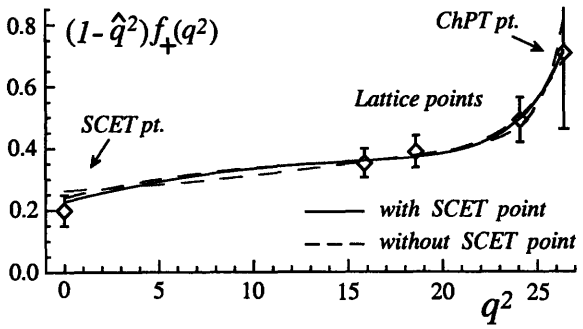

Figure 5-3: Results from the χ^2 fit of $|V_{ub}|$ and f^{0-4} to the q^2 spectra ($\hat{q}^2 = q^2/m_{B^*}^2$). The two solid lines are obtained using either the F_+ or F_- solutions from Eq. (5.19). The two dashed lines repeat this analysis without using the SCET point.

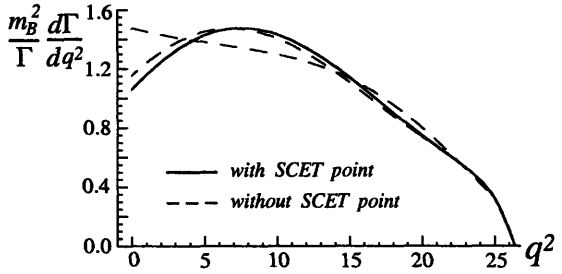

Figure 5-4: The curves are as in Fig.2, but for the decay rate.

so the q^2 spectra brought this theory error down to 12%. Other uncertainties are small as shown in Table 5.1. The experimental spectra favor a larger form factor between the lattice and SCET points. This decreases the value of $|V_{ub}|$ from that in (5.20). Using Eqs. (5.14,5.17) this fit yields

$$f_+(0) = 0.227 \pm 0.047\,, \quad g\,f_B = 96 \pm 29\,\mathrm{MeV}\,, \tag{5.23}$$

consistent with our inputs. This $f_+(0)$ has 21% error.

If we entirely remove the SCET point f^0 from Eq. (5.21) then we obtain a fit that uses only semileptonic data, shown by the dashed red lines in Figs. 5-3 and 5-4. The spectrum is now determined less precisely at small q^2, since this data only bounds the area in the smallest q^2-bin. The result is $|V_{ub}| = (3.56 \pm 0.48) \times 10^{-3}$. It has the same input point error as Eq. (5.22) and a somewhat larger bound error, $\delta|V_{ub}| =$ 1.8%. Turning the use of Eq.(5.14) around, we can combine it with $f_+(0)$ to get an independent method of fixing $|V_{ub}|$ from the nonleptonic data. The semileptonic fit gives $f_+(0) = 0.25 \pm 0.06$, so Eq. (5.14) yields $|V_{ub}|^{nonlep} = (2.9 \pm 1.0) \times 10^{-3}$.

Our final result for $|V_{ub}|$ is given in (5.22). The final theory error is dominated by the lattice points, and is very close to their error. It will decrease with this error in the future.

5.7 Improving the determination

We are presently in the preliminary stages of an exhaustive analysis of all sources of error and the influence of the fit specifics on the determination of $|V_{ub}|$. To this end, we have written a more sophisticated FORTRAN code, still making use of the CERN program libraries routine MINUIT for minimization. The code fits directly for $|V_{ub}|$ and the form factor series coefficients a_k in Eq. (5.7) instead of first solving for the a_k's in terms of the form factor inputs as above. The code is menu-driven and includes options for toggling: experimental data on the $B \to \pi \ell \bar{\nu}$ branching fractions; form factor inputs from Fermilab/MILC [127], HPQCD [133, 73], and the SCET and ChPT points described above. The menu also includes options for changing the number of terms ($Q + 1$ in Eq. (5.11)) in the truncated series expansions. We find a mild sensitivity ($\sim 10\%$) to variations in this choice. We can also vary assumptions about the behavior of the systematic errors, both theoretical and experimental. We change the correlation of the errors as well as the "slope" (*i.e.* whether an 11% systematic error should be interpreted as 11% of the input value or 11% of the fit value). We find that the fit value of $|V_{ub}|$ is insensitive (<1%) to these variations, provided just a few widely-spaced lattice points are included in the fit, as above. We find that the fit value of $|V_{ub}|$ is again insensitive to whether we enforce the "kinematic condition" Eq. (5.5) at $q^2 = 0$ and use lattice data on both f_+ and f_0 or use the SCET point as above. Our default fit uses Br data from: Belle in 3 bins [98], BaBar charge-averaged partial rates in 3 bins for each semi-leptonic and hadronic tagging methods [7], CLEO partial rates in 3 bins [6], BaBar data in 12 bins using untagged loose νs [8], and preliminary data on the total branching fraction from Belle using hadronic tagging presented at ICHEP06 [95]. The fit has three paramters in the truncated f_+ series and two in the truncated f_0 series. As above, we assume 100% correlation of the lattice systematic

errors. With the three widely-spaced Fermilab points in Eq. (5.15), we find

$$10^3|V_{ub}^{\mathrm{FNAL}}| = 3.83 \pm 0.44 \tag{5.24}$$

while using the three widely-spaced lattice points from HPQCD [73]

$$10^3|V_{ub}^{\mathrm{HPQCD}}| = 4.24 \pm 0.45\,. \tag{5.25}$$

From this we see that the choice of which lattice group we use for the form factor normalization changes the determination of $|V_{ub}|$ at the 10% level. As mentioned, this is work in progress, and these results, preliminary.

Chapter 6

Conclusions

This thesis described original contributions of the author and his collaborators to the field of particle physics, in particular, theoretical aspects of B-meson decays in the Standard Model. Strong-interaction effects described by QCD pose the most significant challenge in this undertaking. Effective field theories help simplify and clarify the calculation of these QCD effects. The EFTs used in this thesis were introduced in Chapter 2. In that chapter, we also investigated the completeness of reparametrization-invariance (RPI) constraints derived on a projected surface and the path dependence of ultrasoft Wilson lines in the soft-collinear effective theory (SCET).

In Chapter 3, we constructed a complete basis for heavy-to-light currents to second order in the SCET power counting. These operators enter many SCET calculations, including $B \to X_s\gamma$ and $B \to X_u\ell\bar{\nu}$ in the endpoint region of large energy but moderate invariant mass. We derived relations between the currents' Wilson coefficients by enforcing RPI. These relations determine subleading Wilson coefficients in terms of the leading ones to all orders in α_s without the need for additional matching calculations.

In Chapter 4, we classified, according to their perturbative order and strong phases, all the $\Lambda_{\rm QCD}/m_b$–suppressed decay amplitudes for B decays to two light mesons. We calculated, by explicit tree-level matching, the leading "annihilation" contributions, where the spectator quark is Wick-contracted with a field in the weak

effective Hamiltonian. We showed, using recent results on mode factorization in quantum field theory [124], that the leading annihilation amplitude is real with a magnitude of $\sim 15\%$ of the observed "penguin" amplitude. The origin of the large relative phase between the penguin and tree amplitudes has yet to be determined, but our results eliminate one of the suggested SM explanations.

In Chapter 5, we presented a model-independent method for determining the CKM matrix element $|V_{ub}|$ based on the exclusive mode $B \to \pi \ell \bar{\nu}$ and QCD dispersion-relation based parametrization of the $B \to \pi$ hadronic form factors. Our final result is given in (5.22). The final theory error is dominated by the lattice inputs, and is very close to their error. It will decrease with this error in the future, and provides a competitive and complementary determination for the current best direct estimates based on inclusive $B \to X_u \ell \bar{\nu}$.

Appendix A

Zero-bin subtractions for a 2D distribution

In this appendix we derive a result for the action of the zero-bin subtractions on the integrand obtained from the chirally enhanced annihilation computation, shown in Eq. (4.64). Since the result involves a correlation in the x and y integrals it cannot be read off from the results in Ref. [124]. It is convenient to write the momentum fraction factor coming from the offshell b-quark propagator as $(1-x\bar{y}) = (\bar{x}+y-\bar{x}y)$. Including the rapidity convergence factors [124], the integral we need is

$$I = \sum_{x\neq 1,\, y\neq 0} \int dx_r dy_r \, \frac{\phi_{pp}^{M_1}(y)\phi^{M_2}(x)}{(\bar{x}+y-\bar{x}y)\bar{x}y^2}\, \Theta_x\Theta_y \, |x(1-x)|^{\epsilon} \, |y(1-y)|^{\epsilon} \left(\frac{\mu_+\mu_-}{\bar{n}\cdot p_1 \, n\cdot p_2}\right)^{2\epsilon}, \tag{A.1}$$

where $\Theta_x = \theta(x)\theta(1-x)$. To determine the subtraction terms we must look at the singular behavior as we scale towards the $x = 1$ and $y = 0$ bins, which we do by taking $\bar{x} \sim \eta$ and $y \sim \eta$. In this limit the gluon and b-quark in Fig. 4-2 become soft, and this region would be double counted without the zero-bin conditions. First consider the denominator,

$$\frac{1}{\bar{x}+y-\bar{x}y} = \frac{1}{(\bar{x}+y)} + \frac{\bar{x}y}{(\bar{x}+y)^2} + \dots . \tag{A.2}$$

In the first term the x and y dependence does not decouple, so we must consider them simultaneously. All terms beyond the first one produce finite integrals and are dropped in the minimal subtraction scheme. For the numerator in Eq. (A.1) we use $\phi_{pp}^{M_1}(0) = \phi^{M_2}(1) = 0$ and expand

$$\begin{aligned}\phi_{pp}(y)\,\phi(x) &= -y\phi'_{pp}(0)\,\bar{x}\phi'(1) - \frac{y^2}{2}\phi''_{pp}(0)\,\bar{x}\phi'(1) + y\phi'_{pp}(0)\,\frac{\bar{x}^2}{2}\,\phi''(1) + \dots \\ &= y\phi'_{pp}(0)\sum_{n=1}^{\infty}\frac{(-\bar{x})^n}{n!}\,\phi^{(n)}(1) - \frac{y^2}{2}\,\phi''_{pp}(0)\,\bar{x}\phi'(1) + \dots\,. \end{aligned} \tag{A.3}$$

In the first term on the last line we have identified all terms which remain singular when multiplied by $1/[\bar{x}y^2(\bar{x}+y)]$. This term is equal to $y\phi'_{pp}(0)\phi(x)$. Taken together with the expansion of $\Theta_x\Theta_y$ we therefore find that the required minimal subtraction is

$$\frac{y\phi_{pp}^{M_1\prime}(0)\phi^{M_2}(x)}{(\bar{x}+y)\bar{x}y^2}\,\Theta_x\,\theta(y)\,. \tag{A.4}$$

Following Ref. [124] we use this to convert Eq. (A.1) into an integral that includes the $x = 1$ and $y = 0$ regions,

$$\begin{aligned} I &= \int_0^1 dx \int_0^1 dy \left[\frac{\phi_{pp}^{M_1}(y)\phi^{M_2}(x)}{(\bar{x}+y-\bar{x}y)\bar{x}y^2} - \frac{y\phi_{pp}^{M_1\prime}(0)\phi^{M_2}(x)}{(\bar{x}+y)\bar{x}y^2}\right] \\ &\quad - \int_0^1 dx \int_1^\infty dy\,\frac{y\phi_{pp}^{M_1\prime}(0)\phi^{M_2}(x)}{(\bar{x}+y)\bar{x}y^2}\,x^\epsilon(1-x)^\epsilon\,y^\epsilon(y-1)^\epsilon\left(\frac{\mu_+\mu_-}{\bar{n}\cdot p_1\, n\cdot p_2}\right)^{2\epsilon} \qquad \text{(A.5)} \\ &= \int_0^1 dx\,\frac{\phi^{M_2}(x)}{\bar{x}}\int_0^1 dy\left[\frac{\phi_{pp}^{M_1}(y)}{(\bar{x}+y-\bar{x}y)y^2} - \frac{\phi_{pp}^{M_1\prime}(0)}{(\bar{x}+y)y}\right] - \int_0^1 dx\int_1^\infty dy\,\frac{\phi_{pp}^{M_1\prime}(0)\phi^{M_2}(x)}{(\bar{x}+y)\bar{x}y}\,y^\epsilon(y-1)^\epsilon \\ &= \int_0^1 dx\,\frac{\phi^{M_2}(x)}{\bar{x}}\int_0^1 dy\left[\frac{\phi_{pp}^{M_1}(y)}{(\bar{x}+y-\bar{x}y)y^2} - \frac{\phi_{pp}^{M_1\prime}(0)}{(\bar{x}+y)y}\right] - \phi_{pp}^{M_1\prime}(0)\int_0^1 dx\,\frac{\phi^{M_2}(x)\ln(2-x)}{(1-x)^2}\,. \end{aligned}$$

Here in simplifying the term carrying the $y \to \infty$ limit, we noted that the integral is finite, and so it does not induce $\mu_\pm$ dependence in our subtraction scheme. This result for I was used in Eq. (4.64). For the asymptotic pion wave functions, $\phi^\pi(x) = 6x(1-x)$ and $\phi_{pp}^\pi(y) = 6y(1-y)$, we obtain $I = 6 + \pi^2 - 24\ln 2 = -0.766$. $I = 36 + 6\pi^2 - 144\ln 2 = -4.60$. Note that the steps used here to derive the subtraction also give the correct result for cases where the x and y integrals factorize, such as an integrand $\phi(x)\phi(y)/(x^2y^2)$.

Bibliography

[1] K. Abe et al. Measurement of exclusive $B \to X_u \ell\nu$ decays with $D^{(*)}\ell\nu$ decay tagging. 2004, hep-ex/0408145.

[2] Christian M. Arnesen, Joydip Kundu, and Iain W. Stewart. Constraint equations for heavy-to-light currents in SCET. *Phys. Rev.*, D72:114002, 2005, hep-ph/0508214.

[3] Christian M. Arnesen, Zoltan Ligeti, Ira Z. Rothstein, and Iain W. Stewart. Power corrections in charmless nonleptonic B decays: Annihilation is factorizable and real. 2006, hep-ph/0607001.

[4] Christian M. Arnesen, Ira Z. Rothstein, and Iain W. Stewart. Three-parton contributions to $B \to M_1 M_2$ annihilation at leading order. *Phys. Lett.*, B647:405–412, 2007, hep-ph/0611356.

[5] M. Christian Arnesen, Benjamin Grinstein, Ira Z. Rothstein, and Iain W. Stewart. Precision model-independent determination of $|V_{ub}|$ from $B \to \pi e\nu$. *Phys. Rev. Lett.*, 95:071802, 2005, hep-ph/0504209.

[6] S. B. Athar et al. Study of the q^2 dependence of $B \to \pi\ell\nu$ and $B \to \rho(\omega)\ell\nu$ decay and extraction of $|V_{ub}|$. *Phys. Rev.*, D68:072003, 2003, hep-ex/0304019.

[7] B. Aubert et al. Measurement of the b –¿ pi l nu branching fraction and determination of —v(ub)— with tagged B mesons. 2006, hep-ex/0607089.

[8] B. Aubert et al. Measurement of the $B^0 \to \pi^- \ell^+ \nu$ form factor shape and branching fraction, and determination of $|V_{ub}|$ with a loose neutrino reconstruction technique. 2006, hep-ex/0607060.

[9] Borut Bajc, Alejandra Melfo, Goran Senjanovic, and Francesco Vissani. The minimal supersymmetric grand unified theory. I: Symmetry breaking and the particle spectrum. *Phys. Rev.*, D70:035007, 2004, hep-ph/0402122.

[10] Patricia Ball, V. M. Braun, and A. Lenz. Higher-twist distribution amplitudes of the K meson in QCD. *JHEP*, 05:004, 2006, hep-ph/0603063.

[11] Patricia Ball and Roman Zwicky. $|V_{ub}|$ and constraints on the leading-twist pion distribution amplitude from $B \to \pi \ell \nu$. *Phys. Lett.*, B625:225–233, 2005, hep-ph/0507076.

[12] Myron Bander, D. Silverman, and A. Soni. CP noninvariance in the decays of heavy charged quark systems. *Phys. Rev. Lett.*, 43:242, 1979.

[13] Christian W. Bauer, Sean Fleming, and Michael E. Luke. Summing sudakov logarithms in $B \to X_s \gamma$ in effective field theory. *Phys. Rev.*, D63:014006, 2001, hep-ph/0005275.

[14] Christian W. Bauer, Sean Fleming, Dan Pirjol, Ira Z. Rothstein, and Iain W. Stewart. Hard scattering factorization from effective field theory. *Phys. Rev.*, D66:014017, 2002, hep-ph/0202088.

[15] Christian W. Bauer, Sean Fleming, Dan Pirjol, and Iain W. Stewart. An effective field theory for collinear and soft gluons: Heavy to light decays. *Phys. Rev.*, D63:114020, 2001, hep-ph/0011336.

[16] Christian W. Bauer, Christopher Lee, Aneesh V. Manohar, and Mark B. Wise. Enhanced nonperturbative effects in Z decays to hadrons. *Phys. Rev.*, D70:034014, 2004, hep-ph/0309278.

[17] Christian W. Bauer and Aneesh V. Manohar. Shape function effects in $B \to X_s\gamma$ and $B \to X_u\ell\nu$ decays. *Phys. Rev.*, D70:034024, 2004, hep-ph/0312109.

[18] Christian W. Bauer, Aneesh V. Manohar, and Mark B. Wise. Enhanced nonperturbative effects in jet distributions. *Phys. Rev. Lett.*, 91:122001, 2003, hep-ph/0212255.

[19] Christian W. Bauer, Dan Pirjol, Ira Z. Rothstein, and Iain W. Stewart. $B \to M_1M_2$: Factorization, charming penguins, strong phases, and polarization. *Phys. Rev.*, D70:054015, 2004, hep-ph/0401188.

[20] Christian W. Bauer, Dan Pirjol, Ira Z. Rothstein, and Iain W. Stewart. On differences between SCET and QCDF for $B \to \pi\pi$ decays. *Phys. Rev.*, D72:098502, 2005, hep-ph/0502094.

[21] Christian W. Bauer, Dan Pirjol, and Iain W. Stewart. A proof of factorization for $B \to D\pi$. *Phys. Rev. Lett.*, 87:201806, 2001, hep-ph/0107002.

[22] Christian W. Bauer, Dan Pirjol, and Iain W. Stewart. Soft-collinear factorization in effective field theory. *Phys. Rev.*, D65:054022, 2002, hep-ph/0109045.

[23] Christian W. Bauer, Dan Pirjol, and Iain W. Stewart. Factorization and endpoint singularities in heavy-to-light decays. *Phys. Rev.*, D67:071502, 2003, hep-ph/0211069.

[24] Christian W. Bauer, Dan Pirjol, and Iain W. Stewart. On power suppressed operators and gauge invariance in SCET. *Phys. Rev.*, D68:034021, 2003, hep-ph/0303156.

[25] Christian W. Bauer, Ira Z. Rothstein, and Iain W. Stewart. Determining γ from $B \to \pi\pi$ decays without the CP- asymmetry $C(\pi_0\pi_0)$. *Phys. Rev. Lett.*, 94:231802, 2005, hep-ph/0412120.

[26] Christian W. Bauer, Ira Z. Rothstein, and Iain W. Stewart. SCET analysis of $B \to K\pi$, $B \to K\bar{K}$, and $B \to \pi\pi$ decays. *Phys. Rev.*, D74:034010, 2006, hep-ph/0510241.

[27] Christian W. Bauer and Iain W. Stewart. Invariant operators in collinear effective theory. *Phys. Lett.*, B516:134–142, 2001, hep-ph/0107001.

[28] Thomas Becher and Richard J. Hill. Loop corrections to heavy-to-light form factors and evanescent operators in SCET. *JHEP*, 10:055, 2004, hep-ph/0408344.

[29] Thomas Becher, Richard J. Hill, and Matthias Neubert. Factorization in $B \to V\gamma$ decays. *Phys. Rev.*, D72:094017, 2005, hep-ph/0503263.

[30] M. Beneke, G. Buchalla, M. Neubert, and C. T. Sachrajda. Comment on "$B \to M_1 M_2$: Factorization, charming penguins, strong phases, and polarization". *Phys. Rev.*, D72:098501, 2005, hep-ph/0411171.

[31] M. Beneke, G. Buchalla, M. Neubert, and Christopher T. Sachrajda. QCD factorization for $B \to \pi\pi$ decays: Strong phases and CP violation in the heavy quark limit. *Phys. Rev. Lett.*, 83:1914–1917, 1999, hep-ph/9905312.

[32] M. Beneke, G. Buchalla, M. Neubert, and Christopher T. Sachrajda. QCD traveling waves beyond leading logarithms factorization for exclusive, non-leptonic B-meson decays: General arguments and the case of heavy-light final states. *Nucl. Phys.*, B591:313–418, 2000, hep-ph/0006124.

[33] M. Beneke, G. Buchalla, M. Neubert, and Christopher T. Sachrajda. QCD factorization in $B \to \pi K$, $\pi\pi$ decays and extraction of Wolfenstein parameters. *Nucl. Phys.*, B606:245–321, 2001, hep-ph/0104110.

[34] M. Beneke, F. Campanario, T. Mannel, and B. D. Pecjak. Power corrections to $\bar{B} \to X_u \ell \bar{\nu}\, (X_s \gamma)$ decay spectra in the 'shape-function' region. *JHEP*, 06:071, 2005, hep-ph/0411395.

[35] M. Beneke, A. P. Chapovsky, M. Diehl, and T. Feldmann. Soft-collinear effective theory and heavy-to-light currents beyond leading power. *Nucl. Phys.*, B643:431–476, 2002, hep-ph/0206152.

[36] M. Beneke and T. Feldmann. Multipole-expanded soft-collinear effective theory with non-abelian gauge symmetry. *Phys. Lett.*, B553:267–276, 2003, hep-ph/0211358.

[37] M. Beneke and T. Feldmann. Factorization of heavy-to-light form factors in soft-collinear effective theory. *Nucl. Phys.*, B685:249–296, 2004, hep-ph/0311335.

[38] M. Beneke and S. Jager. Spectator scattering at NLO in non-leptonic B decays: Tree amplitudes. *Nucl. Phys.*, B751:160–185, 2006, hep-ph/0512351.

[39] M. Beneke, Y. Kiyo, and D. S. Yang. Loop corrections to sub-leading heavy quark currents in SCET. *Nucl. Phys.*, B692:232–248, 2004, hep-ph/0402241.

[40] Martin Beneke and Matthias Neubert. QCD factorization for $B \to PP$ and $B \to PV$ decays. *Nucl. Phys.*, B675:333–415, 2003, hep-ph/0308039.

[41] I. I. Bigi. Studying CP violation: Chances for a new alliance. 2002, hep-ph/0206261.

[42] B. Blok, J. G. Korner, D. Pirjol, and J. C. Rojas. Spectator effects in the heavy quark effective theory. *Nucl. Phys.*, B496:358–374, 1997, hep-ph/9607233.

[43] Boris Blok, Michael Gronau, and Jonathan L. Rosner. Annihilation, rescattering, and CP asymmetries in B-meson decays. *Phys. Rev. Lett.*, 78:3999–4002, 1997, hep-ph/9701396.

[44] Geoffrey T. Bodwin. Factorization of the Drell-Yan cross-section in perturbation theory. *Phys. Rev.*, D31:2616, 1985.

[45] S. W. Bosch, B. O. Lange, M. Neubert, and Gil Paz. Factorization and shape-function effects in inclusive B-meson decays. *Nucl. Phys.*, B699:335–386, 2004, hep-ph/0402094.

[46] Stefan W. Bosch, Matthias Neubert, and Gil Paz. Subleading shape functions in inclusive B decays. *JHEP*, 11:073, 2004, hep-ph/0409115.

[47] C. Bourrely, B. Machet, and E. de Rafael. Semileptonic decays of pseudoscalar particles (M $\rightarrow$ M- prime lepton lepton-neutrino) and short distance behavior of quantum chromodynamics. *Nucl. Phys.*, B189:157, 1981.

[48] C. Glenn Boyd, Benjamin Grinstein, and Richard F. Lebed. Constraints on form-factors for exclusive semileptonic heavy to light meson decays. *Phys. Rev. Lett.*, 74:4603–4606, 1995, hep-ph/9412324.

[49] C. Glenn Boyd, Benjamin Grinstein, and Richard F. Lebed. Model independent determinations of $\bar{B} \rightarrow D\ell\nu$, $D^*\ell\nu$ form-factors. *Nucl. Phys.*, B461:493–511, 1996, hep-ph/9508211.

[50] C. Glenn Boyd and Richard F. Lebed. Improved QCD form factor constraints and $\Lambda_b \rightarrow \Lambda_c \ell\bar{\nu}$. *Nucl. Phys.*, B485:275–290, 1997, hep-ph/9512363.

[51] C. Glenn Boyd and Martin J. Savage. Analyticity, shapes of semileptonic form factors, and $\bar{B} \rightarrow \pi\ell\bar{\nu}$. *Phys. Rev.*, D56:303–311, 1997, hep-ph/9702300.

[52] V. M. Braun et al. Moments of pseudoscalar meson distribution amplitudes from the lattice. 2006, hep-lat/0606012.

[53] Gerhard Buchalla, Andrzej J. Buras, and Markus E. Lautenbacher. Weak decays beyond leading logarithms. *Rev. Mod. Phys.*, 68:1125–1144, 1996, hep-ph/9512380.

[54] Andrzej J. Buras. Weak hamiltonian, CP violation and rare decays. 1998, hep-ph/9806471.

[55] J. Charles et al. CP violation and the CKM matrix: Assessing the impact of the asymmetric B factories. *Eur. Phys. J.*, C41:1–131, 2005, hep-ph/0406184.

[56] Ling-Lie Chau and Wai-Yee Keung. Comments on the parametrization of the Kobayashi-Maskawa matrix. *Phys. Rev. Lett.*, 53:1802, 1984.

[57] June-gone Chay and Chul Kim. Factorization of B decays into two light mesons in soft- collinear effective theory. *Phys. Rev.*, D68:071502, 2003, hep-ph/0301055.

[58] June-gone Chay and Chul Kim. Rare radiative exclusive B decays in soft-collinear effective theory. *Phys. Rev.*, D68:034013, 2003, hep-ph/0305033.

[59] Junegone Chay and Chul Kim. Collinear effective theory at subleading order and its application to heavy-light currents. *Phys. Rev.*, D65:114016, 2002, hep-ph/0201197.

[60] Junegone Chay and Chul Kim. Nonleptonic B decays into two light mesons in soft- collinear effective theory. *Nucl. Phys.*, B680:302–338, 2004, hep-ph/0301262.

[61] Junegone Chay, Chul Kim, Yeong Gyun Kim, and Jong-Phil Lee. Soft Wilson lines in soft-collinear effective theory. *Phys. Rev.*, D71:056001, 2005, hep-ph/0412110.

[62] Junegone Chay, Chul Kim, and Adam K. Leibovich. Quark mass effects in the soft-collinear effective theory and $\bar{B} \to X_s\gamma$ in the endpoint region in the endpoint region. *Phys. Rev.*, D72:014010, 2005, hep-ph/0505030.

[63] V. L. Chernyak and A. R. Zhitnitsky. Asymptotic behavior of exclusive processes in QCD. *Phys. Rept.*, 112:173, 1984.

[64] Cheng-Wei Chiang, Michael Gronau, Jonathan L. Rosner, and Denis A. Suprun. Charmless $B \to PP$ decays using flavor SU(3) symmetry. *Phys. Rev.*, D70:034020, 2004, hep-ph/0404073.

[65] J. H. Christenson, J. W. Cronin, V. L. Fitch, and R. Turlay. Evidence for the 2 pi decay of the k(2)0 meson. *Phys. Rev. Lett.*, 13:138–140, 1964.

[66] Marco Ciuchini, E. Franco, G. Martinelli, M. Pierini, and L. Silvestrini. Charming penguins strike back. *Phys. Lett.*, B515:33–41, 2001, hep-ph/0104126.

[67] Marco Ciuchini, E. Franco, G. Martinelli, and L. Silvestrini. Charming penguins in B decays. *Nucl. Phys.*, B501:271–296, 1997, hep-ph/9703353.

[68] P. Colangelo, G. Nardulli, N. Paver, and Riazuddin. Long distance effects in b $\rightarrow$ s exclusive decays. *Z. Phys.*, C45:575, 1990.

[69] John C. Collins. Leading-twist single-transverse-spin asymmetries: Drell-yan and deep-inelastic scattering. *Phys. Lett.*, B536:43–48, 2002, hep-ph/0204004.

[70] John C. Collins and Andreas Metz. Universality of soft and collinear factors in hard- scattering factorization. *Phys. Rev. Lett.*, 93:252001, 2004, hep-ph/0408249.

[71] John C. Collins, Davison E. Soper, and George Sterman. Soft gluons and factorization. *Nucl. Phys.*, B308:833, 1988.

[72] John C. Collins and George Sterman. Soft partons in QCD. *Nucl. Phys.*, B185:172, 1981.

[73] Emel Dalgic et al. B meson semileptonic form factors from unquenched lattice QCD. *Phys. Rev.*, D73:074502, 2006, hep-lat/0601021.

[74] C. T. H. Davies et al. High-precision lattice QCD confronts experiment. *Phys. Rev. Lett.*, 92:022001, 2004, hep-lat/0304004.

[75] J. Dingfelder (BaBar Collaboration). contribution to CKM2005. 2005.

[76] Estia Eichten and Brian Hill. An effective field theory for the calculation of matrix elements involving heavy quarks. *Phys. Lett.*, B234:511, 1990.

[77] Adam F. Falk and Benjamin Grinstein. Power corrections to leading logs and their application to heavy quark decays. *Phys. Lett.*, B247:406–411, 1990.

[78] Adam F. Falk, Matthias Neubert, and Michael E. Luke. The residual mass term in the heavy quark effective theory. *Nucl. Phys.*, B388:363–375, 1992, hep-ph/9204229.

[79] Thorsten Feldmann and Tobias Hurth. Non-factorizable contributions to $B \to \pi\pi$ decays. *JHEP*, 11:037, 2004, hep-ph/0408188.

[80] The Tevatron Electroweak Working Group for the CDF and D0 Collaborations. A combination of CDF and D0 results on the mass of the top quark. 2007, hep-ex/0703034.

[81] Masaru Fukunaga and Tetsuya Onogi. A model independent determination of $|V_{ub}|$ using the global q^2 dependence of the dispersive bounds on the $B \to \pi\ell\nu$ form factors. *Phys. Rev.*, D71:034506, 2005, hep-lat/0408037.

[82] S. C. Generalis. Light quark current correlators. *J. Phys.*, G16:367–373, 1990.

[83] H. Georgi. Effective field theory. *Ann. Rev. Nucl. Part. Sci.*, 43:209–252, 1993.

[84] Howard Georgi. An effective field theory for heavy quarks at low- energies. *Phys. Lett.*, B240:447–450, 1990.

[85] Alan Gray et al. The B meson decay constant from unquenched lattice QCD. *Phys. Rev. Lett.*, 95:212001, 2005, hep-lat/0507015.

[86] Benjamin Grinstein. The static quark effective theory. *Nucl. Phys.*, B339:253–268, 1990.

[87] Benjamin Grinstein, Yuval Grossman, Zoltan Ligeti, and Dan Pirjol. The photon polarization in $B \to X_s\gamma$ in the standard model. *Phys. Rev.*, D71:011504, 2005, hep-ph/0412019.

[88] Michael Gronau, Oscar F. Hernandez, David London, and Jonathan L. Rosner. Decays of B mesons to two light pseudoscalars. *Phys. Rev.*, D50:4529–4543, 1994, hep-ph/9404283.

[89] D. J. Gross and Frank Wilczek. Asymptotically free gauge theories. 1. *Phys. Rev.*, D8:3633–3652, 1973.

[90] Yuval Grossman, Andreas Hocker, Zoltan Ligeti, and Dan Pirjol. Testing the dynamics of $B \to \pi\pi$ and constraints on α. *Phys. Rev.*, D72:094033, 2005, hep-ph/0506228.

[91] Heavy Flavor Averaging Group. Averages of b-hadron properties at the end of 2006. 2007, arXiv:0704.3575 [hep-ex].

[92] Andri Hardmeier, Enrico Lunghi, Dan Pirjol, and Daniel Wyler. Subleading collinear operators and their matrix elements. *Nucl. Phys.*, B682:150–182, 2004, hep-ph/0307171.

[93] ed. Harrison, P. F. and ed. Quinn, Helen R. *The BaBar physics book: Physics at an asymmetric B factory.* Papers from Workshop on Physics at an Asymmetric B Factory (BaBar Collaboration Meeting), Rome, Italy, 11-14 Nov 1996, Princeton, NJ, 17-20 Mar 1997, Orsay, France, 16-19 Jun 1997 and Pasadena, CA, 22-24 Sep 1997.

[94] Shoji Hashimoto. Recent results from lattice calculations. *Int. J. Mod. Phys.*, A20:5133–5144, 2005, hep-ph/0411126.

[95] HFAG, http://www.slac.stanford.edu/xorg/hfag/.

[96] R. J. Hill, T. Becher, S. J. Lee, and M. Neubert. Sudakov resummation for subleading SCET currents and heavy- to-light form factors. *JHEP*, 07:081, 2004, hep-ph/0404217.

[97] Richard J. Hill and Matthias Neubert. Spectator interactions in soft-collinear effective theory. *Nucl. Phys.*, B657:229–256, 2003, hep-ph/0211018.

[98] T. Hokuue et al. Measurements of branching fractions and q^2 distributions for $B \to \pi\ell\nu$ and $B \to \rho\ell\nu$ decays with $B \to D^*\ell\nu$ decay tagging. 2006, hep-ex/0604024.

[99] Nathan Isgur and Mark B. Wise. Weak transition form-factors between heavy mesons. *Phys. Lett.*, B237:527, 1990.

[100] Xiang-dong Ji, Jian-ping Ma, and Feng Yuan. QCD factorization for semi-inclusive deep-inelastic scattering at low transverse momentum. *Phys. Rev.*, D71:034005, 2005, hep-ph/0404183.

[101] Alexander L. Kagan. Polarization in $B \to VV$ decays. *Phys. Lett.*, B601:151–163, 2004, hep-ph/0405134.

[102] Y. Y. Keum, Hsiang-Nan Li, and A. I. Sanda. Penguin enhancement and $B \to K\pi$ decays in perturbative QCD. *Phys. Rev.*, D63:054008, 2001, hep-ph/0004173.

[103] Yong-Yeon Keum, Hsiang-nan Li, and A. I. Sanda. Fat penguins and imaginary penguins in perturbative QCD. *Phys. Lett.*, B504:6–14, 2001, hep-ph/0004004.

[104] A. Khodjamirian, Th. Mannel, M. Melcher, and B. Melic. Annihilation effects in $B \to \pi\pi$ from QCD light-cone sum rules. *Phys. Rev.*, D72:094012, 2005, hep-ph/0509049.

[105] Makoto Kobayashi and Toshihide Maskawa. CP violation in the renormalizable theory of weak interaction. *Prog. Theor. Phys.*, 49:652–657, 1973.

[106] G. P. Korchemsky and G. Marchesini. Structure function for large x and renormalization of Wilson loop. *Nucl. Phys.*, B406:225–258, 1993, hep-ph/9210281.

[107] Gregory P. Korchemsky and George Sterman. Power corrections to event shapes and factorization. *Nucl. Phys.*, B555:335–351, 1999, hep-ph/9902341.

[108] Bjorn O. Lange and Matthias Neubert. Factorization and the soft overlap contribution to heavy- to-light form factors. *Nucl. Phys.*, B690:249–278, 2004, hep-ph/0311345.

[109] Bjorn O. Lange, Matthias Neubert, and Gil Paz. Theory of charmless inclusive B decays and the extraction of V_{ub}. *Phys. Rev.*, D72:073006, 2005, hep-ph/0504071.

[110] Bjorn O. Lange, Iain W. Stewart, and Aneesh V. Manohar. in preparation.

[111] Keith S. M. Lee and Iain W. Stewart. Factorization for power corrections to $B \to X_s\gamma$ and $B \to X_u\ell\bar{\nu}$. *Nucl. Phys.*, B721:325–406, 2005, hep-ph/0409045.

[112] Adam K. Leibovich, Zoltan Ligeti, and Mark B. Wise. Comment on quark masses in SCET. *Phys. Lett.*, B564:231–234, 2003, hep-ph/0303099.

[113] Laurent Lellouch. Lattice-constrained unitarity bounds for $\bar{B}^0 \to \pi^+\ell^-\bar{\nu}_\ell$ decays. *Nucl. Phys.*, B479:353–391, 1996, hep-ph/9509358.

[114] Hsiang-nan Li. QCD aspects of exclusive B meson decays. *Prog. Part. Nucl. Phys.*, 51:85–171, 2003, hep-ph/0303116.

[115] Hsiang-nan Li. k_T factorization of exclusive B meson decays. 2004, hep-ph/0408232.

[116] Eric V. Linder. Theory challenges of the accelerating universe. 2006, astro-ph/0610173.

[117] Cai-Dian Lu, Kazumasa Ukai, and Mao-Zhi Yang. Branching ratio and CP violation of $B \to \pi\pi$ decays in perturbative QCD approach. *Phys. Rev.*, D63:074009, 2001, hep-ph/0004213.

[118] Michael E. Luke and Aneesh V. Manohar. Reparametrization invariance constraints on heavy particle effective field theories. *Phys. Lett.*, B286:348–354, 1992, hep-ph/9205228.

[119] Michael E. Luke, Aneesh V. Manohar, and Ira Z. Rothstein. Renormalization group scaling in nonrelativistic QCD. *Phys. Rev.*, D61:074025, 2000, hep-ph/9910209.

[120] Julie Malcles. Depuzzling $B \to K\pi$: Constraints on the unitarity triangle from $B, B_s \to \pi\pi, K\pi, KK$ decays in the SU(3) limit. 2006, hep-ph/0606083.

[121] Aneesh V. Manohar. Effective field theories. 1996, hep-ph/9606222.

[122] Aneesh V. Manohar. Deep inelastic scattering as $x \to 1$ using soft-collinear effective theory. *Phys. Rev.*, D68:114019, 2003, hep-ph/0309176.

[123] Aneesh V. Manohar, Thomas Mehen, Dan Pirjol, and Iain W. Stewart. Reparameterization invariance for collinear operators. *Phys. Lett.*, B539:59–66, 2002, hep-ph/0204229.

[124] Aneesh V. Manohar and Iain W. Stewart. The zero-bin and mode factorization in quantum field theory. 2006, hep-ph/0605001.

[125] Aneesh V. Manohar and Mark B. Wise. Heavy quark physics. *Camb. Monogr. Part. Phys. Nucl. Phys. Cosmol.*, 10:1–191, 2000.

[126] Sonny Mantry, Dan Pirjol, and Iain W. Stewart. Strong phases and factorization for color suppressed decays. *Phys. Rev.*, D68:114009, 2003, hep-ph/0306254.

[127] M. Okamoto et al. Semileptonic $D \to \pi/K$ and $B \to \pi/D$ decays in 2+1 flavor lattice QCD. *Nucl. Phys. Proc. Suppl.*, 140:461–463, 2005, hep-lat/0409116.

[128] Michael E. Peskin and D. V. Schroeder. An introduction to quantum field theory. Reading, USA: Addison-Wesley (1995) 842 p.

[129] Dan Pirjol. Factorization in color-suppressed $\bar{B} \to D^{(*)0}\pi^0$ decays from the soft-collinear effective theory. 2004, hep-ph/0411124.

[130] Dan Pirjol and Iain W. Stewart. A complete basis for power suppressed collinear-ultrasoft operators. *Phys. Rev.*, D67:094005, 2003, hep-ph/0211251.

[131] H. David Politzer. Reliable perturbative results for strong interactions? *Phys. Rev. Lett.*, 30:1346–1349, 1973.

[132] Mikhail A. Shifman, A. I. Vainshtein, and Valentin I. Zakharov. Light quarks and the origin of the $\Delta I = 1/2$ rule in the nonleptonic decays of strange particles. *Nucl. Phys.*, B120:316, 1977.

[133] J. Shigemitsu et al. Semileptonic B decays with $N_f = 2+1$ dynamical quarks. *Nucl. Phys. Proc. Suppl.*, 140:464–466, 2005, hep-lat/0408019.

[134] Iain W. Stewart. Extraction of the $D^*D\pi$ coupling from D^* decays. *Nucl. Phys.*, B529:62–80, 1998, hep-ph/9803227.

[135] Iain W. Stewart. Theoretical introduction to B decays and the soft-collinear effective theory. 2003, hep-ph/0308185.

[136] S. Wandzura and Frank Wilczek. Sum rules for spin dependent electroproduction: Test of relativistic constituent quarks. *Phys. Lett.*, B72:195, 1977.

[137] Alexander R. Williamson and Jure Zupan. Two body B decays with isosinglet final states in SCET. *Phys. Rev.*, D74:014003, 2006, hep-ph/0601214.

[138] Lincoln Wolfenstein. Parametrization of the Kobayashi-Maskawa matrix. *Phys. Rev. Lett.*, 51:1945, 1983.

[139] Yue-Liang Wu and Yu-Feng Zhou. Charmless decays $B \to \pi\pi$, pi k and k k in broken SU(3) symmetry. *Phys. Rev.*, D72:034037, 2005, hep-ph/0503077.

[140] W. M. Yao et al. Review of particle physics. *J. Phys.*, G33:1–1232, 2006.

[141] A. R. Zhitnitsky, I. R. Zhitnitsky, and V. L. Chernyak. QCD sum rules and properties of wave functions of nonleading twist. (in Russian). *Sov. J. Nucl. Phys.*, 41:284, 1985.